'The Development and Application of Novel Analytical Techniques in the Determination of Geographical Origin and Adulteration of Vegetable Oils'

Alison Parry-Jones

A Thesis submitted to the
University of Glamorgan
for the Degree of Doctor of Philosophy

School of Applied Science
University of Glamorgan
UK

This research programme was carried out
in collaboration with the
Institute for Spectrochemistry and Applied Spectroscopy,
Dortmund, Germany

July 2001

Declaration

This thesis has not been nor is currently being submitted for the award of any other degree or similar qualification.

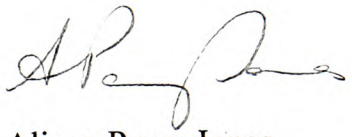

Alison Parry-Jones
July 2001

ABSTRACT

Extra virgin olive oil is expensive to produce and its rising popularity as part of a healthy diet over the last two decades has increased world demand. This has led to olive oil being diluted with cheaper vegetable oils in an attempt to increase output and, therefore, profit. Some oil producing areas are considered to produce a superior quality olive oil and some suppliers import oil from other, less fashionable, areas and export the oil as 'bottled in' the more favoured region. This thesis examines the questions that arise concerning the authenticity of olive oil. It investigates whether spectroscopic data (NMR and IR) analysed by multivariate analysis (Unscrambler 7.5, Camo ASA) can reliably characterise Greek olive oil samples by their area and year or identify adulteration with sunflower oil. Extraction of the volatile compounds would also be considered to discover whether this fraction of olive oil could be useful in the determination of oil origin.

The PLS1 regression models constructed using IR data for a set of samples from the Crete 1995/96 harvest gave a low error of prediction for the measured percentage sunflower adulteration against the predicted values. An RMSEP of 0.795% sunflower oil with an offset of 0.147% using 11 regression components gave good prediction of adulteration of unknown samples.

PCA models of proton NMR data produced classification plots with clear separation between oils originating from Crete and those from other areas of Greece. They also gave unequivocal classification of each year's harvest, making it possible to ascertain the year and area of olive growth.

SFE and SPME were both used for the extraction of the volatile fraction of olive oil with separation and detection by GC-MS. Hierarchical clustering (SPSS) showed rudimentary grouping of the oils by area of origin using both techniques. Coupling the two extraction techniques gave a novel methodology, which with improvements, could become an exciting new procedure.

CONTENTS

INDEX OF FIGURES

INDEX OF TABLES

ABBREVIATIONS

ANOVA	Analysis of Variance
ATR	Attenuated Total Reflectance
DEPT	Distortionless Enhancement by Polarisation Transfer
DPPO	Diphenyl-*p*- phenylene oxide
FFA	Free Fatty Acid
HDL	High Density Lipoprotein
HMQC	Heteronuclear Multiple Quantum Correlation
IDA	Isotope Dilution Assay
IOOC	International Olive Oil Council
ISAS	Institute for Spectrochemistry and Applied Spectroscopy
LDL	Low Density Lipoprotein
MCT	Mercury-cadmium-telluride
MLR	Multiple Linear Regression
MUFA	Monounsaturated Fatty Acid
ODS	Octadecylsilica
ORAC	Oxygen Radical Absorbance Capacity
PC	Principal Component
PCA	Principal Component Analysis
PCR	Principal Component Regression
PDMS	Polydimethylsiloxane
PDMS/CAR	Polydimethylsiloxane/Carboxen
PDMS/DVB	Polydimethylsiloxane/Divinylbenzene
PFPH	Pentafluorophenylhydrazine
PLS	Partial Least Squares
PUFA	Polyunsaturated Fatty Acid
RMSEC	Root Mean Squared Error of Calibration
RMSEP	Root Mean Squared Error of Prediction
ROS	Reactive Oxygen Species
R/T	Retention Time
SC-CO_2	Supercritical Carbon Dioxide
SDE	Steam Distillation-Solvent Extraction
SEP	Standard Error of Prediction
SIMCA	Soft Independent Modelling of Class Analogy
SLDA	Stepwise Linear Discrimination Analysis
SNIF-NMR/IRMS	Site-Specific Natural Isotopic Fractionation studied by Nuclear Magnetic Resonance/Isotope Ratio Mass Spectrometry
SPME	Solid Phase Micro Extraction
SPSS	Statistical Package for the Social Sciences
TIC	Total Ion Chromatogram
TMS	Tetramethylsilane

STATISTICAL GLOSSARY

Calibration – The fitting of a model to the observed data to describe the data as fully as possible

Calibration samples – Samples used to observe the variation in the data on which the model is built

Classification – The prediction, using models constructed from known data, to determine in which category a new sample belongs

Correlation - A measurement of the linear relationship between two variables

Cross-validation – A validation method where samples are omitted from the calibration and used as test samples. This is repeated until all the samples have been used as test samples.

Explained variance – The fraction of the total variance that has been explained by the model

Influence – How much impact a single variable has on the model

Leverage – How extreme a variable is compared to the majority of variables. Variables with a high leverage have a high influence on the model

Loadings – The loadings show how well a variable is taken in to account by the model components

Model – Mathematical equation detailing the variations in a data set, consisting of structure and error information

Offset – The point where a regression line intercepts the y-axis

Outlier – A variable that is abnormal compared to the other variables (occupies an extreme point on the model)

Overfitting – Describing too much of the variation by taking into account noise

Partial least squares regression – A method which relates the variation in a response variable (e.g. % sunflower adulteration) to the variation in the data set (e.g. oil spectra)

Prediction – Using regression models, the ability to compute response values from predictor values

Preprocessing – Operations that reduce the noise from background effects especially in spectroscopic data

Principal component – A linear function of the original variable which contains information to describe the data

Principal component analysis – A modelling method to observe relationships between different variables and detect sample grouping

Regression coefficient – Numerical coefficients that describe the connection between variation in the predictors and in the response

Residual variance – The amount of variance not explained by the model

Root mean squared error of prediction – A measurement of the average difference between measured and predicted response values

Scores – Scores show sample differences or similarities with respect to individual principal components

Test samples – Samples which are not used during the construction of the calibration model but are used to validate the model

Validation – Checking how well a model describes the data

Variance – A measure of a variable's spread around its mean value

Acknowledgements

I would like to thank the following people for their guidance and support throughout the course of this work:

My supervisors at the University of Glamorgan; Dr P S McIntyre, Dr A J Berry and Dr E Morgan

Dr A N Davies, Dr J Lambert, Dr L Küpper and Brigitte Stubenrauch at the Institute for Spectrochemisty and Applied Spectroscopy in Dortmund, Germany for sharing their considerable technical experience and assisting in the preparation and analysis of olive oil samples. Also for supplying a set of IR results for statistical comparison.

The technical staff at the University of Glamorgan.

On a personal note I would like to thank my husband, David, and children, William and Philippa, for putting up with the disruption especially over the last year and my parents and in-laws for their invaluable assistance with school runs and child minding.

CHAPTER 1

1 Introduction

Olive oil has been a valuable commodity since ancient times. It has been widely used and revered as a health product but only in modern times has a greater understanding of the chemistry of olive oil given an insight into its properties. Olive oil is unusual compared to other vegetable oils by virtue of its chemical composition. Whereas most vegetable oils contain a large proportion of polyunsaturated fats, olive oil contains a larger proportion of monounsaturated fat. Olive oil also contains antioxidants which have been shown, in humans, to inhibit the oxidation of low density lipoproteins (LDL cholesterol), which are the most atherogenic (capacity to initiate or accelerate the formation of lipid deposits in the arteries) lipoproteins (Visioli *et al.*, 1998). The antioxidant properties of olive oil have also been linked with possible cancer prevention by protecting cells from damage to DNA caused by reactive oxygen species (ROS). When excess levels of ROS (e.g. ·OH radicals) react with unsaturated fatty acids, oxidative damage occurs in cell membranes that can result in cell mutation and possible carcinogenesis (Lopaczynski *et al.*, 2001). These peroxidative chain reactions are terminated by antioxidants, which break the chain, such as α-tocopherol and β-carotene, both of which are found in olive oils. Polyunsaturated fatty acids (PUFA) play an important role in the initiation of this chain reaction and have also been shown to contribute to the oxidative modification of LDL cholesterol which increases the progression of atherosclerosis (Caruso *et al.*, 1999). Both monounsaturated fatty acids (MUFA) and PUFA lower total cholesterol compared to saturated fatty acids when cholesterol intake is moderate (Trautwein *et al.*, 1999).

As a result of the reported benefits of consuming olive oil there has been an upsurge in its popularity over the last two decades and annual consumption is beginning to outstrip annual production (www.oliveoilsource.com, 2001). Extra virgin olive oil is expensive to produce and some growers and suppliers attempt to increase output and therefore profit by 'watering down' the oil with cheaper seed/vegetable oils. The chemical differences between these cheaper seed/vegetable oils and olive oil are such that this type of adulteration can be exposed by monitoring the chemical structure of the oil components. The fatty acid composition and the unsaponifiable fraction of the oil can both give valuable information.

The uncertainty of the origin of oils due to ambiguous labelling is another issue which has been highlighted. Many suppliers import olive oil from the less 'desirable' producing areas and sell it as originating from areas which are deemed to produce more highly regarded oils. Olive oils that are labelled as 'bottled in Italy' are not necessarily produced in Italy. The chemical composition of oil varies because of a range of factors. Geographical origin is chief amongst these and encompasses many influences such as the topography of the growing area (mountain or plains), climatic variation and the variety of the olive used. The time of harvest can be affected by the weather and this can also alter the composition of the oil. Statistical analysis of data spanning 24 years of Greek olive oil harvests concluded that fatty acid compositional data was a valuable tool for the classification of origin of oils (Tsimidou *et al.*, 1993). Therefore, it would appear that large geographical differences, such as country to country, should be detectable by spectroscopic means and one of the aims of this work was to attempt to distinguish between oils from the same country but different areas of origin.

1.1 AIMS

The aims of the work were to approach the problems of oil identity using two methods, spectroscopic techniques and extraction development. Within the spectroscopic techniques, two methods would attempt to lower the limits of detectable adulteration and separate oils on the basis of area or year of origin. Extraction techniques would be developed to try to isolate the volatile compounds from the oil matrix and discover whether the variation in composition in adulterated oils or geographically separate oils was sufficient to allow classification of unknown samples.

1.1.1 Adulteration Detection

The primary aim of this work was to develop novel methods of adulteration detection using various analytical techniques and statistically analyse the resulting data using chemometrics, to observe whether the method employed reliably identified adulteration. The challenge is to develop methods that can detect lower and lower levels of adulteration and also to detect adulteration with oils that more closely resemble the chemical structure of olive oil. Nuclear magnetic resonance, both ^{13}C and ^{1}H NMR, of pure Greek oils and spiked samples from two harvest years supplied data that could be statistically analysed using multivariate analysis. This type of analysis correlates important variables with specific samples and allows classification models to be constructed which determine whether an unknown sample 'fits' into a certain model. It also provides a measurement of the error of prediction between measured and predicted samples to conclude how well the model fits the particular data set. Infra red spectroscopy would also be employed following the development of a fibre optic probe at the collaborating institute in Germany. This would require no sample preparation,

enabling rapid sampling of a large quantity of samples. Oils from three harvest years, pure and adulterated, would be investigated using this method.

1.1.2 Geographical Differentiation

Distinguishing between oils produced from olives grown in different countries has been investigated and spectroscopic techniques shown to be valuable tools (Zamora *et al.*, 2001). The oils used in this study originated from areas of Greece including some from island producers. If the growing areas experienced suitably different conditions throughout the growth and harvesting of the olives then a difference in oil composition would be expected. The second aim of this work was to investigate whether such variations could, when subjected to statistical analysis, reliably separate oils from different areas.

1.1.3 Harvest Differentiation

It has been previously noted (Mavromoustakos *et al.*, 1997) that *'samples from the same area gave repeatably the same results within a 3 year period'*. However, a project for the European Commission (Lees *et al.*, 1998) used SNIF-NMR/IRMS (Site-specific Natural Isotopic Fractionation studied by Nuclear Magnetic Resonance/Isotope Ratio Mass Spectrometry) to look at isotopic characterisation of oils and concluded that *'the data analysis showed that the year of production had a significant influence on the isotopic composition of the oils'* and *'all three years were differentiated'*. This project obtained samples from 3 concurrent harvest years and aimed to investigate whether the composition of olive oils from the same areas is indeed consistent from year to year. If the variation in growing factors was sufficient, then discrepancy in the oil composition would be expected.

1.1.4 Extraction of the volatile fraction of olive oil

The majority of previous work has concentrated on the fatty acid fraction of olive oil and less work has been carried out using the volatile fraction of the oil. The volatile fraction is composed of chemicals responsible for the flavour and fragrance of the oil and although work has focussed on sensory qualities and how the volatile fraction alters during storage, using the volatile compounds to detect adulteration or geographical origin is less widely reported. This study aimed to develop extraction techniques to enable the volatile compounds to be removed from the oil and analysed using Gas Chromatography/Mass Spectrometry (GC/MS). Removing the compounds from the oil matrix would simplify separation and detection. Techniques would be investigated that would allow rapid, solventless extraction thereby producing a more time efficient, environmentally sound procedure. Supercritical fluid extraction and solid phase microextraction would both be used to attempt to distinguish between commercially bought vegetable oils and olive oil. A comparison of the two techniques using the Greek olive oils would also be undertaken and multivariate analysis carried out on the resulting data to verify whether these techniques could be utilised in the determination of adulteration or geographical origin.

1.2 THESIS SYNOPSIS

The background to olive oil production, chemistry and early analysis techniques is detailed in Chapter 2, with maps showing the origin of the Greek olive oils used throughout this project and tables detailing the sample codes, areas and altitude of origin and the variety and ripeness of the olives at harvest time. Chapter 3 introduces the concept of multivariate analysis and describes the statistical processes utilised in the characterisation of adulteration, and the differentiation of area and harvest origin. As a

result of the number of different techniques employed during this work, each different procedure is the subject of a separate chapter. Each chapter is autonomous and contains theory, a literature review particular to that technique, method, results and discussion and conclusions. Chapters 4 and 5 concentrate on the spectroscopic investigations using Nuclear Magnetic Resonance (NMR) and Infra-red (IR) respectively. Chapters 6 and 7 focus on two different extraction techniques, Supercritical Fluid Extraction (SFE) and Solid-Phase Microextraction (SPME). The SPME chapter (7) also gives preliminary findings obtained from coupling the two extraction techniques. Chapter 8 assimilates the conclusions from the individual chapters and provides method comparison and suggestions for further refinement and additional work.

CHAPTER 2

2 Olive Oil

2.1 HISTORY AND BACKGROUND

The olive was originally native to Asia Minor and spread to the Mediterranean basin 5,000 years ago. It is one of the oldest known cultivated trees in the world, and the olive branch has become a symbol of peace and goodwill. In Greek mythology the olive tree is presented to man as a gift from the gods of Olympus. During the dispute for the possession of Attica between Athena and Poseidon, the Goddess Athena caused an olive tree to sprout on the Acropolis. This was considered more useful than Poseidon's gift of a salt spring and the city was named for Athena. In ancient Egypt the goddess Isis was believed to have introduced olive oil to mankind and it was infused with flowers and grasses to produce medicines and cosmetics in the belief that the oil conferred strength and youth. The trees were so sacred that anyone who felled a tree could be condemned to death (www.museodellolivo.com/eng/emuseo, 2000).

In the Bible the dove returned to Noah carrying an olive branch after the flood, symbolising the re-establishment of peace between God and man. Hebrew culture used olive oil to anoint religious symbols, to consecrate the Ark of the Covenant, religious ornaments and the priests. Its properties were greatly revered and it was used for medicinal purposes as well as religious ceremony. Homer deemed olive oil the *'liquid gold'* and Hippocrates prescribed it as the *'great therapeutic'* (www.globalgourmet.com/food/egg/egg0397/oohistory.html, 1997). The Romans expanded the tree throughout their empire, mainly using the oil for fuel and in baths. They did not widely use it for edible purposes, considering it to be of insufficient quality.

Olive farming reached a peak in the fourteenth century when the oil was used primarily as a lighting fuel. According to the Scriptures the lamps burning on the altars before the Blessed Sacrament could only be fuelled by olive oil and the consecrated oil was used to administer the Sacraments. The settlers introduced olive trees into America, where they remain mainly cultivated in California, Chile and Argentina. Olives are now grown world-wide although the chief producing countries remain those in the Mediterranean basin. The oil is now used predominantly for edible purposes but is also used in the pharmaceutical and cosmetic industries. Some religions still use olive oil with water during baptism to *'enable the baby to slip away from the grasp of evil'* and signify salvation (Zwingle, 1999).

2.2 OLIVE OIL PRODUCTION

The most common olive tree (*Olea Europea*) has a life span in excess of 150 years. It doesn't become fully productive until it is 35 years old and can then yield constantly for over 100 years. The green olives appear in September, subsequently turn purple and then black when fully ripe. The weight of the fruit increases until November at which point it decreases, due to lack of moisture, resulting in a rise in oil content. The oil content reaches a maximum when the olives are black (Boskou, 1996). The olives can be harvested at any stage, by hand picking or machine shaking, and the degree of ripeness at harvest affects the composition of the olive oil produced (Koutsaftakis *et al.*, 1999). The time of picking mainly affects the concentrations of phenolic (Cinquanta *et al.*, 1997) and volatile compounds in the olive, responsible for taste and aroma. Both these classes of compounds decrease as the fruit ripens, leading to the conclusion that oil produced from olives picked prior to full maturation would have a stronger aroma and taste. One study did find that the concentration of tyrosol, hydroxytyrosol and luteolin (a

flavonoid) increased with maturation (Brenes *et al.*, 1999). Other variables such as peroxide value and free acidity, depend on the quality of the olives. Therefore, these characteristics do not fluctuate significantly with degree of ripeness (Boskou, 1996). The way in which the olives are stored/transported before processing has been shown to affect the chemical composition of the resulting oil. A recent study compared the effects of different aqueous storage methods on the volatile compounds in olive oil. It compared olives stored in shallow boxes open to the air with olives placed in jars filled with sea water, jars filled with 4% NaCl solution and jars filled with drinking water. It concluded that storing olives in aqueous media does alter the composition and content of volatile compounds (Koprivnjak *et al.*, 2000). Other studies have compared storage temperatures (Kiritsakis *et al.*, 1998) and their influence on peroxide values, chlorophyll content, phenol content and fatty acid content.

Virgin olive oil is extracted by pressure, centrifugation and percolation systems. Before the oil can be extracted the olives have been traditionally washed and deleafed. The presence of leaves gives the resulting oil a 'green leaf' organoleptic characteristic. Washing the olives can potentially damage the fruit and reduce the oil yield, so it is becoming a less widespread practice. The olives are then crushed to let the oil run out of the vacuoles. There are various methods of crushing, stone mills, hammer crushers or metal crushers. Oils obtained using different crushing methods have different organoleptic characteristics. The olive paste, obtained from the crushing, is then mixed to increase the amount of oil that is released by helping the droplets of oil to merge into larger drops that can be separated into a continuous liquid phase and also to break up the oil/water emulsion. Separation of the oil from the liquid and solid phases is then achieved using pressure, centrifugation or percolation.

The oldest extraction technique is the use of pressure. The solid phase is separated from the liquid by applying pressure to a stack of mats smeared with olive paste. This method requires simple machinery and is the cheapest form of extraction. However, it is the most labour intensive. Centrifugation requires high-speed centrifuges, which are expensive and need a specialised work force. The solid phase is separated from the liquid phase by diluting the olive paste with water. A major drawback with this system is that it produces a lot of vegetation water that still contains a high percentage of oil. Percolation uses a steel plate, which is immersed into the olive paste and becomes coated with oil because of the different surface tensions of the liquid phase in the paste. This method is also called selective filtration. Percolation is often combined with another extraction method to overcome the drawback that it does not completely deplete the olive paste (Boskou, 1996).

It requires approximately 5 kg of olives to produce 1 litre of oil and each tree usually yields 20-30 kg of olives annually. World wide olive oil production is approximately 2,100,000,000 litres per annum. Spain and Italy are the largest producers, followed by Greece, Portugal, Tunisia, Turkey and Syria. A large proportion of olive oil is consumed in the producing country. The three largest producing countries are also the three largest consuming countries. The trend for world consumption has steadily increased over the last decade due to the reported benefits of the 'Mediterranean diet'.

The import/export of olive oil is an expanding market that is carefully regulated by the International Olive Oil Council (IOOC) and the European Union (EU). Typical annual import/export data is given in Figure 2.1 (www.oliveoilsource.com, 2001).

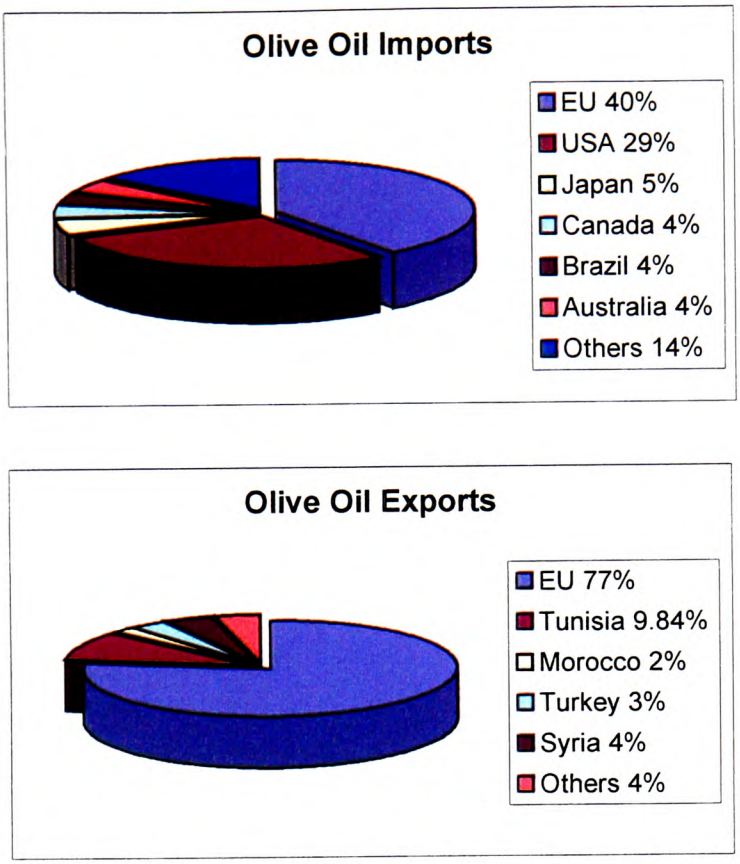

Figure 2.1 - Typical annual % import/export of olive oil 1999/2000

The IOOC was set up under Article 21 of the International Agreement on Olive Oil of 1956. The Agreements are regularly updated and the Council's primary aim is to facilitate international co-operation in all areas concerned with olive oil. It is funded by contributions from producing and importing countries and meets twice a year. It assembles and circulates economic and commercial information on olives and olive oil as well as scientific, technical and agricultural findings.

The Commission of the European Communities has set down regulations that fix the price and define the grade of olive oil produced. The grades of oil are defined using acidity levels. Extra virgin olive oil should have '*perfect flavour and odour with a maximum acidity (oleic acid) of 1g/100g – 1%, with maximum peroxide value mequiv O_2/kg of O_2*'. Fine virgin olive oil can have a maximum acidity of 2%, ordinary olive oil

3.3% (Communities, 1966). Extra virgin oil accounts for less than 10% of produced oil in many countries.

2.3 CHEMISTRY OF OLIVE OIL

Chemically olive oil belongs in the 'Fats and Oils' category. Fats and oils are hydrophobic, water-insoluble substances of animal or plant origin. They consist predominantly of triglycerides, glyceryl esters of fatty acids. Figure 2.2 shows the basic structure of a triglyceride.

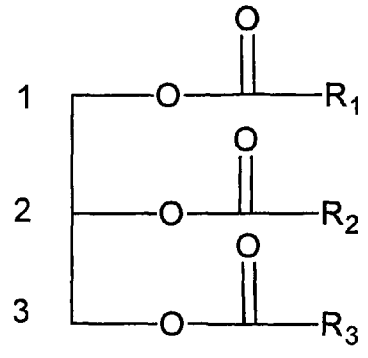

where: R = Fatty acids that can be attached at either the 1,3- (α) position, or the 2- (β) position of the glycerol backbone

Figure 2.2 - Structure of a triglyceride containing three different fatty acids

Fatty acids are sub-divided into:

- Saturated fatty acids, found predominantly in animal fats (e.g. stearic acid).
- Unsaturated fatty acids, found in plant and animal fats

The unsaturated fatty acids can be further sub-divided into:

- Monounsaturated fatty acids (MUFA), e.g. oleic acid
- Polyunsaturated fatty acids (PUFA), which the body requires but can not produce, e.g. linoleic acid

Triglycerides can be composed of up to three different fatty acids. The fatty acids attach either at the primary hydroxyl groups, 1 and 3 (α) or the secondary or central hydroxyl group, 2 (β) (Figure 2.2). The fatty acids account for 94 - 96% of the total weight of the triglyceride molecule and so they greatly influence the physical and chemical properties. As a result differences in fatty acid composition account for many of the observed differences between oils. Genetic variation of the plant, geographical, climatic, environmental and harvesting times and conditions can also affect the fatty acid composition of the oil. Comparisons of olive oil samples from Greece (1992-93 harvest) show how the fatty acid composition varies (Table 2.1) (Boskou, 1996).

Table 2.1 - Variation of fatty acid composition of oils within a harvest year

Fatty Acid	Minimum %	Maximum %	Mean %
Palmitic	7.9	12.3	10.5
Palmitoleic	0.5	0.9	0.6
Heptadecanoic	0.00	0.17	0.05
Heptadecenoic	0.04	0.29	0.09
Stearic	2.0	3.2	2.6
Oleic	68.8	82.8	76.9
Linoleic	4.6	14.5	7.5
Linolenic	0.5	0.9	0.6
Arachidic	0.3	0.6	0.4
Eicosenic	0.2	0.4	0.3

Table 2.2 characterises the fatty acid composition of some common fats and oils, including the oils used as adulterants in this study. Numerous studies have attempted to characterise the distribution of fatty acids in various oils. It was found in oilseed fats and olive oil that a high proportion (96 - 99%) of the acyl groups attached at the 2-position, on the glycerol backbone, consisted of oleic and/or linoleic acid. However, saturated

fatty acids, any other unsaturated acids or any excess of oleic and linoleic acids were found to be attached to the 1 and 3-positions (Swern, 1979; Vlahov, 1999).

Table 2.2 - % composition fatty acid profile of common fats and oils

Number of Carbon Atoms: Number of Double Bonds	Common Name of Fatty Acid	Butter	Olive	Corn	Soya	Sunflower	Sesame
4:0	Butyric	2.8-4.0	-	-	-	-	-
6:0	Caproic	1.4-3.0	-	-	-	-	-
8:0	Caprylic	0.5-1.7	-	-	-	-	-
10:0	Capric	1.7-3.2	-	-	-	-	-
12:0	Lauric	2.2-4.5	-	-	-	-	-
14:0	Myristic	5.4-14.6	-	Tr-1.7	Tr-0.5	⟨0.5	⟨0.5
16:0	Palmitic	26-41	7.5-20	8.0-12.0	7.0-11.0	3.0-10.0	7.0-12.0
16:1	Palmitoleic	6.1-11.2	0.5-3.0	⟨0.5	2.0-6.0	⟨1.0	⟨0.5
18:0	Stearic	1.2-2.4	0.5-5.0	Tr-0.2	0.3-3.0	1.0-10.0	3.5-6.0
18:1	Oleic	18.7-33.4	55.0-85.0	19.0-49.0	15.0-33.0	14.0-65.0	35.0-50.0
18:2	Linoleic	0.9-3.7	7-12.0	34.0-62.0	43.0-56.0	20.0-75.0	35.0-50.0
18:3	Linolenic	1.2	0.1-0.6	Tr	5.0-11.0	⟨0.7	⟨1.0
20:0–22:0	Arachidic, Behenic	0.8-3.0	0.1-0.8	Tr-0.2	0.3-3.0	0.5-1.0	0.5-1.0

Tr – Trace

Olive oil is high in unsaturated fatty acids and contains relatively small proportions of saturated fatty acids; palmitic acid (7.5 - 20%) and stearic acid (0.5 - 5%). The primary unsaturated fatty acids present in olive oil are oleic acid ($C_{17}H_{33}COOH$), linoleic acid ($C_{17}H_{31}COOH$) and linolenic acid ($C_{17}H_{29}COOH$). Oleic acid (monounsaturated) makes up 55 - 85% of olive oil, linoleic acid (polyunsaturated) makes up approximately 9% and linolenic acid (polyunsaturated) up 0 - 1.5%. Structures of these are shown in Figure 2.3. Naturally occuring fatty acids are generally *cis-* isomers. *Trans-* fatty acids occur because of incomplete hydrogenation reactions in the unsaturated fatty acids and degrade the oil quality, which is possibly linked to heart disease and arteriosclerosis (Li *et al.*, 2000).

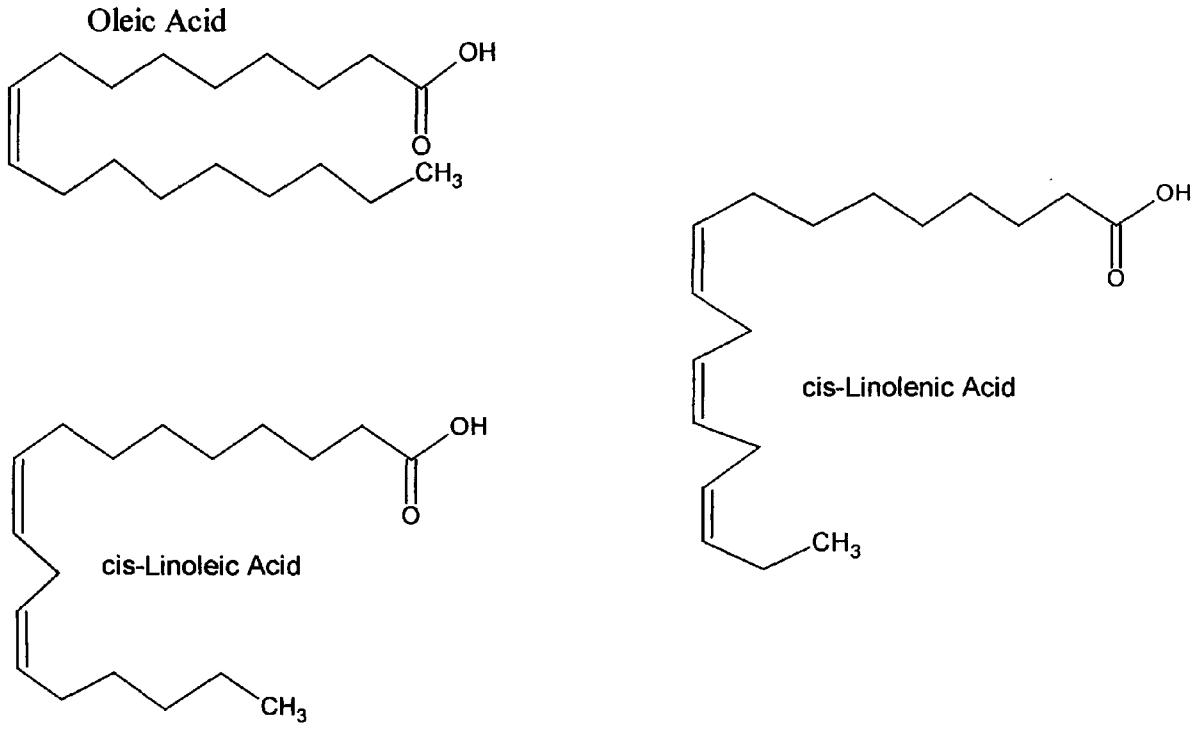

Figure 2.3 - Unsaturated fatty acid structures found in olive oil

The major constituents of olive oil are the triglyceride molecules. They constitute up to 98% of the olive oil matrix.

The remaining 2% of the matrix is made up of:

- phosphatides
- sterols
- triterpene alcohols and fatty alcohols
- hydrocarbons
- pigments
- phenolic compounds
- vitamins and minerals
- volatile and aroma compounds

2.3.1 Phosphatides

Phosphatides consist of a polyhydric alcohol, usually glycerol, which is esterified with phosphoric acid as well as fatty acids. The phosphoric acid is combined with nitrogen compounds such as choline. Lecithin and cephalin are two common phosphatides (Structures shown in Appendix A).

2.3.2 Sterols

Sterols are unsaponifiable alcohols which occur in fats and oils as esters of fatty acids. The most well known and abundant animal fat sterol is cholesterol. The sterols found in plant oils are called phytosterols.

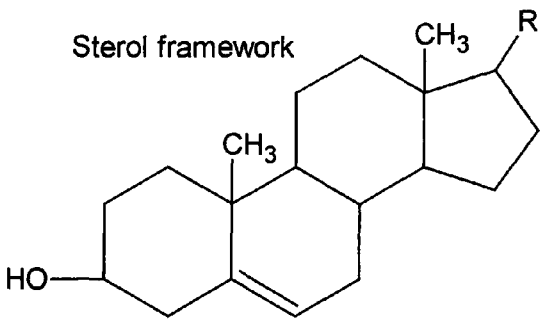

Figure 2.4 – Basic sterol framework structure

The phytosterols found in olive oil include:

β sitosterol where R = $CH(CH_3CH_2CH_2CH(C_2H_5)CH(CH_3)_2$,

campesterol where R = $CH(CH_3)CH{=}CHCH(CH_3)CH(CH_3)_2$,

avenasterol where R = $CH(CH_3)CH_2CH_2C{=}(CHCH_3)CH(CH_3)_2$,

stigmasterol where R = $CH(CH_3)CH{=}CHCH(C_2H_5)CH(CH_3)_2$.

(Swern, 1979)

2.3.3 Alcohols

Alcohols occur in fats and oils as triterpene alcohols and fatty alcohols. Fatty alcohols occur almost exclusively in marine oils. Triterpene alcohols occur in plants and consist of five condensed cyclohexane rings (Structures shown in Appendix A).

2.3.4 Hydrocarbons

Olive oil contains saturated and unsaturated hydrocarbons. The hydrocarbon content has been used to authenticate olive oil (Webster *et al.*, 1999) and the detection of hydrocarbons occupies several studies (Zamora *et al.*, 1994; Angerosa *et al.*, 1998). The most abundant hydrocarbon in olive oil is squalene, $C_{30}H_{50}$. It is an unsaturated triterpene and is an intermediate of the cholesterol biosynthesis pathway. The structure of squalene is shown in Figure 2.5. The amount of squalene in olive oil has been investigated using different analytical methods such as NMR (Zamora *et al.*, 1994), GLC (De Leonardis *et al.*, 1998) and HPLC (Owen *et al.*, 2000). It has been found to be an oxygen carrier and its antioxidant potential has been explored (Manzi *et al.*, 1998; Owen *et al.*, 2000), with encouraging results in its role to decrease the risk of various cancers in animals (Smith, 2000) by acting as a tumour inhibitor (Newmark, 1999).

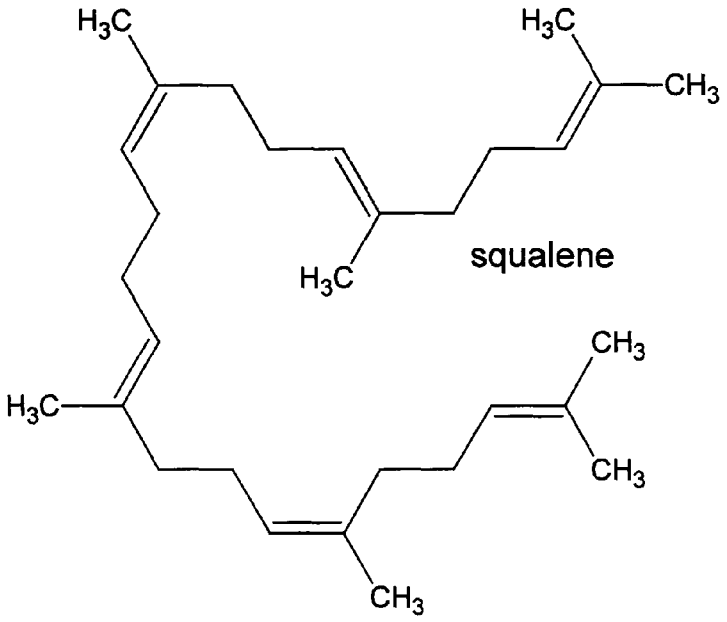

Figure 2.5 - Structure of squalene

2.3.5 Pigments

Pigments give oils their colour. The most obvious pigment in some olive oils is chlorophyll, which gives the characteristic green colour. Carotenoids are pigments, which give a yellow/red colour. The best known carotenoids are α, β and γ-carotenes. The carotenes are present in olive oil and β-carotene is the precursor of Vitamin A (Structures shown in Appendix A).

2.3.6 Phenolic compounds

Phenolic compounds in olive oil affect the stability and flavour of the oil. Various phenolic compounds in olive oil have been shown to display antioxidant properties. Antioxidants inhibit the oxidation of the triglycerides, which would result in rancidity. This increases the stability of the oil. Vegetable oils show greater stability than animal fats because of their increased levels of antioxidants. Tocopherols have been extracted from olive oil by supercritical fluid extraction (Ibanez *et al.*, 2000) and used to identify adulteration (Dionisi *et al.*, 1995; Lee *et al.*, 1998; Ibanez *et al.*, 2000). The tocopherol

content of olive oil is lower than other vegetable oils but the amount of other phenolic compounds is higher. Structures of the most abundant phenolic compounds found in olive oil that have been shown to exhibit antioxidant properties are shown in Figure 2.6.

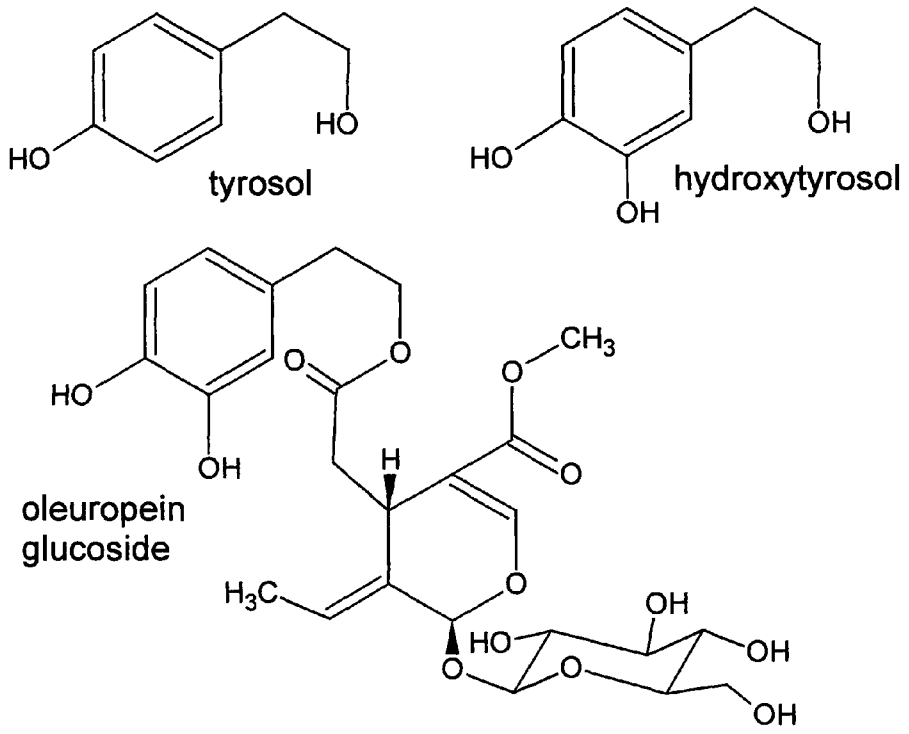

Figure 2.6 – Structures of phenolic antioxidants found in olive oil – tyrosol, hydroxytyrosol and oleuropein glucoside

Hydroxytyrosol and oleuropein have been shown to scavenge free radicals both *in vitro* and *ex vivo* (Visioli *et al.*, 1998). The biological importance of hydroxytyrosol as an antioxidant has also been looked at in terms of cancer prevention (Manna *et al.*, 1999). The removal of free radicals, including superoxide, by these compounds could explain the stability of olive oil compared with other vegetable oils.

The biophenol content of table olives has been studied using HPLC and proton NMR and the results used to characterise the olives by country of origin. The study found that oleuropein was present in larger quantities in olives originating in Italy and Greece than

in olives from Spain and Portugal. Hydroxytyrosol was consistently the major phenolic compound present in all the samples but Italian olives contain the highest percentage overall and Greek olives had significant quantities of tyrosol (Bastoni *et al.*, 2001).

A recent study isolated two phenolic compounds, not previously seen in olive oil, by HPLC, pinoresinol and 1-acetoxypinoresinol (Brenes *et al.*, 2000). The antioxidant capacity of olive oils has been investigated by measuring the oxygen radical absorbance capacity (ORAC) of the oils using spectrofluorimetry (Ninfali *et al.*, 2001) and was proposed as a new parameter to assess the quality and oxidative stability of extra virgin olive oils. Flavour analysis of different oils has been carried out by several researchers, with human tasting panels assigning characteristics to each oil (Servili *et al.*, 1995; Angerosa *et al.*, 1996; Aparicio *et al.*, 1996; Aparicio *et al.*, 1996; Aparicio *et al.*, 1997; Kiritsakis, 1998; Jelen *et al.*, 2000).

2.3.7 Vitamins and Minerals

Olive oil contains significant amounts of vitamin E (α-tocopherol) and provitamin A (carotene). The vitamin E content of olive oil has been shown to play an important role in health. Vitamin E is a natural anti-oxidant and the anti-oxidant properties of olive oil have been explored with encouraging results (Manzi *et al.*, 1998; Bradley, 1999; Galli *et al.*, 1999). It has also been linked as a possible contributing factor in cancer prevention (Lipworth *et al.*, 1997; Levi, 1999).

2.3.8 Volatile and Aroma Compounds

Several classes of volatile compounds in olive oil contribute to its aroma, including hydrocarbons, alcohols, aldehydes, esters, phenols and phenol derivatives, furan

derivatives and oxygenated terpenes. Several studies have attempted to characterise olive oils by their aroma (Morales *et al.*, 1995; Servili *et al.*, 1995; Angerosa *et al.*, 2000), assigning odour description to the volatile components. Fresh olive oil contains a relatively low amount of volatile compounds. In cold-pressed oil hexanal is the most abundant. The majority of volatiles are the products of degradation caused by oxidation of the fatty acids with increased storage time and temperature. The allyl groups in unsaturated fatty acids are highly susceptible to free radical reactions and will decompose, in the presence of oxygen, even at low temperatures. Saturated fatty acids are more stable at lower temperatures ($\langle 60^{\circ}C$) but oxidise at higher temperatures. Monohydroperoxides are formed, which in turn break down to form the aldehydes, ketones, acids, hydrocarbons, furanones and lactones. One study found that after 10 days storage 2-heptenal replaced hexanal as the most abundant volatile component in cold-pressed oil. Octanal and nonanal are the main volatiles derived from oleic acid, hexanal, 2-heptenal, 2-octenal and 2,4-decadienal derive from linoleic acid and 2,4-heptadienal, 2-pentenal and 3-hexenal are the main oxidation products of linolenic acid. Many of these oxidation products are responsible for the unsavoury sensory properties of oils. The presence of 2-hexenal and 4-heptenal have been found to give a green/grassy odour/flavour and they concluded that the samples with the least amount of volatiles were the most desirable oils according to a sensory panel (Jelen *et al.*, 2000). The rapid increase in aldehyde content, with storage at increased temperatures, paralleled the decrease in acceptability of the oils (Structures shown in Appendix A).

2.4 EARLY ANALYSIS OF OLIVE OIL

In the first half of the twentieth century extensive data were gathered from several European countries, to attempt to characterise virgin olive oil by physical properties such as density, refractive index and colour. Fluorescence in ultraviolet light was widely used but relied on colour interpretation and was subject to interference. The Bureau of Standards wrote an official report in 1927 in an attempt to persuade manufacturers and dealers to use the fluorescence methods to detect the addition of refined oil to virgin oil. It was claimed that down to 1% addition could be detected by this method. Refined oils show blue fluorescence whereas virgin oils show a range of colours from yellow to burnt sienna. A range of work was embarked upon to try and overcome the drawbacks of the method. Chlorophyll and carotenes masked the blue fluorescence of the refined oils. Some virgin oils also gave a slight blue fluorescence and the observed colour could alter with storage of virgin oil. Refined seed oils also vary in their fluorescence. Differences in absorption of ultraviolet light (UV) were studied in the 1920s and 30s and the resulting spectra were found to differ with virgin olive oil and refined oils or vegetable oils. The olive maturation at harvest also influenced the UV spectra obtained, as did the degree of oxidation resulting from heating and/or prolonged storage (Gracian, 1968).

Chemical properties such as free fatty acid content, saponification value, iodine value and the Bellier number have also been used to categorise olive oils. The Bellier number test originated in the late nineteenth century to detect groundnut oil and involved saponifying the oil, adding ethanol, acidifying at 16°C and observing the transparency of the solution. A clear precipitation or turbidity indicated the presence of groundnut oil. This test was used with slight variation for many years, the Bellier number being defined as the temperature at which the precipitation was initiated. The identification of

adulterants posed a greater problem, as the physical and chemical properties previously relied upon were of little value. Colour reactions were extensively used, the first being developed in 1842 by Heydenreich. It utilised the reaction of sulphuric acid with a small quantity of the oil under investigation. A few drops of the oil were added to a small quantity (2 or 3 ml) of sulphuric acid and left to stand without stirring. Olive oils, in general, kept their original colour turning slowly to bright yellow. Seed oils, other than groundnut and almond, gave immediate reddish colours of varying intensity. Several other colour reactions were developed and used intermittently throughout the early part of the twentieth century. Many reactions were developed for the detection of specific adulterant oils (Gracian, 1968). Thin-layer chromatography, gas chromatography and infrared spectroscopy gradually began to supersede initial methodologies during the 1940s, 50s and 60s. Infrared spectroscopy of lipids dates back to the beginning of the twentieth century when the spectra of fatty acids and vegetable oils appeared in the first compilation of IR spectra, published by Coblentz in 1905. IR has been used to determine the geometric configuration of double bonds, to study the autoxidation in lipids and, more recently, to detect adulteration of virgin olive oils (Ismail *et al.*, 1999). This led on to the more sophisticated methods of gas chromatography coupled to mass spectrometry (GC-MS), nuclear magnetic resonance (NMR) and high performance liquid chromatography (HPLC).

2.5 IMPORTANCE OF FATS IN THE HUMAN DIET

Fats are a vital source of energy. 25% of daily calorie intake should be from fats or oils in a balanced diet, less than 10% of which should be saturated fats. Fats provide energy, they form part of the membrane surrounding each cell and they are precursors of prostaglandins and other chemical messengers. Most of the fat needed by the body is produced from sugars and starch. However, polyunsaturated fats cannot be synthesised by the body and need to be introduced through diet. Linoleic and alpha-linolenic acids are essential fatty acids used by the body to produce omega-6 and omega-3 fatty acids respectively. These fatty acids (found mainly in oily fish) are thought to contribute to reducing the risk of heart disease (Sinclair, 2000). The main benefits attributed to consuming olive oil arise from its high content of monounsaturated fatty acids. It has been shown that these reduce the level of the 'bad' LDL cholesterol whilst having little effect on the 'good' HDL cholesterol. The reduction of LDL cholesterol reduces the risk of arteriosclerosis and cardiovascular diseases (Caruso *et al.*, 1999). Olive oil is more easily absorbed in the body than other oils because of its unsaturated fatty acid composition. It facilitates the transfer within the body of fat-soluble vitamins, which aid bone growth, essential for child development. Lack of fat in a diet causes deficiency of vitamins A, D, E and K, as these vitamins are only soluble in fat.

2.6 SAMPLE SET ORIGIN

A unique sample set was obtained directly from Greece that consisted of olive oil from three consecutive harvests, 1994/95, 1995/96 and 1996/97. Each harvest was given a sample code letter (D, E and F respectively). Within each harvest oils from various

districts of Greece were represented including oils from Crete. Extra virgin olive oil and other vegetable oils used for the optimisation and investigations using SFE and SPME were obtained from a high street retailer (Tesco).

2.6.1 Maps

The maps below (Figures 2.7 and 2.8) show the geographical detail of sample sets.

2.6.2 Sample set information

The origins of each oil, the harvest conditions and degree of ripeness of the harvested olives are shown in the following tables. Information on the D set can be found in Table 2.3, information on the E set can be found in Tables 2.4 and 2.5 and information on the F set in Tables 2.6 and 2.7.

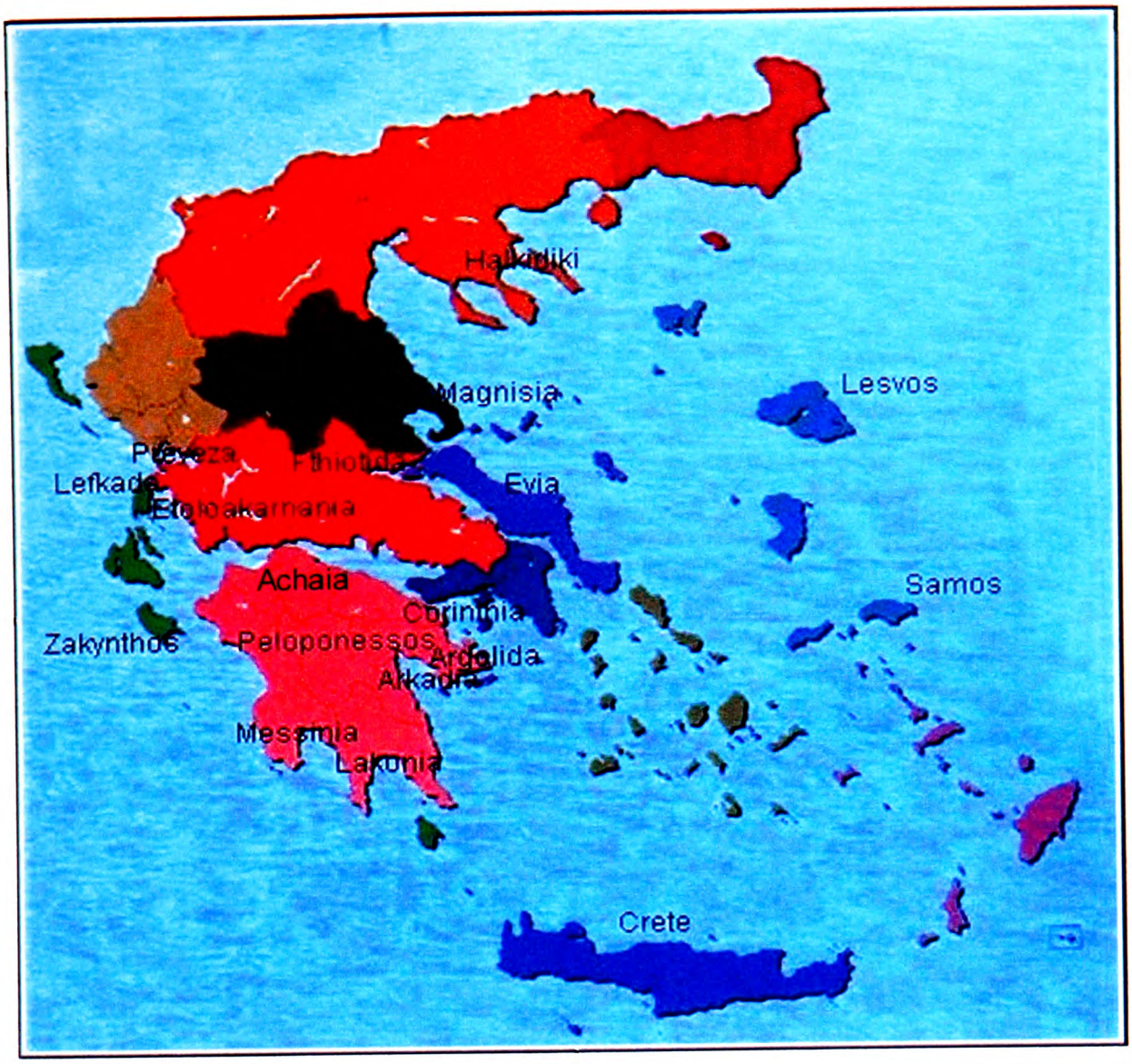

Figure 2.7 – Map of Greece showing geographical origins of oil samples

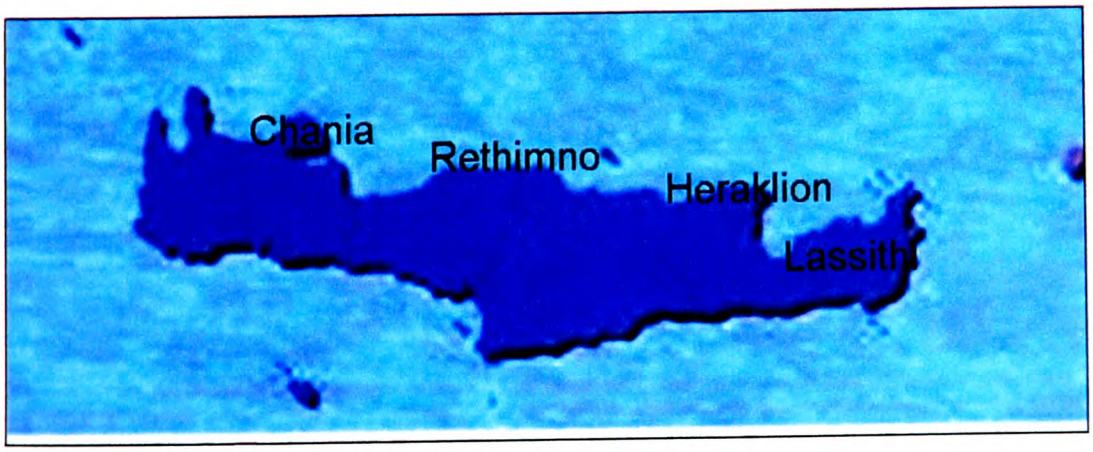

Figure 2.8 - Map of Crete showing specific districts

Table 2.3 - D set, Sample Information 1994/95 harvest (D1-D22)

Sample code	Sample origin		Altitute	Variety of olive	Degree of ripeness
	Area	*District*			
D1	Crete	Chania	Mid-mountain	Koroneiki	Semi-ripe
D2	Crete	Chania	Plain	Koroneiki	Semi-ripe
D3	Crete	Chania	Plain	Koroneiki	Ripe
D4	Crete	Heraklion	Mid-mountain	Koroneiki	Ripe
D5	Crete	Lassithi	Mid-mountain	Koroneiki	Ripe
D6	Crete	Lassithi	Mid-mountain	Koroneiki	Ripe
D7	Crete	Argolida	Mid-mountain	Tsounati 40%	Ripe
D8	Peloponessos	Corinthia	Mid-mountain	Patrini	Semi-ripe
D9	Peloponessos	Lakonia	Mid-mountain	Koroneiki 50%	Ripe
D10	Peloponessos	Lakonia	Mid-mountain	Koroneiki 40%	Ripe
D11	Peloponessos	Lakonia	Mid-mountain	Koroneiki	
D12	Peloponessos	Ilia	Mid-mountain	Botsikoelia	Ripe
D13	Peloponessos	Ilia	Mid-mountain	Koroneiki	Ripe
D14	Peloponessos	Messinia	Plain	Koroneiki	Ripe
D15	Peloponessos	Messinia	Mid-mountain	Koroneiki	Ripe
D16	Peloponessos	Messinia	Mid-mountain	Koroneiki	Ripe
D17	Peloponessos	Messinia	Plain	Koroneiki	Ripe
D18	Peloponessos	Messinia	Plain	Koroneiki	Ripe
D19	Evia Island	Evia	Mid-mountain	Chondrolia, Amphissa	Unripe
D20	Central	Ftiotida	Mid-mountain	Amphissa, Megaritikes	Semi-ripe
D21	Ionian	Kefalinia	Mountain	Koroneiki, Ordinaria	Ripe
D22	Ionian	Zakynthos	Mid-mountain	Koroneiki	Ripe

Table 2.4 - E set, Sample Information 1995/96 harvest (E1-E31)

Sample code	Sample origin			Altitute	Variety of olive	Degree of ripeness
	Area	*District*	*Village*			
E1	Crete	Chania	Cabanl Kldonius	Mountain	Koroneiki	Ripe
E2	Crete	Chania	Colbari Chisamou	Plain	Koroneiki	Ripe
E3	Crete	Chania	Patsianos Sfachion	Mid-mountain	Koroneiki	Ripe
E4	Crete	Chania	Katyves Apokoronou (Vamos)	Plain	Koroneiki	Ripe
E5	Crete	Rethimno	Fourfouras Amariou	Mountain	Chondrolia	Ripe
E6	Crete	Rethimno	Panormo Milopotamou	Mid-mountain	Koroneiki	Ripe
E7	Crete	Heraklion	Gergeni Kenourgiou	Mid-mountain	Chondrolia	Ripe
E8	Crete	Heraklion	Archanes Temenous	Plain	Koroneiki	Ripe
E9	Crete	Heraklion	Ebaros Pediados	Plain	Koroneiki	Ripe
E10	Crete	Heraklion	Vagioria Monofatsiou	Mid-mountain	Koroneiki	Ripe
E11	Crete	Heraklion	Arkalochori Monofatsiou	Mid-mountain	Koroneiki	Ripe
E12	Crete	Heraklion	Ligortinos Monofatsiou	Mid-mountain	Koroneiki	Ripe
E13	Crete	Lassithi	Latsida Meramvelou	Plain	Koroneiki	Ripe
E14	Crete	Lassithi	Vraxasi Meramvelou	Mid-mountain	Koroneiki	Ripe
E15	Crete	Lassithi	Ierepetra	Mid-mountain	Koroneiki	Ripe
E16	Crete	Lassithi	Ano Zarkos Sitias	Mid-mountain	Koroneiki	Ripe
E17	Crete	Lassithi	Lithines Sitias	Mid-mountain	Koroneiki	Ripe
E18	Crete	Lassithi	Cavousi Lerapetras	Mid-mountain	Koroneiki	Ripe
E19	Peloponessos	Achaia	Marmara	Mid-mountain	Koroneiki	Unripe
E20	Peloponessos	Corinthia	Pitsa	Mid-mountain	Chondrolia, Manaki, Megaritikes	Unripe
E21	Peloponessos	Argolida	Pirgiotica Nafpliou	Mid-mountain	Manaki, Chondrolia	Unripe
E22	Peloponessos	Argolida	Koutsopodi	Mid-mountain	Chondrolia	Ripe
E23	Peloponessos	Arkadia	Doliana	Mid-mountain	Manaki	Semi-ripe
E24	Peloponessos	Lakonia	Melana	Mountain	Athinolia	Semi-ripe
E25	Peloponessos	Lakonia	Xirocabi	Mid-mountain	Koroneiki 20%, Athinolia 80%	
E26	Peloponessos	Lakonia	Goritsa	Mid-mountain	Koutsourclia	Ripe
E27	Peloponessos	Lakonia	Geraki	Mid-mountain	Kalamon 50%, Asprolia 50%	
E28	Peloponessos	Lakonia	Vlacniotis	Plain	Koroneiki	
E29	Peloponessos	Lakonia	Molai	Mid-mountain	Athinolia	Ripe
E30	Peloponessos	Lakonia	Nomia Monemvasias		Koroneiki 95%, Athinolia	
E31	Peloponessos	Lakonia	Vellies	Mid-mountain	Koroneiki	Semi-ripe

Table 2.5 - E set, Sample Information 1995/96 harvest (E32-E65)

Sample code	Sample origin			Altitute	Variety of olive	Degree of ripeness
	Area	*District*	*Village*			
E32	Peloponessos	Messinia	Stavropigio	Mountain	Koroneiki	Semi-ripe
E33	Peloponessos	Messinia	Androusa	Plain	Koroneiki	Semi-ripe
E34	Peloponessos	Messinia	Messini	Plain	Koroneiki	Semi-ripe
E35	Peloponessos	Messinia	Petalldi	Flat	Koroneiki	Ripe
E36	Peloponessos	Messinia	Chora Trifillias	Mid-mountain	Koroneiki	Ripe
E37	Peloponessos	Messinia	Gargaliani	Plain	Koroneiki	Unripe
E38	Peloponessos	Messinia	Filiafra	Plain	Koroneiki	Unripe
E39	Peloponessos	Messinia	Mili Kiparisias	Mid-mountain	Koroneiki	Unripe+Semi-ripe
E40	Peloponessos	Ilia	Geraki Amallados	Mid-mountain	Koroneiki	Ripe
E41	Peloponessos	Ilia	Varvaseina	Mid-mountain	Koroneiki	Semi-ripe
E42	Peloponessos	Ilia	Zacharo	Mid-mountain	Koroneiki	Ripe
E43	Peloponessos	Ilia	Gianistochori	Mid-mountain	Koroneiki	Over-ripe
E44	Peloponessos	Ilia	Krestena	Mid-mountain	Koroneiki	Semi-ripe
E45	Peloponessos	Achaia	Psathopirgos	Plain	Koroneiki 25%, Chondrolia 75%	Semi-ripe
E46	Peloponessos	Achaia	Eghira	Mid-mountain	Koroneiki	Unripe
E47	West Hellas	Etolnia	Nafpaktos	Mountain	Koroneiki, Chondrolia	Unripe
E48	West Hellas	Etolnia		Mid-mountain	Chondrolia	Semi-ripe
E49	Evia Island	Evia	Castella Psachnon	Mid-mountain	Chondrolia, Throumba	Ripe
E50	Evia Island	Evia	Kechries	Mid-mountain	Kalamon, amfissis	Semi-ripe
E51	Central Hellas	Fthiotida	Atalarili	Mid-mountain	Amfissis	Semi-ripe
E52	Central Hellas	Fthiotida	Karavomilos Stilidas	Mid-mountain	Amfissis	Semi-ripe
E53	Central Hellas	Magnisia	Agria (Vroxia, Ag Lavrentis)	Mid-mountain	Amfissis	Semi-ripe
E54	Central Hellas	Magnisia	Almiros	Plain	Amfissis, Piliou	Semi-ripe
E55	Ionian Islands	Lefkada		Mid-mountain	Llanolia	Semi-ripe
E56	West Hellas	Preveza		Mid-mountain	Chondrolia	Semi-ripe
E57	Ionian Islands	Zakynthos	Argasi	Mid-mountain	Koroneiki	Semi-ripe
E58	Ionian Islands	Zakynthos	Gaitani	Mountain	Koroneiki	Semi-ripe
E59	Aegean Islands	Lesvos	Kato Tritos	Mid-mountain	Adramatianes	Semi-ripe
E60	Aegean Islands	Lesvos	Plagia Plomariou	Mid-mountain	Kolovi	Ripe
E61	North Hellas	Chalkidiki	Ormilia	Mid-mountain	Chondrolia	Unripe
E62	North Hellas	Chalkidiki	Vrastama		Chondrolia	
E63	North Hellas	Chalkidiki	Polighiros		Chondrolia	
E64	Aegean Islands	Samos	Mili	Mid-mountain	Koron, Chondr, Throumbalia	Unripe, Semi-ripe
E65	Aegean Islands	Samos	Mitilinii	Mid-mountain	Koron, Chondr, Tsounari	

Table 2.6 - F set, Sample Information 1996/97 harvest (F1-F34)

Sample code	Sample origin			Altitute	Variety of olive	Degree of ripeness
	Area	*District*	*Village*			
F1	Crete	Chania	Sternes Kidonias	Mountain	Koroneiki	Unripe
F2	Crete	Chania	Malame Kidonias	Mid-mountain	Koroneiki	Semi-ripe
F3	Crete	Chania	Voukolles Chisamou	Mid-mountain	Koroneiki	Semi-ripe
F4	Crete	Chania	Potamida Chisamou	Plain	Koroneiki	Semi-ripe
F5	Crete	Chania	Galatas Kidonias	Plain	Tsounati	Unripe
F6	Crete	Rethimno	Episkopi Rethimnis	Mid-mountain	Koroneiki	Semi-ripe
F7	Crete	Chania	Kalives Apokoronou	Plain	Koroneiki	Semi-ripe
F8	Crete	Heraklion	Archanes Temenous	Mountain	Koroneiki	Unripe
F9	Crete	Heraklion	Kastelli Pediados	Mid-mountain	Koroneiki	Semi-ripe
F10	Crete	Heraklion	Episkopi Pediados	Plain	Koroneiki	Ripe
F11	Crete	Heraklion	Avdou Pediados	Mid-mountain	Koroneiki	Ripe
F12	Crete	Heraklion	Meshorio Monofatsiou	Mid-mountain	Koroneiki	Ripe
F13	Crete	Heraklion	Arkalohori Monofatsiou	Mid-mountain	Koroneiki	Ripe
F14	Crete	Heraklion	Protaria Monofatsiou	Plain	Koroneiki	Semi-ripe
F15	Crete	Lassithi	Houmeriako Meramvelou	Plain	Koroneiki	Ripe
F16	Crete	Lassithi	Vrahassi Meramvelou	Plain	Koroneiki	Semi-ripe
F17	Crete	Heraklion	Ano Vianos	Mid-mountain	Koroneiki	Semi-ripe
F18	Crete	Lassithi	Nea Malla Ierapetras	Mid-mountain	Koroneiki	Semi-ripe
F19	Crete	Lassithi	Krista Meramvelou	Mid-mountain	Koroneiki	Unripe
F20	Crete	Lassithi	Lithines Sitias	Mid-mountain	Koroneiki	Ripe
F21	Crete	Lassithi	Kavoussi Ierapetras	Mid-mountain	Koroneiki	Ripe
F22	Crete	Lassithi	Exo Mouliana Cooperation	Mountain	Koroneiki	Ripe
F23	Peloponessos	Korinthia	Kiato	Plain	Psilolia Patrini	Semi-ripe
F24	Peloponessos	Korinthia	Kamari	Mid-mountain	Koroneiki	Semi-ripe
F25	Peloponessos	Korinthia	Pitsa	Plain	Petrines	Semi-ripe
F26	Peloponessos	Korinthia	Athikia	Mid-mountain	Manaki	Ripe
F27	Peloponessos	Argolida	Didima	Mid-mountain	Manaki	
F28	Peloponessos	Argolida	Koutsopodi	Mid-mountain	Manaki	Ripe
F29	Peloponessos	Arkadia	Astros	Plain	Ladolia	Ripe
F30	Peloponessos	Lakonia	Pelena	Mid-mountain	Athinolia	Semi-ripe
F31	Peloponessos	Lakonia	Skoura	Mid-mountain	Koutsourolia	Ripe
F32	Peloponessos	Lakonia	Krokees	Mid-mountain	Koroneiki	Ripe
F33	Peloponessos	Lakonia	Githio	Mid-mountain	Koroneiki	Ripe
F34	Peloponessos	Lakonia	Platana	Mountain	Koutsourolia	

Table 2.7 - F set, Sample Information 1996/97 harvest (F35-F65)

Sample Code	Sample origin			Altitute	Variety of olive	Degree of ripeness
	Area	*District*	*Village*			
F35	Peloponessos	Lakonia	Vlaniotis	Mid-mountain	Tsounati or Manaki	Semi-ripe
F36	Peloponessos	Lakonia	Glikovrissi	Mid-mountain	Tsounati or Manaki	Semi-ripe
F37	Peloponessos	Lakonia	Apidia	Mid-mountain	Koroneiki	Semi-ripe
F38	Peloponessos	Messinia	Neohoriou Lefktro	Plain	Koroneiki	Over-ripe
F39	Peloponessos	Messinia	Androussa	Mid-mountain	Koroneiki	Semi-ripe
F40	Peloponessos	Messinia	Messini	Mid-mountain	Koroneiki	Ripe
F41	Peloponessos	Messinia	Diavolitsi	Mid-mountain	Koroneiki	Semi-ripe
F42	Peloponessos	Messinia	Lampaina	Plain/Mountain	Koroneiki	Over-ripe
F43	Peloponessos	Messinia	Romanou Pilias	Plain	Koroneiki	Over-ripe
F44	Peloponessos	Messinia	Loggas	Plain	Koroneiki	Ripe
F45	Peloponessos	Messinia	Adriani	Mountain	Koroneiki	Ripe
F46	Peloponessos	Messinia	Gargaliani	Plain	Koroneiki	Ripe
F47	Peloponessos	Messinia	Fillatra	Plain	Koroneiki	Ripe
F48	Peloponessos	Messinia	Fillatra	Plain	Koroneiki	Ripe
F49	Peloponessos	Messinia	Mili Kiparissias	Plain	Koroneiki	Over-ripe
F50	Peloponessos	Messinia	Kopananki	Mid-mountain	Koroneiki	Semi-ripe
F51	Peloponessos	Ilia	Varvasaina	Mid-mountain	Koroneiki	Over-ripe
F52	Peloponessos	Ilia	Elea	Plain	Koroneiki	Semi-ripe
F53	Peloponessos	Achaia	Ziria	Mid-mountain	Chondrolia	Semi-ripe
F54	Peloponessos	Achaia	Exo Agia	Plain	Chondrolia 80%, Psilolia 20%	Ripe
F55	Evia Islands	Evia	Politika	Mid-mountain	Chondrolia 80%, Koroneiki 20%	Semi-ripe
F56	Evia Islands	Evia	Eretria	Mid-mountain	Ladolia 70%, Tsounati 30%	Semi-ripe
F57	Ionian Islands	Zakynthos	Argasi	Mid-mountain	Koroneiki	Rpe
F58	Aegean Islands	Rodos	Archaggelos	Mid-mountain	Chondrolia	Semi-ripe
F59	Aegean Islands	Lesvos	Keramia	Mid-mountain	Kolovl 80%, Andramitiani 20%	Semi-ripe
F60	Aegean Islands	Lesvos	Polihnitos	Mid-mountain	Adramatiani	Ripe
F61	Aegean Islands	Lesvos	Plagia Plomariou	Mountain	Kolovl	Semi-ripe
F62	Aegean Islands	Lesvos	Kato Tritos	Mid-mountain	Kolovl	Semi-ripe
F63	Aegean Islands	Lesvos	Lpplios	Mid-mountain	Kolovl	Ripe
F64	North Hellas	Chalkidiki	Poligyros	Mountain	Chondrolia	Unripe
F65	North Hellas	Chalkidiki	Ormilia	Mid-mountain	Chondrolia	

CHAPTER 3

3 Multivariate Analysis

3.1 THEORY AND TECHNIQUE

Multivariate analysis is an area of chemometrics, which is the application of modern statistical methods such as experimental design, calibration, pattern recognition and signal analysis to chemical data. Most chemical measurements are multivariate, i.e. more than one measurement can be made on a sample. For example, a spectrum scanned at hundreds of wavelengths is multivariate, whereas a spectrum scanned at a single wavelength is univariate (contains only one measurement).

There are many multivariate methods, some of which are appropriate to this study and include:

- Principal Components Analysis (PCA)
- Soft Independent Modelling of Class Analogy (SIMCA)
- Cluster Analysis
- Regression Methods:

  Multiple Linear Regression (MLR)

  Partial Least Squares Regression (PLS)

  Principal Components Regression (PCR)

Multivariate analysis will provide a powerful tool to analyse and classify the olive oil samples used in this work. Cluster analysis will offer initial insight into whether the oil samples can be differentiated on the basis of geographical origin and harvest year. PCA of the data can then produce models specific to oils from a certain area/year and SIMCA

results in the form of Cooman's plots will give a visual representation of the sample-to-model distance. Additional results from SIMCA will also give information on which spectroscopic variables are important to the model and how well specific variables discriminate between the two models, giving opportunity to discover which peaks are responsible (in NMR and IR) for the differences in geographical/year of origin.

Regression techniques will be used to characterise pure olive oil samples compared to olive oil adulterated with vegetable oil. Depending on the robustness of the resulting models, adulteration prediction can be attempted using PLS1 to determine the lowest level of adulteration that can be detected with confidence and reproducibility.

3.1.1 Principal Components Analysis (PCA)

PCA is a projection method which investigates in what respect samples differ from each other, which variables contribute most to this difference and the extent to which the variables are correlated. It also detects any patterns present in the data, which allows sample grouping. PCA forms the basis for other multivariate methods, regression (PLS/PCR) and classification methods (SIMCA). PCA reduces and therefore simplifies the dimensionality of the data set while retaining its information content (Adams, 1995).

The linear combinations of the initial variables that contribute most to the difference between the samples are called Principal Components (PCs). They are computed so that the first PC carries the most explained variance, the second PC carries the maximum share of the residual variance not taken into account by the first PC, and so on. The first PCs therefore contain the most valuable information and so carry a higher ranking, the latter PCs contain little information of value and large proportions of noise. PCA rotates

and transforms the original axes, in which each represent an original variable, into new axes, which are orthogonal (i.e. new variables are uncorrelated). PCA, like other methods of multivariate analysis, calibrates and validates results in the computation of each model component (PC). Calibration finds the new component and validation checks whether the component describes the new data well. The resulting graphs produced by PCA give information on three sets of attributes, variances, loadings and scores.

3.1.1.1 Variances

Variances are error measurements and express the importance of a principal component. Residual variance shows how much variation in the data remains to be explained after taking into account the current PC. It is expressed as the mean square of its residuals for all model components. Sample residuals are defined as the difference between the original location of a data point and its location after projection on to the model. The total residual variance shows the overall modelling error over all variables. Explained variance is a measurement of the proportion of variation in the data accounted for by the current PC. It is also computed as the mean square variation and the total explained variance measures the proportion of the original variation in the data that is described by the model. Both forms of variance therefore show how well the model fits the data. Most of the variation in the data can be explained if the model has a total residual variance close to 0 or a total explained variance close to 100%. Figure 3.1 shows an example of a residual variance plot where the green line shows the variance in the validation set and the red line the calibration set variance. The residual variance in the calibration set after the first PC is 0.22%, PC 2 explains a further proportion of the

variance as do PCs 3 and 4 until after PC 5 virtually all the variance has been accounted for in the calibration set.

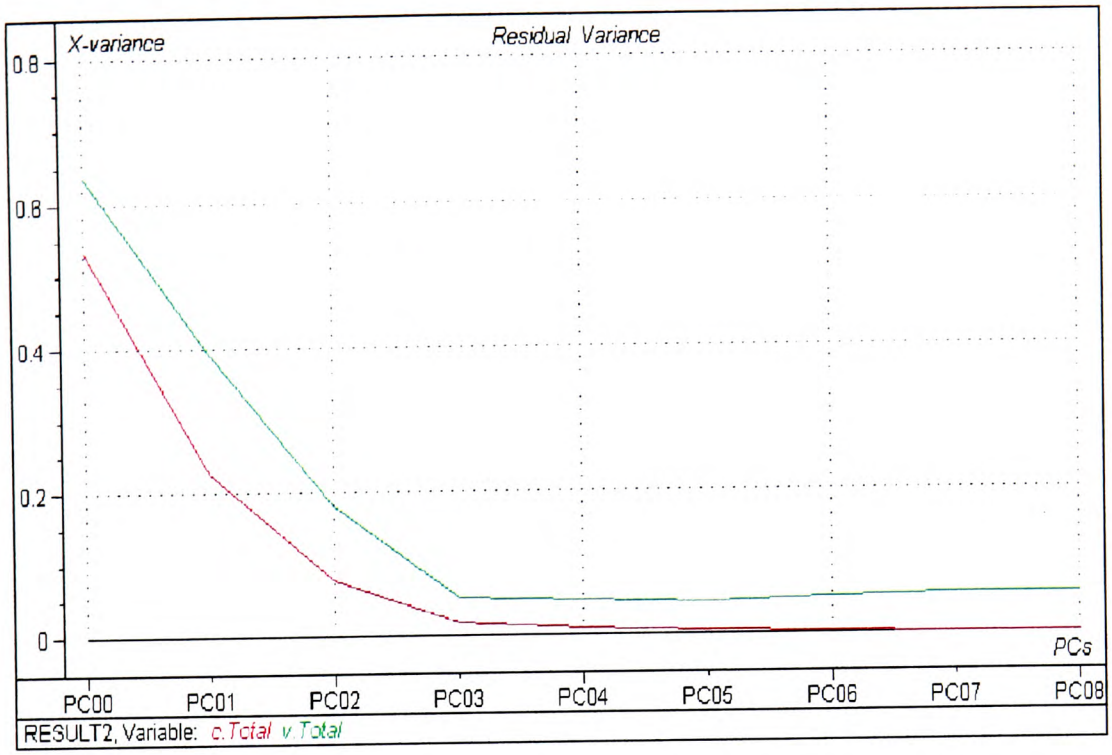

Figure 3.1 – Example of a PCA plot of residual variance for validation and calibration sets

Models where the residual variance does not go to zero with the minimum number of components, suggests the presence of large amounts of noise within the data. The presence of outliers is another possible reason for a large residual variance. Outliers are measurements which appear significantly different to other samples and detrimentally influence the model.

3.1.1.2 Loadings

Loadings describe the relationships between variables. Each variable has a loading on a PC and it shows how much the variable contributes to the particular PC and how well the PC accounts for the variation of the variable over the data points. It is the cosine of the angle between the variable and the particular PC. Loadings range between –1 and +1.

The higher the correlation between the variable and the PC, the higher the loading. If variables have high loadings along the same PC it means they are highly correlated with that PC. The following examples, using jam characteristics, are all taken from tutorials in the Unscrambler manual (Camo, 1998).

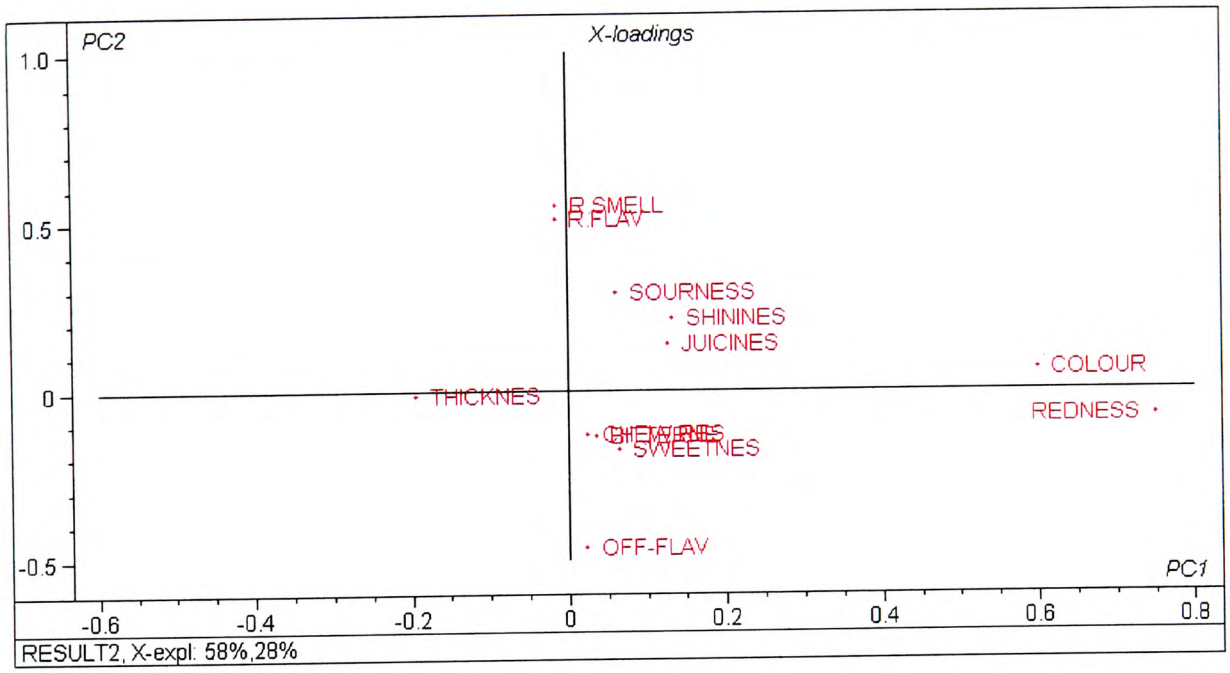

Figure 3.2 - Example of a loading plot of the sensory characteristics of jam samples

Figure 3.2 shows an example loadings plot for the first two principal components, where redness and colour (of jams) are close together (on the right of the plot) with a relatively high loading along PC 1 (x axis). This shows that redness and colour are positively correlated with each other and are described by the first PC.

The second PC (y axis) separates off-flavour (negative loading) from raspberry smell and flavour (positive loadings). Raspberry smell and raspberry flavour are positively correlated with each other and appear at the top of the plot. Cross referencing with the scores plots would indicate that the further up the scores plot the samples (on the second PC), the more the samples would have a raspberry smell and flavour (Figure 3.3).

3.1.1.3 Scores

Scores describe the properties of the samples and show differences or similarities in sample patterns. Each sample has a score on each PC, it shows the sample location along that PC and describes the major features of the sample. Samples with similar scores along the same PC are similar and vice versa. Scores, like loadings, can have positive or negative values. If the loading of a variable and the score of a sample on a PC have the same sign, the sample has a higher than average value for that variable and the larger the loadings and scores the stronger the relationship.

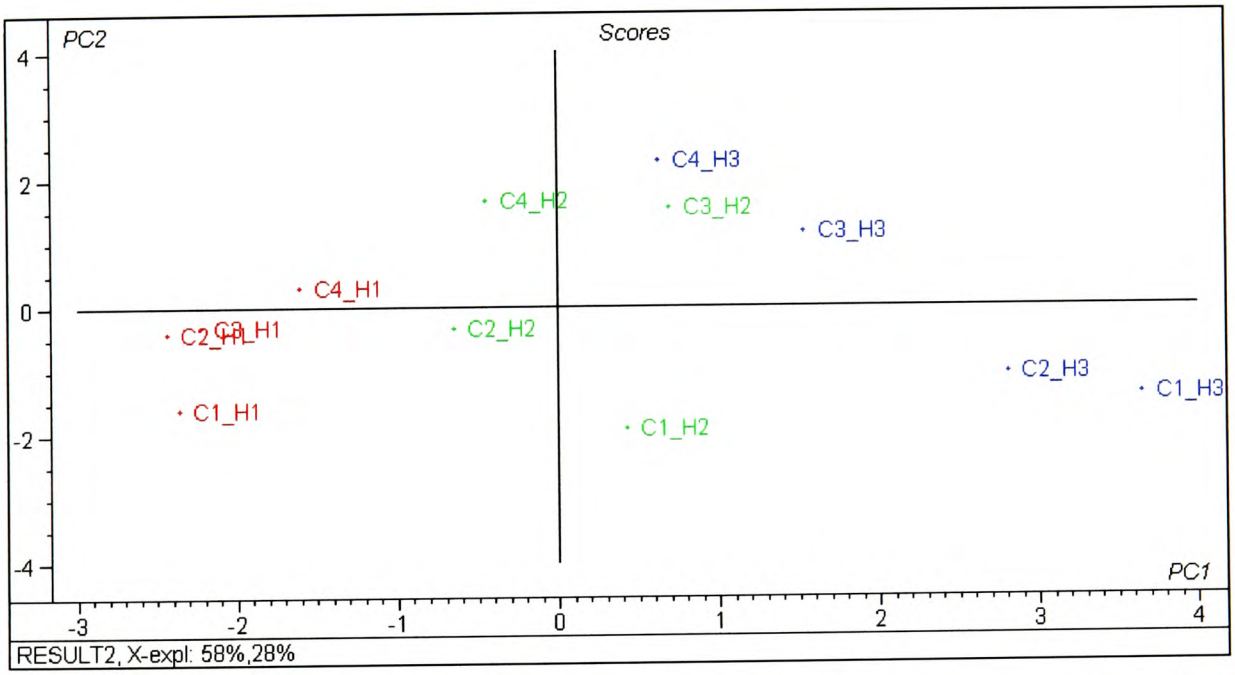

Figure 3.3 - Scores plot of jam fruit by harvest time (H) and cultivar (C).

Figure 3.3 shows an example of a scores plot using jam samples from different fruit cultivars, (C1-C4), harvested at different times, (H1-H3). Sensory qualities (Figure 3.2) were evaluated and compared to spectroscopic data (Camo, 1998). The scores plot (Figure 3.3) shows sample grouping along the first PC by harvest time (first harvest - red, second harvest – green, latest harvest – blue) therefore, the first PC describes characteristics found between fruit picked at different times. The second PC describes

the differences encountered due to differing cultivars, with the C4 samples at the top of the plot, moving down to the C1 samples at the bottom.

The loadings (Figure 3.2) and scores (Figure 3.3) plots can be combined, as samples that appear in a specific area of the scores plot have much of the properties of the variables in the same area of the loadings plot, to give valuable information. For example, C1H3 and C2H3 samples both have relatively high positive scores and appear in a similar area of the plot as strong redness and colour intensity along the first PC in the loadings plot. Therefore, these two samples would be expected to have strong colour intensity. C4H3 and C4H2 have a positive score along the second PC, which from the loadings plot (Figure 3.3) differentiates between raspberry smell and flavour (positive loading) and off-flavours (negative loading). C4H3 and C4H2 would therefore, be expected to have a more characteristic raspberry smell and flavour than C1H2 which has a negative score along the second PC.

3.1.2 Soft Independent Modelling of Class Analogy (SIMCA)

SIMCA is a classification method which makes a PCA model for each class in a training set (samples on which the calibration is based). It then compares unknown samples and places them in corresponding classes to establish whether they fit the model in the particular class. Each class requires a PCA model (mathematical equation summarising the variations in a data set arising from principal component analysis) which, therefore, requires that sufficient samples are present for each distinct class and that there are enough variables to describe accurately the samples. Provided the classes do not overlap significantly, unknown samples can be fitted to each model or left as unclassified. PCR

or PLS models can also be used for SIMCA classification where only the X part (e.g. spectroscopic data) of the model is used.

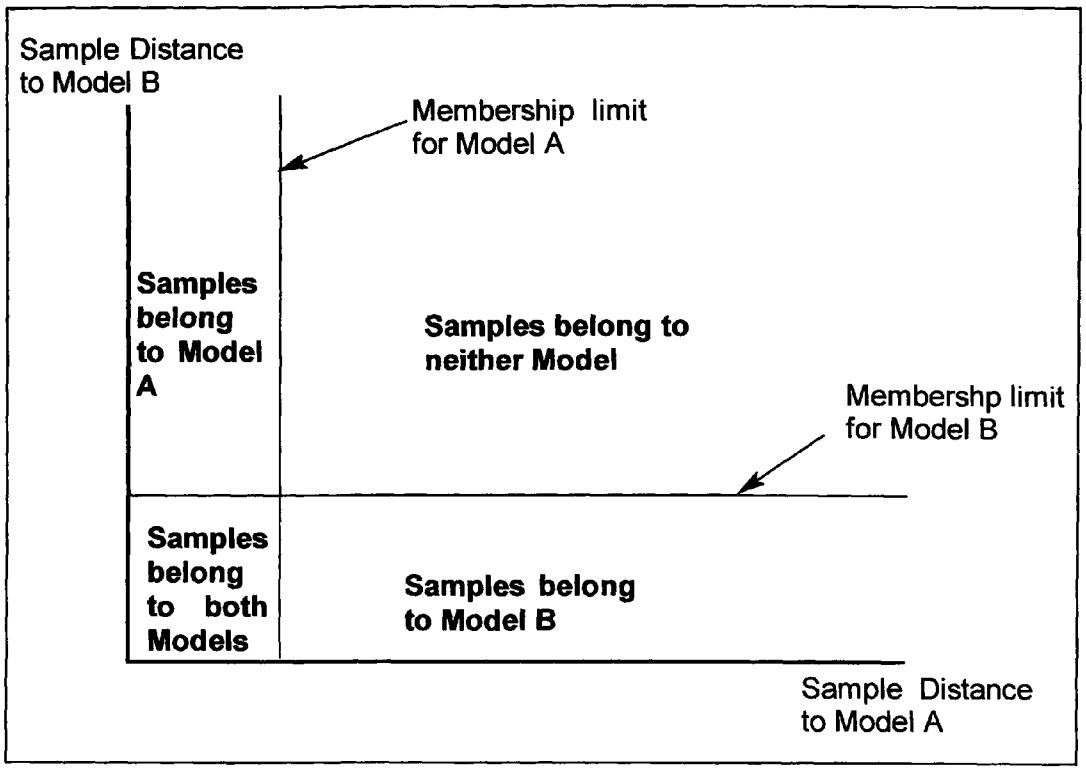

Figure 3.4 – Explanation of a Cooman's Plot

A Cooman's Plot (Figure 3.4) gives graphical representation of the orthogonal distances from samples to two different classes (models). Samples that fall within the membership limit of a class can be said to belong to that class. Samples which appear in the bottom left area of the plot are doubly classified as belonging to both models and satisfactory classification has not been achieved.

3.1.3 Cluster Analysis

Cluster analysis arranges groups of similar samples into clusters by means of different classification algorithms. It is often the first method of data analysis employed to explore the diversity in a data set and to determine whether patterns exist within the data.

Hierarchical clustering starts with each object (e.g. an oil sample) in its own cluster and sequentially links clusters of similar samples until large clusters of increasing dissimliar samples are aggregated. The visual representation of this type of clustering is usually a dendrogram which show the clusters being combined and the values of the distance coefficients between each group. The actual distances are rescaled to between 0 and 25 and connected vertical lines designate clustered samples. There are several forms of linkage and ways to describe distance measurements between samples. Ward's method of creating clusters uses analysis of variance to evaluate the distance between groups and minimises the sum of the squares of any two clusters that could be hypothetically formed at each stage. Ward's method is regarded as a very efficient method of linkage (StatSoft, 2001). The distance between two samples in multidimensional space is used as a measure of their dissimilarity and the squared Euclidean distance is the sum of the squared differences between the values for the samples (Ooyen, 2001). This is the most commonly used type of distance measurement.

3.1.4 Regression Methods

Regression methods are used to try to fit a model to observed data to quantify the relationship between two data matrices relating to groups of variables, X (spectroscopic measurements) and Y (percentage composition of oil mixture). The model is then used to describe the relationship and to predict new values. The model is constructed involving the two data matrices X and Y and tries to predict the variations in the Y variables from the variation in the X variables by building the model so that $Y = f(X)$.

3.1.4.1 Partial Least Squares Regression (PLS)

PLS is a projection method similar to PCA in that the first PC in a model carries the largest amount of information, followed by the second PC etc. PLS models the X and Y matrices concurrently to find latent variables (variables derived from measured variables e.g. PCs) in X that will best predict the latent variables in Y (Livingstone, 1995). There are two applications of PLS:

- PLS1 uses one response variable (i.e. measured output variables that describe the outcome of the experiments, e.g. % adulteration) at a time
- PLS2 can handle several response variables simultaneously

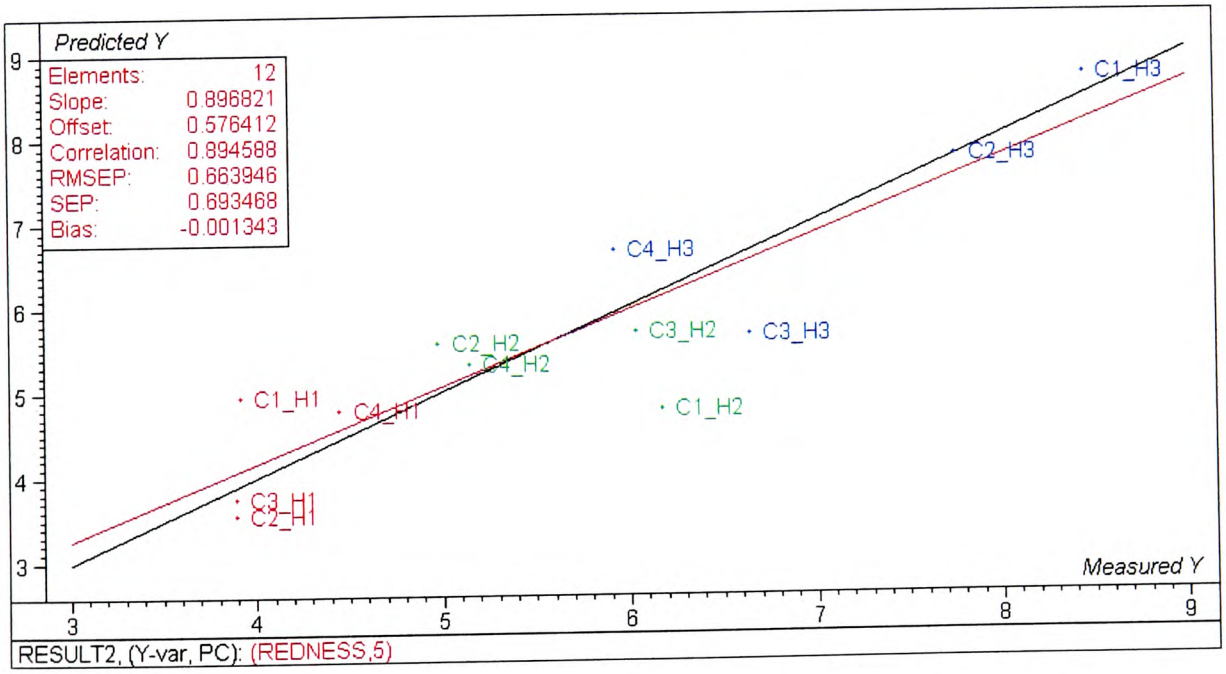

Figure 3.5 - Example of PLS1 regression plot for the prediction of redness of jam samples by spectroscopic data

Using the jam example, Figure 3.5 shows a plot of predicted y-values against measured y-values for the prediction of variations in sensory variables (redness) of jam samples from spectroscopic variables. This plot checks the quality of the regression model by

comparing the two sets of y-values and calculating a root mean squared error of prediction (RMSEP). The lower the RMSEP the better the model fits the data. If the model is a good fit the plot will show samples lying close to a straight line, which goes through the origin (offset close to 0) and has a slope close to 1. The relevant statistics are detailed in the top left corner box (Camo, 1998).

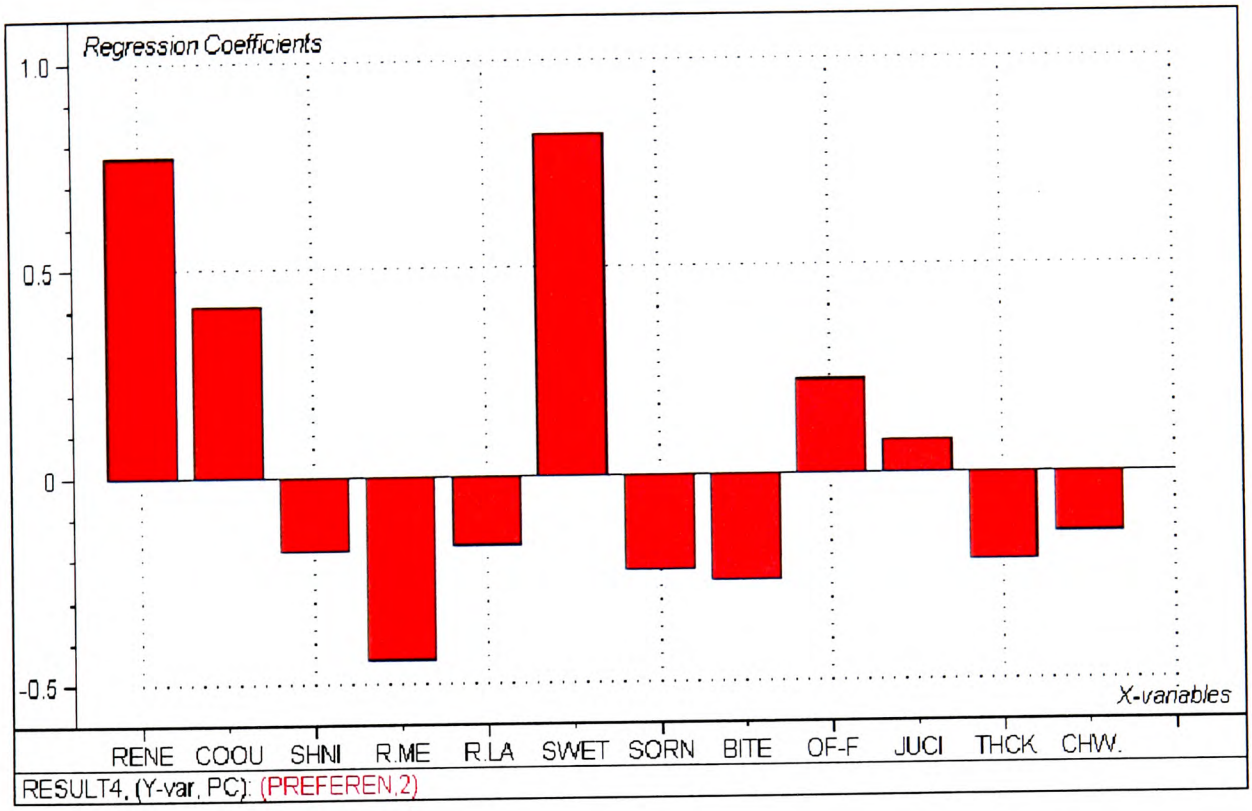

Figure 3.6 - Plot showing regression coefficients for jam sensory characteristics

Figure 3.6 shows examples of regression coefficients, which give the cumulative importance of each of the variables to consumer preference. Redness, colour and sweetness are the most important qualities in jam according to the sensory evaluation. PLS calculates the latent variables and the regression coefficients concurrently (Livingstone, 1995).

3.1.4.2 Multiple Linear Regression (MLR)

MLR involves a matrix inversion where the variables must be linearly independent in order to use variables as predictors. In order for the matrix to be inverted MLR requires that there be more samples than predictors. MLR produced models are used in principal components regression.

3.1.4.3 Principal Components Regression (PCR)

PCR is a two step method, which decomposes the X matrix by PCA then fits an MLR model using the resulting PCs. PCR results give information on scores, loadings, predicted Y values, error measurements, residuals and regression coefficients. As X variables must participate independently in the model for MLR only Y variance (residual and explained) is apposite. The Root Mean Square Error of Calibration (RMSEC) gives information on the average modelling error and is a measurement of the average difference between predicted and measured response values at the calibration stage. The Root Mean Square Error of Prediction gives the average prediction error at the validation stage (Martens *et al.*, 1991).

.

3.1.5 Comparison of Regression Methods

Certain factors need to be considered when choosing a relevant regression method for data analysis. For MLR the number of variables must be smaller than the number of samples and if data is used with a high noise content MLR can overfit (i.e. describe too much of the variation in data by using noise as well as true sample variation). MLR and PCR only model one Y variable at a time whereas PLS uses the dependent and independent variables alternating repeatedly between X and Y to find the correct number of PCs. PLS therefore reaches an optimal solution with fewer PCs than PCR. PLS2 is a

useful method if it is necessary to interpret all variables simultaneously but PLS1 or PCR generally gives improved prediction, as they model each Y variable separately. PLS1 requires fewer components than PCR and gives analogous results (Camo, 1998). Therefore PLS1 will be the regression method used throughout this study to characterise and predict olive oil adulteration.

3.1.6 Validation

Validation is an extremely important step in any multivariate analysis. Once a model has been described, validation checks how well the model would predict unknown samples. The model is said to be valid if the uncertainty of future predictions is low. There are different forms of validation and the one used throughout this work is cross validation. Cross validation tests the robustness of regression models by showing that the omission of samples should not greatly affect the regression coefficients if the model is sound (Livingstone, 1995).

3.1.6.1 Cross Validation

Cross validation can be used in both PCA and PLS investigations. Model estimation and model testing are carried out using the same samples. Some samples are omitted from the calibration data set and these are used as test samples to assess the prediction ability of the model. This is repeated using different test samples until each sample has been used in the test group. All the resulting prediction residuals are combined to give the validation residual variance and the RMSEP. Validation residual variances are computed using prediction residuals instead of calibration residuals and they are used to find the optimum number of model components. The RMSEP gives the average uncertainty when predicting Y values for unknown samples. Full cross validation omits one sample

at a time. Although this is a slower method than validation methods which omit groups of samples at a time (segmented cross validation or test-set switch), it improves the power and relevance of the analysis (Martens *et al.*, 1991).

3.1.7 Prediction

Once a regression model has been constructed, calibrated and validated the prediction of Y variables for unknown samples can be investigated. A prediction plot shows the predicted Y values for all samples with deviation. Deviation conveys how similar the prediction sample is to the calibration samples. The smaller the deviation the more similar the samples (Camo, 1998).

3.2 LITERATURE REVIEW OF MULTIVARIATE ANALYSIS IN EDIBLE OIL ANALYSIS

Multivariate analysis has been used extensively in the characterisation of oils over the last two decades and its use in analytical methodology development was discussed in a review of recent approaches (Miller, 1995). It enables large sets of data, such as chemical spectra, to be analysed rapidly and the data classified and predicted by pattern detection arising from any variation in the data set. This facility of sample grouping has proved useful in many investigations into the geographic origin of olive oils, olive oil characterisation due to olive variety and the adulteration of olive oil.

3.2.1 Principal Component Analysis (PCA)

Principal Component Analysis (PCA) has been used in various research studies using different methods of initial sample analysis. It has been used with infra-red data to explore the viability of distinguishing between olive oil and potential adulterant oils (Lai

et al., 1994; Wesley *et al.*, 1995; Dupuy *et al.*, 1996; Wesley *et al.*, 1996; Guillen *et al.*, 1999). In all cases proving satisfactory sample grouping that identified variances between the composition of the pure adulterant oil and that of olive oil. Sample separations using chromatographic techniques, such as high performance liquid chromatography (HPLC) and gas chromatography (GC), have also successfully separated olive oil from pure adulterant oils using PCA (Tsimidou *et al.*, 1987; Lee *et al.*, 1998; Webster *et al.*, 1999). A large study comprising of fatty acid compositional data of Greek olive oils collected over 24 years, used PCA to geographically classify oil origins in an attempt to encourage the labelling of olive oil bottles with the area of origin (Tsimidou *et al.*, 1993). Tsimidou had previously used HPLC and GC to geographically separate a smaller sample set of Greek oils and concluded that performing PCA on triglyceride compositional data had proved to be a promising technique for the classification of olive oils (Tsimidou *et al.*, 1987). NMR data has also been subjected to PCA to determine adulteration detection (Shaw *et al.*, 1997) and differentiate between olive varieties and geographical origin (Vlahov *et al.*, 1999; Sacco *et al.*, 2000).

3.2.2 Cluster Analysis

Cluster analysis is a good indication of sample grouping and has therefore been used in olive oil studies to attempt to distinguish between oils originating from different areas or different olive varieties. Proton NMR of the minor components of olive oil has been used to try to identify oils from the same olive variety (Sacchi *et al.*, 1996) and to try to distinguish between oils originating from four regions of Italy (Sacchi *et al.*, 1998). Both of these studies used hierarchical cluster analysis to produce dendrograms which concluded, in the second study, that 96% of samples were correctly clustered into geographical origin. Another group also used hierarchical clustering to distinguish

between olive variety and origin, using ^{1}H NMR data. They concluded that the fatty acid composition was more useful for determining olive variety, whereas the phenolic fraction of olive oil was more successful in correctly classifying oil origin (Sacco *et al.*, 2000). Clustering has also been used to investigate the differences between vegetable oils and argania oil. Argania oil originates from Morocco and in its country of origin it is considered to be the best culinary oil. It is ten times the price of olive oil and therefore open to similar adulteration problems. The study considered cluster analysis one of the best methods of determining oil similarity on the basis of fatty acid content (Rezanka *et al.*, 1999).

3.2.3 Partial Least Squares (PLS)

Regression methods, such as PLS, enable the prediction of unknown samples once a model has been constructed for the observed data. This has shown to be constructive in the prediction of adulteration of olive oil sample with other vegetable oils (Lai *et al.*, 1995; Wesley *et al.*, 1996) and also for the determination of geographical origin using ^{13}C NMR (Shaw *et al.*, 1997; Vlahov *et al.*, 1999). PLS has been used for compositional investigations, using FTIR, to determine the free fatty acid range and content (Bertran *et al.*, 1999) and to establish the *trans*- content of edible oils (Li *et al.*, 2000).

Characteristics of olive oils described by sensory panels were related to the headspace analysis of volatile components in olive oil and found that PCA of the GC-MS headspace data gave similar clustering of samples to the sensory panel. PLS of the headspace data was used to predict specific descriptive qualities and attempted to identify the compounds responsible (Servili *et al.*, 1995).

CHAPTER 4

4 Nuclear Magnetic Resonance (NMR) Spectroscopy

4.1 THEORY AND TECHNIQUE

Nuclear Magnetic Resonance (NMR) is a technique which detects the presence of chemical elements that have one or more isotopes whose nuclei are considered to spin and therefore generate a magnetic moment. Nuclei which have a spin of ½, such as a hydrogen nucleus, have two possible alignments of the magnetic moment and can therefore exist in one of two energy levels (Figure 4.1), with the external field (parallel) or against it (anti-parallel).

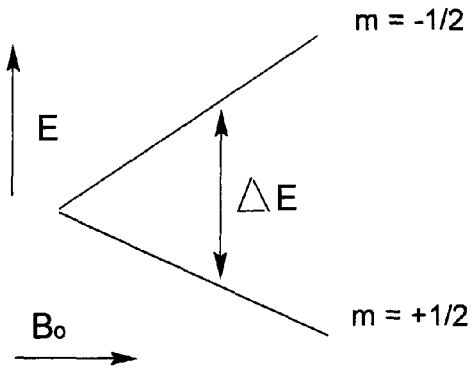

Figure 4.1 - Energy level diagram for a single spin system

Alignment with the field (m = +½) is the more stable arrangement and energy (E) needs to be absorbed in order to make the proton flip to the less stable alignment, against the field. The difference in energy between the two states (ΔE) is 2μBo, where μ is the magnetic moment and Bo is the magnetic flux density of the applied field:

$$\Delta E = h\nu = 2\mu Bo$$

The stronger the external field, the higher the frequency (ν) of the radiation needed to flip the proton (Duckett *et al.*, 2000). A radio-frequency (*rf*) coil surrounds the sample to

provide the necessary radiation. The spin system is subjected to a short intense pulse of *rf* power and at a specific field strength value the energy required to flip the proton matches the energy of the radiation and a signal is observed.

Fourier transformation (FT) is a mathematical transformation that relates time and frequency so that results obtained as a function of time can be expressed as a function of frequency. A nucleus does not remain in one energy state. It either absorbs energy to the anti-parallel alignment or loses energy to the parallel alignment. When equilibrium is reached between the two states the greater population of nuclei are parallel to the field. The time taken to reach equilibrium can be described using an exponential time constant T_1, the spin-lattice relaxation time. This varies and depends on several factors, the temperature, viscosity and the strength of interaction between the nuclei and the rest of the sample. The magnitude of the magnetic moment (μ) of the nuclei and the magnetic moments of other atoms within the sample affects T_1. The effective magnetic field strength felt by a nuclei varies depending on the chemical environment of that nuclei. It will therefore require a slightly different applied field strength to produce the same effective field strength for protons in different environments. Depending on the chemical environment, nuclei of the same species absorb energy at different frequencies because of altered magnetic fields arising from shielding effects of orbital electron motion. This leads to a separation in the signals termed the chemical shift (δ). The chemical shift is field dependent so, to avoid confusion with different magnetic fields being used in different spectrometers, they are quoted as a ratio between the frequency difference and the frequency of a reference compound. The values obtained are very small and therefore are multiplied by 10^6 hence the resulting chemical shifts are represented in parts per million (ppm) (Shaw, 1976). The reference compound used to determine shift

values (in ^{13}C and ^{1}H NMR) is tetramethylsilane (TMS). It is very unreactive, easily removed from a sample due to its volatility, gives an intense single absorption line arising from twelve equivalent protons and very few other resonances fall close to it at 0.0ppm. The majority of chemical substances give positive shifts (lower applied magnetic fields) with relatively few at higher magnetic field (negative shift).

4.1.1 ^{13}C NMR

A carbon NMR spectrum gives information on the carbon skeleton of a molecule, the number of different carbons and the electronic environment with respect to functional groups. Due to the smaller magnetogyric ratio and low natural abundance of ^{13}C (1.108%), it is less sensitive to NMR than ^{1}H. The magnetogyric ratio is the magnitude of the nuclear magnetic moment, which is the ratio of the magnetic moment to the associated angular momentum. ^{13}C spectra are also subject to large nuclear Overhauser enhancements (nOe), which result in unreliable integration, making it unsuitable for quantitative work.

4.1.1.1 Nuclear Overhauser Enhancement (nOe)

Spin-lattice relaxation occurs along the z axis and is a through-space connection which gives information on the distance between spins. One result of such relaxation is nOe. Following the excitation of the spin population, by electromagnetic radiation at an appropriate frequency, its return to equilibrium where excess energy passes from the spins to the surroundings (lattice) is called spin-lattice relaxation. The dominant magnetic fields, in diamagnetic molecules, are due to the dipole-dipole interactions produced by the magnetic moments of protons in the same molecules as they tumble in solution (Sanders *et al.*, 1993). The rate of dipole-dipole relaxation depends on the

cubed distance between the nuclei involved, the effective correlation time of the vectors that join the nuclei (τ_c) and the nature of the nuclei. The rate at which nOe grows and decays is a measure of the strength of the dipole-dipole interactions between two spins. As this is dependent on the proximity of the nuclei the efficiency of the relaxation decreases with increasing interatomic distance. Carbon nuclei are primarily relaxed by neighbouring protons, the more protons attached to the carbon, the faster it relaxes and the broader the signal becomes. Proton-proton interactions tend to be the dominant relaxation process for protons in diamagnetic molecules as the strength of the dipole-dipole interaction depends on the square of the product of the magnetogyric ratios. To demonstrate, Figure 4.2 shows the equilibrium population distribution for dipole-dipole relaxation in a two-spin system. It consists of homonuclear protons I and S, which relax each other but are not J coupled.

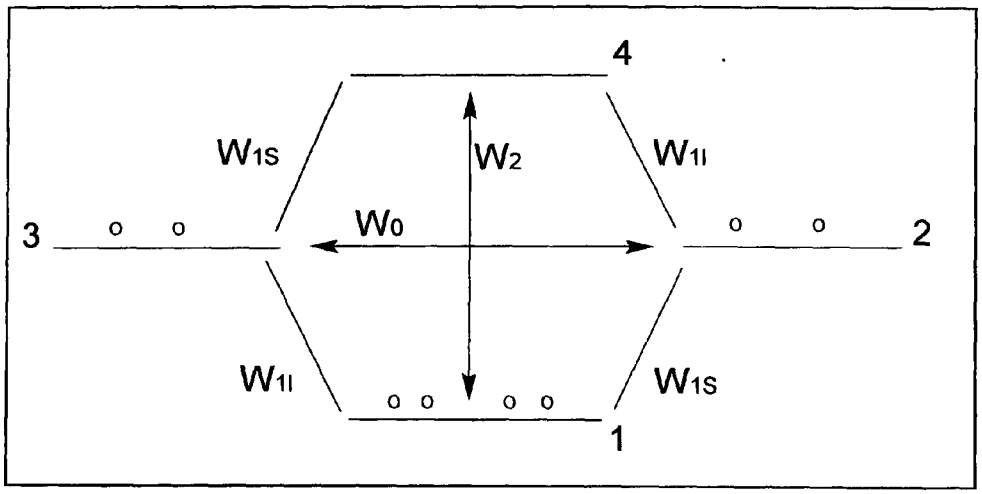

Figure 4.2 - Energy level diagram to explain nOe based on a two-spin system

where:

W_{1I} - Transition probability single quantum

W_{1S} - Transition probability single quantum

W_2 - Double-quantum process that corresponds to the simultaneous relaxation of both spins

W_0 - Zero-quantum process corresponding to a mutual spin-flip – excess energy moved from one spin to another not to surroundings.

Spectrum of I corresponds to the transitions 1,3 and 2,4, spectrum of S corresponds to the transitions 1,2 and 3,4.

If spin S is saturated a new population distribution develops as relaxation occurs through W_2 and W_0. By establishing a Boltzmann distribution between levels 1 and 4, W_2 increases the intensity of I transitions while W_0 decreases the intensity of I by attempting to equilibriate levels 2 and 3. The competition between W_2 and W_0 results in a net change in the intensity of I, which is the nuclear Overhauser effect. The sign of the observed nOe is dictated by whichever is the dominant relaxation pathway between W_2 and W_0 (Claridge, 1999). If both I and S have the same magnetogyric ratio (e.g. both protons) then the maximum enhancement in signal will be 50% irrespective of the inter-atomic distance. A much greater enhancement (198%) is seen when carbon spectra are acquired with proton irradiation. This gives a threefold improvement in signal-to-noise (Sanders *et al.*, 1993).

For protons:

$$\vartheta = \frac{\gamma_{irr}}{2\gamma_{obs}} = \frac{1}{2} \qquad \text{s/n} = 1 + \vartheta = 1.5$$

For ^{13}C:

$$\vartheta = \frac{\gamma_{irr}}{2\gamma_{obs}} = \frac{1}{2\times\frac{1}{4}} = 2 \qquad \text{s/n} = 1 + 2 = 3$$

where ϑ = frequency

γ = magnetogyric ratio

s/n = maximum signal to noise enhancement

In order to achieve comparable integrals in ^{13}C NMR, the range of nOe in a molecule need to be equalised. Using an inverse gated program where the decoupler is on during

pulse and acquisition but is off during relaxation delay equalises the nOe to zero as none of the carbon signals would be enhanced. Due to the increase in signal-to-noise when nOe is present, a much longer time (5 x T_1 of the longest relaxation time) is needed to achieve a comparable signal without nOe and this equates to approximately a ninefold increase in acquisition time.

4.1.1.2 Literature Review - ^{13}C NMR

^{13}C NMR has been used extensively in olive oil studies. Studies have attempted to discriminate between cultivars/geographical origin, using the fatty acid distribution or the unsaponifiable fraction of olive oil (Section 4.1.1.3). ^{13}C NMR has also been used to characterise composition of oils by their fatty acid content and the phenolic compounds present (Section 4.1.1.4). The different grades of olive oil have been investigated and characterised using the composition of mono-, di- and triglycerides in superior grade oil (Vlahov, 1996) and also by characterising the unsaponifiable matter in olive oil (Zamora *et al.*, 1994). The detection of adulteration has also been well documented using methods including fatty acid composition (Section 4.1.1.5).

4.1.1.3 Discrimination between cultivars/geographical origin

It was shown for the first time in 1997 how ^{13}C NMR could be used, with advanced chemometric techniques, to differentiate between olive oils from different regions and of different varieties (Shaw *et al.*, 1997). The ^{13}C spectra were obtained using an inverse-gated proton decoupled arrangement to overcome the nOe and a waiting time of 20 seconds between pulses was adopted to ensure all magnetisation was recovered between pulses, therefore satisfying the requirement of 5 x T_1 relaxation times. The data obtained for the carbonyl, olefinic and aliphatic regions was analysed using in-house

chemometrics programs. The dilemma of selecting variables was discussed for multivariate analysis and whether there is value in reducing the variable set size before the initial calibration model is created. They quote other studies which have concluded that variable reduction generally improves the results of PCA and PLS. It has also been shown that the greater the number of independent variables the greater the possibility of chance correlations between unrelated variables (Horchner *et al.*, 1995; Miller, 1995). Shaw *et al.* concluded that although regional variation was more difficult to separate than variety of olive, ^{13}C NMR discriminated and classified variety and geographical origin. Variable selection improved the predictions and multiple PLS 1 models performed better than a single PLS 2 model (Shaw *et al.*, 1997).

Distortionless Enhancement by Polarisation Transfer (DEPT) was used in a study to discriminate between oil cultivars. The DEPT pulse sequence enhances the ^{13}C spectra by transferring the nuclear spin polarisation from spins with large Boltzmann population differences, such as protons, to species with low Boltzmann factors, such as ^{13}C. Coupled with PCA and PLS multivariate analysis, they agreed with the Shaw study that geographical discrimination was more difficult than variety classification. Their results compared favourably with their previous studies despite the lack of signals in the important carbonyl region, which detects the presence of saturated chains, with the DEPT sequence (Vlahov *et al.*, 1999). The ratio of α (1,3) positions to β (2) position oleic and linoleic acids were used to quantify results for oils from different areas of Greece (Mavromoustakos *et al.*, 1997) and it was suggested that these ratios could be used to identify adulteration.

4.1.1.4 Characterisation of oil composition

The phenolic constituents of olive oil have been well researched due to the link between phenolics and antioxidant properties. Studies have compared other techniques for structure elucidation with NMR (Brenes *et al.*, 1999; Bianco *et al.*, 2000; Brenes *et al.*, 2000), employing various NMR pulse sequences such as DEPT (Owen *et al.*, 2000) and using both 1D and 2D NMR (Servili *et al.*, 1999). Investigating the fatty acid composition of oils has occupied several research groups with quantitative work generally using the inverse gated program to suppress the nOe (Sacchi *et al.*, 1991; Vlahov *et al.*, 1996). Vlahov did find that the nOe enhancement factors of different fatty acids chains on the carbonyl carbon resonances were affected by proton decoupling to the same extent (Vlahov, 1998), leading to the conclusion that this region of the spectra can be acquired with full nOe for quantitative purposes. This gives higher signal-to-noise ratios with shorter experimental times. This information was then used to characterise the triacylglycerols in different parts of the olive fruit (Vlahov *et al.*, 1999) and to obtain detailed carbonyl composition information (Vlahov, 1999). However, to acquire an entire ^{13}C spectra the inverse gated sequence was used.

The carbon atoms of $\alpha-$ and $\beta-$acyl chains show different chemical shifts that have been used to characterise olive oils. However, variations in observed values from different research groups have not given conclusive values. The values of the ^{13}C chemical shifts are dependent on concentration, which can lead to disparity in data from different sources. The shifts for the carbonyl carbons for position 1,3- of the oleic, linoleic and eicosenoic chains and the 2- position of the oleic and linoleic chains are particularly susceptible to concentration fluctuation and it is these areas that have been proposed as characterisation markers. A study undertaken to assign the ^{13}C NMR

spectra of oils as a function of concentration, attempted to ratify the concentration dependence (Mannina *et al.*, 2000) and concluded, in contrast to previous studies, that the shifts of a fatty acid in a triglyceride are independent of the other two fatty acid substituents. They added pure triglycerides to various edible oils, including olive oil, and observed increases in signal intensity of some of the peaks but no new shifted signals were apparent. The chemical shift for any fatty acid in any position, irrespective of the composition of the triglyceride, as a function of concentration should therefore allow the reliable characterisation of oils.

^{31}P has also been investigated to characterise fatty acid composition in an attempt to overcome the long relaxation times necessary in ^{13}C NMR and the problem of overlapped peaks in ^{1}H NMR (Spyros *et al.*, 2000).

4.1.1.5 Determination of adulteration

Many of the research projects that have classified oils by their fatty acid composition have suggested the methods employed, especially the ratio of oleic to linoleic acids, could be used to detect adulteration of olive oil with cheaper oils higher in linoleic/linolenic acids. One study used an inverse gated pulse sequence to suppress the nOe and selected specific peaks from the olefinic area (127 - 130 ppm) to subject to statistical analysis (Mavromoustakos *et al.*, 2000). Adulteration levels of between 5 and 80% were tested using discriminant analysis and they found that adulteration levels of above 40% were classified with 100% success, with 80% success $\leq$40% adulteration and none of the adulterated samples were misclassed as unadulterated olive oil. DEPT was used (Vlahov, 1997) to detect soybean adulteration by plotting calibration graphs of the oleyl C-9, the linoleyl and linolenyl C-10 against the percentage soybean

adulteration. The limits of detection for oleyl, linoleyl and linolenyl chains were calculated and it was determined that the linear correlations observed were not random.

4.1.2 Literature Review - ^{1}H NMR

Proton NMR has been used to shorten the acquisition times and circumvent the problem of nOe associated with ^{13}C NMR analysis (nOe only affects spin-decoupled ^{1}H NMR). As ^{1}H NMR is more sensitive than ^{13}C NMR, it has been used to analyse the phenolic fraction and the volatile components of olive oil, for use in determining geographical origin and adulteration. It was found that the volatile components produced by oxidation of olive oils at high temperatures were formed in two stages (Moreno *et al.*, 1999). Up to 150°C the fats take up oxygen to form hydroperoxides and then a second oxidation takes place to form carbonyl compounds, mainly aldehydes. Signals were recorded at 8 - 8.5 ppm for the hydroperoxides (at 150°C) and at 300°C the peaks disappeared being replaced by aldehydic signals at 9.4 and 9.6 ppm. They concluded that there was a significant increase in the amount of carbonyl compounds formed over 200°C, a temperature regularly exceeded whilst frying food, and that olive oil and sunflower oil had shown the greatest increase in these potentially harmful degradation products.

Two dimensional proton NMR was used (Sacchi *et al.*, 1996) to look at the composition of olive oil with PCA and clustering statistics used to analyse the data. An attempt to characterise Italian olive oils by region used the proton NMR of the phenolic and fatty acid components (Sacco *et al.*, 2000). It was concluded that using data from the phenolic fraction of the oils in multivariate analysis gave better geographical separation. They found no correlation between fatty acid composition and geographical origin in their

limited sample set of 28 oils. The differences in fatty acid composition were used on selected proton peaks to differentiate between olive, hazelnut and sunflower oils (Fauhl *et al.*, 2000). Using discriminant analysis this study demonstrated that there was significant difference between the oils and a plot of discriminant functions showed that adulterated oils would fall outside the defined groups, therefore making detection possible.

Another study used NMR and gas chromatography (GC) to detect adulteration of olive oil with hazelnut oil. They concentrated on the terminal methyl region of the spectrum (0.6 - 1.0 ppm) where the saturated and monounsaturated glyceride signals overlap but the terminal methyl of linoleic acid has one distinguishable peak at 0.84ppm and the triplet arising from linolenic acid occurs at 0.925 ppm. Direct comparison of this triplet intensity and the intensity of the ^{13}C satellites of the main methyl resonance is indicative of the amount of linolenic acid present in a sample. A level of between 0.4 and 0.8% linolenic acid is expected in olive oil and 0.9% is the maximum set by EU regulation (Mannina *et al.*, 1999). Anything above this percentage is suggestive of seed oil adulteration. The discriminant analysis used gave good grouping for hazelnut and olive oils and the minimum hazelnut adulteration detectable was 10%.

Fifty-five Italian oils were also subjected to high-field proton NMR and multivariate analysis to characterise them using the minor unsaponifiable components (Sacchi *et al.*, 1998). Cluster analysis of the data set was performed and gave good classification for the four main geographical areas. 96% of the samples were correctly classified and they concluded that the combination of proton NMR and multivariate statistics was a useful tool in geographical classification.

4.1.2.1 ^{1}H Peak Assignment

Figure 4.3 shows a typical proton NMR spectrum with a key, relating to Figure 4.4, showing which protons in a triacylglyceride give rise to a specific signal. An example of a possible triacylglyceride structure is shown in Figure 4.4. The three fatty acids present are linoleic acid, oleic acid and linolenic acid. The structure is not geometrically correct in order to show clearly the difference in fatty acid structure to assign peaks on the NMR spectrum. Olive oil has a large percentage of oleic acid and is naturally low in linoleic and linolenic acids (polyunsaturated acids). Adulteration with oils high in these polyunsaturates, such as sunflower oil, is detectable by monitoring the peak at 2.73 ppm (H5) or the peak at 5.2 ppm (H1). A ratio of less than 4:3 of H7:H11 indicates the presence of a saturated fatty acid in the triacylglceride (Vlahov, 1999).

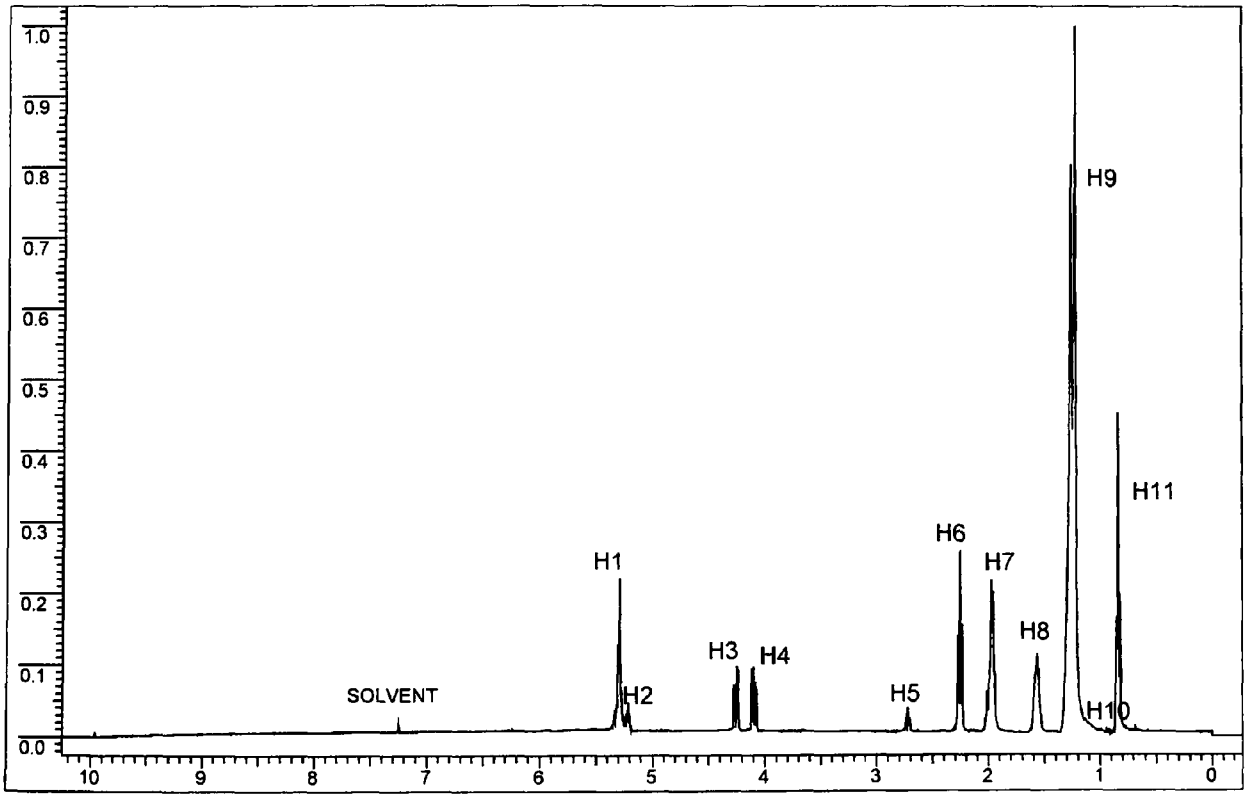

Figure 4.3- Example of proton NMR spectrum of adulterated olive oil

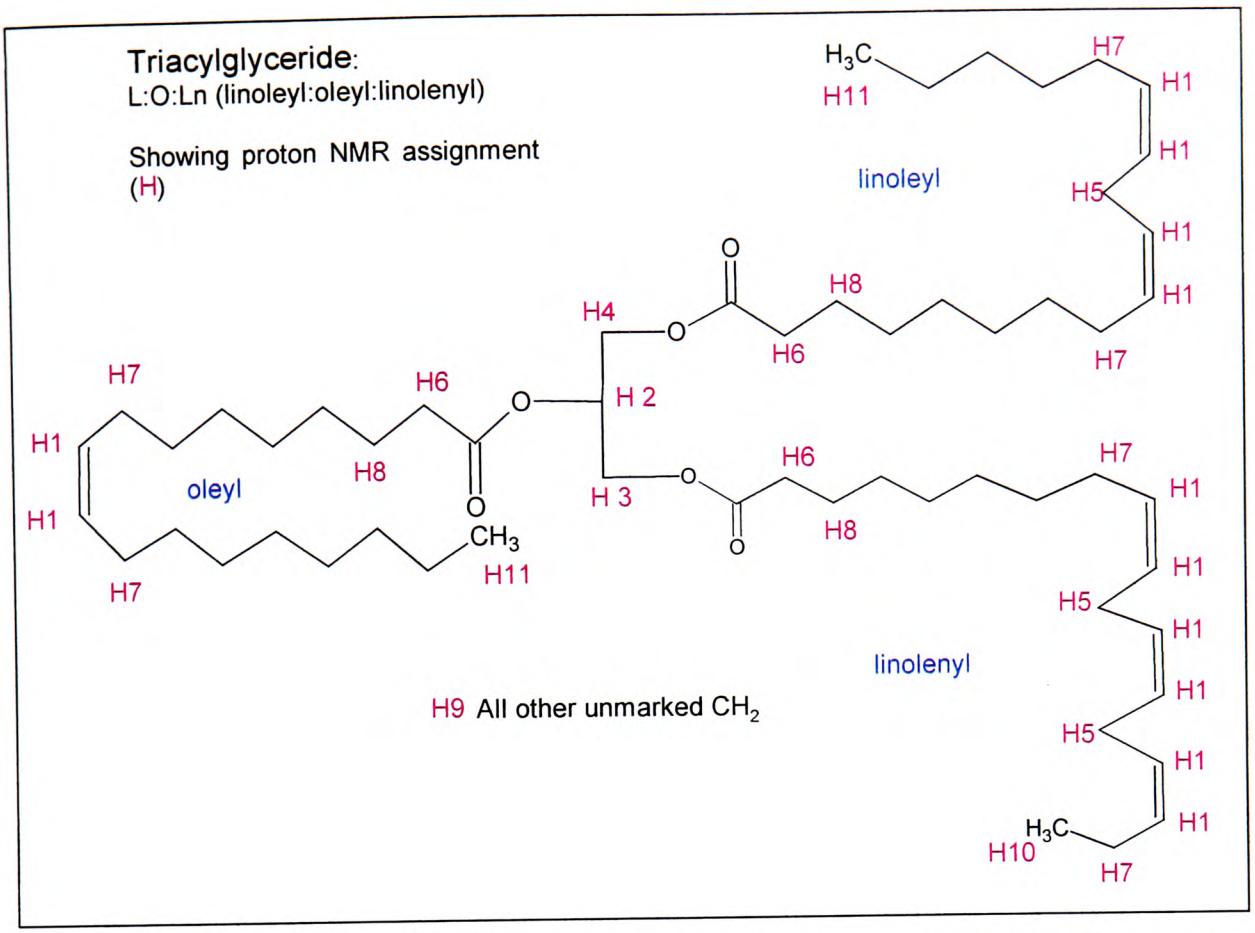

Figure 4.4 - Example of triacylglyceride structure with proton NMR assignment with reference to Figure 4.3

4.2 METHOD

4.2.1 ^{13}C NMR METHODOLOGY

Olive oil samples from 1995/96 harvest (E set) from Crete were diluted 28.5% w/v in deuterated chloroform. Each oil was also adulterated with 2% and 5% sunflower, soya, corn and cotton oil. Pyrazine (0.015 g) was added as an internal standard. Actual weighings are shown in Appendix B. Spectra were obtained for the pure oils and for each of the contaminated samples.

The ^{13}C spectra were run on a Jeol 270 MHz spectrometer using the parameters detailed in Table 4.1. Long repetition times were used to allow for adequate relaxation.

Table 4.1 – ^{13}C NMR parameters

PARAMETER	VALUE
Frequency	13560 Hz
Pulse angle	90°
Pulse width	7.5 μs
Acquisition time	2.7 s
Repetition time	41.8 s
Data points	128000
Broadening factor	0.16 Hz
Temperature	40°C
Number of scans	400

The resulting spectra were imported into the Grams 32 software package to allow peak alignment and peak picking with relevant individual values assembled and imported in Microsoft Excel. The peak areas were then standardised for 0.015 g of pyrazine and for a total weight of 4.0 g oil. The information was then imported into Unscrambler 7.5 (Camo ASA, Norway) software for multivariate statistical analysis.

To attempt to overcome any nuclear Overhauser enhancement resulting from ^{13}C NMR, heteronuclear multiple quantum correlation (HMQC) was undertaken. HMQC is a heteronulear correlation technique that identifies protons with their directly bound carbons. The pulse sequence utilises zero and double quantum coherence between coupled protons and carbons and labels each proton with the frequency of the directly bonded carbon. Magnetisation is transferred from the proton to its directly attached carbon and back to the proton, for higher sensitivity. The results are displayed as a 2D map, with one dimension representing ^{13}C shifts and the other ^{1}H shifts.

4.2.2 ^{1}H NMR METHODOLOGY

^{1}H NMR spectra were obtained for the E set of Greek oils at different sunflower oil adulteration levels, 0%, 1%, 5% and 10% for the Crete oils and 0%, 1% and 5% for the non-Crete oils. The F set of Crete oils was also investigated at 0%, 1% and 5% sunflower oil adulteration. The spectra were run on a JEOL 400 MHz spectrometer in the Institute for Spectrochemistry and Applied Spectroscopy in Dortmund, Germany, using the parameters detailed in Table 4.2.

Table 4.2 – ^{1}H NMR Parameters

PARAMETER	VALUE
Frequency	13560 Hz
Pulse width	5.75 μs
Pulse angle	45°
Acquisition time	2 s
Data points	16384
Broadening factor	0.122 Hz
Temperature	40°C
Number of scans	8

The resulting spectra were imported through the Grams 32 software (Galactic, USA) to align spectra and allow importation into the Unscrambler multivariate statistics program. All spectra were standardised for actual amounts of oil and Principal Component Analysis (PCA) and Partial Least Squares (PLS) carried out on all samples. PCA and PLS investigations were carried out using all variables and also selected variables, chosen for their chemical importance (Fauhl *et al.*, 2000). The selected peaks and their origins are detailed in Table 4.3 below:

Table 4.3 – Selected peaks and their chemical shifts used throughout the ^{1}H NMR multivariate investigations

Range of Chemical Shift (ppm)	Peak Assignment in a triacylglyceride
0.80 – 1.00	Terminal linolenyl methyl group
1.38 – 1.57	β - carboxyl CH_2-CH_2-COOR
2.50 – 2.77	C*H* between C=C in PUFAs
5.07 – 5.19	C*H* at β - position on glycerol molecule
5.19 – 5.35	C*H* on C=C in unsaturated triglycerides

4.3 RESULTS AND DISCUSSION

4.3.1 ^{13}C NMR

The ^{13}C spectra were imported into the Grams 32 software to allow manipulation and then into Microsoft Excel to standardise the peak areas relative to actual oil and pyrazine (internal standard) content. Table B1 in Appendix B details the exact sample content and percentage dilution.

Each unsaturated carbon signal was split depending on the chain position occupied on the glycerol backbone and Table 4.4 details ^{13}C NMR peak assignment from literature values.

Table 4.4 - ^{13}C NMR peaks (ppm) assigned from literature data (Mavromoustakos *et al.*, 1997)

Peak (ppm)	Fatty acid	Carbon	Position
127.63	Linoleyl	12	β (2)
127.64	Linoleyl	12	α (1,3)
127.81	Linoleyl	10	α (1,3)
127.82	Linoleyl	10	β (2)
129.35	Oleyl	9	β (2)
129.37	Oleyl	9	α (1,3)
129.61	Linoleyl	9	β (2)
129.63	Linoleyl	9	α (1,3)
129.67	Oleyl	10	α (1,3)
129.68	Oleyl	10	β (2)
129.83	Linoleyl	13	α (1,3)
129.84	Linoleyl	13	β (2)

Example spectra of the ethylenic region of an unadulterated oil compared to the same oil adulterated with 5% soya oil is shown in Figure 4.5, and the carbonyl region in Figure 4.6. The ethylenic (127 - 130 ppm) and carbonyl (170 - 173 ppm) regions showed an increase in peak heights when adulterated with oils higher in linoleic/linolenic acid.

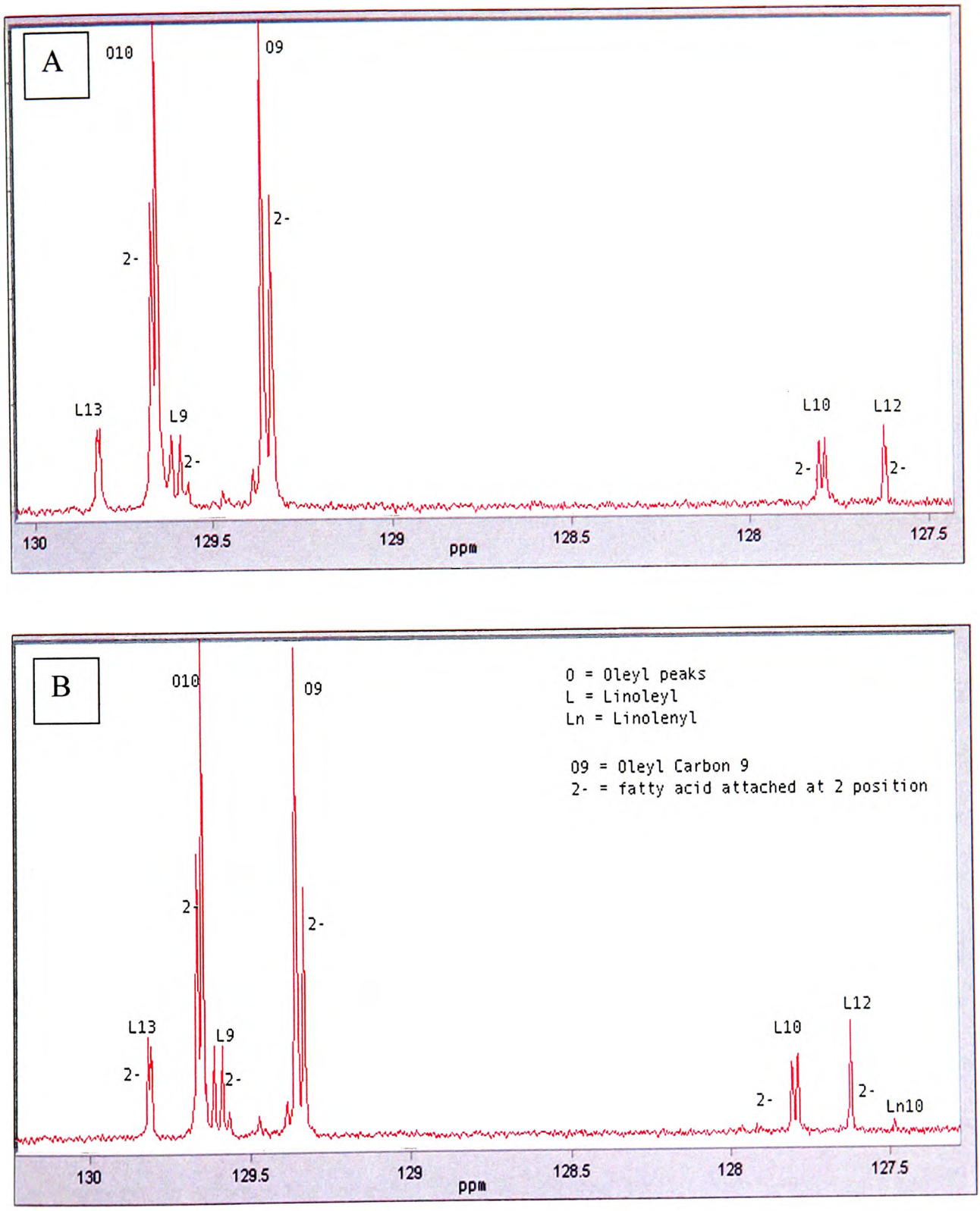

Figure 4.5 - Comparison of unadulterated (A) and 5% soya adulterated (B) ^{13}C NMR spectra in the ethylenic region of the spectrum of olive oil

In Figure 4.5, the peaks arising from carbons 10 and 12 in a linoleyl chain (127.6 - 127.8 ppm) showed an increase in peak height when soya oil was added to the olive oil (bottom spectrum). Linoleyl peaks (C-9 and 13) at 129.6 ppm and 129.8 ppm were also increased. The larger peaks, at 129.3 ppm and 129.7 ppm arise from the oleic acid present. As olive oil contains a greater percentage of oleic acid than the adulterant oils, no increase would be expected or was seen. The spectra showing 5% soya adulteration also detected a peak at 127.5 ppm, which is due to linolenic acid (C-10) not seen in the unadulterated spectra.

The carbonyl region (Figure 4.6) for unadulterated oils showed the presence of linoleic acid as shoulders on the oleyl peaks (172-174 ppm). When adulterated with 5% soya oil, the peaks showed an increase in resolution. The carbonyl region gives structural information on the positional distribution of fatty acids on the glycerol backbone. There is a shift of 0.4 ppm observed between the carbonyl peaks depending on whether the fatty acid is attached at the 1,3- or the 2- position on the glycerol backbone. The resonating frequency is higher when the chains are attached at the 1,3- position. The carbonyl carbons of the chains attached at the 2- position have decreased mobility compared to those attached at the 1,3- position and so have a shorter relaxation time (Vlahov, 1998). At the 2- position (172.85 ppm) there is partial overlap between the linoleyl (L) and oleyl (O) signals. However, at the 1,3- position (172.68 ppm) there is good separation between the saturated (S), oleyl (O) and linoleyl (L) components and the overall content of saturated fatty acids can be measured from their intensities (Sacchi *et al.*, 1997). Free fatty acids (F) were also detected at 172.77 ppm.

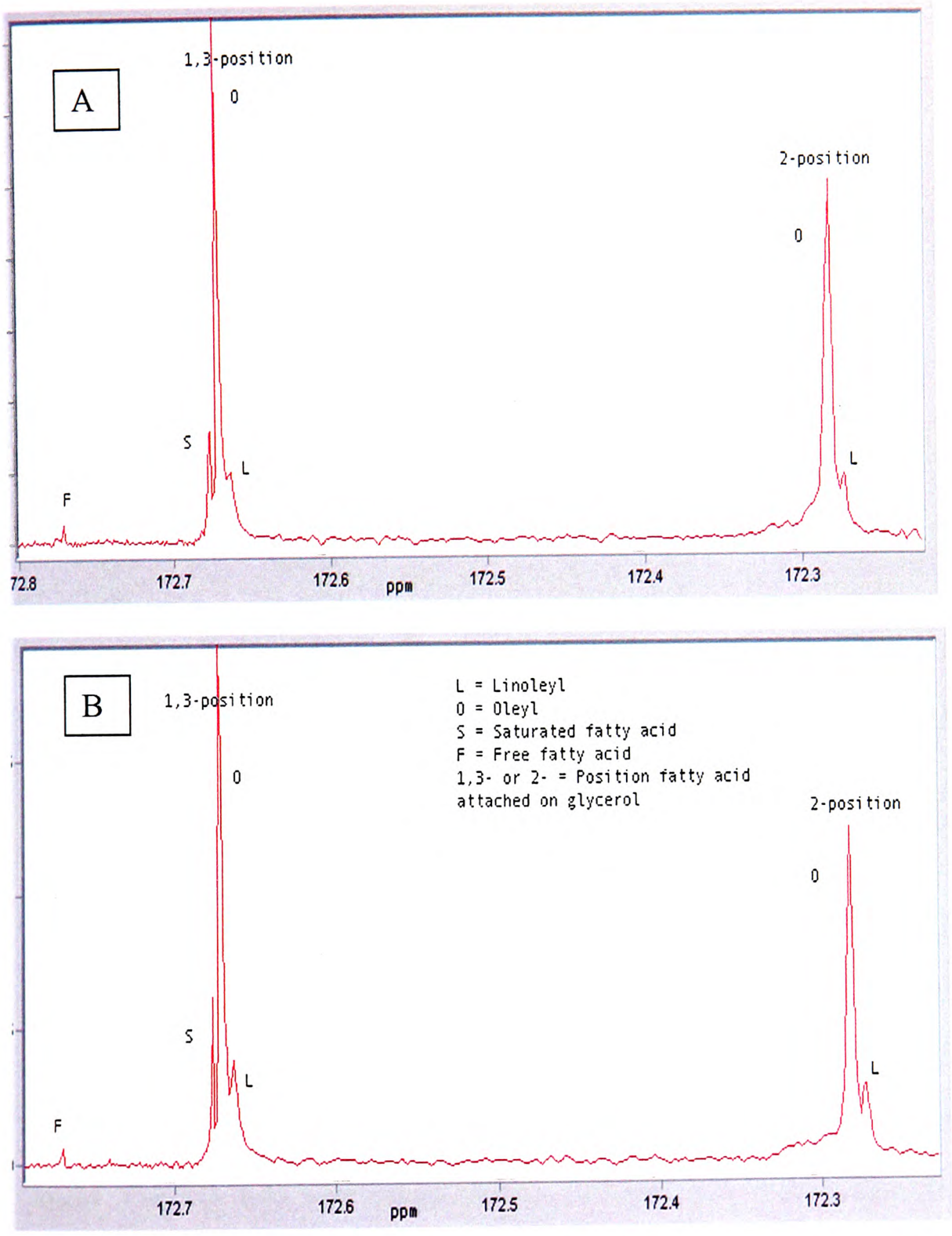

Figure 4.6 - Comparison of unadulterated (A) and 5% soya adulterated (B) ^{13}C NMR spectra in the carbonyl region of the spectrum of olive oil

Using the internal standard peak as a reference, a ratio of peak heights was obtained. An example of this data, using the peak at 127.63 ppm, linoleic acid – carbon 12, attached at the α position, is shown in Table 4.5, full data set shown in Appendix B.

Table 4.5 - Example of ^{13}C NMR peak ratio data

Linoleic peak – carbon 12 α position – 127.63 ppm			
Sample	Unadulterated	2% soya oil	5% soya oil
E1	0.1404	0.1565	0.2200
E2	0.1213	0.1423	0.1605
E3	0.1538	0.1772	0.1789
E4	0.1248	0.1367	0.1760
E5	0.1865	0.1980	0.2050
E6	0.1156	0.1376	0.1465
E7	0.1071	0.2855	0.2972
E8	0.1415	0.1695	0.1849
E9	0.1344	0.1875	0.1896

The spectra were manipulated using Grams 32 software to limit the size of the data file to be exported to the Unscrambler software. This excluded any unnecessary peaks or noise which would prolong statistical processing. Principal Component Analysis (PCA) was carried out to create models for the four separate adulterant oils and also for the pure Greek olive oils. The modelling power plots were evaluated to establish which peak variables the software had assigned to have the most significance for the particular model. The PCA tasks were repeated using only these variables and compared to the results obtained when peaks were picked manually on the basis of chemical importance (Table 4.6)

Table 4.6 – Table comparing ^{13}C NMR peaks chosen by chemical importance and those chosen by the software as being important to the models

Manually picked peaks (ppm)	Software picked peaks (ppm)
126.87 – 127.97	126.87
129.46 – 129.61	127.62
129.81 – 129.82	127.79 – 127.92
172.27	128.47 – 128.52
172.66	129.25
172.68	129.39 – 129.46
	129.50 – 129.59
	129.81
	172.16 – 172.27
	172.77

Figure 4.7 shows the Cooman's plot resulting from classification using the software assigned peaks. Figure 4.8 shows the plot resulting from manually assigned peaks, peaks that show enhancement arising from increased linoleic acid (as in Table 4.6). Although both classifications have a large degree of overlap and doubly classify many of the samples, the manually picked variable plot gave better separation and some of the samples were successfully classified. A full set of classification plots is given in Appendix B.

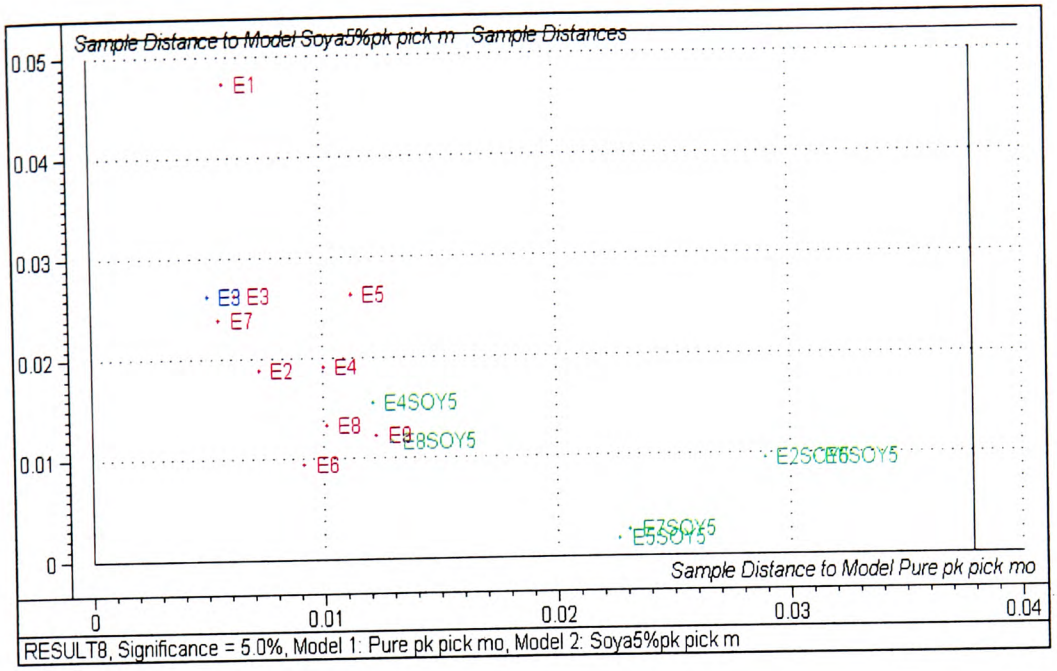

Figure 4.7 - Cooman's Plot showing classification of pure olive oils v 5% soya adulterated olive oil (software assigned)

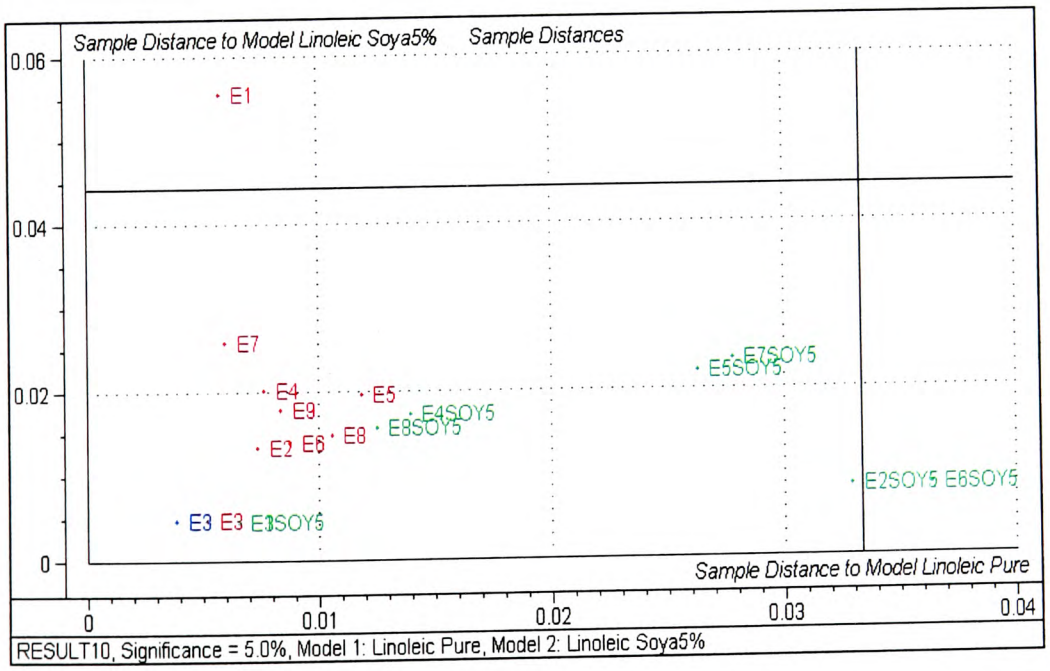

Figure 4.8 - Cooman's Plot showing classification of pure olive oils v 5% soya adulterated olive oil (manually assigned)

To overcome the nuclear Overhauser effect an inverse polarisation pulse sequence was employed. The first HMQC (Heteronuclear multiple quantum correlation) test 1D spectrum measured, produced spectra where the areas of interest were overlapped and poorly resolved in the region 2 - 8 ppm. This would not yield the necessary data to allow multivariate analysis. HMQC 2D projection produced a ^{13}C spectrum projection with very poor signal to noise and took 8 hours to run. The digital resolution was 0.6Hz compared to 0.2 Hz obtained in the original ^{13}C measurements. It was therefore decided that it was not a viable option and ^{1}H NMR would be used.

4.3.2 ^{1}H NMR

The test ^{1}H NMR obtained gave clearly defined spectra, with a short acquisition time which would enable the method to be used to investigate statistically the differences in oil composition with regard to geographical origin, year of harvest and adulteration with sunflower oil.

4.3.2.1 Geographical Origin of the E set

Figure 4.9 shows the results obtained using hierarchical cluster analysis in SPSS (SPSS 9.0 for Windows) using selected peaks (Table 4.3) from the ^{1}H NMR data. Cluster analysis (Section 3.1.3) was the first statistical investigation performed on the E set samples as this would give a good indication of the degree of separation possible using subsequent Principal Component Analysis.

The dendrogram resulting from hierarchical cluster analysis using Ward's method and squared Euclidean distance measurements (Figure 4.9) showed excellent clustering of the

Crete (black) and Non-Crete (red) samples from the E set. This suggested that further analysis would provide well separated models that could be used to predict the geographic origin of unknown samples.

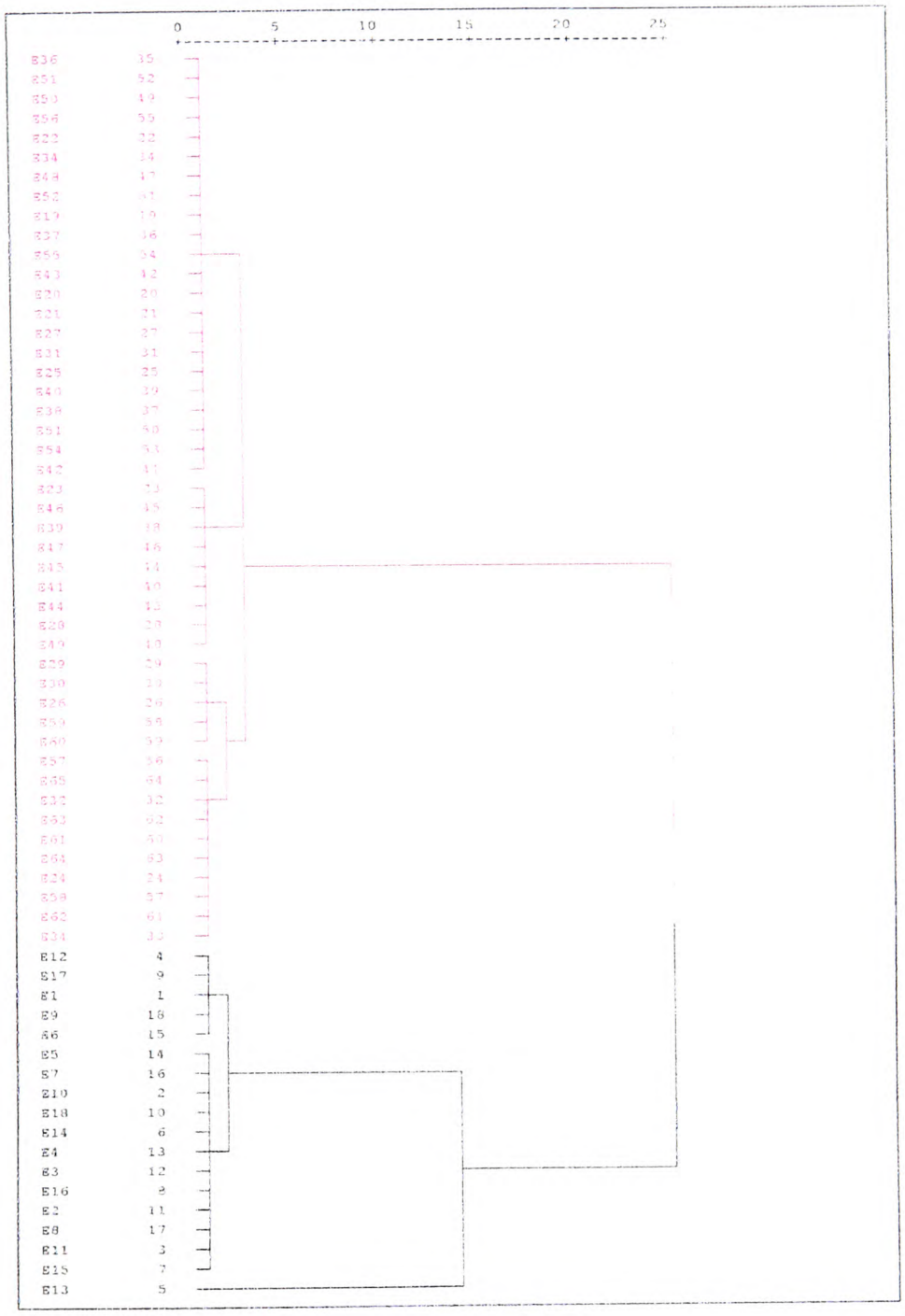

Figure 4.9 - Dendrogram showing hierarchical cluster analysis of the E set of Greek oils by geographical origin

E13 was the only sample from the Crete set which did not cluster well. A study of the oil's origin (Table 2.4) gave no indication of any obvious anomaly in the growing or harvesting conditions. This sample was consistently marked as an outlier in the regression plots used for adulteration prediction and was omitted from further investigations.

Figure 4.10 shows the Cooman's plot for the classification of Crete (red) and non-Crete (green) pure oils from the E set. It gave very good separation for the two models, which were obtained using PCA on selected peaks in the ^{1}H NMR spectra. The selected peaks (Table 4.3) gave better separation than models based on full spectral data. The blue samples were test vectors that were omitted from the original PCA models and in all cases were correctly classified as either Crete or non-Crete oils. The peaks selected all arose from protons in the fatty acid component of the olive oil. Previous work has used the minor volatile compounds to assess geographical origin (Sacco *et al.*, 2000) deeming the fatty acid profile to be inconclusive.

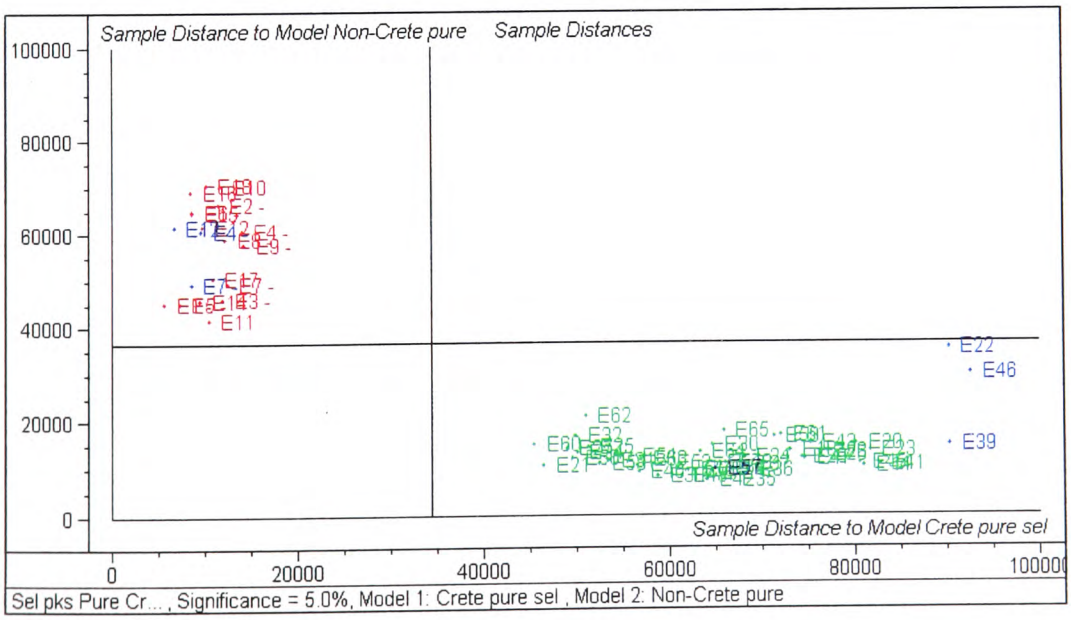

Figure 4.10 – Cooman's plot showing geographical differentiation within the E set. Red = Crete oils, green = non-Crete oils, blue = test samples

NMR Measurements were not taken for the non-Crete oils from the F set, therefore, geographical comparison of the F series could not be undertaken.

4.3.2.2 Harvest Differentiation

Principal Component Analysis was carried out on the E and F oils as a whole data set to ascertain whether separation was possible using all variables. The scores (Figure 4.11) and loadings (PC1) plots (Figure 4.12) detail which variables were paramount in differentiating between the E and F oils. The first principal component described the majority of the variance detected in the oils as shown by the close scores observed for the two groups of samples along PC 1. Samples with positive scores have higher than average values for variables with high positive loadings on the same PC. Therefore, variables that are positive in plot B (loadings on first PC) are the variables which describe the samples that have positive scores for PC1 (E set). Variables with negative loadings for PC1 are correlated with samples with negative scores for that PC (F set).

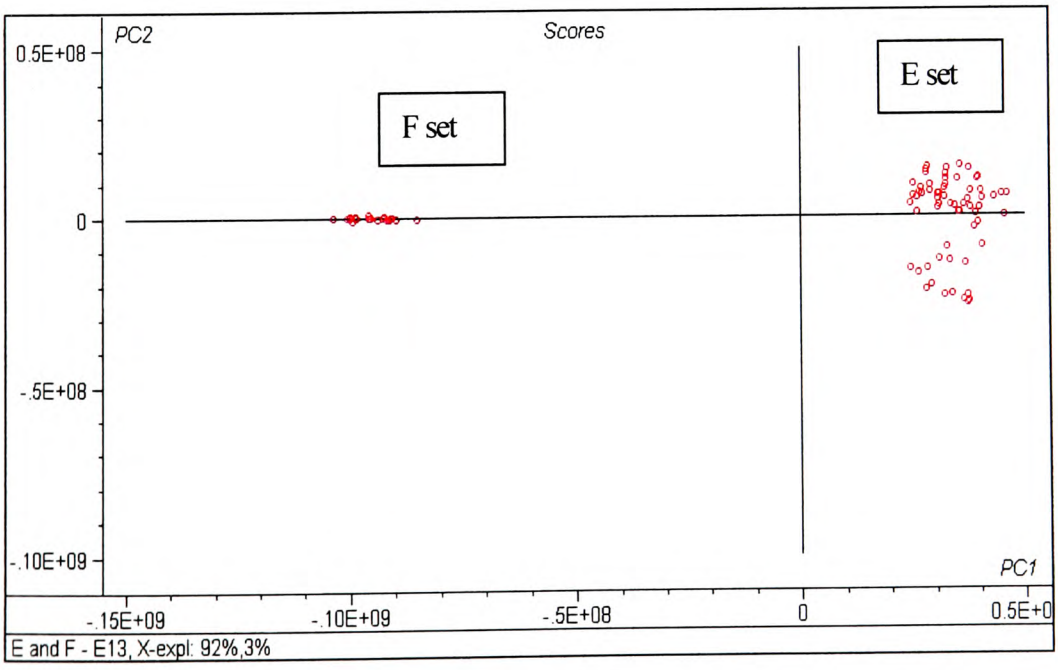

Figure 4.11 – PCA Scores plot for E and F oils, PCs 1 and 2

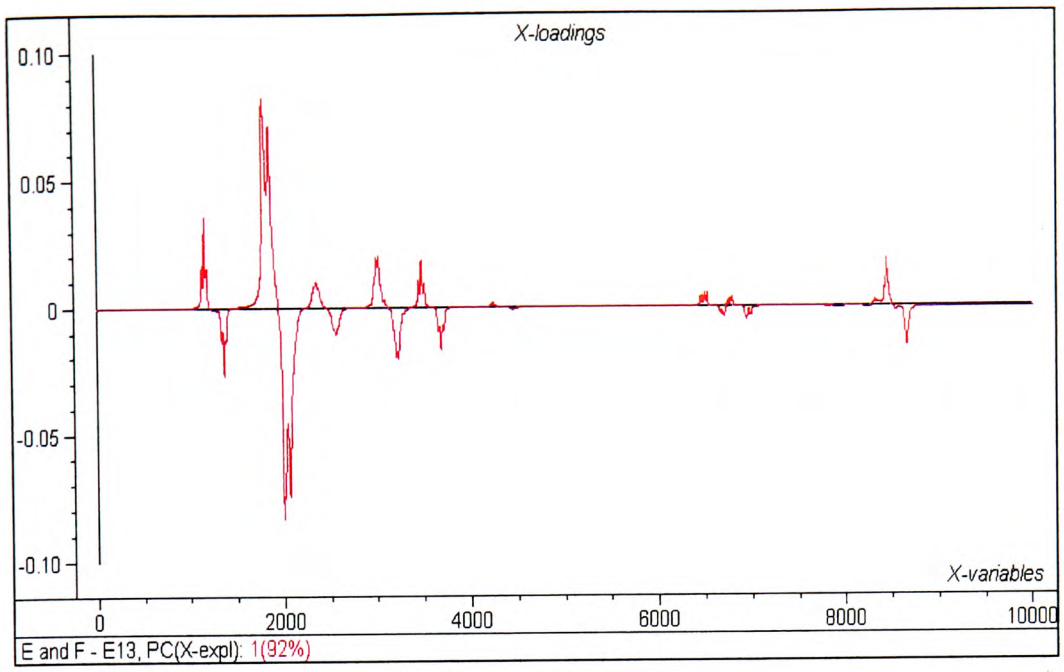

Figure 4.12 - Loadings (PC 1) plot for PCA of E and F pure oils

This suggested that the following peaks (Table 4.7) described the model for the F set of oils and differentiated it from the E set model. Peaks reference Figures 4.3 and 4.4.

Table 4.7 – ^{1}H NMR Peaks important to the F set as suggested by the loadings plot (PC1) from PCA models using all variables

Chemical shift (ppm)	Peaks
0.81 – 0.84	H10 (terminal linolenyl methyl)
1.20 – 1.30	H9 all acyl chains (C***H*****$_2$**)*n*
1.53 – 1.59	H8 all acyl chains (C***H*****$_2$**CH_2COOH)
1.93 – 1.99	H7 unsaturated (C***H*****$_2$**$CH=CH$)
2.22 – 2.28	H6 all acyl chains (C***H*****$_2$**$COOH$)
5.24 – 5.30	H1 unsaturated (C***H***$=CH$)

Figure 4.13 shows the Cooman's plot classification of Crete oils from two harvest years. The oils originating from the 1995/96 harvest (E set) are shown in red, those from the

1996/97 harvest (F set) are shown in green and test samples (blue crosses) which were all correctly identified to their year of origin. The classification was based on PCA models using all variables.

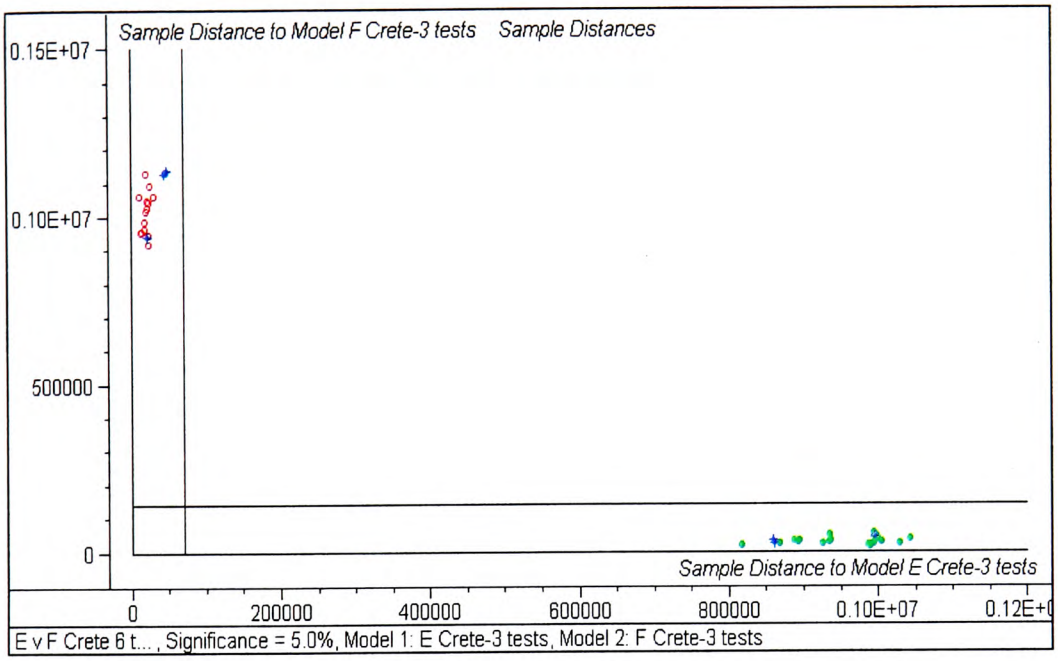

Figure 4.13 -Cooman's plot showing harvest differentiation in Crete oils. Red = 95/96, green = 96/97, blue = test samples

4.3.2.3 Adulteration Determination

Regression plots were obtained using PLS1for all adulterated samples from the E and F sets. Using all oil samples for a single regression plot produced a plot with a RMSEP of 2.09% sunflower adulteration. As it has been shown that the Crete and non-Crete oils vary sufficiently in their fatty acid profile to allow satisfactory separation of the two models (Figure 4.10), it was perceived that this could adversely affect the analysis, leading to the Crete and non-Crete oils being treated separately. Figure 4.15 shows the predicted v measured % sunflower adulteration plot for the E set of Crete oils over all variables, giving an RMSEP of 1.65% sunflower adulteration and offset of 0.511% using

9 principal components, as suggested from Figure 4.14, the residual validation variance plot. Regression plots were also acquired for Crete and non-Crete samples using only the proton signals arising from the CH_2 between unsaturated carbons (2.6 ppm) and the CH on the C=C (5.2 ppm), H5 and H1 respectively in Figures 4.3 and 4.4. The error of prediction observed using specific peak picking was greater than with the full spectral data. Plots in Appendix C.

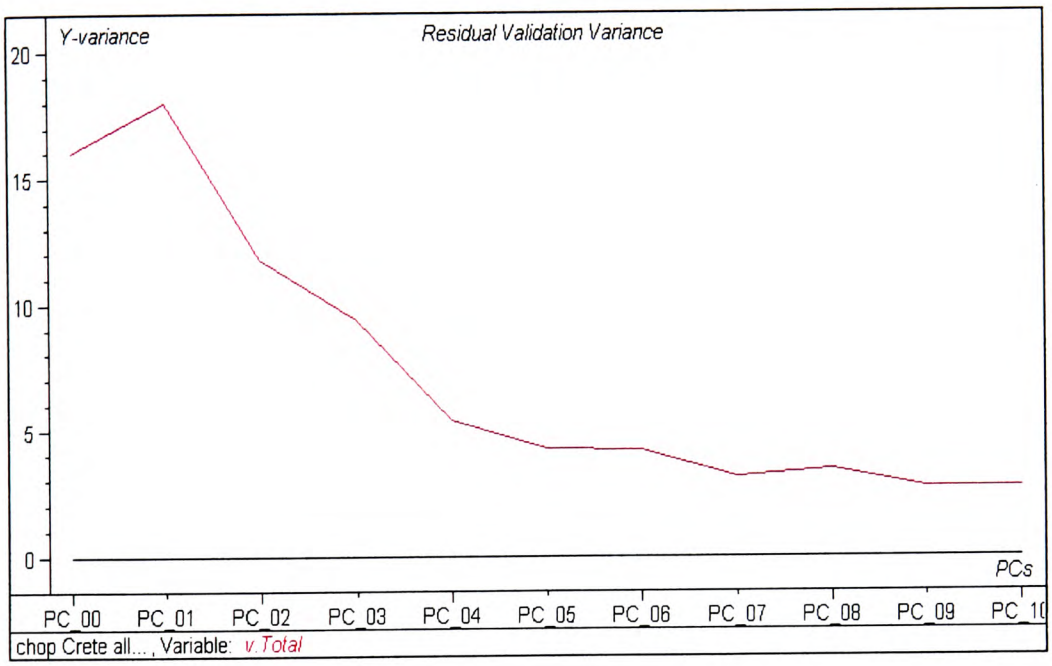

Figure 4.14 – PLS 1 residual validation variance plot for E set Crete

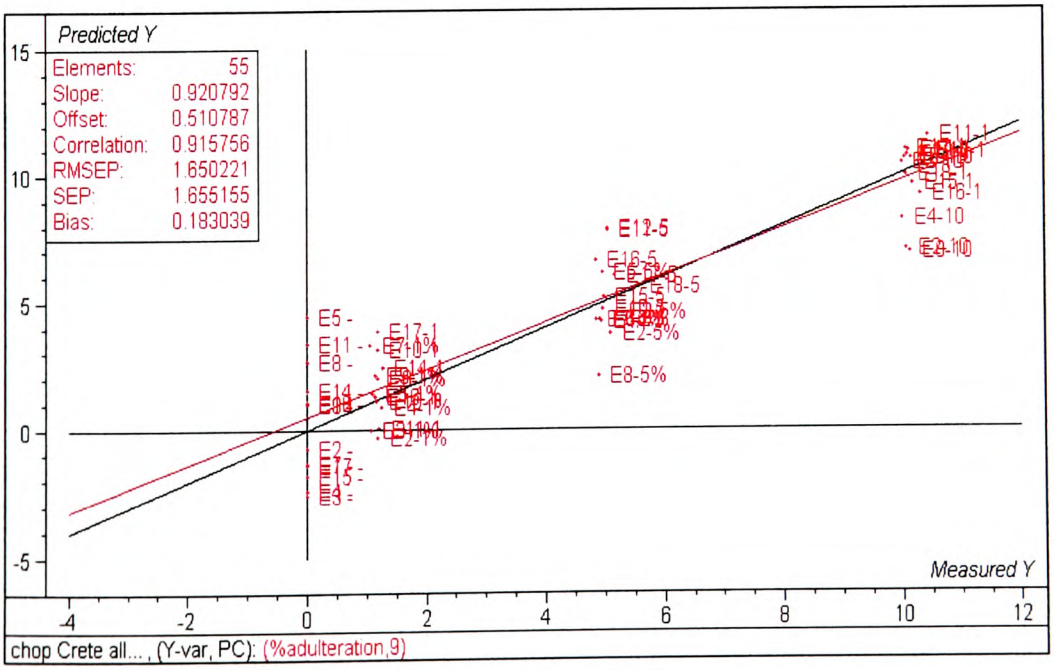

Figure 4.15 - E set Crete PLS1 over all variables, predicted v measured sunflower adulteration using 9 PCs

A root mean squared error of prediction of 1.56% sunflower oil was calculated for the non-Crete E set over all variables (Figure 4.17), using 10 principal components (Figure 4.16).

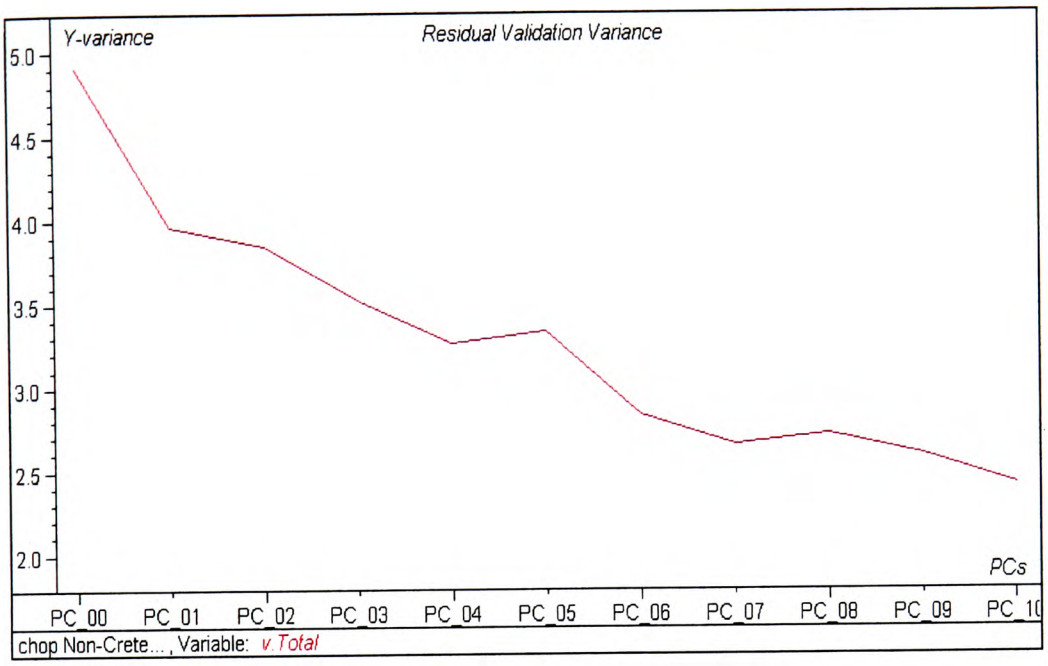

Figure 4.16 – PLS1 E set non-Crete oils, residual validation variance plot

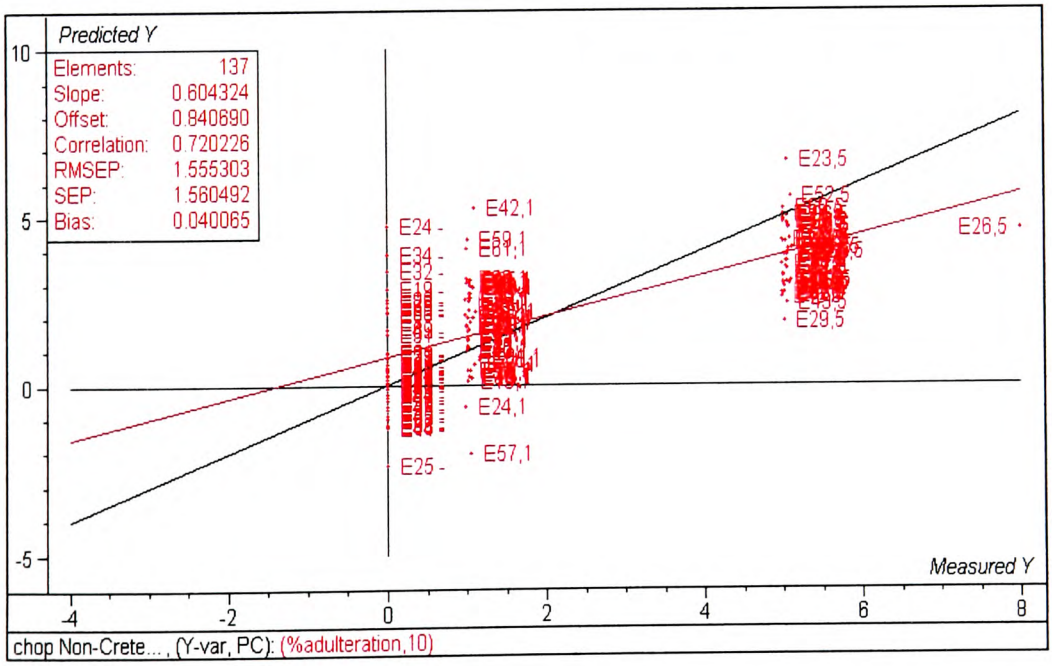

Figure 4.17 – PLS1 predicted v measured % sunflower adulteration for E set, non-Crete oils

The data collected from the F set, Crete oils did not give good statistical results. The initial principal components extracted little of the information deemed to be relevant and

the majority of the samples were marked as outliers, therefore not producing a statistically robust model (Appendix C).

4.4 CONCLUSIONS

4.4.1 ^{13}C NMR

^{13}C NMR has been reported to be a viable method of detecting adulteration of olive oil when the adulterant has a high linoleic/linolenic acid content (Sacchi *et al.*, 1997; Vlahov, 1997; Zamora *et al.*, 2001).

The ^{13}C NMR method employed in this work had a long acquisition time to allow for the long ^{13}C relaxation times. A long acquisition time limits the quantity of samples that can be tested and also increases the possibility of magnetic field drift which adversely affects the resolution of the carbonyl region. The peaks also overlap in the carbonyl region, which complicates interpretation.

The presence of nuclear Overhauser enhancement gives better signal to noise ratio but the spectra are not quantitative. To overcome this problem an inverse polarisation pulse sequence was investigated but needed an untenable acquisition time. It was therefore decided to be an impractical method.

4.4.2 ^{1}H NMR

Proton NMR has been shown to be a rapid, dependable method of analysing olive oils. The statistical analysis of the Greek oils was able to differentiate between oils originating from Crete and those from the rest of Greece. This suggests that the growing conditions

on the island of Crete vary sufficiently to those encountered in other Greek areas, to alter the composition of the fatty acid profile of the oil. The conditions (on Crete) also appear to fluctuate from harvest to harvest as the models produced for each harvest year were clearly distinguishable, and gave 100% classification when tested. Previous work with the sample sets (Lees *et al.*, 1998) had characterised the fatty acid composition of some of the oils by GC (Appendix A). This limited information showed that the concentration of linoleic acid (18:2) tended to be lower in samples from the F set in comparison to analogous samples from the E set. The difference in rainfall during the ripening and harvesting stages has been cited as a possible contributor to the variance in linoleic acid content that allowed harvest differentiation. Mainland Greece had a higher rainfall during the 1996/97 (F) harvest period than for the previous harvest year (E) 1995/96. The majority of cultivars grew the same olive variety, Koroneiki, suggesting that climatic conditions were responsible for the variation in fatty acid composition. The influence of growing area and weather conditions on the fatty acid profile of the oils was investigated by a Greek study. They concluded that oils originating from low-altitude areas with a high temperature had a higher content of saturated acids and agreed with earlier reports that increased humidity produced oils with lower percentages of 18:1 (oleic acid). Areas of high altitude and therefore a cooler climate produced oils with higher levels of 18:1 (Stefanoudaki *et al.*, 1999). Therefore, the increased rainfall could account for the increase in C18:1 observed in oils in the F set and hence influenced the PCA models which attributed the majority of the harvest differentiation to peaks arising from the accompanying fluctuation in C18:2.

CHAPTER 5

5 Infrared (IR) Spectroscopy - Fibre Optic Probe

5.1 THEORY AND TECHNIQUE

Infrared (IR) absorption spectroscopy is the measurement of the intensity and wavelength of the absorption of infrared light by a sample. Mid IR (4000 - 400 cm^{-1}) is energetic enough to excite molecular vibrations to higher energy levels during which the dipole moment must change for a molecule to absorb IR radiation. The wavelengths of many IR absorption bands are characteristic of specific types of chemical bonds and can therefore be used to identify unknown samples. Mid IR spectroscopy has been widely used in research on fats and lipids (Lai *et al.*, 1994; Lai *et al.*, 1995; Dupuy *et al.*, 1996) but near-infrared (NIR) is becoming more extensively used both for adulteration determination and fatty acid characterisation (Sato, 1994; Wesley *et al.*, 1995; Wesley *et al.*, 1996; Hourant *et al.*, 2000). Molecular absorption of energy in the near-infrared region (14000 - 4000 cm^{-1}) results from the excitation of overtones and combinations of the fundamental vibrational modes that give rise to mid-IR absorption (Cast, 1995). This type of absorption is only observed for bonds involving hydrogen and is generally a weak absorption. Therefore, NIR provides less detailed structural information than mid-IR and is of less value in qualitative work than in quantitative work (Colthup *et al.*, 1990).

Fourier Transform Infrared Spectroscopy (FTIR) was developed in the late 1960s and uses an interferometer, typically a Michelson interferometer (Figure 5.1), to encode frequency and intensity information in the signal. This eliminates the need for a prism or a grating to disperse the radiation emitted by the infrared source into its component

wavelengths. Interferometry increases the speed of data collection, increases signal-to-noise ratio, increases the wavelength precision by the use of an internal reference laser and gives a higher energy throughput (Guillen *et al.*, 1997).

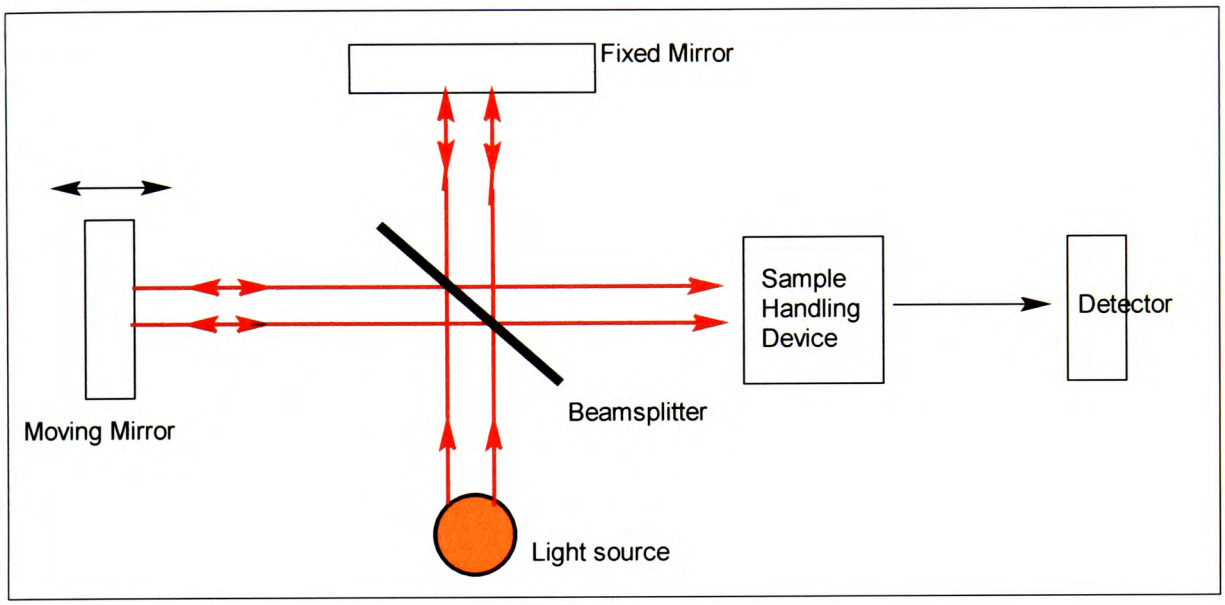

Figure 5.1 - Schematic of a Michelson Interferometer

The beam of light is divided into two equal components by a beamsplitter in an interferometer, one component travels to a fixed mirror and the other travels to a moving mirror. A laser beam tracks the moving mirror. The two beams recombine at the beamsplitter after being reflected back by the mirrors and produce a constructive/destructive interference pattern due to the varying differences in the distances travelled by each component. Half of the recombined IR beam is reflected to the sample where is it selectively absorbed by the sample. The other half of the beam is reflected back to the source. The detector response is measured continuously and the analogue signal is converted to a digital signal, thereby giving an interferogram, which is a plot of the spectral data in the time domain. A fast Fourier transform (FFT) algorithm converts it to the frequency domain and the resulting spectrum is a plot of the intensity reaching the detector against the frequency of the radiation. The transmittance spectrum

is obtained by digitally ratioing this spectrum against the emittance spectrum of a blank sample (Cast, 1995).

Attenuated Total Reflectance (ATR) is often used for sampling oils using IR (Bertran *et al.*, 1999; Li *et al.*, 2000). ATR devices are based on the phenomenon of the total internal reflection of light. The measurement of the energy of the total internally reflected light as a function of frequency gives the absorption spectrum. The sample is placed in contact with an internal reflection element, which is generally a crystal of an IR transmitting material of high refractive index (Cast, 1995).

5.2 LITERATURE REVIEW

NIR has been used to classify a range of oils and fats following fatty acid quantification by high-performance gas chromatography (HPGC), to show that only a minimal number of selected bands need be statistically analysed, with stepwise linear discriminant analysis (SLDA) to classify a large data set (Hourant *et al.*, 2000). NIR with statistical analysis using Principal Component Analysis (PCA) successfully classified different vegetable oils (Sato, 1994). They found that the oils separated along the second PC with oils with the highest degree of unsaturation to the right of the plot. As the degree of unsaturation decreased the plots moved to the left of the scatter plot. PCA and PLS were both used to measure the adulteration of virgin olive oils using refined olive oil, corn and sunflower oil (Wesley *et al.*, 1995) and the same authors extended this work to successfully identify specific adulterants (Wesley *et al.*, 1996).

The use of Fourier transform infrared (FTIR) spectroscopy (mid-IR) has been investigated to discriminate between extra virgin and lower grades of olive oil (Lai *et al.*, 1994), resulting in the development of a successful discriminant model with a very short analysis time (2 - 3 minutes). The same authors expanded this work by investigating the potential of quantitative analysis using FTIR spectroscopy combined with attenuated total reflectance (ATR) and multivariate analysis (PLS) to determine levels of walnut and refined olive oil adulteration (Lai *et al.*, 1995). Their results showed that the technique has potential, the lowest standard error of prediction (SEP) being for the addition of walnut oil to extra virgin oil (0.68 g / 100 g). The adulteration of extra virgin olive oil with refined olive oil gave a SEP of 0.92 g / 100 g.

A new procedure was proposed for determining free fatty acids (FFA) in olive oil using FTIR-ATR spectroscopy and PLS regression statistical evaluation (Bertran *et al.*, 1999). They sampled olive oils of different ages, from different geographical origins and different grades of commercially available olive oils. They concentrated on two wavenumber ranges (1775 - 1689 and 1480 - 1050 cm^{-1}) and employed extensive pretreatment methods before statistical assessment. PCA of FTIR spectra of fats and oils including sunflower seed oil, olive oils and peanut oils have been studied for classification using two spectral ranges, 3060 - 2750 cm^{-1} and 1500 - 1000 cm^{-1} to reduce the number of data points (Dupuy *et al.*, 1996). The concentration of polyunsaturated fatty acid ester allowed characterisation of the sunflower oil compared with the olive or peanut, whereas separating olive and peanut samples proved difficult and inconclusive. A comparison of mid-IR and Raman techniques to classify and detect adulteration in edible oils (Marigheto *et al.*, 1998) led the authors to conclude that IR was a more reliable method than Raman for both purposes. Detection limits of 5% adulterant were

achieved with IR even when the adulterant was refined olive oil. Raman spectral quality, in terms of signal to noise, is significantly less than for IR. They also found that linear discriminant analysis (LDA) based on PLS data gave better classification results than artificial neural networks (Marigheto *et al.*, 1998). CO_2 laser Infrared Optothermal Spectroscopy determined the limit of detection for adulteration with sunflower and safflower oils to be 5% w/w (Favier *et al.*, 1998) and the possibility of lowering the detection limit was discussed by using a more stable, discretely tunable CO_2 laser.

The advantages of FTIR over dispersive IR was discussed and techniques highlighted to show the usefulness of FTIR (Guillen *et al.*, 1997). They reviewed procedures that could be used to:

- Determine the degree of unsaturation from the absorbance of the -C=C- stretching band at 1658 cm^{-1} or the olefinic band at 3007 cm^{-1}. The ratio of absorbances of olefinic and aliphatic -C-H stretching vibration bands could also be used.
- Determine the *trans*- unsaturation content and the free fatty acid content.
- Determine the saponification number and solid fat index by combining FTIR with PLS regression statistics.
- Determine peroxide and anisiding values, both of which refer to the concentration of primary or secondary oxidation products of oils.

They concluded that FTIR was an extremely valuable quantitative technique that was efficient, low-cost and simple to use.

5.3 FIBRE OPTIC PROBE

The fibre optic probe used for this work was developed at the Institute for Spectrochemistry and Applied Spectroscopy (ISAS), Dortmund, Germany and utilises a diamond at the tip to act as a prism. The parallel beam from the infra-red spectrometer is focussed by an off-axis parabolic mirror onto the illuminating fibre. A lens at the end of this fibre focuses the light, to allow two internal reflections in the sensor head, the diamond, which is immersed into the sample to be measured. Following detection the detecting fibre takes the beam to the detector. The detector was a liquid nitrogen cooled semiconductive mercury-cadmium-telluride (MCT) detector. In front of the detector element is a lens, which focuses the light onto a 1 x 1 mm detector. The signal is amplified by a pre-amplifier, which is matched to the detector to ensure low noise. The resulting interferogram is Fourier transformed to give the IR spectrum. Figure 5.2 shows a schematic diagram of the probe interfaced to a spectrometer, Figure 5.3 shows a photograph of the probe and Figure 5.4 shows the detector.

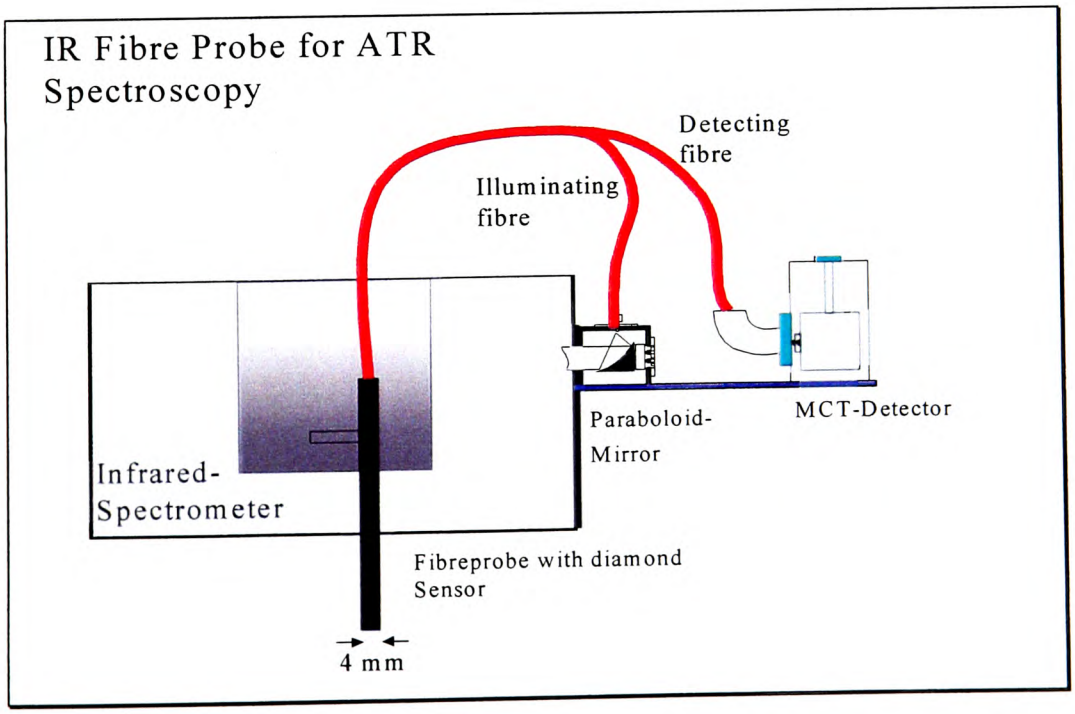

Figure 5.2 – Schematic of the I/R Fibre Probe for ATR spectroscopy

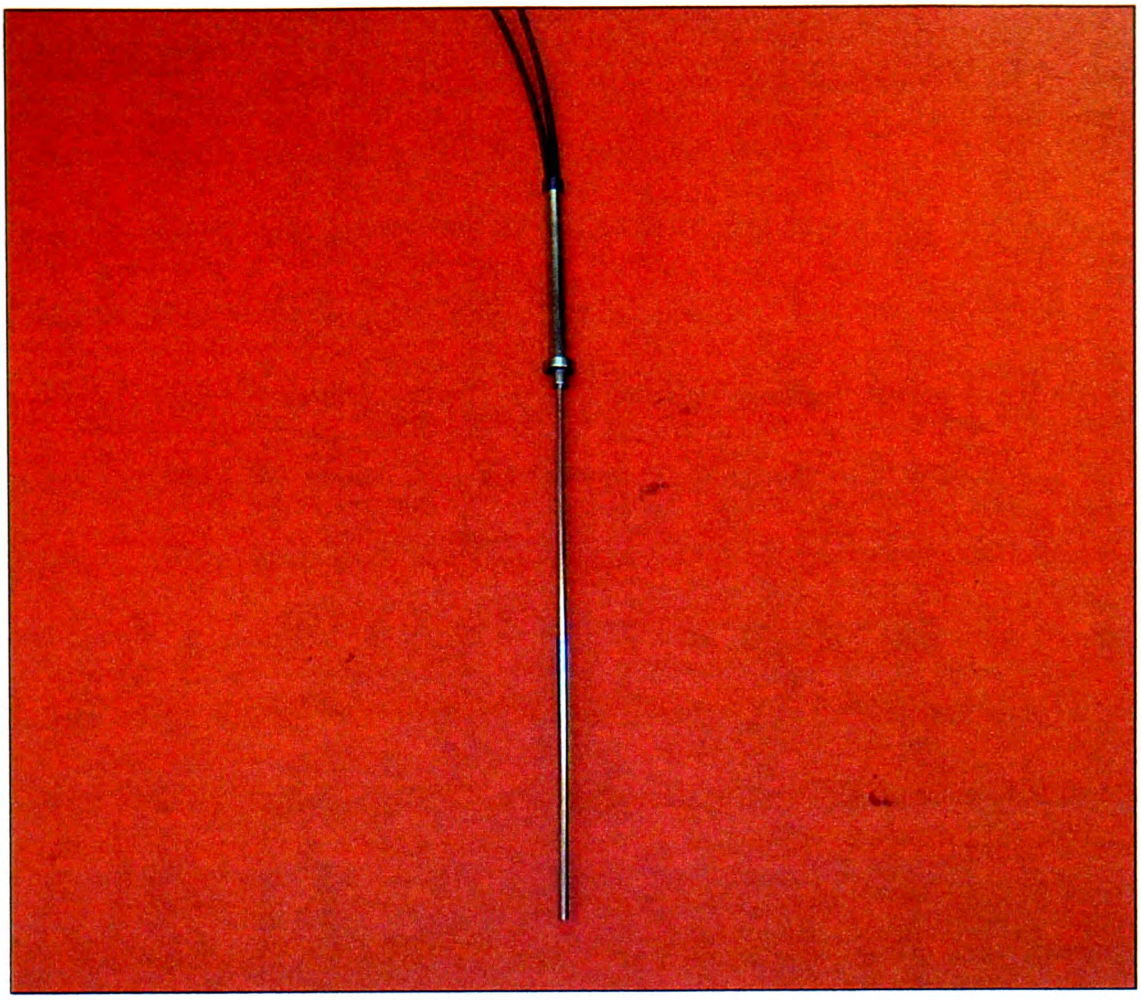

Figure 5.3 - Photograph of the diamond tipped probe

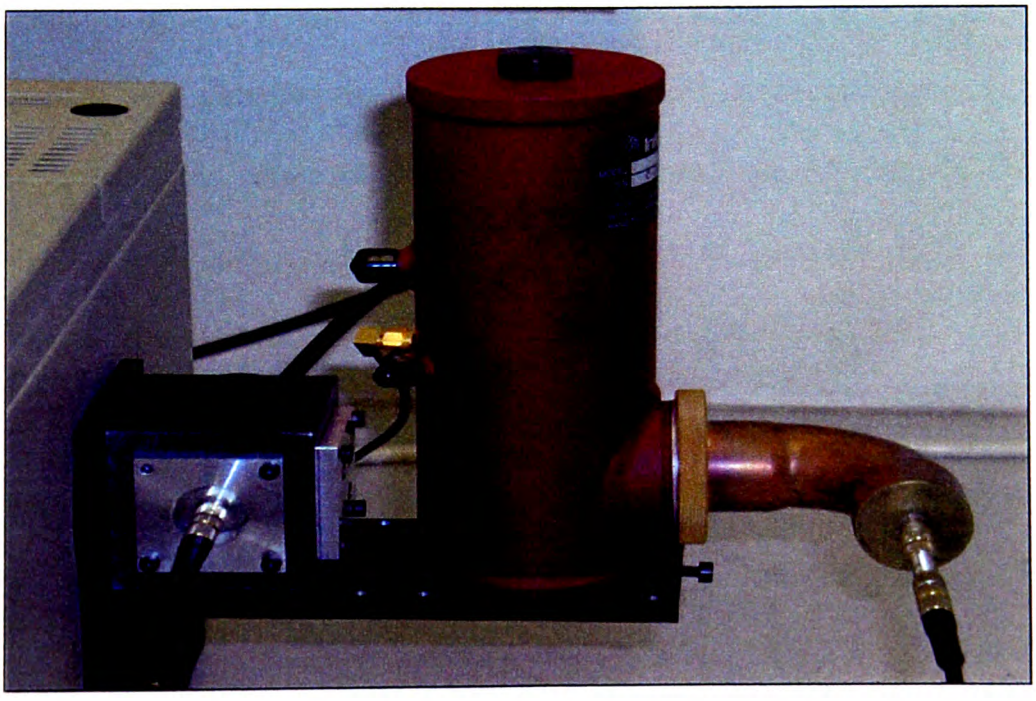

Figure 5.4 - Photograph of the MCT detector interfaced to an IR spectrometer

5.4 METHOD

5.4.1 Greek olive oil sampling with the diamond probe

Measurements were obtained for all 88 samples in the D set (all adulterated), 117 samples in the E set (all pure and Crete oils adulterated). The 109 samples in the F set (Crete oils adulterated and all pure oils) had previously been measured by ISAS and the data made available for statistical comparison. 128 scans were performed for each measurement with a resolution of 4 wavenumbers. Background measurements were recorded every 8 samples to compensate for any possible drift, e.g. change in temperature of the source. The diamond tip and lower casing of the probe, which came into contact with the sample, were cleaned following every measurement using ethanol and dried in nitrogen gas. The spectra were stored as galactic (.spc) files.

5.4.2 Statistical Analysis

The files were imported into the Unscrambler 7.5 (Camo ASA, 1998) multivariate analysis program. PCA (Principal Component Analysis) and PLS1 (Partial least squares) regression plots were obtained for the D, E and F sets. Classification plots (Cooman's plots) were constructed using the PCA models to investigate whether the data could differentiate between geographical origin and/or year of harvest. Plots using only specific wavelength selections of 893 - 1260 cm^{-1} (HC=CH), 1610 - 1776 cm^{-1} (carbonyl), 2730 - 3060 cm^{-1} (CH) allowed the data to be analysed statistically without unnecessary peaks and noise prolonging and complicating the calculation. These selected wavelengths were chosen on the basis of their chemical importance and were used throughout the statistical analysis of the IR data. The wavelength selection corresponds to the areas in the spectrum which would be affected by an increase in

linolenic acid if an adulterant oil higher in these fatty acids, such as sunflower oil, was added to olive oil.

5.5 RESULTS AND DISCUSSION

The diamond probe provided very reproducible results. Figure 5.5 shows the overlaid spectra of the entire F series of pure oils (64 samples) over the three bands of selected wavelengths to demonstrate the reproducibility. The spectra in Figure 5.5 were plotted without any preprocessing of the data, such as normalisation or baseline correction. Based upon the spectra in Figure 5.5 it was decided that preprocessing of the data would not be necessary.

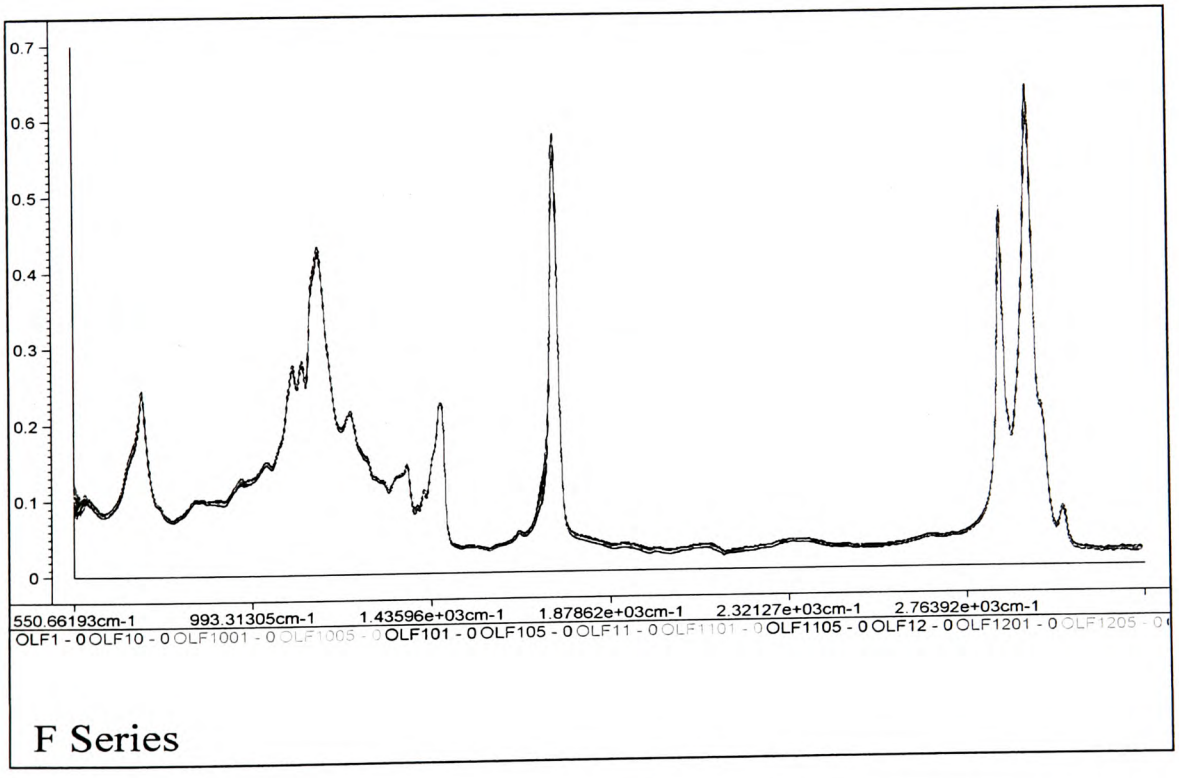

Figure 5.5 - All F series spectra plotted without normalisation or baseline correction.

Figure 5.6 shows the area around 912 cm^{-1}, and how it differs for sunflower oil and the pure E set Crete oils. The spectrum for sunflower oil is shown as a brown line and the mass of different colour lines represent the spectra of the eighteen pure oils. As seen on the spectrum there is some natural variation in the unadulterated oils which may be due to slight geographical variance, growing and harvesting conditions. The pink line (above the rest of the pure oils) represents the spectrum of E5. This oil was marked as an outlier in subsequent statistical investigations and was omitted from further analyses.

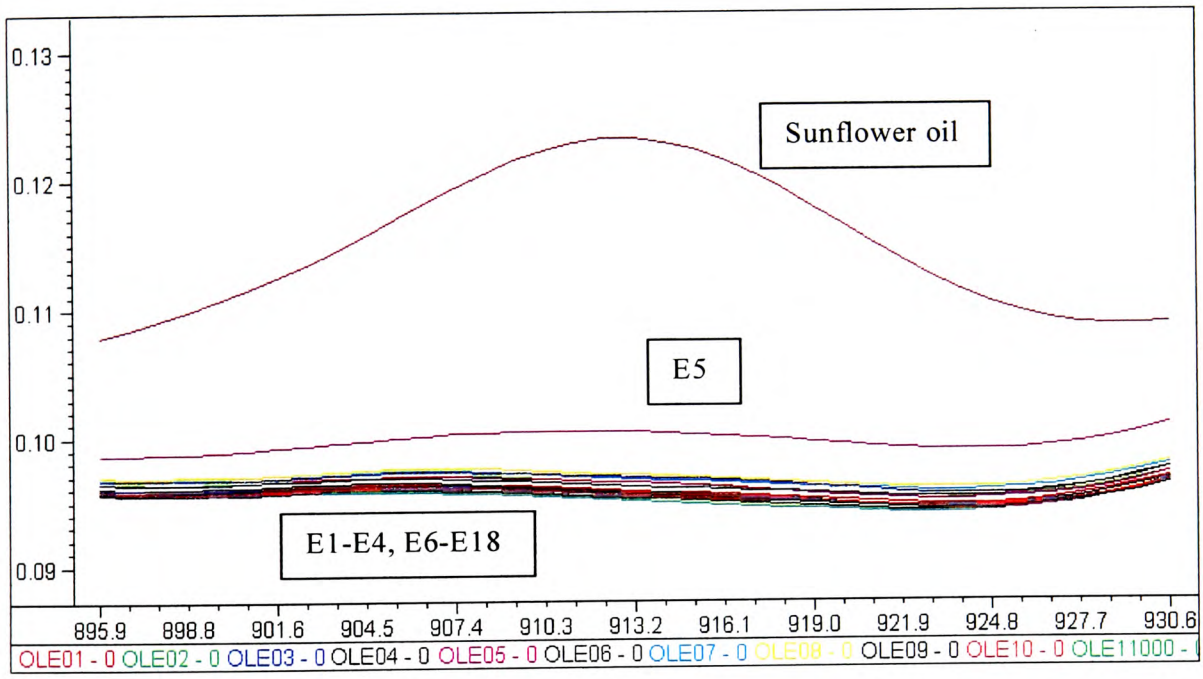

Figure 5.6 – E set Crete unadulterated oils and sunflower oil (brown) at 912 cm^{-1}

Figure 5.7 shows the effects of sunflower adulteration on the area of the IR spectrum around 912 cm^{-1}. An increase in sunflower oil increased the intensity of the peak due to the greater degree of unsaturation present in linoleic acid rich sunflower oil.

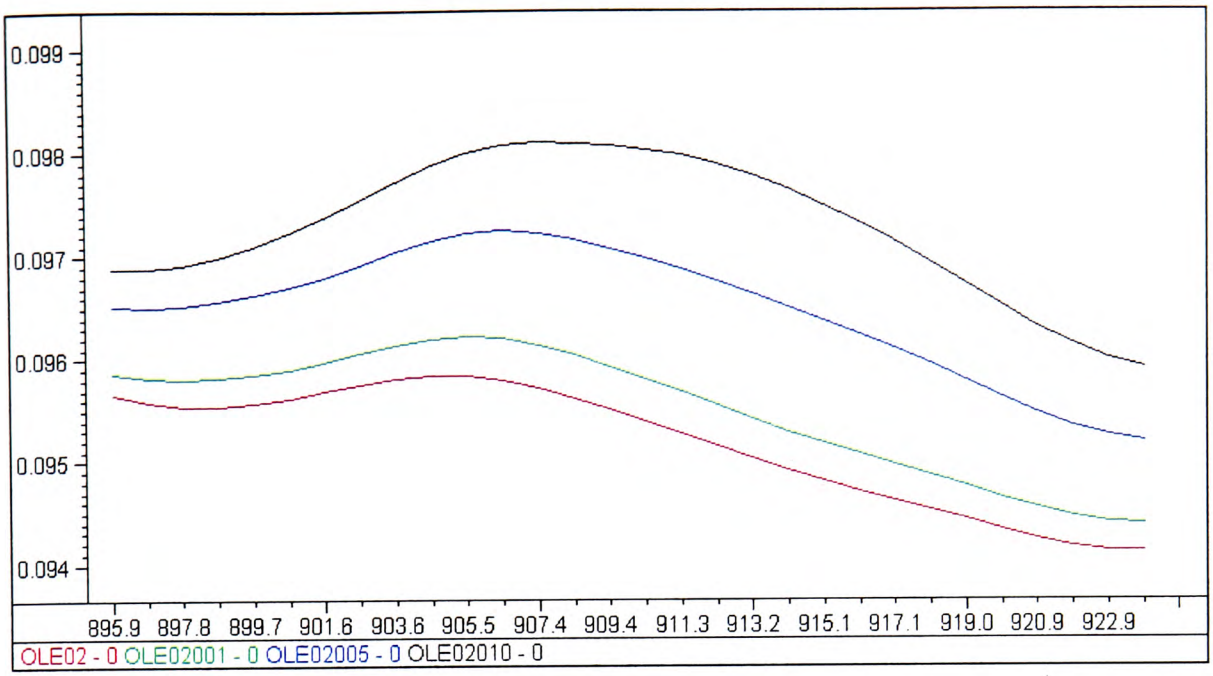

Figure 5.7 - Effects of sunflower adulteration at 912 cm^{-1}. Red = pure olive oil, green = 1% sunflower, blue = 5% sunflower and grey = 10% sunflower

5.5.1 D Set

5.5.1.1 Adulteration

The D set of oils used in this investigation were oil samples that had previously been adulterated with approximately 0, 2, 5 and 10% sunflower oil. Because the exact percentages of adulteration were unavailable, PLS1 regression plots were obtained using the approximated weights. When measuring the D set, one sample (D1 2% sunflower oil) appeared from the spectra to have been contaminated with water. This was excluded from the data set for statistical analysis. Figure 5.8 shows the predicted v measured percentage sunflower adulteration plot for the D series, which gave a RMSEP of 2.151% with an offset (y intercept) of 0.961%, using 11 principal components.

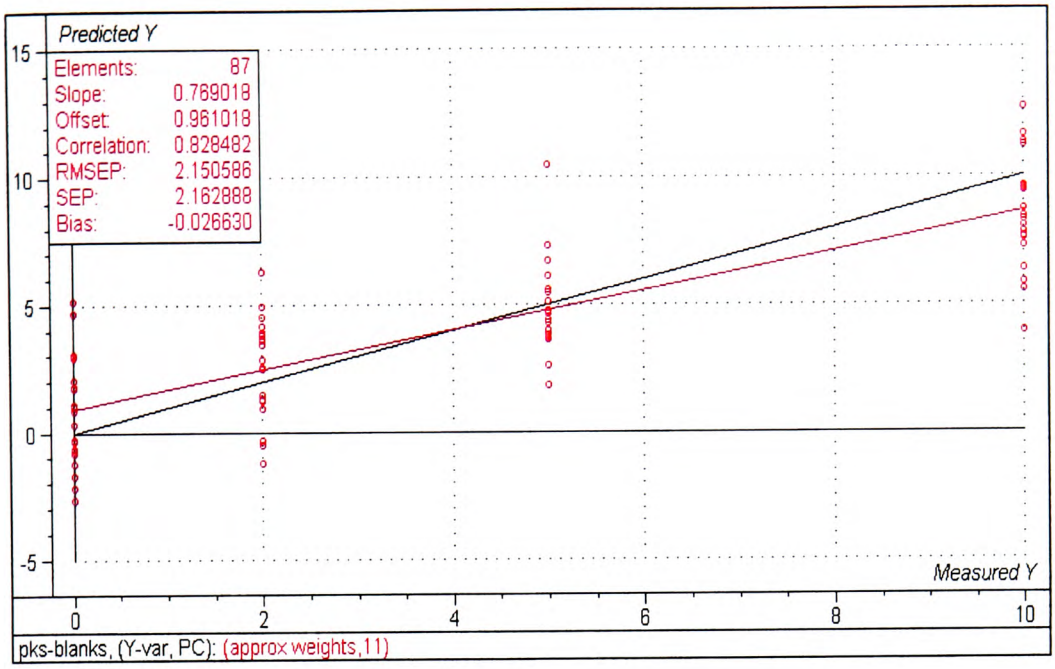

Figure 5.8 – PLS 1 regression plot, predicted v measured % sunflower adulteration plot for the entire D set of oils adulterated with 0, 2, 5 and 10% sunflower oil

5.5.1.2 Geographical Differentiation

The Crete set of oils in the D series was a much smaller sample set (D1-D6) than from the subsequent harvest years. Figure 5.9 shows the Cooman's plot resulting from the attempted classification of the samples by geographical area (Crete or non-Crete). Most of the oils are doubly classified although a few non-Crete oils (green, D7-D22) showed a degree of separation from the opposing Crete model. The models were constructed without two samples which were used as test vectors. D3 (a Crete oil) and D12 (a non-Crete oil) were omitted from the PCA models and treated as unknown oils. They were both doubly classified (as were most of the oils) and both samples (blue) were grouped with the Crete oils.

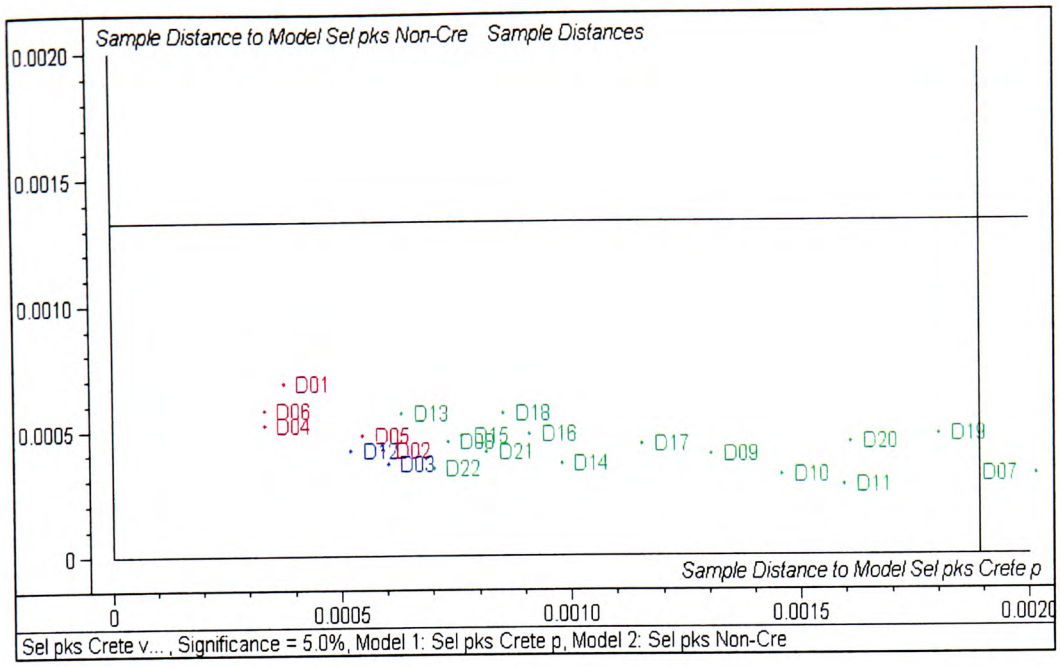

Figure 5.9 – Cooman's Plot to show geographical classification between the Crete oils (red) and non-Crete oils (green) of the D set

5.5.2 E Set

5.5.2.1 Adulteration

The Crete samples (18 oils) had previously been adulterated with 0, 1, 5 and 10% sunflower oil. Exact adulteration percentages are shown in Appendix D. Only the pure non-Crete samples (47 oils) were analysed. Figure 5.10 shows the PLS1 regression plot overview for the Crete oils from the E set using the three ranges of previously selected wavelengths (893 – 1260 cm^{-1}, 1610 – 1776 cm^{-1} and 2730 – 3060 cm^{-1}). The E5 samples were omitted from the calculation as they were marked as outliers. The plot shows the predicted versus measured % adulteration plot (bottom right), which gave an excellent RMSEP of 0.795% and offset of 0.147%, using 11 principal components (PCs) as suggested by the residual validation variance plot (bottom left).

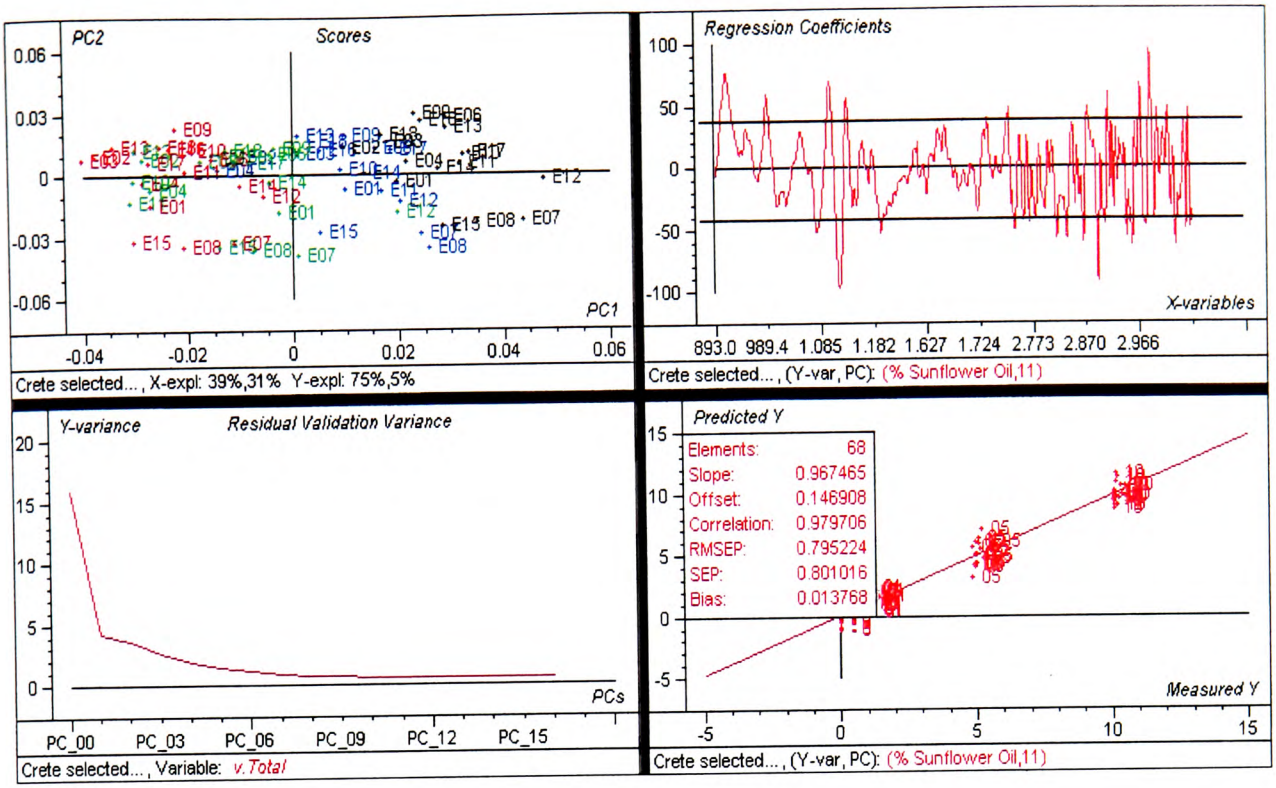

Figure 5.10 – PLS1 regression overview plot for E set Crete oils (E1 – E18) omitting an outlier (E5) over three bands of selected wavelengths

The scores plot (top left) shows that the samples group along the first PC with the pure oils (red) and the 1% sunflower adulterated oils (green) undifferentiated. The 5% sunflower samples (blue) and the 10% sunflower samples (brown) are separated along the first PC. The first PC, therefore, distinguished between the higher percentage adulterated oils (5 and 10%) and the oils with very low (1%) or no adulteration. The regression coefficients plot (top right) shows the cumulative importance of the variables and using this plot, the fifteen most important cumulative variables (peaks with the highest maxima and lowest minima) were extracted and the PLS1 regression repeated using only these variables. The variables chosen from the regression coefficient plot were; 912 cm^{-1}, 985 cm^{-1}, 1099 cm^{-1}, 1130 cm^{-1}, 1168 cm^{-1}, 1196 cm^{-1}, 1776 cm^{-1}, 2815 cm^{-1}, 2863 cm^{-1}, 2890 cm^{-1}, 2908 cm^{-1}, 2953 cm^{-1}, 2967 cm^{-1}, 2984 cm^{-1} and 3031 cm^{-1}.

The regression overview is shown in Figure 5.11. Using 9 PCs the RMSEP of percentage adulteration between the predicted and the measured samples was 0.912% with an offset of 0.235%. Although both of these values are higher than in the original regression plot, the plots show that comparable results can be obtained using a greatly reduced number of variables. The oils group along the first PC according to percentage sunflower adulteration (pure – red, 1% - green, 5% - blue and 10% - brown) with a good separation between the pure and 1% adulterated oils.

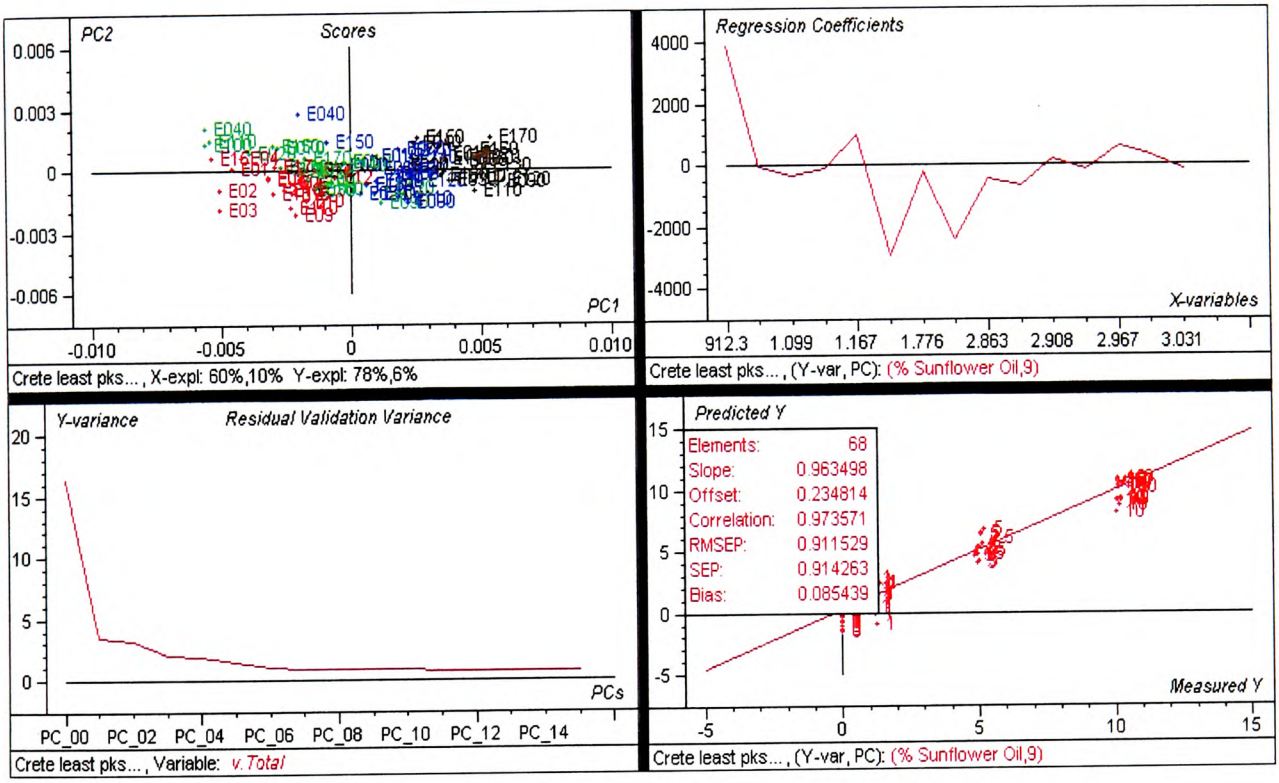

Figure 5.11 - PLS1 regression overview plot for E set Crete oils(E1 – E18) omitting an outlier (E5) using 15 wavelengths

The results were also statistically analysed using Principal Component Analysis (PCA), to determine whether satisfactory classification would allow the prediction of unknown samples. Figure 5.12 shows an example of good classification between unadulterated olive oil and olive oil adulterated with 10% sunflower oil. The Cooman's plot separated the unadulterated and adulterated oils by plotting the distance of the samples to the model set produced by PCA, using only the wavelength range around 912 cm^{-1} to

highlight how a specific area of the spectrum could be used, thereby reducing the number of necessary variables. The unadulterated oils (green) were sufficiently removed from the model produced for 10% adulteration to give good classification, shown by their position on the x-axis. The adulterated oils (red) were also well classified as they are well removed from the model produced for unadulterated oils. From the four test samples (blue), two were correctly classified as being 10% sunflower adulterated oils, one was correctly classified as a pure oil but the second pure oil (E1) was incorrectly assigned as belonging to neither class.

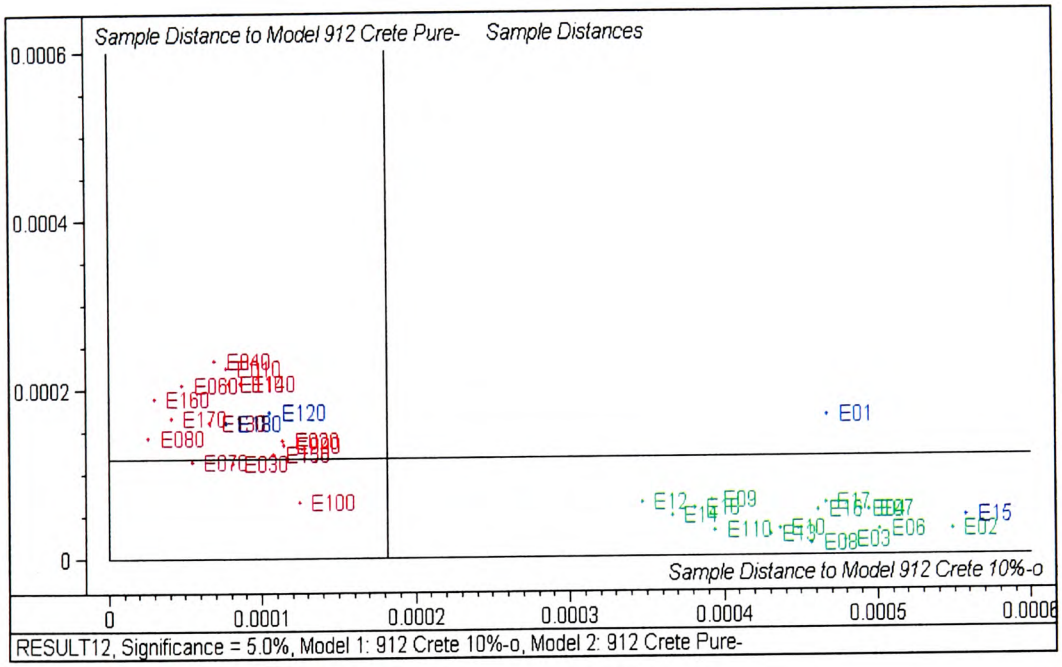

Figure 5.12 – Cooman's Plot showing good classification of E set Crete pure oils (green) and 10% sunflower adulterated oils (red) with test samples (blue).

The classification plots became less well separated as the percentage adulteration decreased, with considerable overlap between the models at 1% adulteration (Figure 5.13). The Cooman's plot showed the majority of samples in the bottom left of the plot denoting that the unadulterated oils (green) were too close to the 1% sunflower model to be discriminated from the adulterated oil (red) which were too close to the pure oil

model. They therefore overlapped and did not afford a satisfactory classification. Five test vectors were employed to test the PCA models, two pure oils, two 1% sunflower adulterated oil and an 10% sunflower adulterated oil. The models did correctly classify the 10% adulterated sample (blue E160) as belonging to neither the pure nor the 1% sunflower adulterated models and one of the pure oils (blue E15) was also assigned to the correct class. Two of the other test samples (blue, pure E01 and 1% adulterated E090) were incorrectly classified as belonging to neither class.

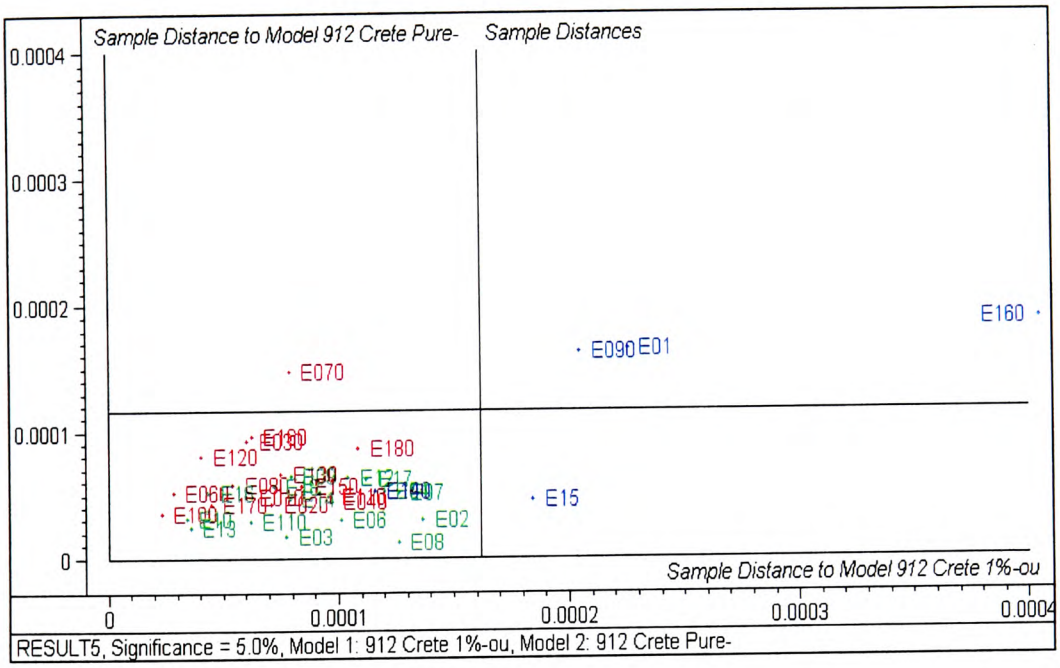

Figure 5.13 – Cooman's Plot showing classification of E set Crete pure oils (green) and 1% sunflower adulterated oils (red) with five test samples (blue)

5.5.2.2 Geographical Discrimination

PCA models were produced for the Crete oils, with the exception of the outlier E5 and the non-Crete oils, with the exception of the outlier E29. The classification plot to discriminate between the two models was calculated using the software suggested 8 PCs for the Crete model and 4 PCs for the non-Crete model. The E set showed clustering of the two representative groups (Figure 5.14) but the separation between the two models

was insufficient to predict the origin of a sample with certainty. Most of the oils were doubly classified but a few of the non-Crete oils (green) were of sufficient distance from the Crete model to be classified correctly.

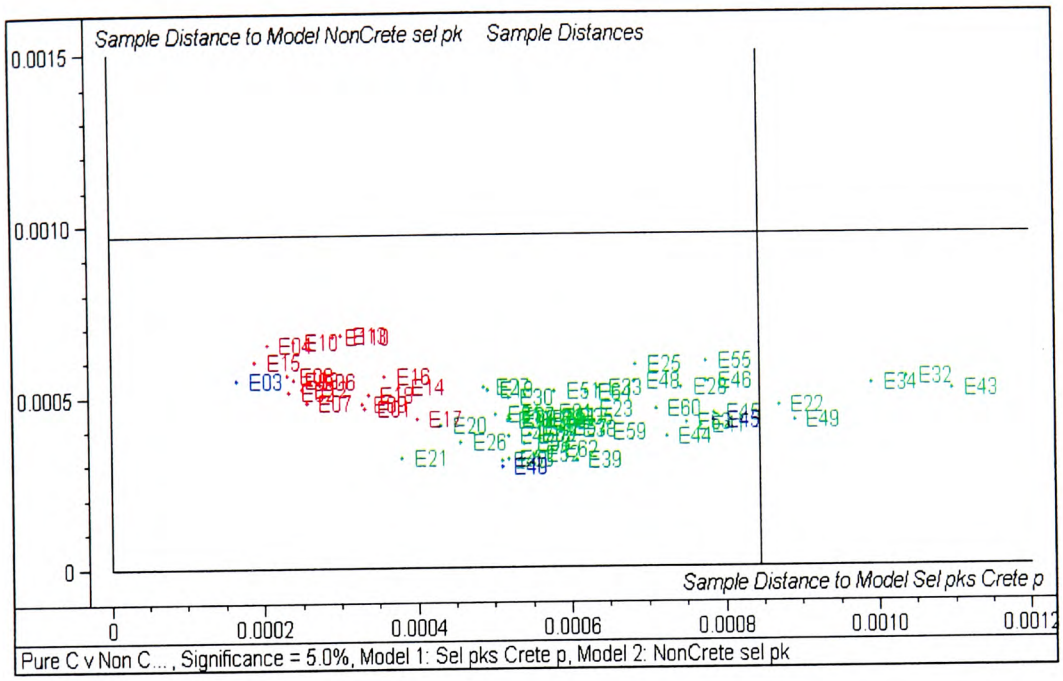

Figure 5.14 – Cooman's plot to separate Crete (red) and non-Crete (green) oils in the E set, using selected wavelengths with three test vectors (blue)

5.5.3 F Set

5.5.3.1 Adulteration

The Crete samples (22 oils) in the F series had previously been adulterated with 0, 1 and 5% sunflower oil. Exact weighings are shown in Appendix D. Only the pure non-Crete samples (43 oils) were analysed. PLS1 regression was applied to the entire F set and Figure 5.15 shows the predicted against measured percentage sunflower adulteration plot for the F series (F1-F65), using 9 PCs as suggested by the residual validation variance plot and giving a RMSEP of 1.411% and an offset of 0.549%. The three selected ranges of wavelengths used were 893 – 1260 cm^{-1}, 1610 – 1776 cm^{-1} and 2730 – 3060 cm^{-1}.

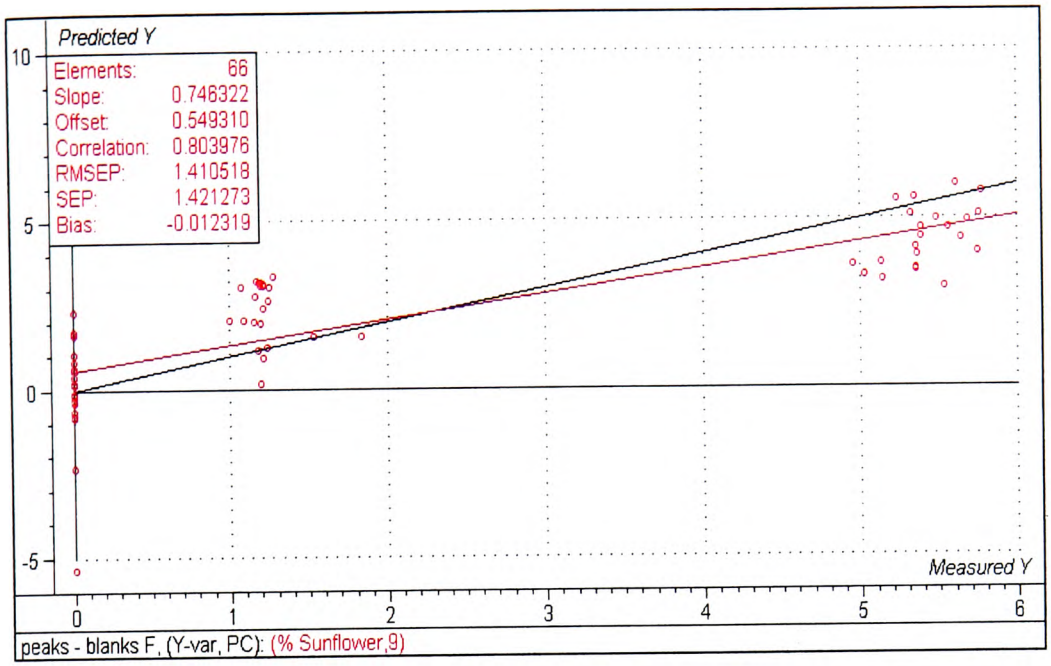

Figure 5.15 – F set PLS1 regression using three ranges of selected wavelengths, predicted v measured % sunflower adulteration using 9 PCs

Figure 5.16 gives the classification plot showing the separation between the models produced using PCA for Crete pure and 5% sunflower adulterated oils. The separation is defined although the samples were doubly classified. Four unknown samples (blue) were correctly grouped with the pure or 5% adulterated oils. A 1% sunflower adulterated sample (blue, F19) was incorrectly classified with the 5% adulterated oils.

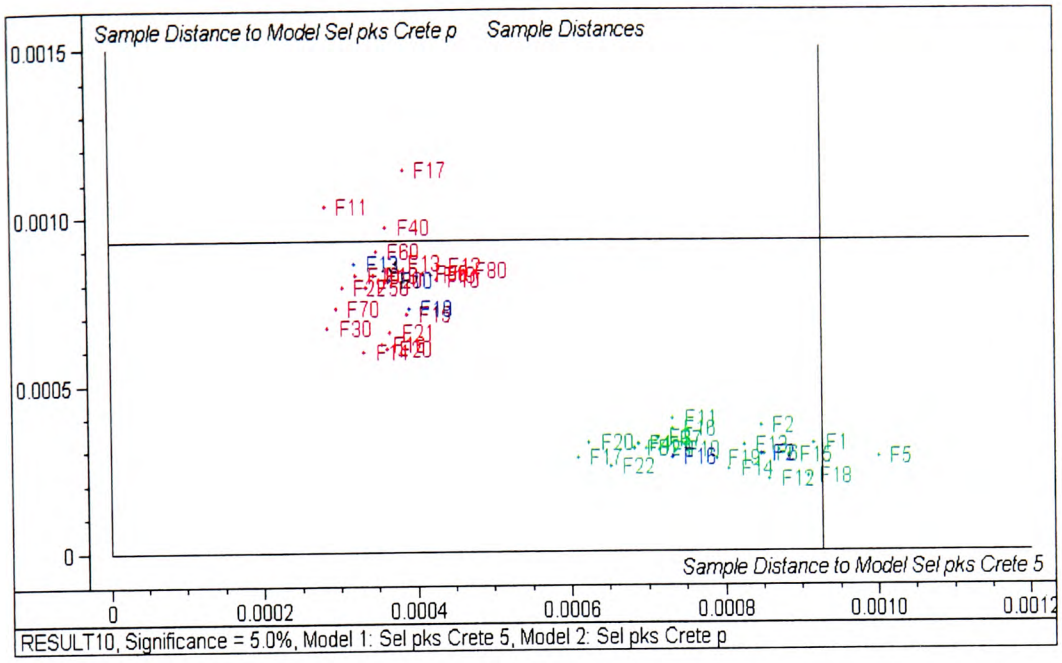

Figure 5.16 – Cooman's plot to show Crete F set pure oils against 5% adulteration

Figure 5.17 demonstrates that the separation became slightly less well defined when the adulteration was decreased to 1% sunflower oil. The unknown samples (blue) were generally correctly classified as pure or adulterated oils, although a 5% sunflower adulterated sample (blue, F10) was grouped with the 1% adulterated samples.

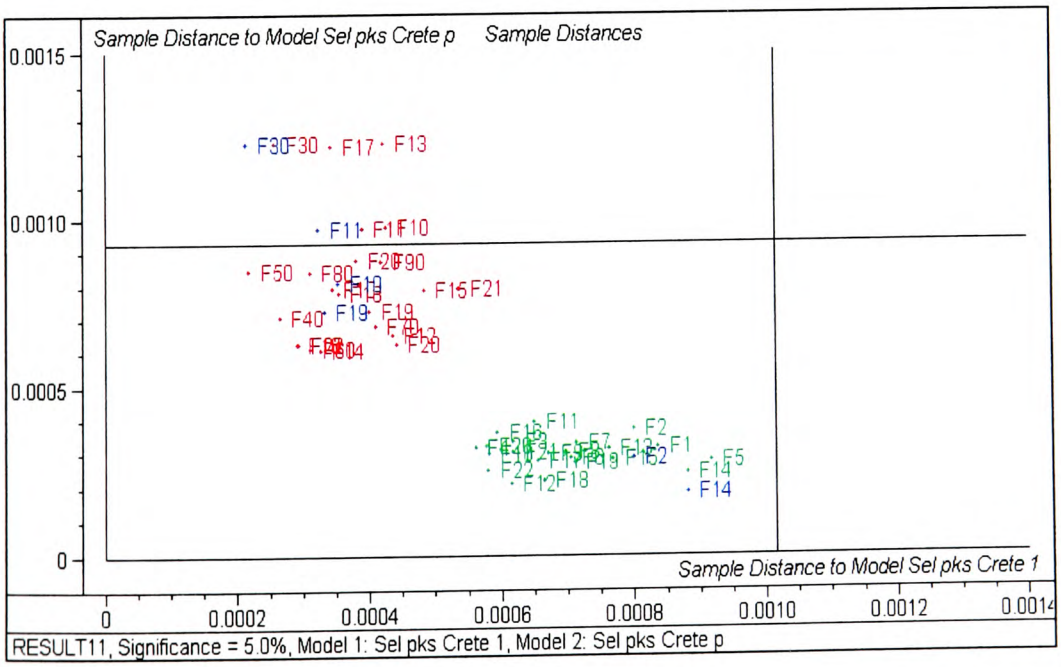

Figure 5.17 – Cooman's plot to distinguish between pure Crete F set oils v 1% sunflower oil adulterated oils

5.5.3.2 Geographical Differentiation

Attempts to classify the F set by region of origin produced similar results to the E set. As seen in Figure 5.18 all of the oils were doubly classified with some evidence of rudimentary clustering of the Crete (red) and non-Crete (green) oils. The PCA models using selected wavelengths (893 – 1260 cm^{-1}, 1610 – 1776 cm^{-1} and 2730 – 3060 cm^{-1}) were constructed without six samples which were treated as unknown test vectors. Three of the unknown test samples (blue) originated from Crete (F7, F11 and F17) and three from other areas of Greece (F32, F41 and F61). They all grouped correctly with their respective classes of oils although all the samples appeared in the region of double classification (bottom left) of the Cooman's plot, therefore not showing satisfactory separation.

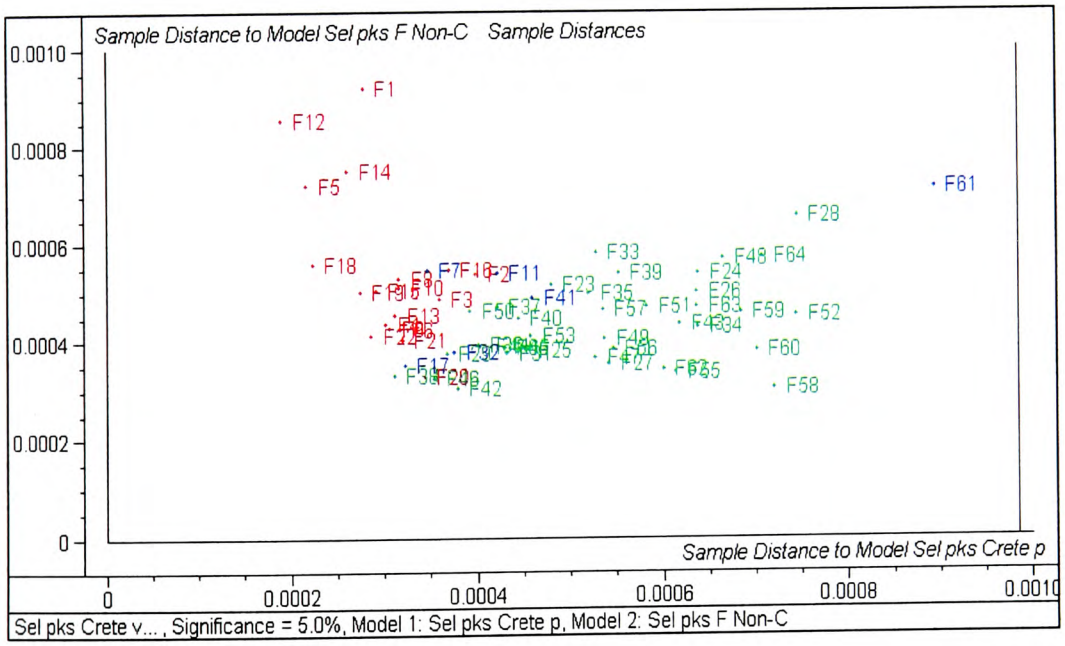

Figure 5.18 – Cooman's plot to show F set geographical differentiation, Crete (red) v non-Crete (green) with test vectors (blue)

5.5.4 Harvest Differentiation

Figure 5.19 shows a Cooman's plot classifying an oil from the F set (blue) onto models obtained from the PCA analysis of non-Crete oils from the D (red) and E sets (green). It

correctly assigns the F set oil as belonging to neither the D nor E models, although the separation between the D and E models was not complete.

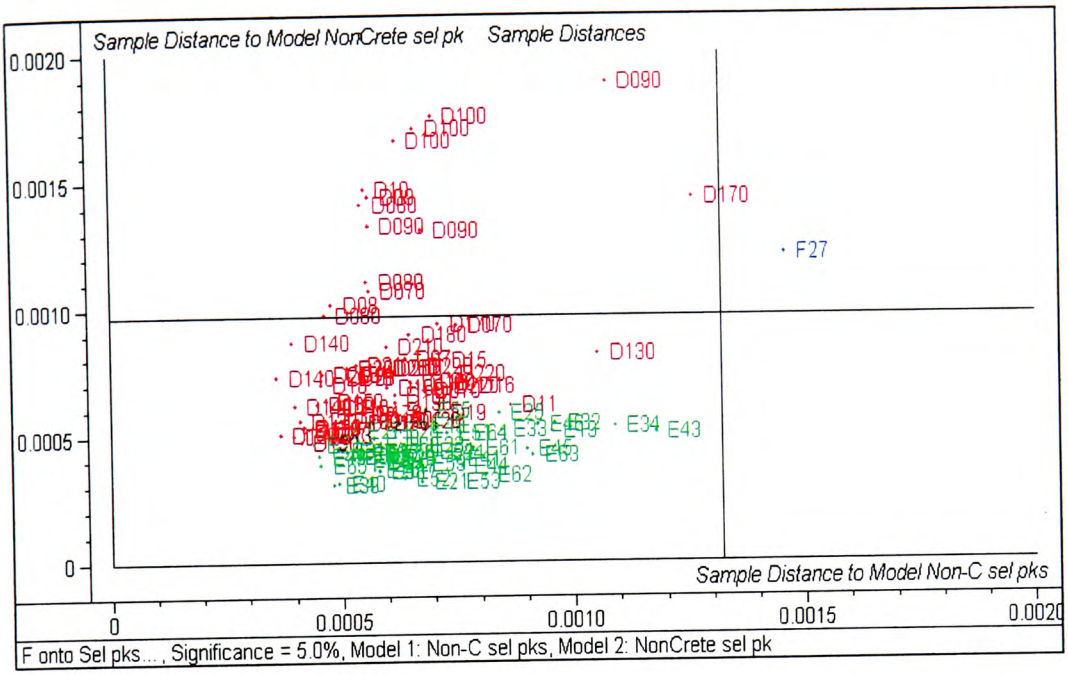

Figure 5.19 – Cooman's plot to show separation between harvest years 1994/95 (red) and 1995/96 (green) with a test sample (blue) from 1996/97

5.6 CONCLUSIONS

This investigation has demonstrated the efficacy of IR as a technique, especially for the rapid detection and classification of adulteration of olive oils with sunflower oil. Regression investigations using three selected wavelength bands (893 – 1260 cm^{-1}, 1610 – 1776 cm^{-1} and 2730 – 3060 cm^{-1}), with the E series of adulterated oils from Crete gave the closest correlation between the observed and the predicted adulteration data, with a RMSEP of 0.795% sunflower oil and an offset of 0.147% using 11 PCs. Reducing the variables to fifteen, chosen by studying the regression coefficients, produced a predicted against measured sunflower adulteration percentage with a good correlation. It gave an RMSEP of 0.912% with an offset of 0.235% using 9 PCs. This would suggest that

comparable results could be obtained using a greatly reduced number of variables, thereby considerably shortening the time required for statistical analysis.

The PCA models of pure oils and 1% adulterated oils for the F Crete samples gave a more reliable separation than the D or E series. The D set of oils was of limited sample size, which could affect the statistical analysis, making the models produced less trustworthy. Although some clustering was observed for the Crete and non-Crete samples the separation was not sufficient to allow confident prediction of unknown samples. The differentiation between harvests did not singly classify the samples, however the models were well enough defined to distinguish a sample from neither model and classify it accordingly.

CHAPTER 6

6 Supercritical Fluid Extraction (SFE)

6.1 THEORY AND TECHNIQUE

Many conventional extraction techniques use solvents which are potentially harmful and difficult to dispose of environmentally. The procedures are often complex and time consuming. An alternative extraction technique utilises supercritical fluids as solvents. Supercritical fluids (SCFs) are so named because they exist at temperatures and pressures beyond the critical point of that compound. The critical point is the temperature and pressure at which the gas and liquid phases become identical. The first reported observation of this phenomena was in 1822 when Baron Cagniard de la Tour noted that the gas-liquid boundary disappeared in certain materials when heated in closed glass containers (Taylor, 1996). In the 1950s a process using propane as a solvent was developed to purify and separate the polyunsaturated triglycerides in vegetable and fish oils. The most common commercial use for supercritical fluid extraction has been the decaffeination of coffee with supercritical CO_2. Figure 6.1 shows the phase diagram for carbon dioxide, which is the most commonly used SCF because of its low critical temperature, low cost and low-toxicity. The fluid is neither a liquid or a gas and has properties intermediate to both phases. Supercritical fluids have the solvating power of liquids and the transport properties common to gases.

6.1.1 Properties of Supercritical Fluids

The solvating power of SCFs is dependent on pressure and temperature. At high pressure the solvent power of CO_2 increases with rising temperature but at low pressure the opposite occurs and it decreases with rising temperature. This is because with an

increase in temperature at low pressure the density decreases, whereas changes in temperature at high pressures have less of an effect on density. Therefore, density is proportional to the solvating power, the dissolving power of a SCF increases with an isothermal increase in density or an isopycnic (constant density) increase in temperature. When temperatures are reached just above the critical temperature (Tc) of a substance, slight increases in pressure will produce liquid-like densities. Further above the critical temperature much larger increases in pressure are required to produce the same effect. The region above $T_R = 1.0$ and $P_R = 1.0$ is the operational supercritical region, where T_R is the reduced temperature (T_{actual} / T_c) and P_R is the reduced pressure (P_{actual} / P_c). Between T_R = 0.95 and 1.0, the region is called the subcritical region (Figure 6.1) (Taylor, 1996).

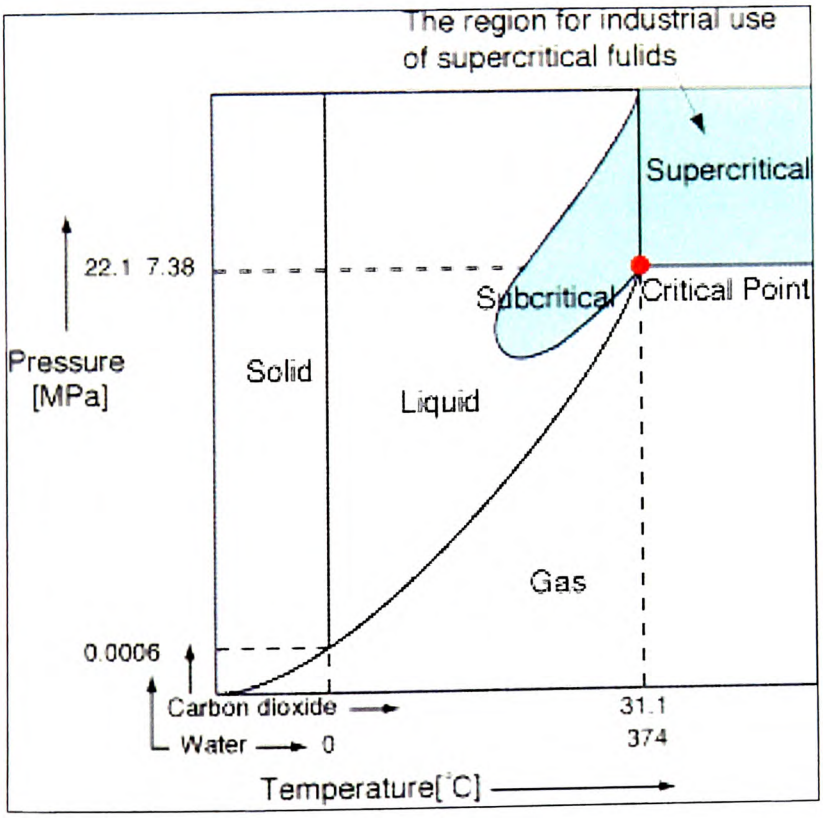

Figure 6.1 - Phase diagram for carbon dioxide and water

Table 6.1 shows a comparison of typical average values for density, viscosity and diffusivity of gases, liquids and supercritical fluids.

Table 6.1 – Comparison of properties

Property	Gas	SCF	Liquid
Density (kg m^{-3})	1	100 – 800	1000
Viscosity (cP)	0.01	0.05 – 0.1	0.5 – 1.0
Diffusivity ($mm^2 s^{-1}$)	1 - 10	0.01 – 0.1	0.001

Diffusivity and viscosity also depend on temperature and pressure. As pressure is increased these properties approach those of a liquid. Increases in temperature lead to a decrease in the viscosity of SCFs but an increase of diffusivity.

As previously discussed CO_2 is the most commonly used SCF but it has limited solvating power for polar analytes. To overcome this problem, polar compounds (modifiers) can be added to the solvating fluid. These enhance the characteristics of supercritical CO_2. The addition of a polar solvent (e.g. methanol) alters the T_c and P_c. The T_c of a solvent mixture lies between the values for the two separate solvents and the P_c is at a maximum at an intermediate composition between the pure modifier or pure CO_2. The arithmetic mean of the critical temperatures and pressures of the two components can be used to approximate the critical constants of the mixture:

$$T_c = X_{CO_2} T_{c(CO_2)} + X_m T_{c(m)}$$

$$P_c = X_{CO_2} P_{c(CO_2)} + X_m P_{c(m)}$$

where X_{CO_2} and $X_{(m)}$ are the mole fractions of CO_2 and modifier respectively.

Adding modifier enhances the solvating power but can adversely affect the mass transfer if the modifier reacts with the solute, e.g. by forming hydrogen bonds (Taylor, 1996).

6.1.2 Extraction

Supercritical fluid extraction has two stages, static extraction and dynamic extraction. The sample is placed in an extraction cell, in a heated and pressurised chamber. The SCF is introduced and the sample is immersed in the fluid for a predetermined time (static extraction) with a shut off valve to the restrictor closed. The SCF then flows through the sample at a given flow rate, for a given time (dynamic extraction), the valve opened to allow the analytes to be collected through the restrictor port onto a trapping system (Figure 6.2).

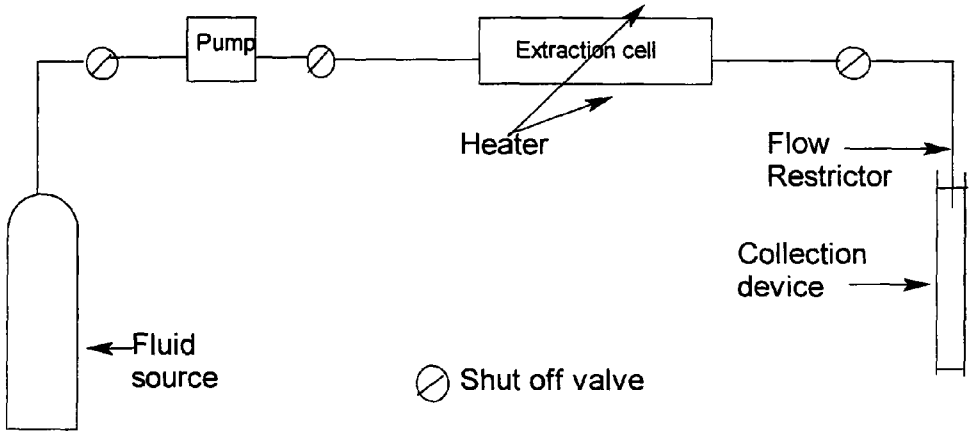

Figure 6.2 - Block diagram showing basic off-line SFE instrumentation

Figure 6.2 shows the basic instrumentation requirements for off-line SFE. The pump supplies extraction media to the sample matrix, which is contained in a heated cell. The analytes are partitioned from the matrix and are subsequently trapped using a suitable collection device after depressurisation via a restrictor. The restrictor provides a back-pressure within the system. Both flow rate and pressure (density) of the extraction fluid can be controlled by variation of the pump output or back-pressure or a combination of the two. The initial step of extraction requires that the analytes be partitioned from the sample matrix, which allows them to be swept from the matrix, out of the extraction cell.

The size and shape of extraction cells have been investigated and no appreciable difference between 'long and thin' or 'short and fat' cells was noted (Hawthorne, 1993).

6.1.3 Trapping/Restrictor Types

Various analyte trapping procedures have been used with SFE:

- Into a solvent filled vial (liquid filled trapping)
- Onto an active solid sorbent
- Onto an inert solid support
- Into an empty bottle

In all cases, trapping occurs after decompression of the extract. The expansion of CO_2 out of the restrictor lowers the fluid density and therefore the solvating power with subsequent precipitation of the extracted analytes. Traps may be cryogenically cooled to maximise recoveries or the more volatile analytes. Inert solid supports include glass beads, stainless steel plates and spheres. Minimal amounts of solvents that have a high solvating power for the trapped analytes are then essential to strip the analytes from the solid support. Liquid solvent trapping is a popular trapping technique where the extract is decompressed into a container of solvent. To ensure efficient trapping the restrictor should be immersed in the solvent and cooling the solvent increases the efficiency of volatile analyte collection. Active sorbent trapping typically involves a chromatographic stationary phase such as octylsilica and octadecylsilica (ODS). In order to trap compounds of varying polarity, modifications to the 100% silica is necessary (Taylor, 1996).

6.2 GAS CHROMATOGRAPHY-MASS SPECTROMETRY (GC-MS)

Gas Chromatography (GC) coupled to Mass Spectrometry (MS) was used to separate and identify the compounds extracted from the oil samples. The sample to be analysed is introduced via the sample inlet into the GC, where it encounters a continuous flow of carrier gas. This gas transports the vaporised sample to a thermostatted column, which performs the separation. The separated components in the sample are then detected and recorded. The mobile carrier gas should be one that is non-interactive with the sample and does not influence selectivity, such as helium. The sample is introduced to the GC by a microsyringe, through a septum which seals the inlet system as the syringe is withdrawn. The injection port is heated to a slightly higher temperature than the column to facilitate vaporisation. The column determines the selectivity and efficiency of the separation. The internal diameter, column length and stationary phase thickness vary from column to column, providing columns suitable for a variety of conditions and requirements. These are three of the parameters that determine the degree of separation and analysis time for a separation. The other three, column temperature, carrier gas and carrier gas velocity, can be altered with each analysis.

The liquid stationary phase needs to exhibit certain properties; a low vapour pressure, thermal and chemical stability, low viscosity, non-reactivity towards sample components and a wide operating-temperature range. It must also show reasonable solvent properties for the solutes to ensure symmetrical peaks. The column temperature is controlled by a thermostatted oven. A separation can either be achieved by using a constant column temperature, isothermal analysis, or by initiating a temperature programme where there are different rates of temperature rise with pauses at intermediate fixed temperatures for

a pre-determined time. With temperature programming the components elute according to their boiling points, making it a suitable operation for samples that contain a large number of compounds that have a wide range of volatility.

There are many different detectors used with GC which fall broadly into two categories, selective detectors which are useful for complex mixtures, and universal detectors that do not exhibit selectivity. A good detector is required to possess several criteria, sensitivity, good signal-to-noise, good detection limit and a good response time. The GC can be coupled to a mass spectrometer (MS), which acts as a detector. GC/MS represents one of the more powerful analytical techniques available. In GC/MS the mass spectrometer acts as a selective detector for the GC and the interface between the two instruments acts as the inlet system for the MS.

When the sample has been introduced into the mass spectrometer, ionisation of the sample occurs in the ion source, either by chemical ionisation or electron impact (EI). In EI the electrons are produced from a heated filament, and accelerated through a voltage, V. V is variable between 5 and 100 V, but maximum ion yield occurs at 70 V and therefore, standard mass spectra are obtained at this voltage. Because of this universally used voltage, data libraries can be compiled enabling computerised library searches of unknown compounds.

When an electron collides with a sample molecule, M, the energy causes an electron to be ejected from M leaving a positively charged ion (M^+):

$$M + e^- \rightarrow M^{+\cdot} + 2e^-$$

An applied electrostatic potential attracts the positive ions which are accelerated through a slit in a negative plate into a magnetic field. Generally, only positively charged ions are accelerated into the analyser for separation. Ions are separated according to their mass-to-charge ratio (*m/z*), the lighter the ion and the greater its charge, the greater the deflection.

Mass spectra show a peak that corresponds to the parent ion of the particular molecule (M^+), at a *m/z* value of the sum of the relative atomic masses. A small peak one mass unit greater than the parent ion (M + 1) is also expected due to the presence of an isotope of one of the constituent atoms. For example, ethanol gives a peak corresponding to the parent ion at *m/z* 46, with the small M + 1 peak at *m/z* 47. As a result of the high energy of the bombarding electrons some of the ethanol ions fragment to give smaller positive ions. Figure 6.3 shows the possible fragmentation pattern of ethanol. The relative intensities of the peaks depend upon the stability of the ion from which it arises. The loss of a $\cdot CH_3$ group (mass 15) by simple cleavage of a single bond results in a large base peak (highest peak to which all other peak height ratios are expressed) at *m/z* 31. Only the charged (carbonium) ion $[CH_2OH]^+$ is recorded on the spectrum (Duckett *et al.*, 2000).

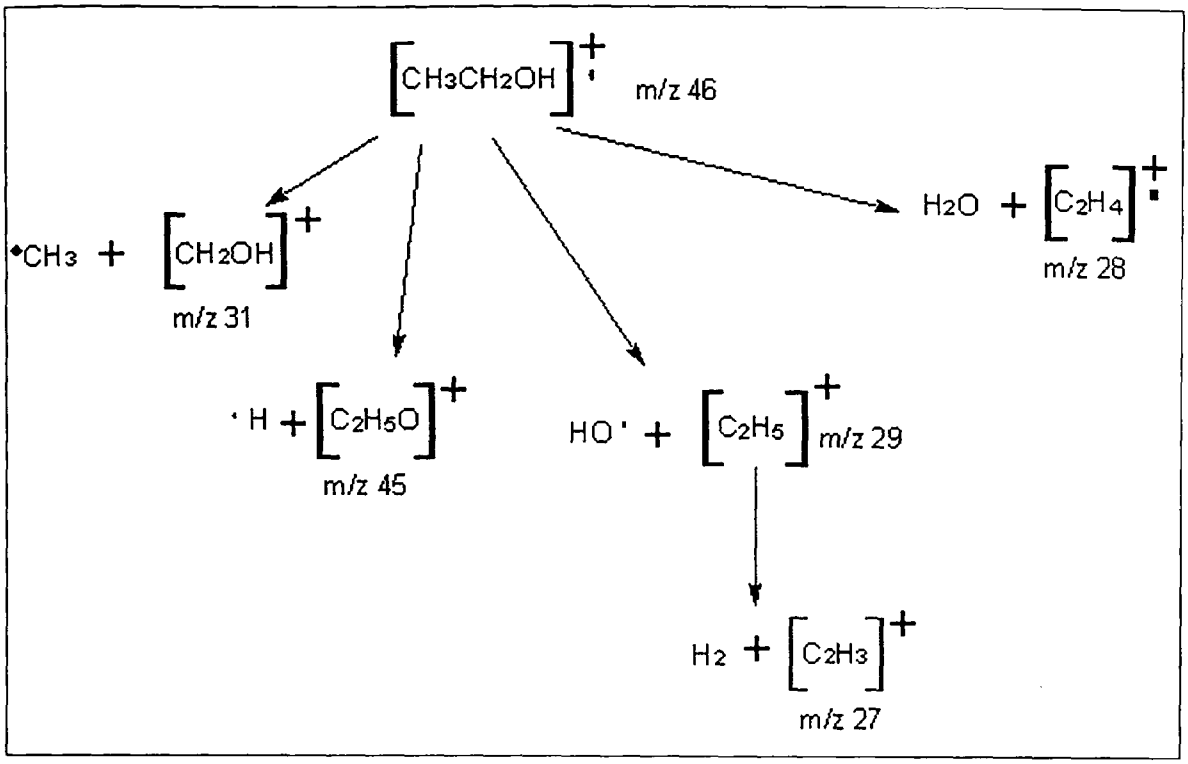

Figure 6.3 - Fragmentation pattern of ethanol

There are several forms of mass analyser, magnetic sector analyser, quadrupole mass filters, quadrupole ion traps, time of flight analysers and ion cyclotron resonance instruments. The one used was a quadrupole mass filter analyser. A quadrupole mass filter consists of four parallel rods of hyperbolic or circular cross-section symmetrical to the z axis. A direct current (*dc*) and a superimposed radio-frequency (*rf*) is applied between each pair of opposite and electrically connected rods. Ions are injected into the filter with a very small accelerating voltage, 10 - 20V, and are made to oscillate in the x and y directions by the electric field. The separation of ions according to mass is achieved by varying the voltages with the *rf/dc* voltage ratio remaining constant. At any point in the scan only one mass can pass through the system, for other masses the oscillations become unstable and the ions are lost on the rod assembly. The resolution required is selected by adjusting the *dc* voltage. The *dc* voltage can be switched off and all ions will then perform stable oscillations for a sufficiently small *rf* voltage. This enables the quadrupole to be used in more sophisticated instruments, such as the triple

quadrupole or hybrid instruments. The control of the rod voltages can be effected more accurately than the control of the magnetic field in a magnetic sector, in particular the rod voltages can be switched very rapidly from one value to another to focus a few selected ions for sensitive quantitative mass spectrometry. Therefore, the quadrupole is automated more easily than a magnetic sector instrument, is smaller, cheaper and easier to run. The ions are detected by either an electron multiplier or a continuous channel multiplier and the resulting signal converted to a digital form compatible with a computer system which produces the mass spectrum. A mass spectrum is a line spectrum that shows the molecular ion, in electron impact, and signals that correspond to the individual fragments comprising the sample. The spectrum obtained is analysed by computer and the results can be library searched to achieve structure elucidation .

6.3 LITERATURE REVIEW

The versatility of SFE has been demonstrated by numerous research projects. These include the extraction of amphetamines from hair samples (Allen *et al.*, 2000), sunscreen agents from cosmetics (Scalia, 2000) and it compares favourably with traditional extraction methods to extract the active compounds from camomile flowers (Scalia *et al.*, 1999). Previous work within the olive oil field has shown the use of SFE to extract olive husk oil evaluated by mathematical models (Esquivel *et al.*, 1999) and the extraction of the volatile components of virgin olive oil followed by head-space analysis (Morales *et al.*, 1998). SFE was included in a range of methods used to evaluate the authenticity of olive and hazelnut oils (Blanch *et al.*, 1998). They concluded that, under the conditions they employed, SFE was not a sufficiently selective method of analysis, compared to the selectivity and sensitivity of Steam Distillation-Solvent Extraction (SDE) using dichloromethane. Supercritical carbon dioxide (SC-CO_2) has also been used to de-

acidify olive oils, without modifying their triglyceride composition, making them more appropriate for human consumption. Disputed solubility data led to further studies to verify the applicability of SC-CO_2 to oil deacidification (Goncalves *et al.*, 1991; Simoes *et al.*, 1996). SFE was used with LC-MS, to extract the compounds reported to have antioxidant activities from rosemary leaves (Senorans *et al.*, 2000). Another group also interested in antioxidant extraction, used SFE to extract tocopherols from olive pomace, thereby making use of a by-product of olive oil production (Ibanez *et al.*, 2000). A study by Maheshwari determined the solubility of various fatty acids in supercritical carbon dioxide (Maheshwari *et al.*, 1992).

6.4 METHOD DEVELOPMENT

In this work, the viability of using Supercritical Fluid Extraction (SFE) to extract the semi-volatile fraction of a variety of oils would be explored. The aim was to develop a technique to extract the semi-volatile components from a variety of vegetable oils. The development of a solid phase trapping system that could be coupled to a supercritical fluid extraction system was the first objective. The optimisation of extraction conditions could then be addressed to ensure maximum performance. A method to separate, detect and identify the semi-volatile compounds extracted by the SFE would be developed and once the oils had been characterised by their semi-volatile composition, the possibility of detecting low level adulteration would be explored. A number of previous studies have used high-performance liquid chromatography (HPLC) either to identify olive oil adulteration by studying the linoleic acid content (El-Hamdy *et al.*, 1995) or to identify geographical origins (Salter *et al.*, 1997). The use of GC-MS to identify adulteration from the semi-volatile fraction had not previously been explored.

6.4.1 Solid Phase Trapping System

Tenax TA™ is a polymer manufactured from diphenyl-*p*-phenylene oxide (DPPO). It is relatively inert, semi-crystalline, macroporous ($\geq$50 nm in diameter) and available in various granular mesh sizes. It can be conditioned to have a very low background, which together with its high temperature stability makes it useful for semi-volatile recovery. In a macroporous system, such as Tenax TA™, the pores are filled by a monolayer followed by multilayer adsorption. The adsorbed molecules are in a condensed phase, which more closely resembles a liquid than a vapour. Tenax TA™ has been compared with other sorbent trapping systems and contrasted with other sampling procedures (Faldt *et al.*, 2000; Harper, 2000) to determine extraction suitability for volatile organic compounds from biologically active compounds and air respectively.

For this work a solid phase trapping system using Tenax TA™ was developed onto which the compounds of interest would adsorb. Tenax TA™ filled glass tubes (0.25″ x 7″) were obtained (Supelco UK, Poole, England) and attached to the restrictor port via silicone rubber tubing. A plug was inserted into the top of the glass tube to prevent the Tenax being pushed out by the pressure of the CO_2.

6.4.2 Sample Preparation

Silica gel Davisil™ (60-100 mesh) was activated by heating, in an oven, at 160° C for 20 hours. The oil to be analysed was loaded onto 20g activated silica (12.5% w/w), in a round bottomed flask and manually agitated for 30 minutes to ensure uniform coating. 3.30g of loaded silica were placed in an SFE extraction cell. A selection of Greek olive oils, obtained directly from Greece, was examined using this method. The other oils

under investigation, sunflower, sweet almond, toasted sesame and extra virgin olive oil were all bought from a high street retailer (Tesco).

6.4.3 Sample extraction

SFE was applied to the loaded silica, using an ISCO SFX™ 220 SFE system, using CO_2 as the extraction medium. The extraction conditions were varied (Table 6.2) to optimise extraction conditions, using parameters:

Density (g/ml)	0.75
Pressure (psi)	5000
Flow rate (ml/min)	2
Restrictor (°C)	85
Dynamic Extraction (min)	20

Table 6.2 – SFE Extraction optimisation conditions applied to oil samples

Run	Oven Temperature	Static Extraction
1	40°C	10min
2	40°C	20min
3	40°C	30min
4	70°C	10min
5	70°C	20min
6	70°C	30min
7	90°C	10min
8	90°C	20min
9	90°C	30min

Using a static extraction time of 20 minutes and an oven temperature of 90°C, an optimum dynamic extraction time was shown to be 20 minutes. Using an internal standard (phenanthrene, $1cm^3$, 10 ppm) to calculate relative quantities, extraction conditions were optimised to provide maximum recovery of the target analytes.

The extract was trapped in a Tenax™ TA tube that had been attached to the restrictor outlet. The Tenax tube was subsequently detached and solvent stripped using high purity HPLC grade hexane (3 ml). The tenax was then washed with a polar solvent, dichloromethane (DCM), to ensure no polar compounds were being left behind. An internal standard ($1cm^3$) was added to the extraction and the sample was concentrated by evaporation using nitrogen.

The sample was introduced onto a Hewlett Packard 5890 GC system with a CP-SIL 8CB Low bleed column (30 m x 0.32 mm ID). The GC temperature program is shown in Table 6.3. A Hewlett Packard 5971A Mass Selective Detector was coupled to the GC and the sample was analysed using electron impact mass spectrometry. Hewlett-Packard Chemstation was the software used. Standards were obtained (Sigma-Aldrich, Poole) to confirm retention times and identification of compounds. Each standard (10 ppm) was run through the GC/MS using the program in Table 6.3. Total Ion Chromatograms (TICs) for the standards are shown in Appendix E.

Table 6.3 - GC Temperature program

Temp (°C)	Time Held (min)	Program Rise (°C/min)	Final Temp(°C)
40	2	0	40
40	0	10	270
270	2	40	280
280	3	0	280

A sample set from the Greek olive oils, which consisted of five oils from Crete and five non-Crete oils were also analysed by the protocol detailed above. Reproducibility was tested by performing several extractions of the same sample and by sequential injections of the same extract. The ratio of detected compound to internal standard peak areas was

calculated and the mean and standard deviation of ratios of repeated injections determined. The resulting spectra were imported into the Grams 32 laboratory software package in order to manipulate the chromatographic traces to allow importation into the Unscrambler statistics program. Principal Component Analysis (PCA) and PLS1 regression were carried out on the sample set, including the vegetable oils, to investigate whether the semi-volatile fraction of olive oil could be used to separate olive oil samples from vegetable oils and also whether the geographical origin (Crete or non-Crete) could be established.

6.5 RESULTS AND DISCUSSION

The optimum parameters for the supercritical fluid extraction had been shown to be a static extraction time of 20 minutes followed by a dynamic extraction time of 20 minutes, at a temperature of 90°C. Figure 6.4 shows a graphical representation of the optimisation results for two compounds, nonanal and 2-decenal. It was found that, at this high temperature, some of the triglyceride oil base was being removed from the silica support and collecting in the tubing attached to the restrictor. To overcome this problem the temperature was dropped to 80°C, this required the pressure to be altered to 4400 psi to maintain the density of CO_2 at 0.75 g/ml.

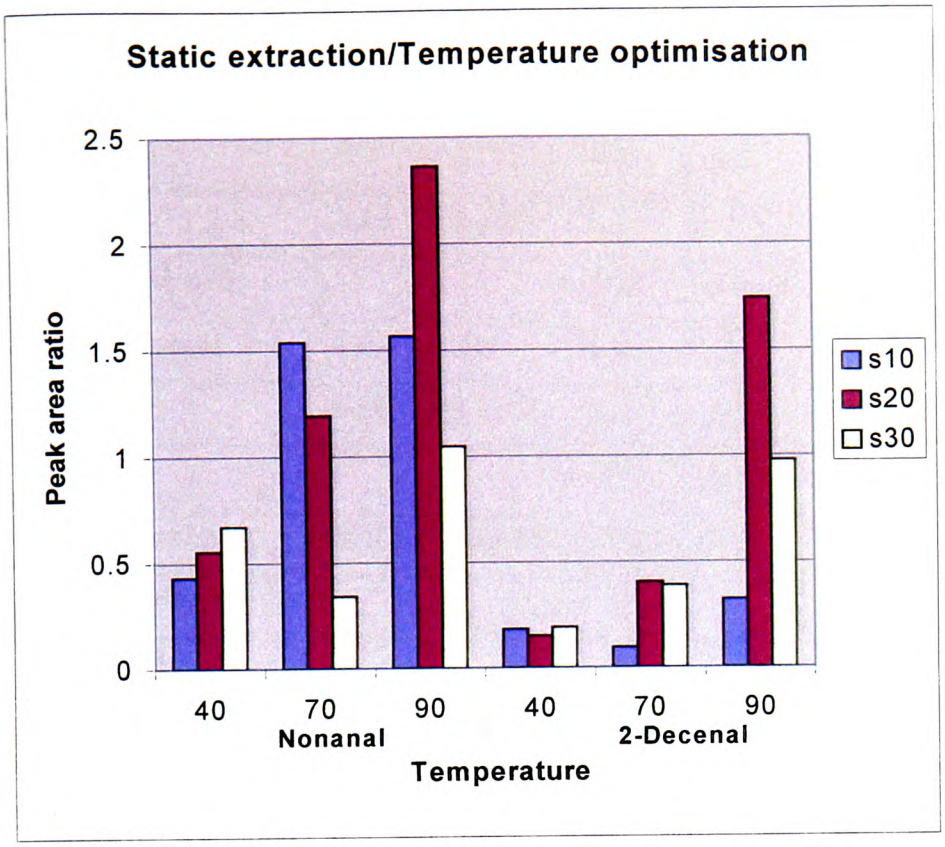

Figure 6.4 - Graphical representation of optimisation of static extraction (s) in minutes and temperature optimisation

6.5.1 Vegetable Oils

The initial extractions identified several semi-volatile components that had not been previously seen using head-space analysis. The continued and unexpected presence of napthalene caused doubts as to possible contamination of equipment or reagents. After ruling out the presence of napthalene in the silica or the tenax and ensuring, by running blanks, that all components were eluting from all instrumentation, it was concluded that napthalene is present, in small amounts, in the oils.

It was decided to use an internal standard that more closely resembled the compounds being detected. Tetradecanal (50 ppm) was chosen, as a series of saturated aldehydes was present in all four of the oils used. The range of compounds detected in the vegetable oils is shown in Table 6.4.

Table 6.4 - Range of compounds extracted by SFE and detected by GC/MS

Compound	Walnut Oil		Olive Oil		Sesame Oil		Almond Oil	
	R/T	*Ratio*	*R/T*	*Ratio*	*R/T*	*Ratio*	*R/T*	*Ratio*
Hexanal	3.14	0.047	3.13	0.103	3.11	0.028	3.10	0.139
Pentanoic acid			4.58	0.0078	4.53	Tr		
2-Heptanone	4.62	Tr	4.65	Tr				
Heptanal	4.88	0.0036	4.88	0.012	4.83		4.86	0.0066
α-Pinene			5.42	0.012	5.36	Tr	5.39	0.0059
2-Heptenal (Z)	5.90	0.0074	5.89	0.011	Tr		5.87	0.0084
Benzaldehyde					5.94	Tr	5.99	0.255
Heptanol			6.14	0.0074				
Hexanoic Acid	6.37	0.011	6.32	Tr	6.34	0.029	6.30	0.016
2,4-Nonadienal	6.47	0.036	6.48	Tr	6.41	Tr	6.45	0.132
2,4 Heptadiene	6.62	0.0036						
Octanal	6.71	0.0033	6.73	0.025	6.66	Tr	6.71	0.0064
Limonene	7.16	0.0068	7.16	0.011	7.10	0.039	7.15	0.0068
2-Octenal (E)	7.69	0.0051	7.71	Tr			7.68	0.0072
Heptanoic acid			8.10	0.045				
Isooctanol					7.88	Tr		
Nonanal			8.49	0.029				
2-Nonenal	9.41	0.0040	9.41	Tr			9.40	0.051
Octanoic acid			9.71	0.115	9.54	Tr		
Napthalene	9.87	0.0050	9.88	0.019	9.81	Tr	9.85	0.015
11-Dodecenol	18.28	Tr						
2-Decenal (E)			11.01	Tr				
Nonanoic acid			11.14	0.080				
α-Farnesene			14.38	0.045				
Hexadecanoicacid	19.65	0.041	19.67	0.058	19.63	0.67	19.66	Tr
9-Hexadecenoic acid	21.43	0.079	21.44	0.269				
Hexadecanal	25.71	0.015	25.72	0.034			25.69	0.046
Octadecanal			27.74	0.131				

Compound	Walnut Oil		Olive Oil		Sesame Oil		Almond Oil	
	R/T	*Ratio*	*R/T*	*Ratio*	*R/T*	*Ratio*	*R/T*	*Ratio*
16-Octadecenal			**30.07**	**0.025**				

R/T – Retention time Tr - Trace

Ratio – Area compound/Area internal standard

Using the temperature program detailed in Table 6.3, the target compounds eluted from the column between 2 and 10 minutes. The Total Ion Chromatographs (TIC) obtained for each of the oils show that this region varies with different oils. This variation could be used to profile specific oils and possibly detect adulteration. Examples of TICs for walnut oil, sesame oil, olive oil and almond oil, are shown in Figures 6.5, 6.6, 6.7 and 6.8 respectively.

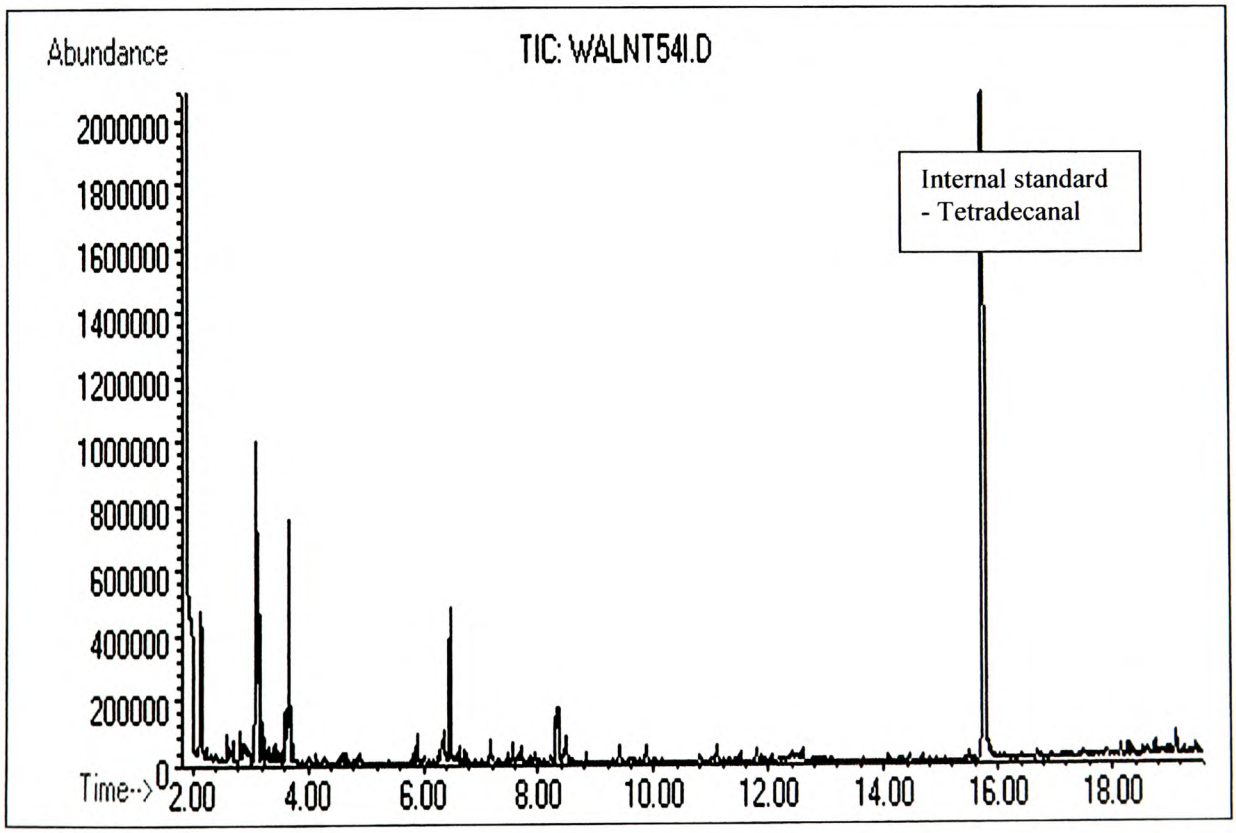

Figure 6.5 – Total Ion Chromatogram for the extraction of walnut oil by SFE

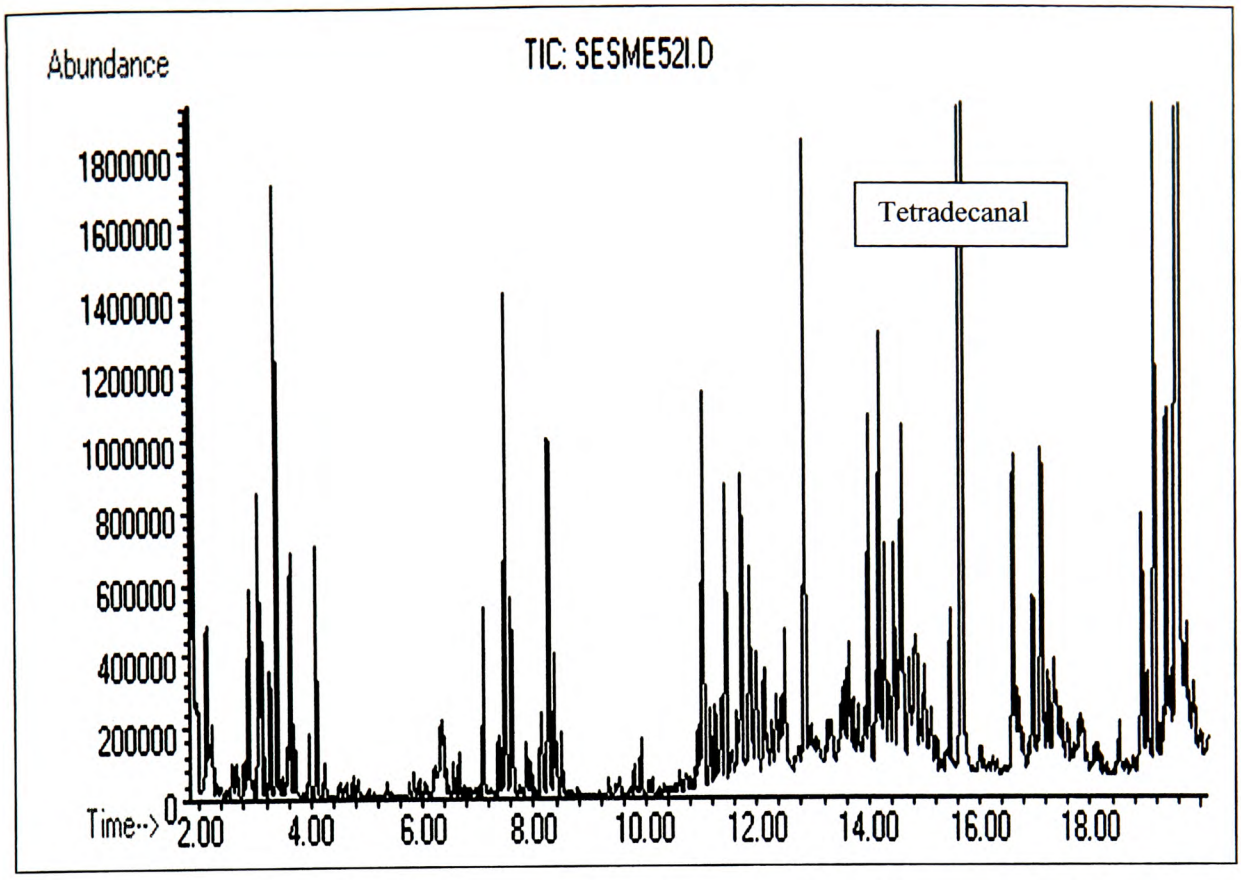

Figure 6.6 - Total Ion Chromatogram for the extraction of sesame oil by SFE

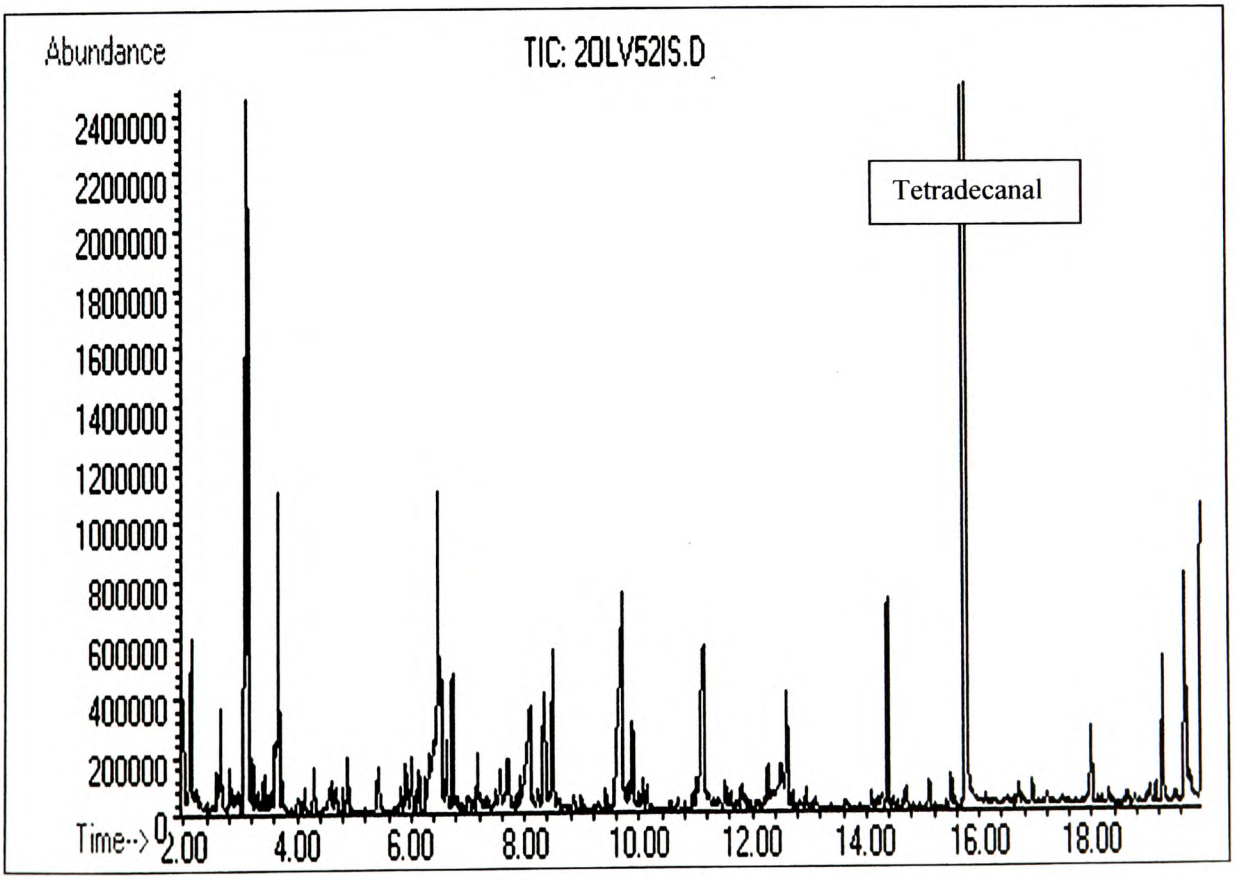

Figure 6.7 - Total Ion Chromatogram for the extraction of olive oil by SFE

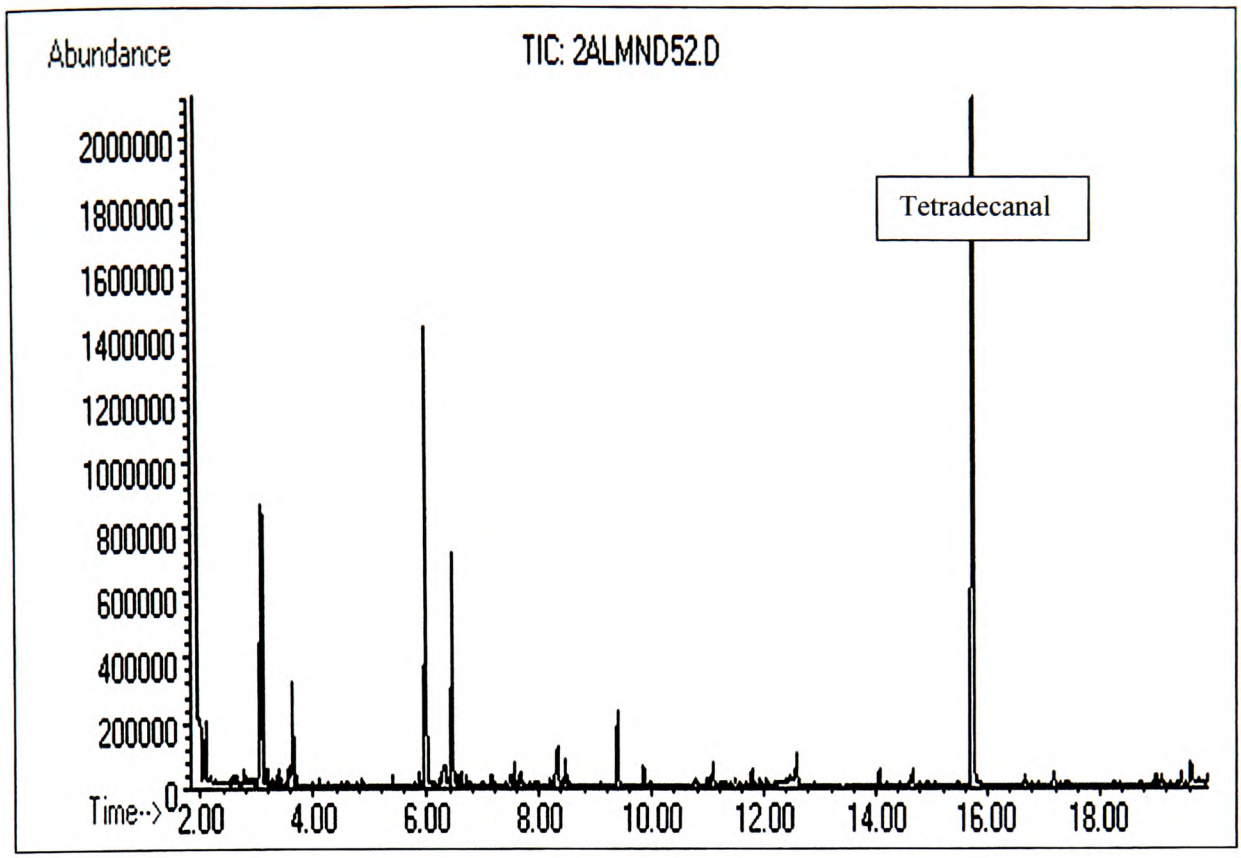

Figure 6.8 - Total Ion Chromatogram for the extraction of almond oil by SFE

6.5.2 Greek Olive oils

The compounds extracted from the Greek oils varied slightly in their semi-volatile components compared to the vegetable oils. Table 6.5 shows the entire list of extracted compounds and their retention times. Not all the compounds were detected in all of the samples.

Table 6.5 – Identified compounds extracted by SFE in the Greek olive oil sample set

Compound	Retention Time in minutes
2-Pentenal	2.22
Hexanal	2.93
2-Hexenal	3.72
3-Hexen-1-ol	3.81
Heptanal	4.63
2,4-Hexadienal	4.74

2,4-Hexadienal	4.74
2-Heptenal	5.60
1-Octen-3-ol	6.08
2,4-Nonadienal	6.28
Octanal	6.48
Limonene	6.91
3-Octen-2-one	7.08
2-Octenal	7.42
Nonanal	7.67
4-Nonenal	8.05
2-Nonen-1-ol	8.22
2-Nonenal	9.14
Naphthalene	9.48
Decanal	9.86
2-Decenal	10.68
2,4-Decadienal	11.19
2-Undecenal	12.20
α -Farnesene	14.19

Four injections were carried out for each extraction to check the reproducibility of the method. Table 6.6 shows an example (sample E14) of the mean and standard deviation calculations. Full set of statistics in Appendix E.

Table 6.6 – Mean and standard deviation of the ratio of extracted compound to internal standard (E14)

Retention time	Mean	Standard Deviation	Sample size
2.93	0.439928	0.030163	4
4.63	0.034041	0.010661	4
5.62	0.06973	0.02296	4
6.08	0.017515	0.002312	2

6.28	0.114788	0.010834	4
6.48	0.108312	0.06115	4
7.44	0.03576	0.004331	4
7.67	0.044051	0.032417	4
8.05	0.140933	0.009943	4
8.22	0.177163	0.010252	3
9.14	0.0406	0.010973	4
9.86	0.050142	0.000351	3
10.72	0.023629	0.015027	2
12.22	0.044675	0.002457	4

6.5.3 Statistical Analysis

The total ion chromatograms from the Greek olive oil samples were imported via Grams 32 software into the Unscrambler multivariate analysis program. The ratio of compound to internal standard was calculated for volatiles eluting from the column between two and twenty minutes. Figure 6.9 shows the result of hierarchical cluster analysis (SPSS), using Ward's clustering method with squared Euclidean distance measurements (Section 3.1.3), performed on this data from the ten Greek oils. The codes of the oils originating from Crete are in black (E15) and the non-Crete oils in red (E33).

The cluster analysis showed some rudimentary grouping of geographical origin and so models were produced using PCA analysis on the ratio of identified compound to internal standard peak heights. The oils were then classified and the resulting Cooman's plot in shown in Figure 6.10, Crete oils in green and non-Crete oils in red. An unknown sample (blue) was doubly classified although it was correctly grouped with other oils from Crete.

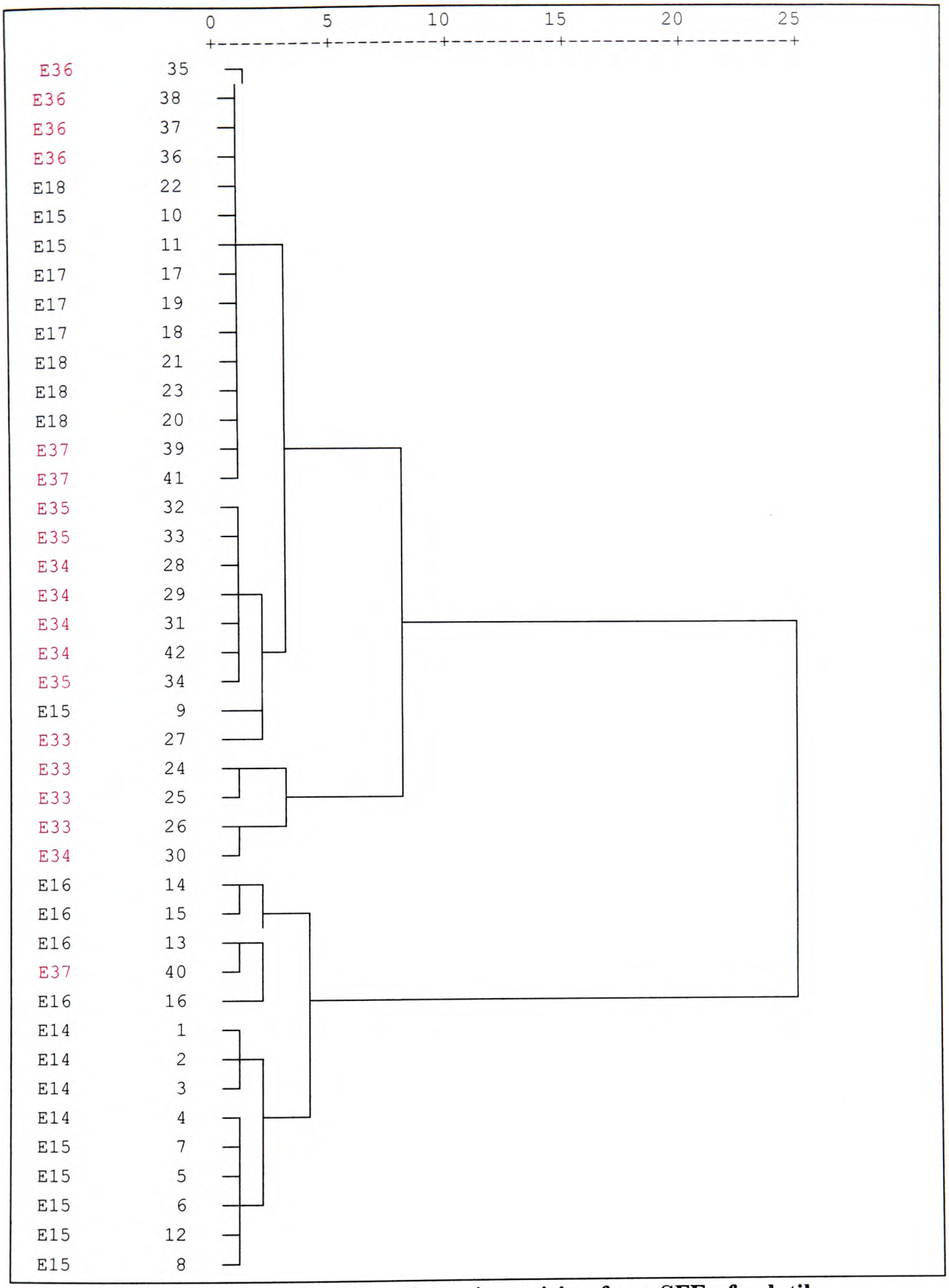

Figure 6.9 - Dendrogram detailing clustering arising from SFE of volatile compounds, using variables between 2 and 20 minutes retention time. Crete oils – black, non-Crete oils – red

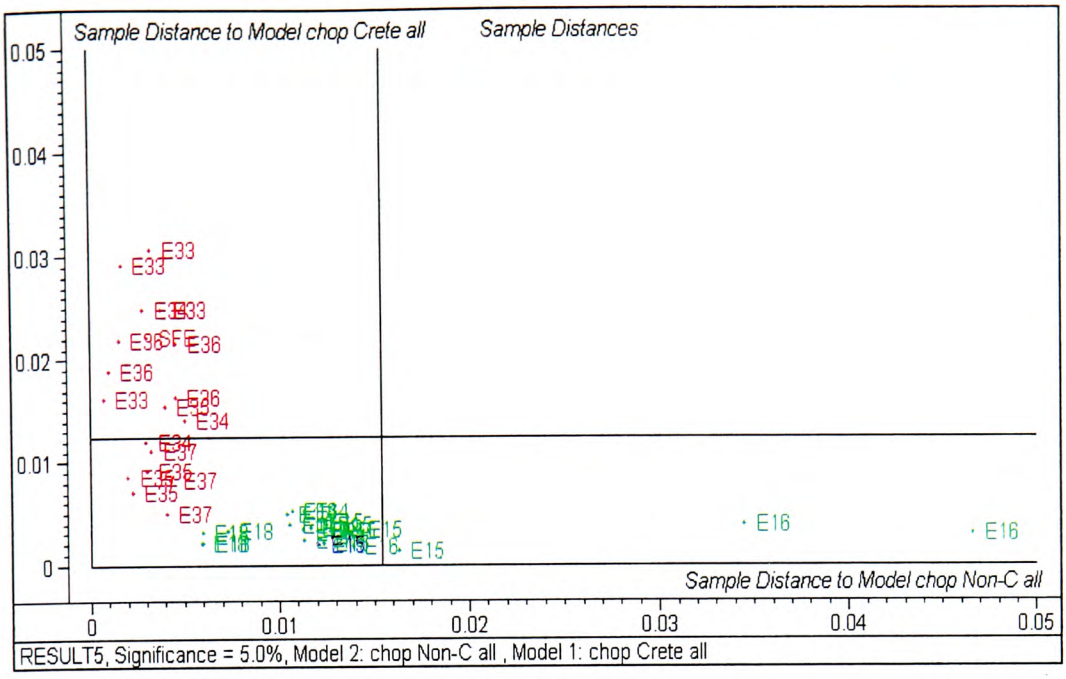

Figure 6.10 – Cooman's plot showing separation between E set, Crete (green) and non-Crete (red) oils by compounds extracted by SFE

Although most of the Crete oils were doubly classified (bottom left of plot), the non-Crete oils showed better classification and the models were showing a degree of separation.

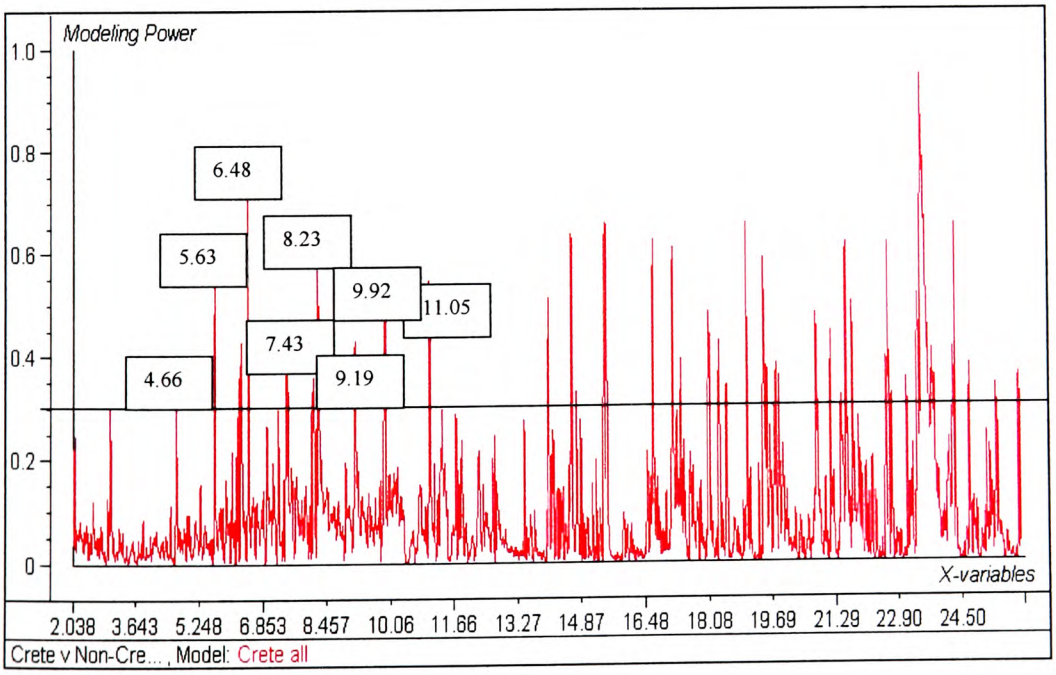

Figure 6.11 – Modelling power plot showing the peaks assigned important (〈0.3) to the Crete PCA model of volatiles extracted by SFE

The plot of the modelling power (Figure 6.11) indicated which of the earlier eluting compounds were influential in the construction of the Crete model. Peaks with a modelling power greater than 0.3 are considered as significant. The peaks marked on Figure 6.11 relate to heptanal, 2-heptenal, 2,4-nonadienal, octanal, 2-octenal, 2-nonen-1-ol, 2-nonenal and decanal.

PLS1 regression plots showed (Figure 6.12) the pure sesame oil well differentiated from the Greek olive oils (black) along the first PC. The other two potential adulterants (walnut and almond) were not so well removed from the olive oils but still showed some separation.

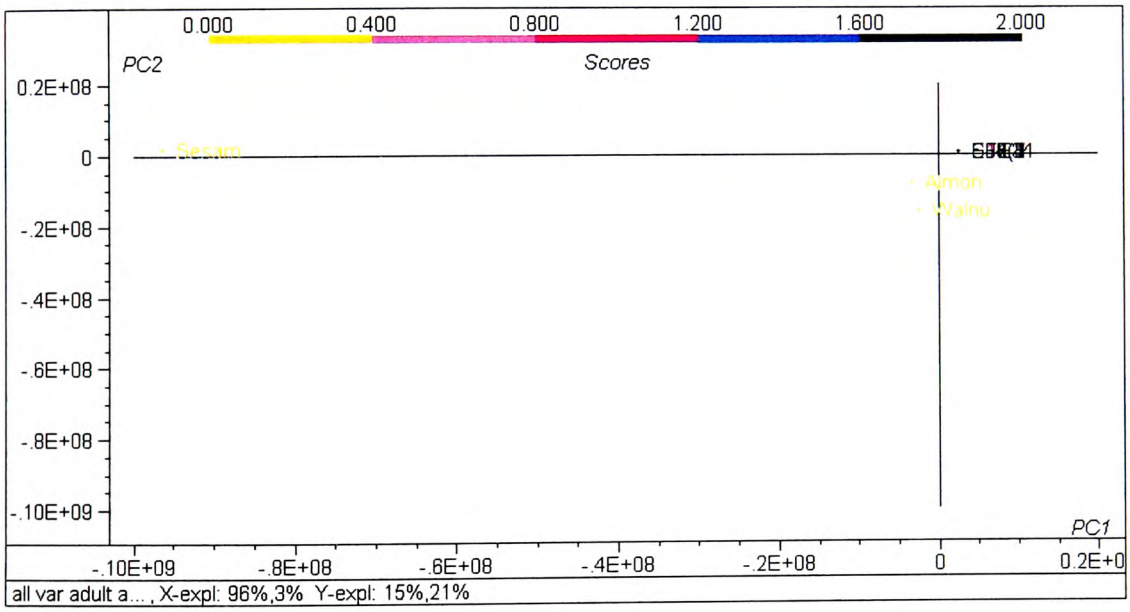

Figure 6.12 – PLS1 regression scores plot showing adulterant oils (yellow) and Greek olive oils (black)

6.6 CONCLUSIONS

The volatile components of olive oil are responsible for the flavour and fragrance of the oil. The most abundant headspace compound is trans-2-hexenal, which has been found to be responsible for the fresh fruity taste of oils (Aparicio *et al.*, 1997; Kiritsakis, 1998).

The majority of volatiles are products of autoxidation, which occurs with storage, exposure to light or heat. These degradation products are responsible for the 'off' flavours and tastes described by sensory panels. Supercritical fluid extraction was successful in selectively extracting a range of these compounds, some that had been observed (Morales *et al.*, 1998) and others not previously reported using this technique. The detection of some of these unreported compounds could be due to the extended storage of the oils used in this study compared to Morales *et al.* Fresh oils contain less of the degradation products and this could explain why they did not report compounds such as octanal, 2-heptenal and 2-octenal, the main oxidation products of oleic and linoleic acids respectively.

The application of multivariate statistical analysis to the data did not show reliable clustering that could confidently predict whether the oil originated in Crete or other areas of Greece. The volatile fraction of olive oil has been used, successfully, to classify oils by origin using other techniques (Sacchi *et al.*, 1998) and a larger sample set could improve the modelling power and hence improve the classification. Investigations into whether the statistical analysis could be applied to the SFE results to determine adulteration showed that some adulterant oils were sufficiently different in composition to olive oil to give some separation. Sesame oil was well differentiated from the olive oils suggesting that adulteration with sesame oil could be easily detected. The adulterant samples were all pure so the ability to detect low level adulteration with these oils would require further analysis using olive oil samples spiked with lower concentrations of adulterant.

CHAPTER 7

7 Solid Phase Micro Extraction (SPME)

7.1 THEORY AND TECHNIQUE

Solid Phase MicroExtraction (SPME) is a relatively new technique, developed in 1990 by Pawliszyn and Arthur, the applications and optimisation of which have been well documented in recent books (Pawliszyn, 1997; Pawliszyn, 1999). A fused-silica fibre is coated in a specific stationary phase, which absorbs or adsorbs the analytes of interest in a sample by direct immersion of the fibre into the sample or suspension in the headspace of the sample. The analytes can then be thermally desorbed in the injection port of a gas chromatograph. The process therefore consists of single step sample preparation, which does not require solvents and has been shown to give good reproducibility and high sensitivity.

SPME relies on the partitioning of analytes between the sample matrix and the polymer coating on the fibre. In headspace SPME there are three phases, condensed phase, its headspace and the SPME polymer. The molecules of analyte need to diffuse from the condensed phase to the polymer through the headspace, therefore giving two interfaces; condensed/headspace interface and headspace/polymer interface.

If a steady-state mass transfer is attained the mass flow rates at the two interfaces should be equal. At the headspace/polymer interface the extraction rate of the analyte is proportional to the mass flow rate at the interface. The net analyte transfer from the condensed phase to the headspace, at the condensed/headspace interface, is related to the headspace concentration variations. Prior to sampling an equilibrium exists between the

headspace and the condensed phase for the analyte and there is no net mass transfer at the interface. When analytes are extracted during sampling onto the polymer on the fibre the equilibrium is disturbed and when the analyte concentration is depleted in the headspace the analyte in the condensed phase will evaporate to the headspace. The headspace concentration deviation from equilibrium is therefore the driving force of analyte evaporation. The mass flow rate at the condensed/headspace interface equals that at the headspace/polymer interface when a steady-state extraction is achieved. This means that the evaporation rate should be proportional to the extraction rate. Mass transfer at either of the two interfaces can be established as the rate determining step (Ai, 1999).

7.1.1 Fibres

The selectivity of extraction depends on the type of polymer coating on the fibre. At this time there are three classes of coatings commercially available (Supelco):

- Non-polar coatings – Polydimethylsiloxane (PDMS) of varying film thickness
- Semipolar coatings – Polydimethylsiloxane/divinylbenzene (PDMS/DVB)
- Polar coatings – Polyacrylate, Carbowax/divinylbenzene and Carbowax/TPR100

These coatings are classified as:

- Homogeneous polymer coating
- Porous particles embedded in a polymeric phase

7.1.1.1 Homogeneous coatings

PDMS and polyacrylate are both homogeneous polymer coatings. PDMS is a liquid coating and the amount of analytes absorbed by the coating at equilibrium is directly related to its concentration in the sample. The amount of analyte extracted by a liquid coated surface is described by Nernst's partition law:

$$n = K_{fs}V_fC_oV_s / K_{fs}V_f + V_s$$

where n = mass analyte absorbed

V_f = volume of coating

V_s = volume of sample

K_{fs} = partition coefficient of analyte between the fibre coating and the sample

C_o = initial concentration of analyte in sample.

This shows that the relationship between the initial concentration of analyte in the sample and the amount adsorbed by the coating is linear. The K_{fs} values for analytes are large when the fibre coatings have strong affinity for the analytes, this leads to good sensitivity and effective concentration. From the equation, if V_s is very large the amount of analyte extracted is not related to sample volume, making the technique suitable for field sampling. SPME does not usually lead to exhaustive extraction as the K_{fs} values are rarely large enough (Pawliszyn, 1997).

PDMS coatings are available as either non-bonded or bonded. The non-bonded fibre is thermally treated and has a lower thermal stability than the bonded fibres. The bonded fibres are crosslinked and this increases the stability of the fibre (Mani, 1999).

Polyacrylate fibres are partially crosslinked and highly polar. Polyacrylate is a solid crystalline coating that turns into liquid at desorption temperatures. Both the polyacrylate and the PDMS extract analytes via absorption. Absorption is based on partitioning of an analyte between two immiscible phases and the process is determined by the relative fugacity of an analyte in each phase. At equilibrium, for a two-phase system it can be described by a partition coefficient *K*. Analytes dissolve in the coating and diffuse into it during extraction (Gorecki, 1999).

7.1.1.2 Porous particles embedded in Polymeric Phase

The porous particles are embedded in partially crosslinked polymeric phases. These fibres have high selectivity but have lower stability than homogeneous fibres. Increasing the porosity of the fibre coating increases the capacity of the fibre, increasing the porosity of the polymer particle retained analytes more efficiently and increasing the pore size of the polymer particle in the coating increased the selectivity of the fibre. Polydimethylsiloxane/Divinylbenzene (PDMS/DVB) is a blend of porous DVB polymer particles with liquid PDMS polymer. DVB has a high degree of porosity 1.5 mLg^{-1}, which gives strong analyte retention. Because it is a solid particle DVB is blended with a liquid phase, PDMS. The amalgamation has better affinity for polar analytes. Polydimethylsiloxane/Carboxen (PDMS/CAR) is again a solid porous particle, CAR, blended into a liquid phase, PDMS. The pores in CAR are smaller than in DVB, making it more suitable for the extraction of smaller molecules. The total pore volume of CAR is 0.78 mLg^{-1} (Mani, 1999). Both PDMS/DVB and PDMS/CAR are mixed coatings where the primary extracting phase is a porous solid. These fibres extract analytes by adsorption, where the analyte remains on the surface of the polymer and does not diffuse into it. Molecules attach to the surface via weak intermolecular forces such as van der

Waals or dipole-dipole interactions. If the sample is in aqueous solution hydrophobic interactions also drive the molecules out of the solution and onto the fibre. In adsorption there are a limited number of surface sites to which the analyte can adsorb so the amount of molecules that adsorb onto the surface is proportional to the total surface area of the polymer coating. Once these sites are full no more analyte can be adsorbed, potentially limiting the percentage uptake of analyte. It also creates a competitive situation where analytes with a higher affinity for the fibre coating will replace an analyte with lower affinity, making quantitation unreliable (Gorecki, 1999).

7.2 LITERATURE REVIEW

Comparisons have been done in various studies to ascertain the suitability of specific fibres for various matrices (Azodanlou *et al.*, 1999; Miller *et al.*, 1999; Jelen *et al.*, 2000; Page *et al.*, 2000; Roberts *et al.*, 2000). The process has been well tested for its applicability to extracting volatile components in several areas. It has been applied to monitoring the volatile compounds produced from monosodium glutamate in cooking (Wu *et al.*, 2000), investigating the formation of volatile compounds during the heating of spice paprika powder (Cremer *et al.*, 2000) and another study extracted the volatiles from kiwi fruit and found that compounds previously only found in kiwi fruit juice were extracted from the fruit and some other, previously undetected, compounds were also identified (Wan *et al.*, 1999).

SPME proved to exceed the extraction performance of static headspace analysis when applied to fruit juice samples (Miller *et al.*, 1999), and was found to be a successful method for extracting and quantifying the aliphatic aldehydes in sunflower oil (Keszler *et al.*, 1998). On-fibre derivatisation was used to extract the volatile carbonyl compounds

from sunflower oil by doping the fibre with pentafluorophenylhydrazine (PFPH) (Stashenko *et al.*, 2000). The PFPH reacts with the carbonyl compounds to form hydrazones which can then be analysed using an electron-capture detector. They concluded that the PDMS-DVB fibre adsorbed more PFPH than the PDMS fibre and 'salting out' the sample by adding potassium chloride (KCl) to the PFPH allowed even higher loading levels. The addition of potassium or sodium chloride (salting out) is used when working with an aqueous solution, to modify the matrix, to give the analytes a greater affinity with the fibre coating than with the water. The oil under investigation was heated to temperatures similar to those found during cooking to explore the degradation of the oil due to thermally induced oxidation (Stashenko *et al.*, 2000).

The volatile compounds in sunflower oil have also been studied with SPME, using refined and oxidized oils, to associate volatile components with oxidative degradation (Keszler *et al.*, 1998). Carboxen-based fibres were used to analyse the volatile contaminants in vegetable oils following the comparison of several fibres (Page *et al.*, 2000). A review of the applicability of SPME to food analysis was published in June 2000 and concluded that the simplicity of the process and the ease of coupling with analytical systems made it highly efficient and widely applicable (Kataoka *et al.*, 2000). The evolution of the technique throughout the 90s was also reviewed in 2000 (Lord *et al.*, 2000). The technique has been developed and optimised to tackle one of the most demanding analytical pharmaceutical tasks, the determination of residual solvent in drug substances (Camarasu, 2000). Coupled with GC-MS, and using a Carboxen/PDMS fibre, it was concluded to be a suitable technique owing to its precision, accuracy and speed of analysis.

The critical optimisation factors for SPME are sample temperature, agitation of the sample and length of time of exposure of the fibre to the sample (Pawliszyn, 1999). The importance of sampling conditions has been investigated in previous studies (Gorecki *et al.*, 1998; Prosen *et al.*, 1999). Adsorption equilibrium in headspace sampling for volatiles has been found to occur in the order of minutes compared with hours for liquid sampling (Ai, 1997). Convection in the gas phase maintains a steady-state diffusion at the fibre surface. In order to obtain reproducible results with good sensitivity in headspace sampling, the sampling should reach equilibrium and increased temperatures decrease the time required, whilst maintaining analyte yield on the fibre. The fibre/air partition coefficient (K_{fa}) decreases with temperature with reduced adsorption. This is offset by an increase in the air/solution partition coefficient (K_{as}) which in turn increases the concentration of analyte in the headspace, thereby promoting increased analyte adsorption by the fibre (Matich, 1999). Therefore, the reduced sensitivity arising from short sampling time can be increased by sampling at elevated temperatures.

Increasing the ratio of sample to headspace volume increases the loading of analyte onto the fibre and reduces equilibrium times, whereas the value of stirring the sample depends upon the volatility of the sample. If the sample is highly volatile then most of the sample will be in the headspace prior to sampling due to rapid solution/headspace equilibration, rendering stirring unnecessary.

Previous research (Roberts *et al.*, 2000) reported that quantification of volatiles using SPME was difficult to achieve because of several factors. Bias can arise due to competition phenomena, the linear range, different affinities to the fibre and the effect of sampling time. Competition phenomena arises when compounds with a high K_{fa} are

highly adsorbed by the fibre and reduce the adsorption of other compounds. The linear range for most compounds using SPME is usually under 1ppm. When compounds have different affinities for the fibre and are in varying concentration, all the compounds may not be in the linear range. Above this concentration there will be less increase in the amount adsorped for equal increase in concentration. Instead of using one internal standard, which would not give absolute quantification because of the different partition coefficient values among compounds they used isotope dilution assays (IDA), where compounds labelled with stable isotopes are used as internal standards. Table 7.1 shows how SPME compares with other techniques (Supelco, 2000).

Table 7.1 – Comparison of SPME with other techniques

Detection limit MS	Precision (% RSD)	Expertise	Time	Solvent Use	Simplicity
Purge & Trap ppb	1-30	high	30 min	none	No
Stripping ppt	3-20	high	2 hr	none	No
Headspace ppm		low	30 min	none	Yes
Liquid-Liquid Extraction ppt	5-80	high	1 hr	1000mL	Yes
Solid Phase Extraction ppt	7-15	medium	30 min	To 100mL	Yes
SPME ppt	〈1-12	low	5 min	none	Yes

This technique eliminates some of the disadvantages of conventional extraction techniques, many of which use organic solvents with the associated risks to health and problematic disposal. A photograph of a manual fibre assembly (Figure 7.1) illustrates

the simplicity of the process. The fibre is retracted into the needle for protection and exposed, for sampling, by depression of the plunger.

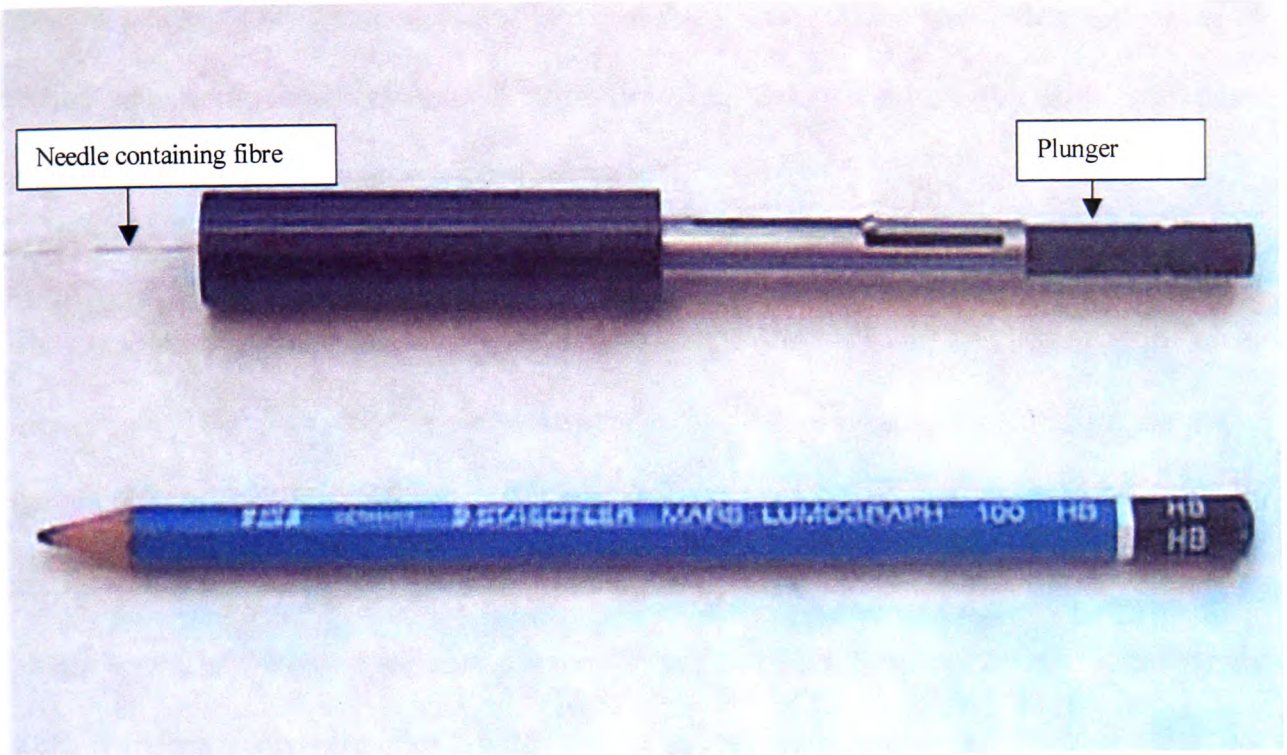

Figure 7.1 – Photograph of an SPME manual fibre assembly

7.3 METHOD

Several different fibres were obtained (Supelco UK, Sigma Aldrich, Poole, UK) to optimise extraction conditions. The main areas of investigation were centred on fibres with the following bonded stationary phases with specified film thickness:

Polydimethylsiloxane/Divinylbenzne (PDMS/DVB) Stableflex™ 65 μm

Carboxen™/Polydimethylsiloxane (CAR/PDMS) 75 μm

Polyacrylate 85 μm

The Stableflex™ fibre has a more stable coating and is less breakable. The fibre is coated on a flexible fused silica core and the coating partially bonds to the flexible core. Both the CAR/PDMS and the PDMS/DVB fibres have a partially crosslinked phase.

All the fibres were conditioned by heating in the injection port of a GC/MS system at 250°C for the time recommended by the manufacturers, half an hour for the PDMS/DVB and CAR/PDMS and two hours for the polyacrylate. The GC oven was then heated to elute any compound that had desorbed from the fibres. Blank runs were performed to ensure any compounds associated with the glue used to attach the fibre had been desorbed.

The compounds of interest, semi-volatiles, would be present in the headspace of the olive oil sample. Therefore, the fibre was suspended in the headspace rather than immersed in the oil. Immersion of the fibres into the oils could potentially damage the fibres as they are lipophillic in character. Three different fibres were used to ascertain which bonded phase would be the most suitable for the extraction of the semi-volatiles. Comparisons were then made on extractions with sample agitation (stirring) and without agitation. The effect of temperature on the compounds extracted was optimised by performing and comparing extractions at room temperature (20°C), 40°C, 48 °C, 67°C and 85°C. The fibres were also exposed to the sample for varying lengths of time, 20 minutes, 30 minutes, 40 minutes and 60 minutes. The amount of sample was also considered using 1 g and 2 g of walnut oil. The fibre was introduced into a Hewlett Packard 5890 GC system with a CP-SIL 8CB Low bleed column (30 m x 0.32 mm ID). A SPME inlet liner, 0.75 mm ID (Supelco UK, Sigma Aldrich, Poole, UK) was inserted into the injection port to decrease the internal diameter of the GC injection port. This increases linear velocity compared to a conventional, larger volume 2 mm ID liner and rapidly introduces the analytes onto the column in a narrow band. In order to curtail sample loss or peak tailing by minimising adsorption of active sample components, the inlet liner is inert. The GC temperature program, identical to the program used for Supercritical Fluid

Extraction apart from exclusion of unnecessary solvent delay, is shown in Table 7.2. A Hewlett Packard 5971A Mass Selective Detector was coupled to the GC and the sample was analysed using electron ionisation.

Table 7.2 - GC Temperature program

Temp (°C)	Time Held (min)	Program Rise (°C/min)	Final Temp(°C)
40	2	0	40
40	0	10	270
270	2	40	280
280	3	0	280

Injector temperature - 200°C Detector temperature - 270°C

Standards of a range of volatile compounds were obtained (Sigma-Aldrich) and run through the GC-MS program to confirm retention times. Standards were also made up to investigate the linear response and therefore reproducibility obtainable with SPME.

Following optimisation the technique was evaluated using samples from the Greek olive oils. Ten oils from the 1995/96 harvest were extracted, five from Crete and five from Peloponessos to determine whether SPME would extract a similar range of compounds to SFE. The resulting chromatograms were imported into Unscrambler and Statistical Package for Social Sciences (SPSS) for multivariate statistical analysis. The two techniques (SFE and SPME) were then combined, for two of the oils, by replacing the Tenax™ tube to adsorb analytes, with the SPME fibre. The SFE program was run as before (Table 7.3) with the SPME fibre exposed during the 20 minutes of dynamic extraction.

Table 7.3 - SFE extraction conditions

Density (g/ml)	0.75
Pressure (psi)	4400
Flow rate (ml/min)	2
Restrictor (°C)	85
Dynamic Extraction (min)	20
Static Extraction (min)	20
Oven Temperature (°C)	80

7.4 RESULTS AND DISCUSSION

7.4.1 Optimisation

Initial investigations with different fibres showed the PDMS/DVB fibre to extract a greater range of semi-volatiles than the CAR/PDMS or the polyacrylate, although the CAR/PDMS fibre did extract greater amounts of hexanal, 2-heptenal and nonanal, but similar amounts of other volatiles including 2-octenal (Figure 7.2).

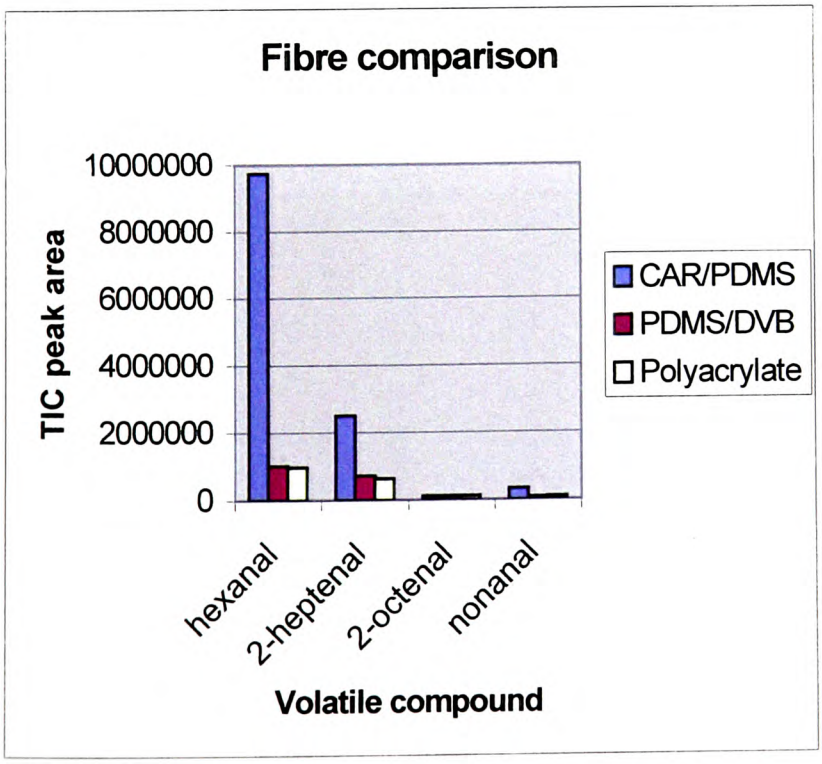

Figure 7.2 – Graph showing range of volatiles extracted by three different fibres, CAR/PDMS (blue), PDMS/DVB (red) and polyacrylate (yellow)

Using the PDMS/DVB fibre, optimum parameters were concluded. Stirring appeared to 'release' more of the target compounds so further samples were stirred. Temperature was the next parameter investigated. First interpretation shows that most of the aldehyde compounds increase in abundance with higher temperature. Elevated temperatures reduce the time required to reach equilibrium whilst maintaining adsorption on to the fibre. The higher the temperature, the greater the degradation of the oil, therefore the factor of sampling time was investigated using a working temp of 67°C.

Figure 7.3 gives a graphical representation of the impact of increased sampling temperature on individual compounds. Figure 7.4 shows the Total Ion Chromatograms (TIC) for the extraction carried out at 20°C (A), compared to the extraction at 85°C, showing enhanced extraction at 85°C (B). TICs for the other temperature optimisations are shown in Appendix E.

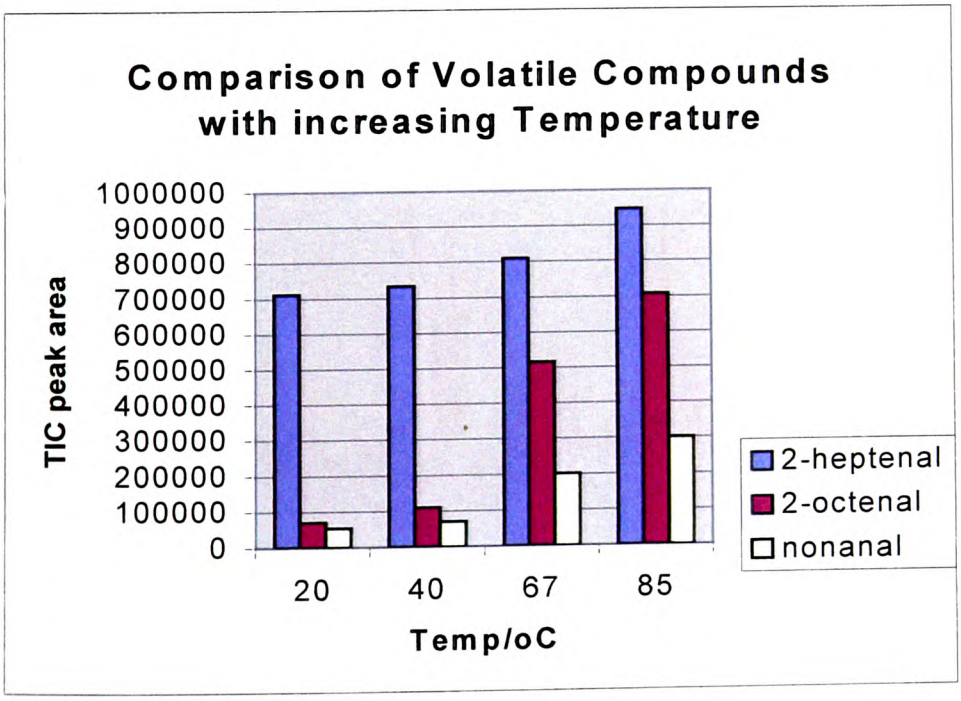

Figure 7.3 - Graph to show increase in three volatile compounds with increased extraction temperature

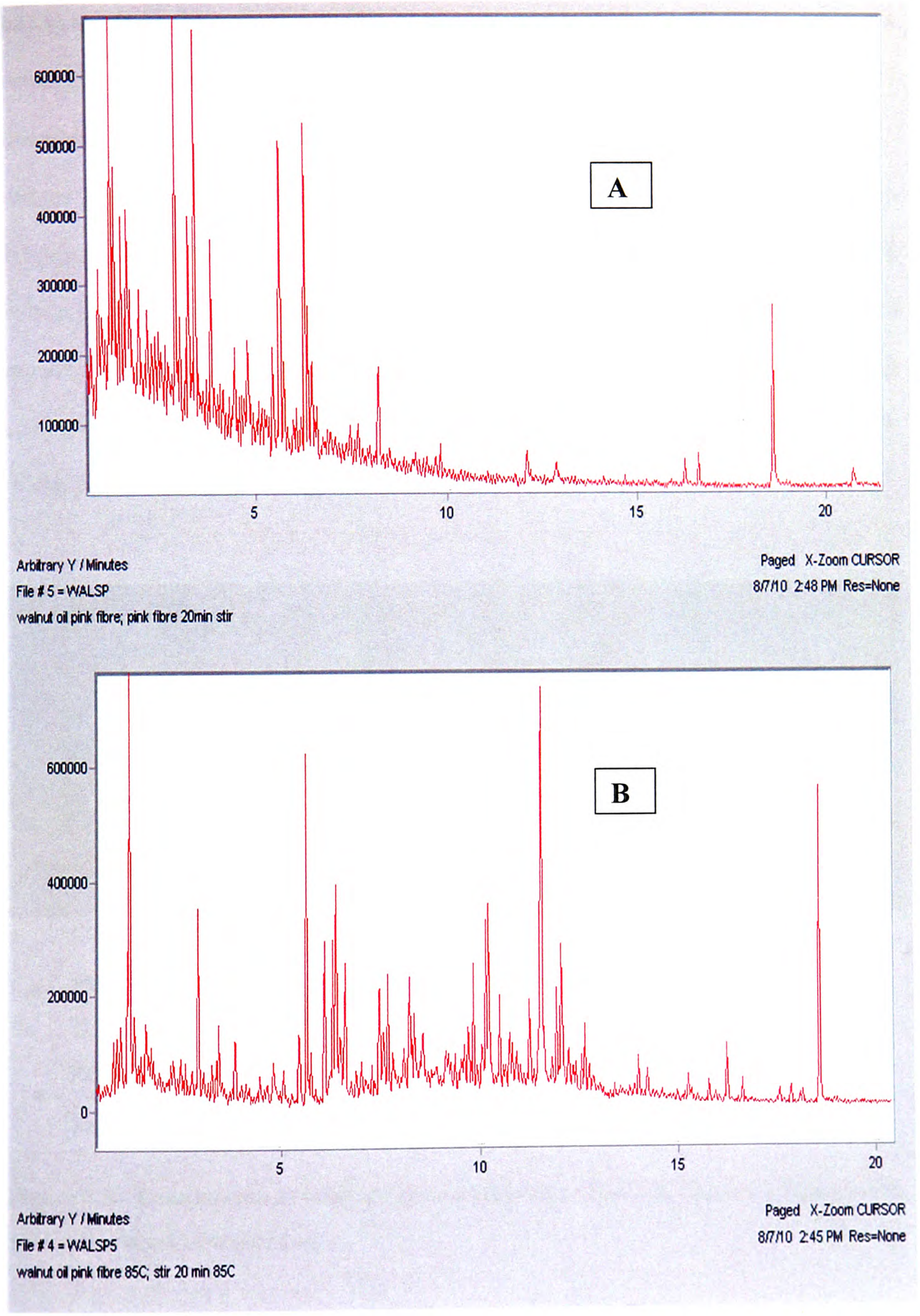

Figure 7.4 - TIC for SPME extractions of walnut oil at 20°C (A) and 85°C (B)

All temperature optimisation was carried out using a sampling time of 40 minutes, which had shown to be the most advantageous. All previous optimisations had been carried out using 2 g of walnut oil. 1g of oil was tested at 40 minutes sampling time and 67°C, however it was concluded that the larger sample size gave better extraction. The size of sample tested was restricted by the vial capacity, 2 g being the maximum to allow headspace. Using the optimised parameters, stirring 2 g of oil at 67°C for 40 minutes the extract of walnut oil using the PDMS/DVB fibre was desorbed in the injection port and run on the GC-MS. The resulting TIC is shown in Figure 7.5 as a negative image compared to the TIC of the same oil extraction using SFE. It shows enhanced extraction of compounds between 4 and 10 minutes using the SPME technique.

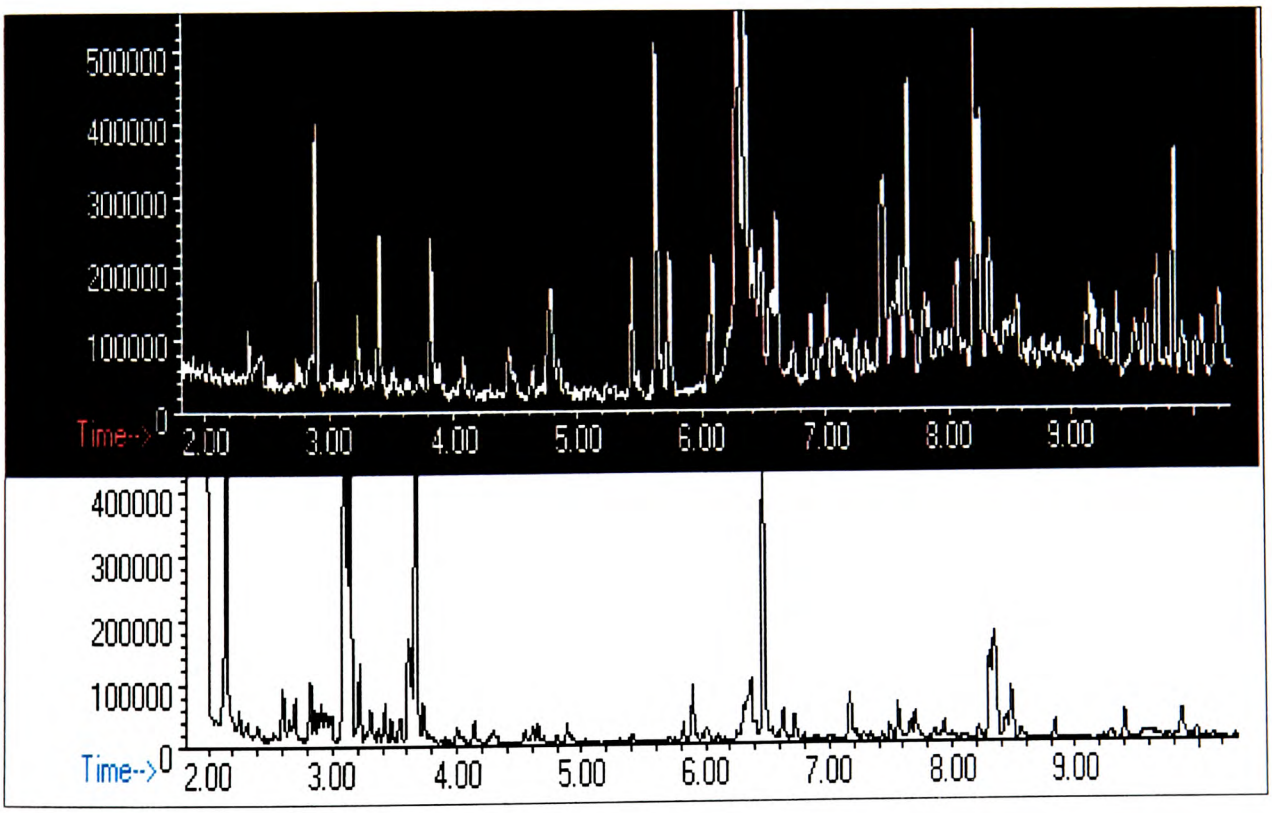

Figure 7.5 - Comparison of total ion chromatograms of SPME (negative image) and SFE extractions of walnut oil

Standard solutions of 2.5 ppm, 5 ppm, 6.25 ppm and 10 ppm of volatile compounds were extracted to investigate the linearity of the response using the PDMS/DVB fibre. The graph in Figure 7.6 shows good linearity for extractions of 2-heptenal.

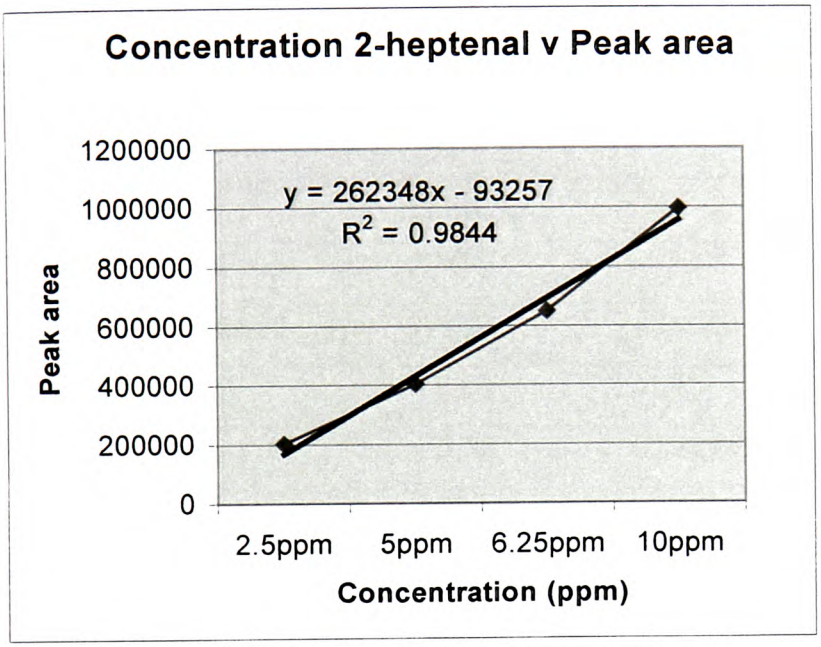

Figure 7.6 - Linearity of SPME extraction for 2-heptenal

7.4.2 Greek Oil Extraction

The range of compounds extracted using SPME on the Greek olive oil was more extensive than was extracted by SFE. Table 7.4 gives a comparison of the compounds extracted from an oil from the 1995/6 harvest from Crete and Table 7.5 an oil from Peloponessos from the same harvest year.

Table 7.4 - Comparison of retention times and peak area of SFE and SPME extracted compounds from Crete oil E15

Compound	SFE		SPME	
	RT	*Peak area*	*RT*	*Peak area*
2-pentenal	ND		2.26	330794
Hexanal	2.96	6844805	2.90	6698597
2-hexenal	ND		3.75	213963
3-hexen-1-ol	ND		4.02	783370
Heptanal	ND		ND	
2,4-hexadienal	ND		ND	
2,4-octadienal	4.48	228030	ND	
2-heptenal	5.61	705514	5.61	4134368
Heptanol	5.89	228894	5.90	581380
1-octen-3-ol	ND		6.07	3820637
2,4 nonadienal	6.27	1370279	6.28	1328777
Octanal	6.46	1317888	ND	
Limonene	ND		ND	
3-octen-2-one	ND		ND	
2-octenal	7.40	696080	7.44	5986265
Nonanal	ND		7.68	1459440
4-nonenal	8.04	2495158	8.05	3619954
2-nonen-1-ol	8.21	3512832	8.23	8778476
Nonanol	ND		ND	
Naphthalene	ND		ND	
Decanal	ND		ND	
2-decenal	10.70	695036	10.73	7018099
2,4-decadienal	ND		11.54	1958063
2-undecenal	12.22	899329	12.22	3399576
α -Farnesene	ND		ND	

Table 7.5 – Comparison of retention times and peak areas of SFE and SPME extracted compounds from Peloponessos oil E33

Compound	SFE		SPME	
	RT	*Peak area*	*RT*	*Peak area*
2-pentenal	ND		2.59	35738
Hexanal	2.92	2453495	2.82	923904
2-hexenal	3.76	342806	3.68	1786999
3-hexen-1-ol	ND		3.76	664521
Heptanal	4.16	Trace	ND	
2,4-hexadienal	ND		ND	
2,4-octadienal	ND		5.36	227509
2-heptenal	5.58	Trace	5.56	222954
Heptanol	ND		ND	
1-octen-3-ol	6.02	Trace	6.02	60972
2,4 nonadienal	6.24	2534967	6.24	172658
Octanal	6.42	544978	6.43	627184
Limonene	ND		6.89	756923
3-octen-2-one	ND		ND	
2-octenal	7.4	Trace	7.4	162186
Nonanal	ND		ND	
4-nonenal	8.00	577563	ND	
2-nonen-1-ol	8.18	2895043	8.2	2073912
Nonanol	ND		ND	
Naphthalene	ND		9.47	172297
Decanal	ND		ND	
2-decenal	10.68	645852	10.70	2009347
2,4-decadienal	ND		ND	
2-undecenal	12.18	219864	12.21	325678
α -Farnesene	ND		14.16	210948

The SPME extracted a greater range of volatile/semi-volatile compounds from the oils in each case. A full set of data for the extractions of the remaining oils can be found in

Appendix E. SPME repeatedly had more success in extracting the lower boiling point compounds. α-Farnesene was extracted and detected in all the Peloponessos oils but none of the Crete oils, indicating that it could possibly be used as a marker to determine geographical origin.

Table 7.6 shows a comparison of the two previously used extraction processes (SFE and SPME) with the unique idea of coupling SFE and SPME. Results could possibly be improved by a modification in the coupling procedure. The SPME fibre was inserted into the unsealed tubing leading from the SFE restrictor, therefore increasing the possibility of loss of analyte to the surroundings.

Table 7.6 – Comparison of three extraction techniques (E34)

Compound	**SFE**		**SPME**		**SFE onto SPME**	
	RT	*Pk area*	*RT*	*Pk area*	*RT*	*Pk area*
2-pentenal	ND		ND		ND	
Hexanal	2.94	1995689	2.85	412944	2.80	308583
2-hexenal	3.79	322195	3.72	2518686	3.69	
3-hexen-1-ol	ND		3.79	617934	ND	
Heptanal	4.64	182448	ND		ND	
2,4-hexadienal	ND		4.74	50198	ND	
2,4-octadienal	ND		ND		ND	
2-heptenal	5.63	178386	5.59	182926	5.57	234810
Heptanol	ND		ND		ND	
1-octen-3-ol	ND		6.04	49189	6.03	
2,4 nonadienal	6.30	2320927	ND		6.25	896508
Octanal	6.48	542884	6.44	182481	6.44	451399
Limonene	ND		ND		ND	
3-octen-2-one	ND		ND		ND	
2-octenal	ND		ND		7.42	289959

Nonanal	ND		ND		7.67	873714
4-nonenal	8.06	939281	ND		8.05	976023
2-nonen-1-ol	8.23	4036898	8.21	1423070	8.23	4505137
Nonanol	ND		ND		ND	
Naphthalene	ND		9.47	193667	9.50	245153
Decanal	ND		9.88	9084475	9.88	681414
2-decenal	10.73	620553	ND		10.73	1557192
2,4-decadienal	ND		11.55	Tr	11.55	344901
2-undecenal	12.24	255017	ND		12.23	699200
α -Farnesene	14.19	233980	14.16	520245	ND	

ND – Not detected Tr – Trace

7.4.3 Statistical Analysis

The total ion chromatograms from the ten Greek oils tested were imported into two statistical packages (Unscrambler and SPSS) to ascertain whether the differences in volatile compounds extracted by SPME are sufficient to allow class separation and/or clustering. Figure 7.7 shows the dendrogram resulting from the hierarchical cluster analysis using Ward's method with squared Euclidean distance measurement from the SPSS program. All variables were used for the cluster analysis, relating to compounds eluting from the column between one and twenty minutes.

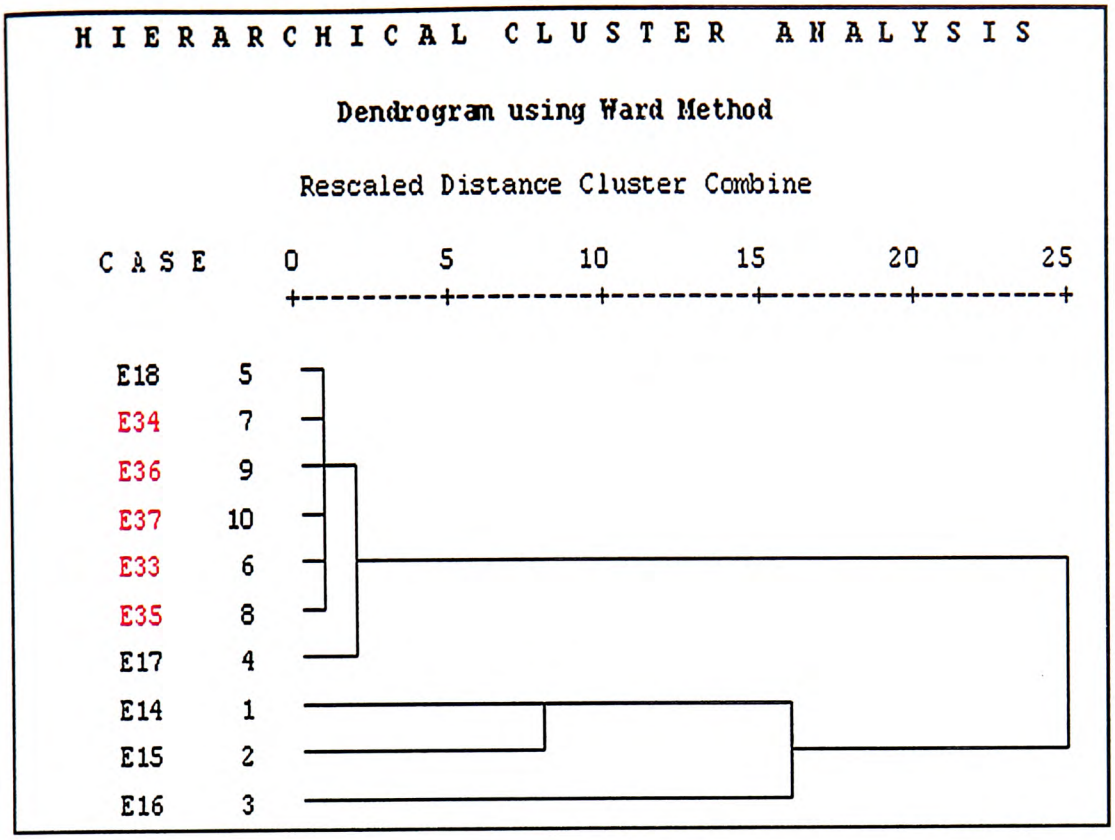

Figure 7.7 - Dendrogram of clustering of SPME extracted volatiles from olive oil, using all variables (1 - 20 minutes)

The dendrogram shows good clustering for the non-Crete samples (red), although one of the Crete oils (E18) was clustered with the non-Cretes. The distance between the Crete oils (black) was greater than the non-Cretes with E14 and 15 showing the closest relationship. The cluster analysis gave an indication that PCA models may show grouping to differentiate between the two areas of geographical origin and possibly classify unknown samples.

Figure 7.8 shows the Cooman's plot, with the non-Crete oils shown in green and the Crete oils shown in red. Although many of the oils are doubly classified (appearing in the bottom left) there is some separation with the Crete oils having greater sample distance from the non-Crete model and the non-Crete oils show a good clustering. The

test sample (blue) was correctly grouped with other non-Crete oils although the distance to the Crete model was not sufficient to afford conclusive separation.

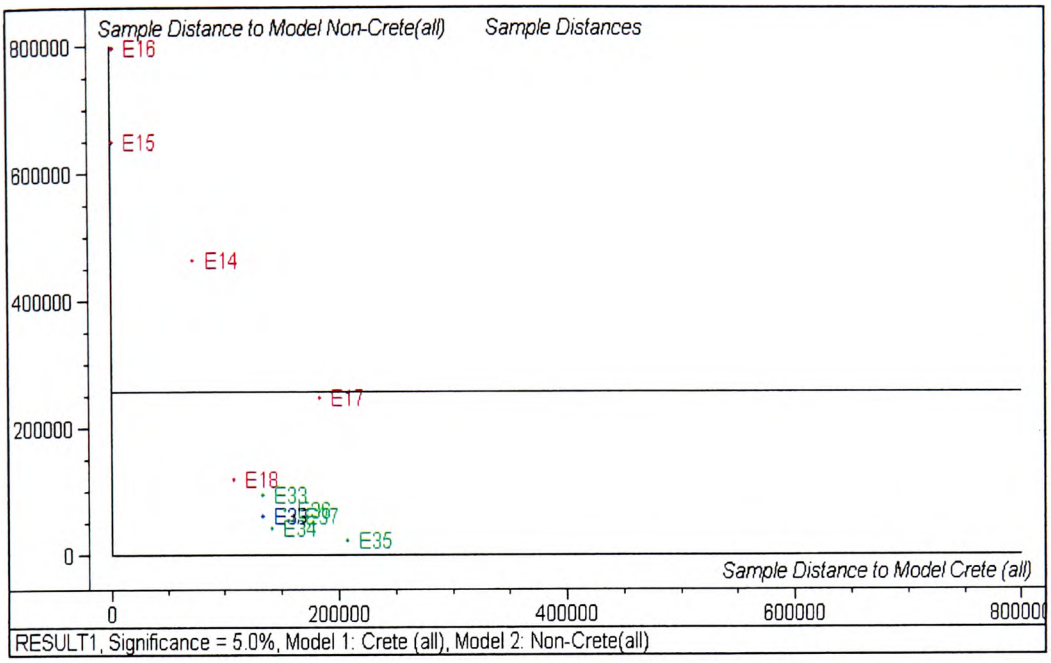

Figure 7.8 – Cooman's plot to show classification of Crete (red) v non-Crete (green) oils by SPME extracted compounds

7.5 CONCLUSIONS

As previously discussed (Chapter 2.3.8), elevated temperatures, increased storage time and exposure to light cause the autoxidation of the fatty acids present in olive oil. The majority of the volatile compounds extracted and detected using SPME (Tables 7.4 and 7.5) are the products of this degradation. Heating the sample, to optimise the volatile adsorption onto the SPME fibre, increases the volatile compounds extracted because heating increases the oxidation of the oil. In olive oil autoxidation is sensitive to heating as both the intermediates of decomposition (hydroperoxides) and the final products are labile and prone to changes. The ideal temperature for extracting fresh oil samples would be room temperature (20°C) but the time required to reach equilibrium at this

temperature would be inhibiting due to the affinity of the volatile compounds to the oil matrix.

Although the statistical analysis was limited by the size of the sample set, the non-Crete oils showed good clustering and the Crete oils demonstrated some separation from the non-Crete model. The discrimination plot (Appendix F) showed no particular compounds as influential in geographic determination, with the full spectra having a discrimination power greater than 3. α-Farnesene was detected in all the non-Crete samples but none of the Crete, leading to the supposition that this compound could potentially be used as a geographical marker.

SPME is an extremely simple, cheap technique that has been shown to be applicable in numerous areas. Within this work SPME was employed as a sampling method rather than a quantitative method as it does not exhaustively extract the sample. The fibre choice was therefore made qualitatively rather than quantitatively, to compare the range of compounds extracted with those using SFE. SPME repeatedly extracted a greater range of compounds especially at the lower boiling points and extractions were performed more rapidly than SFE, which makes SPME the preferred technique.

The novel concept of coupling the two techniques, utilising the solvating power of supercritical fluid with the concentrating effects of SPME, gave encouraging results which provide the basis for exciting and innovative future work.

CHAPTER 8

8 Conclusions

The analysis of olive oil is an area of research which has occupied numerous groups of researchers, especially over the last decade. Reviews appear regularly collating recent findings and assessing new techniques for characterisation, extraction and detection of adulteration (Aparicio *et al.*, 2000; Cert *et al.*, 2000; Lercker *et al.*, 2000; Ulberth *et al.*, 2000).

8.1 EXTRACTION TECHNIQUES

The two techniques used throughout this work (SFE and SPME) to attempt to extract the semi-volatile components in olive oil have both proved valuable tools and the possibility of combining the two processes gave encouraging preliminary results.

8.1.1 Supercritical Fluid Extraction (SFE)

Supercritical fluid extraction (SFE) gave reproducible results on the test samples used from the Greek oils and confirmed compounds seen previously, by other research groups, using different extraction methods. SFE has been shown to be a comparable extraction technique which has the added benefit of using a readily available, low cost, low toxicity solvent with relatively short experimental time. The range of compounds extracted and detected in the locally obtained vegetable oils (walnut, sesame, sweet almond and extra virgin olive oil) varied. Long chain alkanes and alkenes, not of interest in this study, were eluting from the column after 23 minutes. The intensity of these peaks was such that they were affecting the integration of the smaller peaks. This resulted in some compounds of interest not being included in the integration due to their

low concentration and small peak area. A further modification to the GC-MS program of shortening the detection time of the mass spectrometer would be advantageous. The less volatile components could then be eluted from the GC column but not detected by the MS, thereby simplifying the chromatograms and allowing more straightforward integration and identification of the smaller peaks.

The Greek olive oils gave good extraction and detection reproducibility when the oil was repeatedly extracted and the same extract repeatedly injected. The multivariate statistical analysis of the Greek oils showed some separation between the Crete and non-Crete oils with the software assigning the peaks important in differentiating between the two models as being a range of saturated and unsaturated aldehydes. The amount of volatile compounds in an olive oil is, to a certain extent, indicative of the degree of oxidation experienced by the oil either from extended storage or exposure to heat or light. Information from a recent SPME work (Jelen *et al.*, 2000) demonstrated that some of these saturated and unsaturated aldehydes are oxidation products of fatty acids. For example, the main volatile product of oleic acid oxidation is octanal whereas linoleic oxidation produces 2-heptenal and 2-octenal. This would suggest that the fatty acids that influence the Crete oil model were oleic and linoleic acids.

Regression plots were constructed using the ratio of peak area of extracted volatile compounds to internal standard for the Greek olive oils and potential adulterants. PLS1 plots showed clear separation, along the first regression component, between olive oil and 100% sesame oil. This indicated that the difference in volatile composition between these two oils was sufficient to allow statistical classification. Other adulterant oils were not so well defined and if the concentrations were less than 100% (as would be expected

if used for adulteration) it is inconclusive, from this work, whether the extracted volatile compounds would vary sufficiently to detect and predict adulteration.

8.1.2 SPME

SPME consistently detected a greater range of volatiles than the SFE. SPME extracted some shorter chain aldehydes including 2-pentenal, one of the main products of linolenic acid oxidation. Unlike the SFE extractions, there was no solvent delay used during the thermal desorption of the fibre and this could account for the detection of the 2-pentenal in the SPME extractions. The extractions were performed qualitatively purely to assess the applicability of the technique. In order to optimise the adsorption of the volatile compounds on to the fibre, the oil samples were heated to 67°C. Heating the oil increases the autoxidation of the fatty acids, thereby increasing the concentration and range of the volatile components. This raised the concern that the enhanced performance of the SPME was due to the method parameters employed. However, a study looking at the degradation of olive oil and monitoring the formation of carbonyl compounds concluded that primary oxidation, to form hydroperoxides, takes place up to 150°C and significant degradation occurred (formation of aldehydes) after 200°C (Moreno *et al.*, 1999). This would suggest that the temperatures, used in this work, for the SPME extractions would cause minimal increase in the volatile fraction. Extra virgin olive oil does have a higher resistance to oxidation than other oils because of its antioxidant component. The length of storage could be another contributor to the increase in volatile compounds. Although the samples tested were not fresh, the absence of noticeable aldehydic peaks in the ^{1}H NMR would suggest that degradation had not occurred to any substantial degree. A true reflection of the volatile components of olive oil would require analysis to be carried out as soon as the oil were produced before any degradation

had occurred. However, the majority of olive oils are consumed following shelf storage for varying amounts of time and so the analysis of the development of degradation products is necessary to predict shelf life. Following the storage recommendations of keeping oil in a dark bottle at 20°C prolongs the shelf life by decelerating the oxidation process.

8.1.3 SFE onto SPME

Coupling the two extraction techniques together was a novel idea which gave promising early results. The extraction is maximised by harnessing the solvating power of the supercritical fluid with the enhanced extraction abilities of the SPME fibre. The coupled technique extracted a greater range of components from the oils than either technique alone and some compounds were detected that had not been detected with either method. It should also be noted that improvement in the physical coupling of the two pieces of equipment could decrease a potential loss of compounds as the SFE restrictor outlet/SPME fibre interface had not been sealed during this work.

8.2 SPECTROSCOPY

The two spectroscopic procedures used in this project gave complementary results, with the ^{1}H NMR identifying geographic and harvest origin and the IR giving better results in the detection of sunflower adulteration. The data gathered using ^{13}C NMR did not constitute a very large sample set, therefore, the statistical analysis could be considered unreliable. Whilst there did appear to be an increase in the peak area ratios arising from linoleic/linolenic acid in the ethylenic region when adulterated with vegetable oils

(sunflower, soya, corn and cotton), the resulting statistics did not support this observation.

8.2.1 Geographic and Harvest Differentiation

Proton NMR gave clearly defined separation between the oils originating from Crete and those from other areas of Greece and also between the Crete oils produced in 1995/96 and 1996/97. Both geographic areas have a variety of growing altitudes and the majority of growers use the same species of olive (Koroneiki). Although both of these factors influence the composition of the oil, there is not sufficient evidence to attribute the appreciable difference in the oils to these features alone. Difference in climatic conditions is possibly a major contributor to the variation in the composition of the oils. A previous study has shown that the percentage of C18:1 (oleic acid) is negatively correlated with the relative humidity of the atmosphere (Stefanoudaki *et al.*, 1999), so that the areas of high altitude with cooler climates produced oils that had a greater level of monounsaturated fatty acids and low altitude areas with high mean temperatures produced oils with a higher content of saturated acids. A previous work (Lees *et al.*, 1998) acquired information regarding rainfall for the Greek mainland during the 1995/96 and 1996/97 growing seasons (E and F sets respectively). There was a greater average rainfall during the 1996/97 growing and harvesting period than for the previous season. From the limited data for the 1995/96 harvest in that study, in general, the ratio of 18:1 was higher in the F set (1996/97) than the E set, 18:2 was lower in the F set, 18:0 was also lower in the F set whereas the amount of linolenic acid (18:3) showed little change. This would suggest that the F oils were grown and harvested in a cooler climate than the previous years' oils but whether a cooler climate can be directly correlated to the increased rainfall in that year is questionable.

NMR looks at specific protons, therefore, when the degree of unsaturation in the fatty acids increases the number of protons between the C=C bonds (Figure 4.4, H5) and the protons on the C=C (Figure 4.4, H1) are greater so the signal will be enhanced. In contrast the number of CH_2 bonds in the chain (Figure 4.4, H9) will be reduced. As shown in the extract from Table 2.1 (Table 8.1 below), the percentage composition of fatty acids varies enormously within a single harvest year (Boskou, 1996) because of climatic and other factors.

Table 8.1 – Extract from Table 2.1 showing variation in percentage fatty acid composition within a single harvest year

Fatty acid	Minimum %	Maximum %	Mean %
Oleic	68.8	82.8	76.9
Linoleic	4.6	14.5	7.5
Linolenic	0.5	0.9	0.6

The natural variation in fatty acid composition can produce oils with a naturally higher linoleic/linolenic content. As seen from Table 8.1 the maximum percentage linoleic acid content in olive oils from a particular year was 14.5% compared to the minimum of 4.6%. This 10% fluctuation is greater than would be expected with adulteration at low levels (1, 2 and 5%), which could explain the ability of ^{1}H NMR to better detect the natural variation over the induced variation of adulteration.

The analysis using the fibre optic probe did not produce statistical models robust enough to give well defined separation between harvest year or geographic origin for any of the three years. Most of the samples were doubly classified with the E Crete v non-Crete oils showing better grouping than the F or D sets. The differentiation between harvest years was again not as specific as with ^{1}H NMR, however the models using only selected

wavelengths (HC=CH, CH and C=O) did correctly assign an F oil as belonging to neither the D or E sets for non-Crete samples.

IR is a more generic technique than NMR, looking at functional groups areas over large wavelength spans (893 - 1260, 1610 - 1776, 2730 - 3060 cm^{-1}). Fluctuations in functional groups in compounds other than the fatty acids will affect the IR spectra, resulting in the unsaponifiable fraction of the oil distorting the result. The carbonyl area (1610 - 1776 cm^{-1}) gives well defined peaks in IR but this area contains less information than the other two areas (HC=CH and CH respectively).

Throughout this study the peaks extracted as being amongst the most important to the PCA models discriminating between year of origin showed accord with the findings of a Greek study (Tsimidou *et al.*, 1993). They found that PCA indicated a greater influence of harvest year on the grouping of oils than either olive variety or place of origin. Palmitic, oleic and linoleic acids contributed equally to PC1, along which axis the oils were spread. PC2 was defined by stearic acid and they concluded this to be characteristic of the year of harvest and that the factor year influenced all the variables as opposed to cultivar, which only affected the oleic and linoleic variables. A variation in the amount of stearic acid would alter the proton peaks H8 (CH_2C=C), H12 (C*H*=CH) and H10 (allyl CH_2), (reference Figures 4.3 and 4.4). These three peak areas have been shown, also by this study, to have a pivotal role in distinguishing between year of origin and also area of origin.

8.2.2 Adulteration with sunflower oil

In all the adulteration investigations the Crete and non-Crete oils were treated separately to avoid the geographical variance influencing the regression plots. Using ^{1}H NMR the errors of prediction were unacceptably high and the number of samples marked as outliers were greater than the accepted samples, proving the model to be unreliable.

The squared errors of prediction (RMSEP) using IR were much lower especially for the Crete oils from the E set (0.795% sunflower oil). The initial PLS components accounted for the majority of the variance with the samples grouped according to adulteration along the first PC. The first principal component separated the higher levels of adulteration and the 0%/1% levels. The lower levels of adulteration (0 and 1%) showed considerable overlap as would be expected at this extremely low level of adulteration. The natural variation in fatty acid composition would account for the overlap and it would be extremely difficult to consistently distinguish adulteration with 1% sunflower oil.

The E set of Crete oils was also used to investigate how reducing the number of variables used for statistical analysis would affect the results. The three selected ranges (893 - 1260, 1610 - 1776, 2730 - 3060 cm^{-1}), on which the majority of the statistical analysis was based, used 899 variables. Fifteen of the most important variables, as concluded from the regression coefficient plot, were used to recalculate the data. The resulting RMSEP was 0.912% (compared to 0.795%) sunflower adulteration, with an offset of 0.235% (compared to 0.147%) using 9 regression components (compared to 11). Although these results were higher than when using 899 variables, they still showed good correlation between the predicted adulteration levels and the measured levels. Using 15 variables reduced the statistical analysis time but increased the error of

prediction. This makes it questionable whether reducing the variables is, in this case, a sound statistical process which would enable future investigations to monitor specific wavelengths, or a statistical exercise purely for the sake of it.

The D and F sets did not produce statistically robust models, giving an RMSEP between the measured and the predicted percentage adulteration greater than 1.5% sunflower oil. The natural fluctuation in composition of olive oils means that low level adulteration (e.g. less than 5%) is only reliably detectable if the corresponding unadulterated samples are available to factor out discrepancies arising from origin or climatic influences.

8.3 FURTHER WORK

The possibility of detecting adulteration with the volatile fraction was looked at briefly by comparing the chromatograms, from SFE, obtained for common adulterant oils with olive oil. The volatiles detected did vary in part and whether this would be sufficient to be confidently used as an adulteration marker would require the collection and analysis of large data sets, beyond the time constraints of this project. Preliminary statistical analysis showed separation between adulterants (at 100%) and olive oil. However, adulteration would occur at much lower concentrations of adulterant oil and further work would need to involve the analysis of spiked olive oil samples using low levels of adulterant oils to ascertain whether the separation was sufficient to detect statistically. SPME would appear to be the preferred method of extraction but further investigation into coupling SFE with SPME could provide a more complete extraction method.

The non-Crete samples from the F set were not evaluated using ^{1}H NMR due to technical difficulties at ISAS. The completion of this set would allow geographical and harvest differentiation investigations for the full F set to be carried out. This would confirm whether the conclusion that ^{1}H NMR was a suitable technique could be substantiated.

The completion of the analysis of the oils using ^{13}C NMR would verify whether a larger sample set would give more robust statistical models for adulteration with all four contaminant oils (corn, cotton, soya and sunflower). The use of other pulse sequences, such as DEPT, could prove to give useful data. DEPT increases the sensitivity of ^{13}C NMR and decreases the long acquisition times by population transfer. The major drawback with DEPT would be the inability to detect the resonance of the unprotonated carbonyl carbon, as this gives important information on the fatty acid composition.

Investigations into reducing the number of applicable variables could be continued to attempt to find the optimum number of variables that would give acceptable statistical results. This would considerably decrease the time involved in both the acquisition and the data processing procedures.

8.4 FINAL SYNOPSIS

The aims of this work were to assess the suitability of various analytical techniques for detecting adulteration, geographical and harvest provenance of Greek olive oils. The development of the diamond tipped fibre optic probe at the Institute for Spectrochemistry and Applied Spectroscopy in Dortmund, Germany, provided a technique additional to the

original research plan. This method proved to be the most rapid and reliable for the detection of adulteration with sunflower oil.

The extraction and detection of the volatile fraction was not fully explored with regard to adulteration. The SFE results reinforced previous investigations (Morales *et al.*, 1998) and extracted previously unseen saturated and unsaturated aldehydes, possibly products of oil degradation. The emphasis moved to the investigation and optimisation of Solid Phase Microextraction, which would enable a completely solventless extraction. A further modification was also instigated that resulted in the unique coupling of SFE and SPME providing an exciting area on which to expand.

The proton NMR results reinforce the side of the argument which concludes that the fatty acid composition is suitable for distinguishing between areas and years of origin. Previous research groups have disagreed as to its suitability but this data confirms the union of NMR and chemometrics as being an extremely valuable technique with minimal sample preparation and short acquisition time.

Results from this work would suggest that there is not a universal technique applicable for all areas of olive oil characterisation. The spectroscopy techniques were successful in different areas and although the extraction of the volatile components posed more questions that it answered, the possibility of further exploring the coupling of SFE and SPME is an area of exciting possibilities.

References

Adams, M. (1995). Chemometrics in Analytical Spectroscopy, Royal Society of Chemistry.

Ai, J. (1997). "Solid-Phase Microextraction for Quantitative Analysis in Nonequilibrium situations." Analytical Chemistry **69**(6): 1230-36.

Ai, J. (1999). Quantitation by SPME before Reaching a Partition Equilibrium. Applications of Solid Phase Microextraction. J. Pawliszyn. Cambridge, Royal Society of Chemistry. **1:** 22-37.

Allen, D. L. and J. S. Oliver (2000). "The use of supercritical fluid extraction for the determination of amphetamines in hair." Forensic Science International **107**(1-3): 191-199.

Angerosa, F., L. Camera, N. d'Alessandro and G. Mellerio (1998). "Characterization of seven new hydrocarbon compounds present in the aroma of virgin olive oil." Journal of Agricultural and Food Chemistry **46**(2): 648-653.

Angerosa, F., L. Di Giacinto, R. Vito and S. Cumitini (1996). "Sensory Evaluation of Virgin Olive Oils by Artificial Neural Network Processing of Dynamic Head-Space Gas Chromatographic Data." Journal of the Science of Food and Agriculture **72**(3): 323-28.

Angerosa, F., R. Mostallino, C. Basti and R. Vito (2000). "Virgin olive oil odour notes: their relationships with volatile compounds from the lipoxygenase pathway and secoiridoid compounds." Food Chemistry **68**(3): 283-287.

Aparicio, R. and R. Aparicio-Ruiz (2000). "Authentication of vegetable oils by chromatographic techniques." Journal of Chromatography A **881**(1-2): 93-104.

Aparicio, R., J. Calvente and M. Morales (1996). "Sensory authentication of European extra virgin olive oil varieties by mathematical procedures." Journal of the science of Food and Agriculture **72**(4): 435-47.

Aparicio, R., M. Morales and M. Alonso (1996). "Relationship between volatile compounds and sensory attributes of olive oils by the sensory wheel." Journal of the American Oil Chemists Society **73**(10): 1253-64.

Aparicio, R., M. Morales and V. Alonso (1997). "Authentication of European virgin olive oils by their chemical compounds, sensory attributes anad consumers attitudes." Journal of Agricultural and Food Chemistry **45**(4): 1076-83.

Azodanlou, R., C. Darbellay, J. L. Luisier, J. C. Villettaz and R. Amado (1999). "A new concept for the measurement of total volatile compound of food." Zeitschrift Fur Lebensmittel-Untersuchung Und-Forschung a-Food Research and Technology **208**(4): 254-258.

Bastoni, L., A. Bianco, F. Piccioni and N. Uccella (2001). "Biophenolic profile in olives by nuclear magnetic resonance." Food Chemistry **73**(2): 145-151.

Bertran, E., M. Blanco, J. Coello, H. Iturriaga, S. Maspoch and I. Montoliu (1999). "Determination of olive oil free fatty acid by Fourier transform infrared spectroscopy." Journal of the American Oil Chemists Society **76**(5): 611-616.

Bianco, A. and N. Uccella (2000). "Biophenolic components of olives." Food Research International **33**(6): 475-485.

Blanch, G. P., M. D. Caja, M. L. R. delCastillo and M. Herraiz (1998). "Comparison of different methods for the evaluation of the authenticity of olive oil and hazelnut oil." Journal of Agricultural and Food Chemistry **46**(8): 3153-3157.

Boskou, D. (1996). Olive Oil ; Chemistry and Technology, AOCS.

Bradley, D. (1999). "Testing olive oil for antioxidants." Chemistry in Britain **35**(10): 19.

Brenes, M., A. Garcia, P. Garcia, J. J. Rios and A. Garrido (1999). "Phenolic compounds in Spanish olive oils." Journal of Agricultural and Food Chemistry **47**(9): 3535-3540.

Brenes, M., F. J. Hidalgo, A. Garcia, J. J. Rios, P. Garcia, R. Zamora and A. Garrido (2000). "Pinoresinol and 1-acetoxypinoresinol, two new phenolic compounds identified in olive oil." Journal of the American Oil Chemists Society **77**(7): 715-720.

Camarasu, C. C. (2000). "Headspace SPME method development for the analysis of volatile polar residual solvents by GC-MS." Journal of Pharmaceutical and Biomedical Analysis **23**(1): 197-210.

Camo (1998). Unscrambler User Manual.

Caruso, D., B. Berra, F. Giavarini, N. Cortesi, E. Fedeli and G. Galli (1999). "Effect of virgin olive oil phenolic compounds on in vitro oxidation of human low density lipoproteins." Nutrition Metabolism and Cardiovascular Diseases **9**(3): 102-107.

Cast, J. (1995). Infrared Spectroscopy of Lipids. Developments in Oils and Fats. R. J. Hamilton. Glasgow, Blackie Academic and Professional: 224-266.

Cert, A., W. Moreda and M. C. Perez-Camino (2000). "Chromatographic analysis of minor constituents in vegetable oils." Journal of Chromatography A **881**(1-2): 131-148.

Cinquanta, L., M. Esti and E. La Notte (1997). "Evolution of Phenolic Compounds in Virgin olive oil during storage." Journal of the American Oil Chemists Society **74**(10): 1259-64.

Claridge, T. D. W. (1999). High-Resolution NMR Techniques in Organic Chemistry, Elsevier Science Ltd.

Colthup, N. B., L. H. Daly and S. E. Wiberley (1990). Introduction to Infrared and Raman Spectroscopy, Academic Press.

Communities, E. (1966). Regulation No: 136/66/EEC, Commission of the European Communities.

Cremer, D. R. and K. Eichner (2000). "Formation of volatile compounds during heating of spice paprika (Capsicum annuum) powder." Journal of Agricultural and Food Chemistry **48**(6): 2454-2460.

De Leonardis, A., V. Macciola and M. De Felice (1998). "Rapid Determination of squalene in virgin olive oils using Gas-liquid chromatography." Italian Journal of Food Science **10**(1): 75-80.

Dionisi, F., J. Prodolliet and E. Tagliaferri (1995). "Assessment of Olive oil adulteration by reversed-phase high-performance liquid chromatography/amperometric detection of tocopherols and tocotrienols." Journal of the American Oil Chemists Society **72**(12): 1505-11.

Duckett, S. and B. Gilbert (2000). Mass Spectrometry. Foundations of Spectroscopy. R. Compton. Oxford, Oxford University Press: 1-18.

Duckett, S. and B. Gilbert (2000). Nuclear Magnetic Resonance Spectroscopy. Foundations of Spectroscopy. R. Compton. Oxford, Oxford University Press. **1:** 54-75.

Dupuy, N., L. Duponchel, J. P. Huvenne, B. Sombret and P. Legrand (1996). "Classification of edible fats and oils by principal component analysis of Fourier transform infrared spectra." Food Chemistry **57**(2): 245-251.

El-Hamdy, A. and N. El-Fizga (1995). "Detection of olive oil adulteration by measuring its authenticity factor using reversed-phase high-performance liquid chromatography." Journal of Chromatology A **708**(2): 351-55.

Esquivel, M. M., M. G. BernardoGil and M. B. King (1999). "Mathematical models for supercritical extraction of olive husk oil." Journal of Supercritical Fluids **16**(1): 43-58.

Faldt, J., M. Eriksson, I. Valterova and A. K. Borg-Karlson (2000). "Comparison of headspace techniques for sampling volatile natural products in a dynamic system." Zeitschrift Fur Naturforschung C-a Journal of Biosciences **55**(3-4): 180-188.

Fauhl, C., F. Reniero and C. Guillou (2000). "H-1 NMR as a tool for the analysis of mixtures of virgin olive oil with oils of different botanical origin." Magnetic Resonance in Chemistry **38**(6): 436-443.

Favier, J., D. Bicanic, J. Cozijnsen, B. van Veldjuizen and P. Helander (1998). "CO_2 laser infrared optothermal spectroscopy for Quantitative adulteration studies in Binary mixtures of extra virgin olive oil." Journal of the American oil Chemists Society **75**(3): 359-62.

Galli, C. and F. Visioli (1999). "Antioxidant and other activities of phenolics in olives/olive oil, typical components of the Mediterranean diet." Lipids **344**(SS): S23-26.

Goncalves, M., A. M. P. Vasconcelos, E. Deazevedo, H. J. C. Dasneves and M. N. Daponte (1991). "On the Application of Supercritical Fluid Extraction to the Deacidification of Olive Oils." Journal of the American Oil Chemists Society **68**(7): 474-480.

Gorecki, T. (1999). Solid versus Liquid Coatings. Applications of Solid Phase Microextraction. J. Pawliszyn. Cambridge, Royal Society of Chemistry. **1:** 92-108.

Gorecki, T., A. Khaled and J. Pawliszyn (1998). "The effect of sample volume on quantitative analysis by solid phase microextraction - Part 2. Experimental verification." Analyst **123**(12): 2819-2824.

Gracian, J. (1968). The Chemistry and analysis of olive oil. Analysis and Characterisation of Oils, Fats and Fat Products. H. A. Boekenoogen, Interscience Publishers. **2:** 317-591.

Guillen, M. D. and N. Cabo (1997). "Infrared spectroscopy in the study of edible oils and fats." Journal of the Science of Food and Agriculture **75**(1): 1-11.

Guillen, M. D. and N. Cabo (1999). "Usefulness of the frequencies of some Fourier transform infrared spectroscopic bands for evaluating the composition of edible oil mixtures." Fett-Lipid **101**(2): 71-76.

Harper, M. (2000). "Sorbent trapping of volatile organic compounds from air." Journal of Chromatography A **885**(1-2): 129-151.

Hawthorne, S. B. (1993). Methodology for off-line supercritical fluid extraction. Supercritical Fluid Extraction and its use in Chromatographic Sample Preparation. S. A. Westwood, Blackie Academic & Professional: 39-64.

Horchner, U. and J. H. Kalivas (1995). "Further Investigation On a Comparative-Study of Simulated Annealing and Genetic Algorithm For Wavelength Selection." Analytica Chimica Acta **311**(1): 1-13.

Hourant, P., V. Baeten, M. T. Morales, M. Meurens and R. Aparicio (2000). "Oil and fat classification by selected bands of near-infrared spectroscopy." Applied Spectroscopy **54**(8): 1168-1174.

Ibanez, E., J. Palacios, F. J. Senorans, G. SantaMaria, J. Tabera and G. Reglero (2000). "Isolation and separation of tocopherols from olive by-products with supercritical fluids." Journal of the American Oil Chemists Society **77**(2): 187-190.

Ismail, A., A. Nicodemo, J. Sedman, F. v. d. Voort and I. E. Holzbaur (1999). Infrared spectroscopy of lipids: Principles and Applications. Spectral Properties of Lipids. R. Hamilton and J. Cast, Sheffield Academic Press: 235-269.

Jelen, H. H., M. Obuchowska, R. Zawirska-Wojtasiak and E. Wasowicz (2000). "Headspace solid-phase microextraction use for the characterization of volatile compounds in vegetable oils of different sensory quality." Journal of Agricultural and Food Chemistry **48**(6): 2360-2367.

Kataoka, H., H. L. Lord and J. Pawliszyn (2000). "Applications of solid-phase microextraction in food analysis." Journal of Chromatography A **880**(1-2): 35-62.

Keszler, A., K. Heberger and M. Gude (1998). "Identification of volatile compounds in sunflower oil by headspace SPME and ion-trap GC/MS." Hrc-Journal of High Resolution Chromatography **21**(6): 368-370.

Keszler, A., K. Heberger and M. Gude (1998). "Quantitative analysis of aliphatic aldehydes by headspace SPME sampling and ion-trap GC-MS." Chromatographia **48**(1-2): 127-132.

Kiritsakis, A. (1998). "Flavour components of olive oil - A review." Journal of the American Oil Chemists Society **75**(6): 673-81.

Kiritsakis, A., G. Nanos, Z. Polymenopoulos, T. Thomai and E. Sfakiotakis (1998). "Effect of Fruit storage conditions on olive oil quality." Journal of the American Oil Chemists Society **75**(6): 721-24.

Koprivnjak, O., G. Procida and T. Zelinotti (2000). "Changes in the volatile components of virgin olive oil during fruit storage in aqueous media." Food Chemistry **70**(3): 377-384.

Koutsaftakis, A., F. Kotsifaki and E. Stefanoudaki (1999). "Effect of extraction system, stage of ripeness, and kneading temperature on the sterol composition of virgin olive oils." Journal of the American Oil Chemists Society **76**(12): 1477-1481.

Lai, Y., E. Kemsley and R. Wilson (1995). "Quantitative analysis of potential adulterants of extra virgin olive oil using infrared spectroscopy." Food Chemistry **53**(1): 95-8.

Lai, Y. W., E. K. Kemsley and R. H. Wilson (1994). "Potential of Fourier Transform-Infrared Spectroscopy For the Authentication of Vegetable-Oils." Journal of Agricultural and Food Chemistry **42**(5): 1154-1159.

Lee, D. S., B. S. Noh, S. Y. Bae and K. Kim (1998). "Characterization of fatty acids composition in vegetable oils by gas chromatography and chemometrics." Analytica Chimica Acta **358**(2): 163-175.

Lees, M., T. Mavromoustakos and P. McIntyre (1998). Molecular and Isotopic Characterisation of Virgin Olive Oil, Institute of Organic and Pharmaceutical Chemistry, The National Hellenic Research Foundation, Athens, Greece

Centre European d'Analyse Istotopique Specifique, Nantes, France

School of Applied Sciences, University of Glamorgan, UK

ELAIS, Pireus, Greece.

Lercker, G. and M. T. Rodriguez-Estrada (2000). "Chromatographic analysis of unsaponifiable compounds of olive oils and fat-containing foods." Journal of Chromatography A **881**(1-2): 105-129.

Levi, F. (1999). "Cancer prevention: Epidemiology and perspectives." European Journal of Cancer **35**(7): 1046-58.

Li, H., F. R. van de Voort, A. A. Ismail, J. Sedman and R. Cox (2000). "Trans determination of edible oils by Fourier transform near- infrared spectroscopy." Journal of the American Oil Chemists Society 77(10): 1061-1067.

Lipworth, L., M. Martinez, J. Angell, C. Hsieh and D. Trichopoulos (1997). "Olive oil and human cancer: An assessment of the evidence." Preventitive Medicine **26**: 181-190.

Livingstone, D. (1995). Data Analysis for Chemists, Oxford University Press.

Lopaczynski, W. and S. H. Zeisel (2001). "Antioxidants, programmed cell death, and cancer." Nutrition Research **21**(1-2): 295-307.

Lord, H. and J. Pawliszyn (2000). "Evolution of solid-phase microextraction technology." Journal of Chromatography A **885**(1-2): 153-193.

Maheshwari, P., Z. L. Nikolov, T. M. White and R. Hartel (1992). "Solubility of Fatty-Acids in Supercritical Carbon-Dioxide." Journal of the American Oil Chemists Society **69**(11): 1069-1076.

Mani, V. (1999). Properties of Commercial SPME Coatings. Applications of Solid Phase Microextraction. J. Pawliszyn. Cambridge, The Royal Society of Chemistry. **1:** 57-72.

Manna, C., F. Della Ragione, V. Cucciolla, A. Borriello, S. D'Angelo, P. Galletti and V. Zappia (1999). Biological effects of hydroxytyrosol, a polyphenol from olive oil endowed with antioxidant activity. Advances in Nutrition and Cancer 2. **472:** 115-130.

Mannina, L., C. Luchinat, M. Patumi, M. C. Emanuele, E. Rossi and A. Segre (2000). "Concentration dependence of C-13 NMR spectra of triglycerides: implications for the NMR analysis of olive oils." Magnetic Resonance in Chemistry **38**(10): 886-890.

Mannina, L., M. Patumi, P. Fiordiponti, M. C. Emanuele and A. L. Segre (1999). "Olive and hazelnut oils: A study by high-field H-1 NMR and gas chromatography." Italian Journal of Food Science **11**(2): 139-149.

Manzi, P., G. Panfili, M. Esti and L. Pizzoferrato (1998). "Natural antioxidants in the unsaponifiable fraction of virgin olive oils from different cultivars." Journal of the Science of Food and Agriculture **77**: 115-120.

Marigheto, N. A., E. K. Kemsley, M. Defernez and R. H. Wilson (1998). "A comparison of mid-infrared and Raman spectroscopies for the authentication of edible oils." Journal of the American Oil Chemists Society **75**(8): 987-992.

Martens, H. and T. Naes (1991). Multivariate Calibration, John Wiley & Sons Ltd.

Matich, A. (1999). Analysis of Food and Plant Volatiles. Applications of Solid Phase Microextraction. J. Pawliszyn. Cambridge, Royal Society of Chemistry. **1:** 349363.

Mavromoustakos, T., M. Zervou, G. Bonas, A. Kolocouris and P. Petrakis (2000). "A novel analytical method to detect adulteration of virgin olive oil by other oils." Journal of the American Oil Chemists Society **77**(4): 405-411.

Mavromoustakos, T., M. Zervou, E. Theodoropoulou, D. Panagiotopoulos, G. Bonas, M. Day and A. Helmis (1997). "^{13}C NMR analysis of the triacylglycerol composition of Greek virgin olilve oils." Magnetic Resonance in Chemistry **35**: S3-S7.

Miller, C. E. (1995). "The use of chemometric techniques in process analytical method development and operation." Chemometrics and Intelligent Laboratory Systems **30**(1): 11-22.

Miller, M. E. and J. D. Stuart (1999). "Comparison of gas-sampled and SPME-Sampled static headspace for the determination of volatile flavor components." Analytical Chemistry **71**(1): 23-27.

Morales, M., M. Alonso, J. Rios and R. Aparicio (1995). "Virgin olive oil aroma: Relationship between volatile compounds and sensory attributes by chemometrics." Journal of Agricultural and Food Chemistry **43**(11): 2925-31.

Morales, M., A. Berry, P. McIntyre and R. Aparicio (1998). "Tentative analysis of virgin olive oil aroma by supercritical fluid extraction - high-resolution gas chromatography/mass spectrometry." Journal of Chromatography A **818**: 267-275.

Moreno, M., D. M. Olivares, F. J. M. Lopez, V. P. Martinez and F. B. Reig (1999). "Study of the formation of carbonyl compounds in edible oils and fats by H-1-NMR and FTIR." Journal of Molecular Structure **483**: 557-561.

Newmark, H. L. (1999). Squalene, olive oil, and cancer risk - Review and hypothesis. Cancer Prevention: Novel Nutrient and Pharmaceutical Developments. **889:** 193-203.

Ninfali, P., G. Aluigi, M. Bacchiocca and M. Magnani (2001). "Antioxidant capacity of extra-virgin olive oils." Journal of the American Oil Chemists Society **78**(3): 243-247.

Ooyen, A. v. (2001). Theorectical aspects of pattern analysis. New Approaches for the Generation and Analysis of Microbial Fingerprints. Amsterdam, Elsevier. **2001**.

Owen, R. W., W. Mier, A. Giacosa, W. E. Hull, B. Spiegelhalder and H. Bartsch (2000). "Identification of lignans as major components in the phenolic fraction of olive oil." Clinical Chemistry **46**(7): 976-988.

Owen, R. W., W. Mier, A. Giacosa, W. E. Hull, B. Spiegelhalder and H. Bartsch (2000). "Phenolic compounds and squalene in olive oils: the concentration and antioxidant potential of total phenols, simple phenols, secoiridoids, lignans and squalene." Food and Chemical Toxicology **38**(8): 647-659.

Page, B. D. and G. Lacroix (2000). "Analysis of volatile contaminants in vegetable oils by headspace solid-phase microextraction with Carboxen-based fibres." Journal of Chromatography A **873**(1): 79-94.

Pawliszyn, J. (1997). Solid Phase Microextraction - Theory and Practice. New York, Wiley-VCH.

Pawliszyn, J. (1999). Applications of Solid Phase Microextraction. Cambridge, Royal Society of Chemistry.

Pawliszyn, J. (1999). Quantitative Aspects of SPME. Applications of Solid Phase Microextraction. J. Pawliszyn. Cambridge, Royal Society of Chemistry. **1:** 3-21.

Prosen, H. and L. Zupancic-Kralj (1999). "Solid-phase microextraction." Trac-Trends in Analytical Chemistry **18**(4): 272-282.

Rezanka, T. and H. Rezankova (1999). "Characterization of fatty acids and triacylglycerols in vegetable oils by gas chromatography and statistical analysis." Analytica Chimica Acta **398**(2-3): 253-261.

Roberts, D. D., P. Pollien and C. Milo (2000). "Solid-phase microextraction method development for headspace analysis of volatile flavor compounds." Journal of Agricultural and Food Chemistry **48**(6): 2430-2437.

Sacchi, R., F. Addeo and L. Paolillo (1997). "^{1}H and ^{13}C NMR of virgin olive oil. An overview." Magnetic Resonance in Chemistry **35**: S133-S145.

Sacchi, R., L. Mannina, P. Fiordiponti, P. Barone, L. Paolillo, M. Patumi and A. Segre (1998). "Characterization of Italian extra virgin olive oils using 1H NMR spectroscopy." Journal of Agricultural and Food Chemistry **46**(10): 3947-51.

Sacchi, R., L. Paolillo, I. Giudicianni and F. Addoe (1991). "Rapid H-1 NMR Determination of 1,2 and 1,3 Diglycerides in Virgin Olive Oils." Italian Journal of Food Science **3**: 235-262.

Sacchi, R., M. Patumi, G. Fontanazza, P. Barone, P. Fiordiponti, L. Mannina, E. Rossi and A. L. Segre (1996). "A high-field H-1 nuclear magnetic resonance study of the minor components in virgin olive oils." Journal of the American Oil Chemists Society **73**(6): 747-758.

Sacco, A., M. A. Brescia, V. Liuzzi, F. Reniero, C. Guillou, S. Ghelli and P. van der Meer (2000). "Characterization of Italian olive oils based on analytical and nuclear magnetic resonance determinations." Journal of the American Oil Chemists Society **77**(6): 619-625.

Salter, G., M. Lazzari, L. Giansante, R. Goodacre, A. Jones, G. Surricchio, D. Kell and G. Bianchi (1997). "Determination of the geographical origin of Italian extra virgin olive oil using pyrolysis mass spectrometry and artificial neural networks." Journal of the analytical and applied pyrolysis **40**(1): 159-70.

Sanders, J. and B. Hunter (1993). Modern NMR Spectroscopy: A Guide for Chemists, Oxford University Press.

Sato, T. (1994). "Application of Principal-Component Analysis On Near-Infrared Spectroscopic Data of Vegetable-Oils For Their Classification." Journal of the American Oil Chemists Society **71**(3): 293-298.

Scalia, S. (2000). "Determination of sunscreen agents in cosmetic products by supercritical fluid extraction and high-performance liquid chromatography." Journal of Chromatography A **870**(1-2): 199-205.

Scalia, S., L. Giuffreda and P. Pallado (1999). "Analytical and preparative supercritical fluid extraction of Chamomile flowers and its comparison with conventional methods." Journal of Pharmaceutical and Biomedical Analysis **21**(3): 549-558.

Senorans, F. J., E. Ibanez, S. Cavero, J. Tabera and G. Reglero (2000). "Liquid chromatographic-mass spectrometric analysis of supercritical- fluid extracts of rosemary plants." Journal of Chromatography A **870**(1-2): 491-499.

Servili, M., M. Baldioli, R. Selvaggini, E. Miniati, A. Macchioni and G. Montedoro (1999). "High-performance liquid chromatography evaluation of phenols in olive fruit, virgin olive oil, vegetation waters, and pomace and 1D-and 2D- nuclear magnetic resonance characterization." Journal of the American Oil Chemists Society **76**(7): 873-882.

Servili, M., J. Conner, J. Piggott, S. Withers and A. Paterson (1995). "Sensory Characterisation of Virgin Olive Oil and Relatonship with Headspace Composition." Journal of the Science of Food and Agriculture **67**(1): 61-70.

Shaw, A. D., A. diCamillo, G. Vlahov, A. Jones, G. Bianchi, J. Rowland and D. B. Kell (1997). "Discrimination of the variety and region of origin of extra virgin olive oils using C-13 NMR and multivariate calibration with variable reduction." Analytica Chimica Acta **348**(1-3): 357-374.

Shaw, D. (1976). Fourier Transform NMR Spectroscopy, Elsevier Scientific.

Simoes, P. and G. Brunner (1996). "Multicomponent phase equilibria of an extra virgin olive oil in supercritical carbon dioxide." Journal of Supercritical fluids **9**(2): 75-81.

Sinclair, R. (2000). "Good, bad or essential fats: what is the story with Omega-3?" Nutrition and Food Science **30**(4): 178-182.

Smith, T. J. (2000). "Squalene: potential chemopreventive agent." Expert Opinion On Investigational Drugs **9**(8): 1841-1848.

Spyros, A. and P. Dais (2000). "Application of P-31 NMR spectroscopy in food analysis. 1. Quantitative determination of the mono- and diglyceride composition of olive oils." Journal of Agricultural and Food Chemistry **48**(3): 802-805.

Stashenko, E. E., M. A. Puertas, W. Salgar, W. Delgado and J. R. Martinez (2000). "Solid-phase microextraction with on-fibre derivatisation applied to the analysis of volatile carbonyl compounds." Journal of Chromatography A **886**(1-2): 175-182.

StatSoft, E. T. (2001). www.ast.cam.ac.uk/~rgm/scratch/statsbook/stcluan.html. **2001**.

Stefanoudaki, E., F. Kotsifaki and A. Koutsaftakis (1999). "Classification of virgin olive oils of the two major Cretan cultivars based on their fatty acid composition." Journal of the American Oil Chemists Society **76**(5): 623-26.

Supelco (2000). Bulletin 923, SPME: Theory and Optimisation of Conditions. http://info.sial.com/cgi-bin/gx.cgi/Applogic+Supelco.Groups.

Swern, D. (1979). Bailey's Industrial Oil and Fat Products, Wiley-Interscience.

Taylor, L. (1996). Supercritical Fluid Extraction, Wiley Interscience.

Trautwein, E. A., D. Rieckhoff, A. KunathRau and H. F. Erbersdobler (1999). "Replacing saturated fat with PUFA-rich (sunflower oil) or MUFA-rich (rapeseed, olive and high-oleic sunflower oil) fats resulted in comparable hypocholesterolemic effects in cholesterol-fed hamsters." Annals of Nutrition and Metabolism **43**(3): 159-172.

Tsimidou, M. and K. X. Karakostas (1993). "Geographical Classification of Greek Virgin Olive Oil By Nonparametric Multivariate Evaluation of Fatty-Acid Composition." Journal of the Science of Food and Agriculture **62**(3): 253-257.

Tsimidou, M., R. Macrae and I. Wilson (1987). "Authentication of Virgin Olive Oils Using Principal Component Analysis of Triglyceride and Fatty-Acid Profiles .1. Classification of Greek Olive Oils." Food Chemistry **25**(3): 227-239.

Tsimidou, M., R. Macrae and I. Wilson (1987). "Authentication of Virgin Olive Oils Using Principal Component Analysis of Triglyceride and Fatty-Acid Profiles .2. Detection of Adulteration With Other Vegetable-Oils." Food Chemistry **25**(4): 251-258.

Ulberth, F. and M. Buchgraber (2000). "Authenticity of fats and oils." European Journal of Lipid Science and Technology **102**(11): 687-694.

Visioli, F., G. Bellomo and C. Galli (1998). "Free radical-scavenging properties of olive oil polyphenols." Biochemical and Biophysical Research Communications **247**(1): 60-64.

Visioli, F. and C. Galli (1998). "Olive oil phenols and their potential effects on human health." Journal of Agricultural and Food Chemistry **46**(10): 4292-4296.

Vlahov, G. (1996). "Improved quantitative 13C NMR criteria for determination of grades of virgin olive oils. The normal ranges for diglycerides in olive oil." Journal of the American Oil Chemists Society **73**(9): 1201-03.

Vlahov, G. (1997). "Quantitative ^{13}C NMR method using the DEPT Pulse sequence for the detection of olive oil adulteration with soybean oil." Magnetic Resonance in Chemistry **35**: S8-S12.

Vlahov, G. (1998). "Regiospecific analysis of natural mixtures of triglycerides using quantitative C-13 nuclear magnetic resonance of acyl chain carbonyl carbons." Magnetic Resonance in Chemistry **36**(5): 359-362.

Vlahov, G. (1999). "Application of NMR to the study of olive oils." Progress in Nuclear Magnetic Resonance Spectroscopy **35**(4): 341-357.

Vlahov, G. and C. S. Angelo (1996). "The structure of triglycerides of monovarietal olive oils: A C- 13-NMR comparative study." Fett-Lipid **98**(6): 203-205.

Vlahov, G., C. Schiavone and N. Simone (1999). "Triacylglycerols of the olive fruit (Olea europaea L.): characterization of mesocarp and seed triacylglycerols in different cultivars by liquid chromatography and C-13 NMR spectroscopy." Fett-Lipid **101**(4): 146-150.

Vlahov, G., A. D. Shaw and D. B. Kell (1999). "Use of C-13 nuclear magnetic resonance distortionless enhancement by polarization transfer pulse sequence and multivariate analysis to discriminate olive oil cultivars." Journal of the American Oil Chemists Society **76**(10): 1223-1231.

Wan, X. M., R. J. Stevenson, X. D. Chen and L. D. Melton (1999). "Application of headspace solid-phase microextraction to volatile flavour profile development during storage and ripening of kiwifruit." Food Research International **32**(3): 175-183.

Webster, L., P. Simpson, A. M. Shanks and C. F. Moffat (1999). "The authentication of olive oil on the basis of hydrocarbon concentration and composition." Analyst **125**(1): 97-104.

Wesley, I. J., R. J. Barnes and A. E. J. McGill (1995). "Measurement of Adulteration of Olive Oils By Near-Infrared Spectroscopy." Journal of the American Oil Chemists Society **72**(3): 289-292.

Wesley, I. J., F. Pacheco and A. E. J. McGill (1996). "Identification of adulterants in olive oils." Journal of the American Oil Chemists Society **73**(4): 515-518.

Wu, C., Z. Wang and Q. H. Wu (2000). "Volatile Compounds produced from Monosodium Glutamate in common food cooking." Journal of Agricultural and Food Chemistry **48**(6): 2438-2442.

www.globalgourmet.com/food/egg/egg0397/oohistory.html (1997). The Electronic Gourmet Guide - Olive Oil History. **2000**.

www.museodellolivo.com/eng/emuseo (2000). The Olive Tree Museum.

www.oliveoilsource.com (2001). The Olive Oil Source.

Zamora, R., V. Alba and F. J. Hidalgo (2001). "Use of high-resolution C-13 nuclear magnetic resonance spectroscopy for the screening of virgin olive oils." Journal of the American Oil Chemists Society **78**(1): 89-94.

Zamora, R., J. L. Navarro and F. J. Hidalgo (1994). "Identification and Classification of Olive Oils By High-Resolution C- 13 Nuclear-Magnetic-Resonance." Journal of the American Oil Chemists Society **71**(4): 361-364.

Zwingle, E. (1999). "Olive oil: Elixir of the Gods." National Geographic **196**(3): 66-81.

APPENDICES

APPENDIX A

Appendix A – Index of Figures

Appendix A – Index of Tables

Chemical Structures

Figure A.1 – Structure of pigments found in olive oil

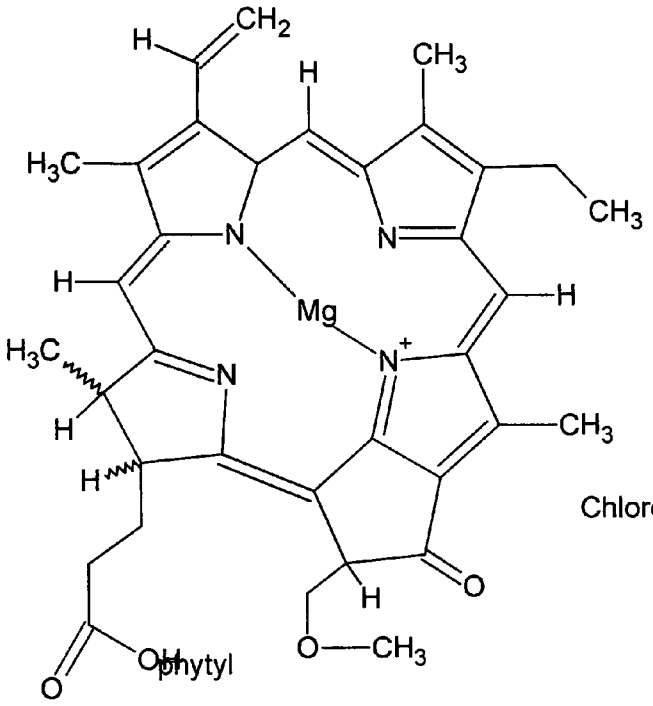

Chlorophyll a

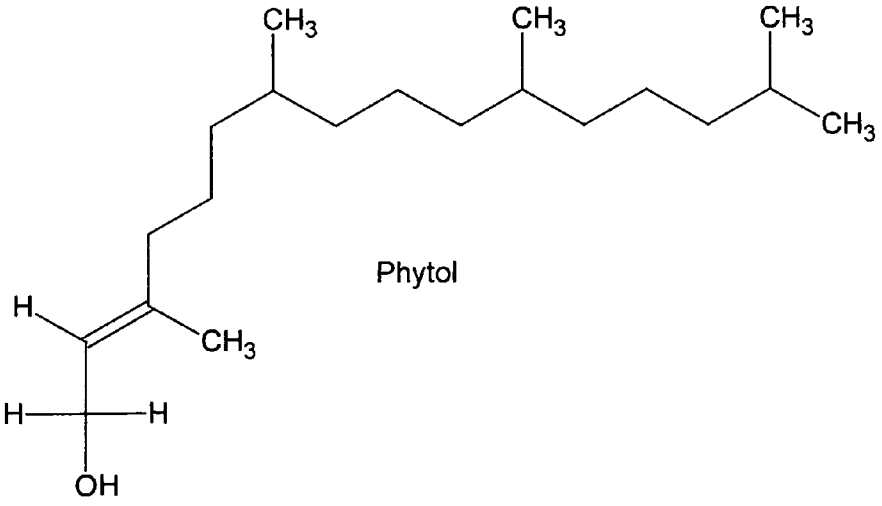

Phytol

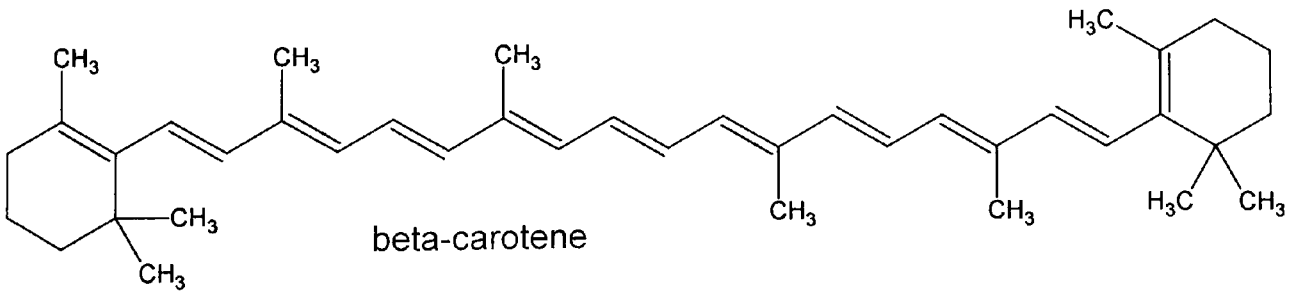

beta-carotene

Figure A.2 - Antioxidant (tocopherol) structure

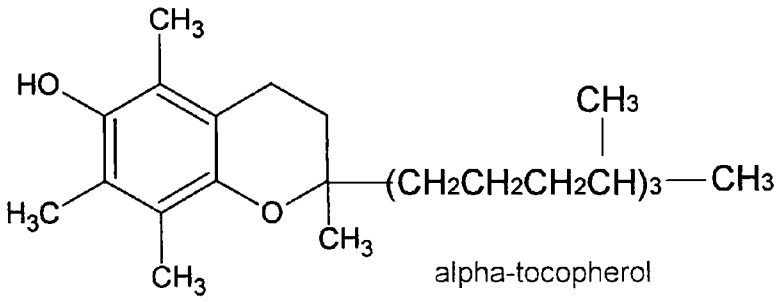

Figure A.3 – Structures of the main triterpene alcohols found in olive oil

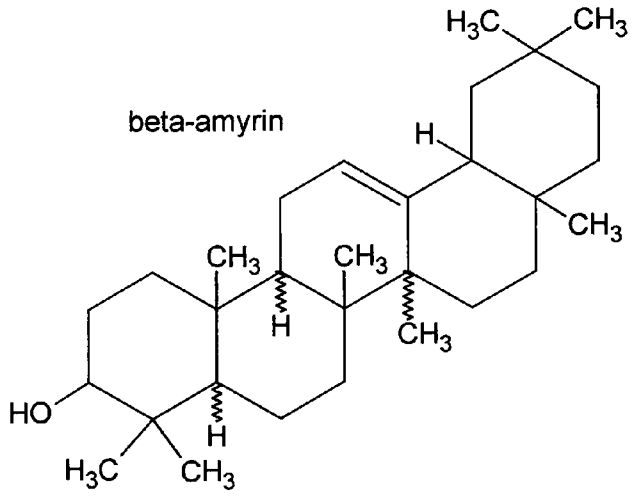

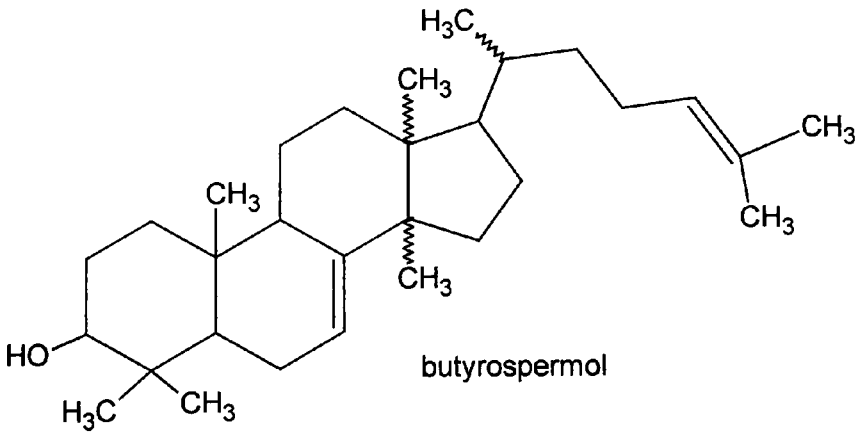

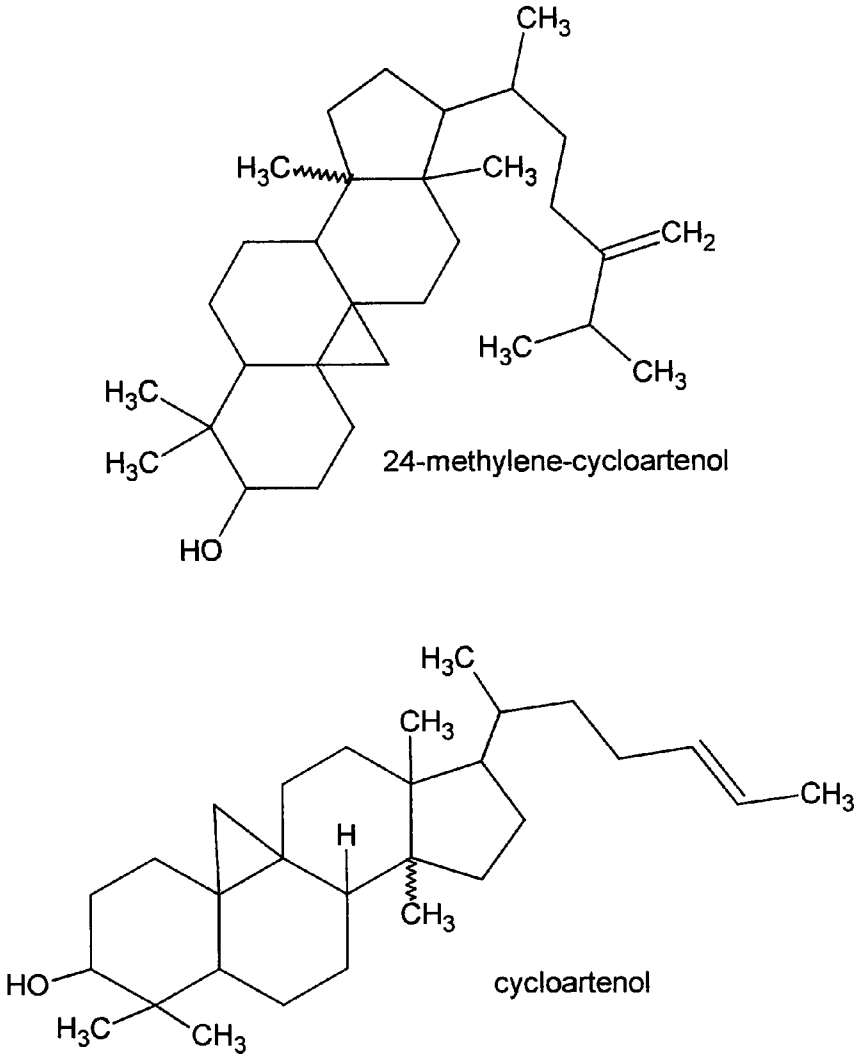

Figure A.4 – Structures of triterpene dialcohols

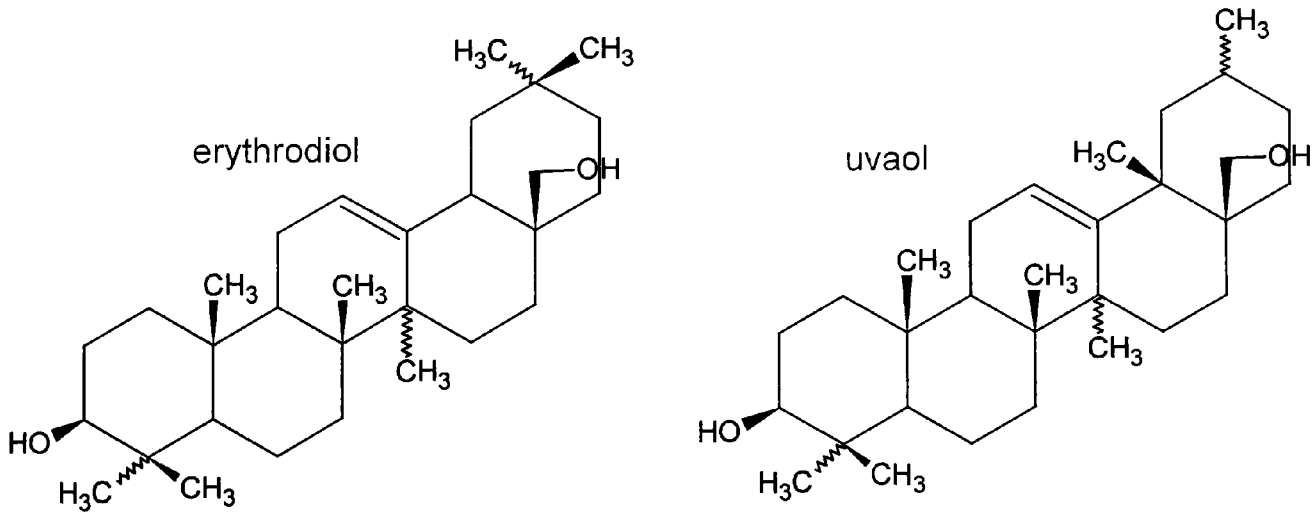

Figure A.5 – Structures of phosphatides in olive oil

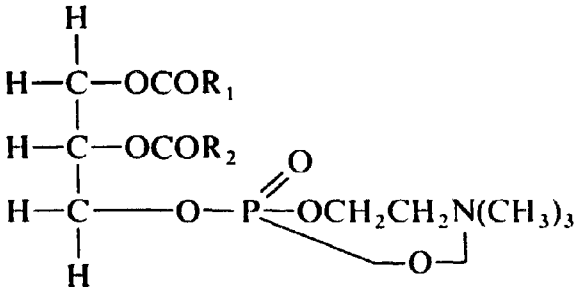

α-Lecithin

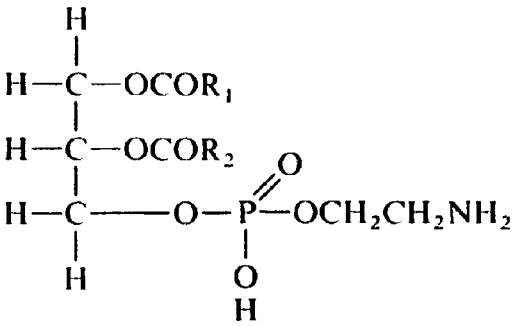

α-Cephalin

R_1 and R_2 = Fatty acids

Figure A.6 - Structure of typical aldehydes found in olive oil

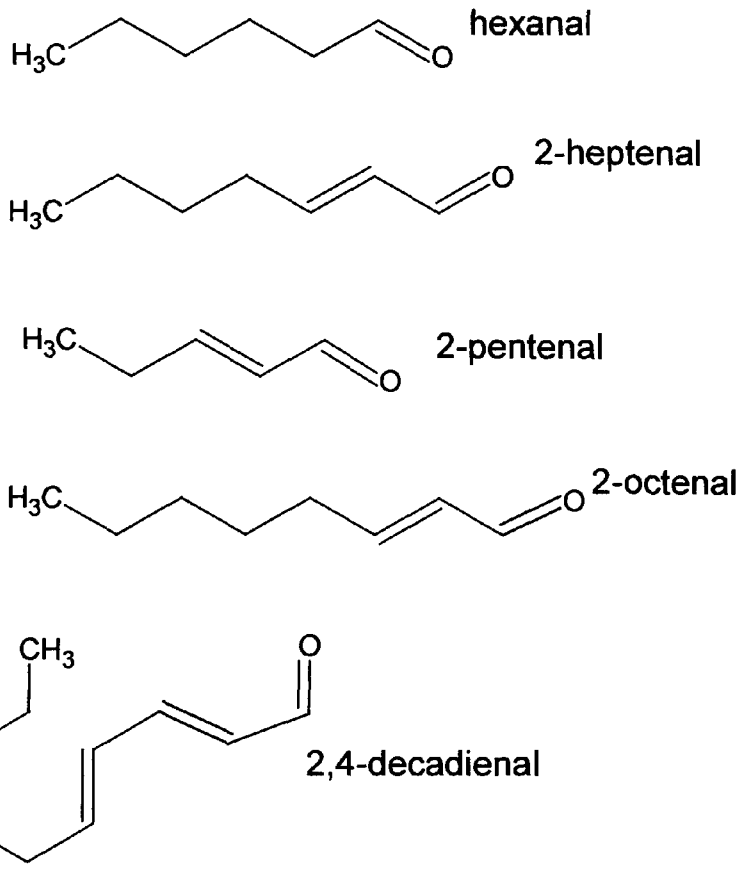

Table A.1 - Fatty acid composition of some of the olive oil samples used in the study

FATTY ACID COMPOSITION													
	Origin of oil		Number of C atoms:Number of double bonds					Origin of oil		Number of C atoms:Number of double bonds			
			18:0	**18:1**	**18:2**	**18:3**				**18:0**	**18:1**	**18:2**	**18:3**
E1	Crete	Chania	2.86	75.81	8.22	0.59	F23	Peloponessos	Korinthia	3.24	75.88	7.97	0.57
E3	"	"	2.86	76.33	6.94	0.64	F24	"	"	2.64	77.79	6.39	0.65
E26	Peloponessos	Lakonia	2.87	75.55	8.52	0.6	F25	"	"	3.01	79.03	5.99	0.56
E27	"	"	2.37	72.69	10.52	0.63	F26	"	"	2.71	74.67	11.45	0.45
E34	"	Messinia	2.82	77.32	5.85	0.71	F27	"	Argolida	2.78	73.72	12.09	0.46
E38	"	"	2.87	76.48	6.17	0.7	F28	"	"	2.49	63.72	15.86	0.68
E47	Central Greece	Etol/nia	3.34	79.47	5.03	0.6	F29	Peloponessos	Arkadia	2.88	74.92	9.38	0.52
E49	C Greece Island	Evia	2.67	66.25	16.33	0.81	F30	"	Lakonia	2.54	80.47	5.19	0.46
E51	Central Greece	Fthiotida	2.3	75.48	9.2	0.73	F31	"	"	2.47	78.22	6.73	0.63
E57	Ionian Island	Zakinthos	3.13	75.49	7.14	0.76	F32	"	"	2.7	78.42	6.22	0.67
E59	Aegean Island	Lesvos	2.59	73.04	10.66	0.66	F33	"	"	2.46	79.03	5.43	0.66
F1	Crete	Chania	2.41	79.46	4.67	0.65	F34	"	"	2.4	77.32	7.46	0.59
F2	"	"	2.5	78.34	5.35	0.65	F35	"	"	2.51	71.7	9.88	0.66
F3	"	"	2.56	78.55	5.42	0.63	F36	"	"	2.29	78.89	5.26	0.68
F4	"	"	2.78	77.86	5.83	0.79	F38	"	Messinia	3.2	74.82	7.68	0.79
F8	"	Heraklion	2.84	77.37	6.52	0.61	F39	"	"	2.33	78.97	5.21	0.81
F9	"	"	2.73	79.26	5.21	0.64	F40	"	"	2.54	78.57	5.06	0.77
F10	"	"	2.74	78.59	5.91	0.69	F41	"	"	2.25	79.25	4.9	0.74
F13	"	"	3.21	77.05	6.63	0.71	F45	"	"	2.64	78.34	5.91	0.62
F14	"	"	2.77	76.88	6.79	0.66	F49	"	"	2.72	78.24	5.97	0.66
F15	"	Lassithi	2.68	76.04	6.6	0.68	F50	"	"	2.73	78.27	5.42	0.69
F16	"	"	3.04	77.19	6.04	0.73	F53	"	Achaia	3.29	78.3	6.79	0.57
F17	"	Heraklion	2.77	77.65	6.67	0.63	F55	C Greece Island	Evia	2.7	73.01	10.91	0.59
F18	"	Lassithi	2.75	78.6	5.35	0.7	F56	"	"	2.68	75.28	9.6	0.59
F19	"	"	3.32	72.77	9.26	0.69	F57	Ionian Island	Zakinthos	2.61	77.4	5.44	0.69
F20	"	"	2.91	75.51	7.49	0.58	F58	Aegean Island	Rodos	2.86	69.19	14.14	0.86
F21	"	"	2.75	74.51	8.19	0.68	F59	"	Lesvos	2.37	78.93	7.98	0.7
F22	"	"	3.09	74.87	8.78	0.78	F60	"	"	2.85	75.23	11.33	0.82

Table A.1 - Fatty acid composition of some of the olive oil samples used in the study (continued)

FATTY ACID COMPOSITION						
	Origin of oil		Number of C atoms:Number of double bonds			
F61	Aegean Island	Lesvos	2.62	77.33	9.58	0.68
F62	"	"	2.66	77.24	8.97	0.71
F63	"	"	2.65	76.75	9.15	0.71
F64	North Greece	Chalkidiki	2.59	80.64	5.74	0.48
F65	"	"	2.72	75.75	8.82	0.61

APPENDIX B

^{13}C NMR

Appendix B – Index of Tables

Appendix B – Index of Figures

Table B.1 - ^{13}C NMR adulterated sample weighings

File Name	g Pyrazine	g Olive oil	g Adulterant	g Total Oil	% adulteration
E1	0.0160g	0.8	0	0.8	0.00
E1SOY2	0.0160g	1.181	0.023	1.204	1.91
E1SOY5	0.014	0.78	0.0431	0.8231	5.24
E1SUN2	0.0143	1.21	0.0232	1.2332	1.88
E1SUN5	0.0147	0.76	0.043	0.803	5.35
E1CORN2	0.0154	0.782	0.0174	0.7994	2.18
E1CORN5	0.0161	0.764	0.0405	0.8045	5.03
E1COTTON2	0.0154	0.7904	0.0171	0.8075	2.12
E1COTTON5	0.0147	0.7511	0.0473	0.7984	5.92
E2	0.015	0.8	0	0.8	0.00
E2SUN2	0.0155	0.783	0.019	0.802	2.37
E2SUN5	0.015	0.76	0.04	0.8	5.00
E2SOY2	0.0153	1.181	0.0262	1.2072	2.17
E2SOY5	0.016	0.763	0.046	0.809	5.69
E2COTTON2	0.017	0.792	0.02	0.812	2.46
E2COTTON5	0.017	0.762	0.044	0.806	5.46
E2CORN2	0.0158	1.1735	0.0246	1.1981	2.05
E2CORN5	0.0144	0.7682	0.0417	0.8099	5.15
E3	0.016	0.803	0	0.803	0.00
E3SUN2	0.0156	1.1156	0.023	1.1386	2.02
E3SUN5	0.0152	0.7615	0.0418	0.8033	5.20
E3SOY2	0.0153	0.7836	0.0168	0.8004	2.10
E3SOY5	0.0155	0.766	0.0401	0.8061	4.97
E3CORN2	0.0157	0.8788	0.0199	0.8987	2.21
E3CORN5	0.0149	0.763	0.046	0.809	5.69
E3COTTON2	0.014	0.7861	0.0164	0.8025	2.04
E3COTTON5	0.0151	0.763	0.0406	0.8036	5.05
E4	0.0158	0.8001	0	0.8001	0.00
E4SUN2	0.0146	0.792	0.0174	0.8094	2.15
E4SUN5	0.0146	0.7592	0.0397	0.7989	4.97

E4SOY2		0.0156	0.7815	0.0172	0.7987	2.15
E4SOY5		0.0146	0.7615	0.0408	0.8023	5.09
E4COTTON2		0.0143	0.7839	0.0166	0.8005	2.07
E4COTTON5		0.0151	0.7632	0.0401	0.8033	4.99
E4CORN2		0.0161	0.789	0.0159	0.8049	1.98
E4CORN5		0.0155	0.771	0.048	0.819	5.86
E5		0.0162	0.8016	0	0.8016	0.00
E5SUN2		0.0147	0.7832	0.0178	0.801	2.22
E5SUN5		0.015	0.7563	0.0441	0.8004	5.51
E5SOY2		0.0154	1.1751	0.0255	1.2006	2.12
E5SOY5		0.0152	0.762	0.0399	0.8019	4.98
E5COTTON2		0.0162	1.5643	0.0316	1.5959	1.98
E5COTTON5		0.0146	0.7563	0.0425	0.7988	5.32
E5CORN2		0.015	0.7851	0.016	0.8011	2.00
E5CORN5		0.0149	0.7604	0.0399	0.8003	4.99
E6		0.0158	0.803	0	0.803	0.00
E6SUN2		0.0147	0.7822	0.019	0.8012	2.37
E6SUN5		0.0153	0.758	0.0439	0.8019	5.47
E6SOY2		0.0154	0.7864	0.0168	0.8032	2.09
E6SOY5		0.016	0.7582	0.042	0.8002	5.25
E6COTTON2		0.0154	0.788	0.016	0.804	1.99
E6COTTON5		0.016	0.762	0.0406	0.8026	5.06
E6CORN2		0.0151	0.7837	0.0162	0.7999	2.03
E6CORN5		0.0147	0.7601	0.0399	0.8	4.99
E7		0.0151	0.805	0	0.805	0.00
E7SUN2		0.0161	0.7852	0.0161	0.8013	2.01
E7SUN5		0.014	0.76	0.0407	0.8007	5.08
E7SOY2		0.0165	1.5668	0.022	1.5888	1.38
E7SOY5		0.0164	0.7594	0.0402	0.7996	5.03
E7COTTON2		0.016	0.7837	0.0171	0.8008	2.14
E7COTTON5		0.015	0.7721	0.045	0.8171	5.51
E7CORN2		0.015	0.787	0.017	0.804	2.11
E7CORN5		0.015	0.7615	0.0412	0.8027	5.13
E8		0.0148	0.7999	0	0.7999	0.00

E8SUN2	0.016	0.7901	0.0164	0.8065	2.03
E8SUN5	0.0147	0.7604	0.0408	0.8012	5.09
E8SOY2	0.0147	0.981	0.0201	1.0011	2.01
E8SOY5	0.0155	0.756	0.045	0.801	5.62
E8CORN2	0.0156	0.7824	0.017	0.7994	2.13
E8CORN5	0.016	0.757	0.0406	0.7976	5.09
E8COTTON2	0.0159	0.782	0.018	0.8	2.25
E8COTTON5	0.0149	0.7553	0.044	0.7993	5.50
E9	0.0153	0.8009	0	0.8009	0.00
E9SOY2	0.0158	0.873	0.019	0.892	2.13
E9SOY5	0.016	0.7576	0.042	0.7996	5.25
E9SUN2	0.0159	0.787	0.0158	0.8028	1.97
E9SUN5	0.0148	0.7607	0.04	0.8007	5.00
E9CORN2	0.0158	0.784	0.0159	0.7999	1.99
E9CORN5	0.0157	0.76	0.0403	0.8003	5.04
E9COTTON2	0.0156	0.7848	0.0161	0.8009	2.01
E9COTTON5	0.0153	0.7601	0.041	0.8011	5.12

Table B.2 - ^{13}C NMR peaks (ppm) assigned from literature data (Mavromoustakos, Zervou, Theodoropoulou *et al.*, 1997)

^{13}C NMR Peak Assignment

Peak (ppm)	Fatty acid	Carbon	Position
127.63	Linoleyl	12	β
127.64	Linoleyl	12	α
127.81	Linoleyl	10	α
127.82	Linoleyl	10	β
129.35	Oleyl	9	β
129.37	Oleyl	9	α
129.61	Linoleyl	9	β
129.63	Linoleyl	9	α
129.67	Oleyl	10	α
129.68	Oleyl	10	β
129.83	Linoleyl	13	α
129.84	Linoleyl	13	β

Table B.3 - Tables detailing the ratio of relative intensity of peak heights, sample/internal standard (pyrazine 144.8 ppm), in the ethylenic region, for Crete oils E1-E9.

E1									
Peak (ppm)	Unadult -erated	2% Sunfl	5% Sunfl	2% Soya	5% Soya	2% Corn	5% Corn	2% Cotton	5% Cotton
127.63	*0.1343*	0.1665	0.1761	0.1376	0.1898	0.1386	0.1504	0.1244	
127.64	*0.1404*	0.1879	0.2131	0.1565	0.2200	0.1728	0.1829	0.1565	0.2241
127.81	*0.1331*	0.1585	0.1803	0.1451	0.2019	0.3122	0.1583	0.1315	0.2016
127.82	*0.1091*	0.1456	0.1470	0.1238	0.1609	0.1208	0.1320	0.1130	0.1766
129.35	*0.8758*	0.9213	0.8287	0.7989	0.9895	0.8075	0.7378	0.7104	0.9147
129.37	*1.3189*	1.4883	1.2778	1.2117	1.5013	1.2600	1.1497	1.1405	1.4481
129.61	*0.1454*	0.1581	0.1753	0.1310	0.2047	0.1463	0.1512	0.1211	0.1977
129.63	*0.1700*	0.1916	0.2101	0.1663	0.2403	0.1730	0.1896	0.1438	0.2362
129.67	*1.3970*	1.4978	1.2853	1.2477	1.5415	1.2905	1.1461	1.1143	1.4756
129.68	*0.8962*	1.0597	0.9013	0.8066	1.0472	0.9102	0.8025	0.8259	1.1118
129.83	*0.1870*	0.2063	0.2283	0.1997	0.2601	0.1741	0.1896	0.1685	0.2479
129.84	*N/a*	0.1956	0.1933	N/a	N/a	0.1612	0.1698	0.1613	N/a

E2									
Peak (ppm)	Unadult -erated	2% Sunfl	5% Sunfl	2% Soya	5% Soya	2% Corn	5% Corn	2% Cotton	5% Cotton
127.63	*0.1316*	0.1519	0.1203	0.1080	0.1277	0.0941	0.1359	0.1194	0.1332
127.64	*0.1213*	0.1829	0.1648	0.1423	0.1605	0.1093	0.1678	0.1286	0.1531
127.81	*0.1190*	0.1615	0.1375	0.1179	0.1255	0.1020	0.3163	0.1188	0.1350
127.82	*0.0938*	0.1345	0.1031	0.1083	0.1004	0.0755	0.1125	0.1027	0.1181
129.35	*1.0779*	1.2294	0.7456	0.8665	0.7069	0.7025	0.7882	0.8415	0.8019
129.37	*1.5366*	1.8610	1.1619	1.3938	1.1235	1.0293	1.2344	1.2728	1.2232
129.61	*0.1468*	0.1645	0.1172	0.1095	0.1168	0.0925	0.1300	0.1263	0.1366
129.63	*0.1906*	0.1952	0.1451	0.1348	0.1462	0.1175	0.1615	0.1541	0.1631
129.67	*1.6461*	1.8914	1.1704	1.3730	1.1245	1.0713	1.2303	1.300	1.2366
129.68	*1.0109*	1.3244	0.8088	1.0467	0.7368	0.6647	0.8499	0.9705	0.8552
129.83	*0.1602*	0.2052	0.1713	0.1739	0.1676	0.1172	0.1778	0.1543	0.1751
129.84	*N/a*	N/a	0.1492	N/a	0.1411	0.0895	N/a	N/a	N/a

E3

Peak (ppm)	Unadult -erated	2% Sunfl	5% Sunfl	2% Soya	5% Soya	2% Corn	5% Corn	2% Cotton	5% Cotton
127.63	*0.1382*	0.1483	0.1464	0.1442	0.1450	0.1295	0.1792	0.1274	0.1422
127.64	*0.1538*	0.1416	0.1562	0.1772	0.1789	0.1491	0.2449	0.1391	0.1516
127.81	*0.1289*	0.1461	0.1580	0.1415	0.1433	0.1266	0.1966	0.1189	0.1372
127.82	*0.1102*	0.1085	0.0990	0.1289	0.1239	0.1011	0.1667	0.1024	0.1169
129.35	*1.0539*	0.9498	0.9234	1.0049	0.8437	0.8665	0.9215	0.8451	0.7633
129.37	*1.5605*	1.3731	1.1536	1.5954	1.2851	1.3060	1.4407	1.2594	1.1488
129.61	*0.1433*	0.1547	0.1738	0.1406	0.1439	0.1284	0.1651	0.1261	0.1392
129.63	*0.1697*	0.1959	0.2182	0.1568	0.1677	0.1540	0.1805	0.1379	0.1658
129.67	*1.5630*	1.4779	1.2804	1.5633	1.3038	1.3323	1.1414	1.2984	1.1748
129.68	*1.0528*	0.9457	0.7425	1.0825	0.9306	0.8788	1.0576	0.8608	0.7616
129.83	*0.1471*	0.1846	0.1991	0.1828	0.1917	0.1548	0.2697	0.1550	0.1656
129.84	*0.1344*	N/a	0.1798	0.1736	0.1747	0.1366	N/a	0.1441	0.1480

E4

Peak (ppm)	Unadult -erated	2% Sunfl	5% Sunfl	2% Soya	5% Soya	2% Corn	5% Corn	2% Cotton	5% Cotton
127.63	*0.1392*	0.1005	0.1270	0.1154	0.1465	0.1136	0.1439	0.1257	0.1406
127.64	*0.1248*	0.1578	0.1660	0.1367	0.1760	0.1323	0.1726	0.1501	0.1513
127.81	*0.1423*	0.1344	0.1448	0.1240	0.1528	0.1145	0.1515	0.1337	0.1373
127.82	*0.0991*	0.1038	0.1119	0.0951	0.1254	0.2053	0.1071	0.1130	0.1129
129.35	*1.0274*	0.8417	0.7458	0.7663	0.8060	0.7339	0.7239	0.8951	0.7977
129.37	*1.3596*	1.2402	1.1539	1.1727	1.2626	1.0655	1.0845	1.3570	1.1771
129.61	*0.1539*	0.1301	0.1265	0.1159	0.1433	0.1089	0.1280	0.1318	0.1491
129.63	*0.1964*	0.1663	0.1538	0.1327	0.1610	0.1378	0.1676	0.1510	0.1838
129.67	*1.5674*	1.2995	1.1783	1.2101	1.2872	1.2678	1.1307	1.3826	1.2284
129.68	*0.9027*	0.8160	0.8018	0.8141	0.8782	0.7107	0.6894	0.9343	0.7812
129.83	*0.1682*	0.1608	0.1830	0.1461	0.1945	0.1309	0.1811	0.1712	0.1754
129.84	*N/a*	0.1394	0.1638	0.1375	0.1756	0.1111	0.1379	N/a	N/a

E5

Peak (ppm)	Unadult -erated	2% Sunfl	5% Sunfl	2% Soya	5% Soya	2% Corn	5% Corn	2% Cotton	5% Cotton
127.63	*0.1746*	0.1931	0.1428	0.2057	0.1990	0.1912	0.2587	0.1949	0.2253
127.64	*0.1865*	0.2193	0.1774	0.1980	0.2050	0.2014	0.2608	0.2044	0.2265
127.81	*0.1660*	0.1857	0.1618	0.1793	0.1882	0.1728	0.2418	0.1789	0.2047
127.82	*0.1455*	0.1715	0.1146	0.1526	0.1571	0.1470	0.1924	0.1557	0.1736
129.35	*0.6540*	0.6797	0.7551	0.6474	0.6130	0.6369	0.7928	0.6549	0.6856
129.37	*1.0515*	1.1470	1.1597	1.0580	0.9718	1.0211	1.2768	1.0372	1.0480
129.61	*0.1689*	0.1857	0.1320	0.1851	0.1843	0.1732	0.2427	0.1796	0.2108
129.63	*0.1743*	0.1970	0.1725	0.1908	0.1935	0.1841	0.2695	0.1845	0.2362
129.67	*1.0711*	1.1554	1.1762	1.0635	1.0230	1.0365	1.3396	1.0889	1.1077
129.68	*0.6814*	0.7326	0.7684	0.6115	0.5984	0.6335	0.7720	0.6519	0.6458
129.83	*0.1871*	0.2278	0.1892	0.1993	0.2211	0.1971	0.3255	0.2070	0.2449
129.84	*0.1941*	0.2278	0.1480	0.1856	0.2059	0.1907	0.2671	0.2023	0.2212

E6

Peak (ppm)	Unadulterated	2% Sunfl	5% Sunfl	2% Soya	5% Soya	2% Corn	5% Corn	2% Cotton	5% Cotton
127.63	*0.0952*	0.1351	0.1470	0.1173	0.1206	0.1088	0.1316	0.1024	0.1656
127.64	*0.1156*	0.1693	0.1766	0.1376	0.1465	0.1392	0.1711	0.1212	0.1864
127.81	*0.0941*	0.1509	0.1622	0.1174	0.1249	0.1174	0.1389	0.1099	0.1627
127.82	*0.0727*	0.1099	0.1127	0.0894	0.0911	0.0899	0.1120	0.0869	0.1218
129.35	*0.7267*	0.9091	0.7684	0.7312	0.6235	0.6973	0.7403	0.7291	0.7821
129.37	*1.0627*	1.4172	1.1413	1.0788	0.9851	1.1480	1.1467	1.1254	1.1498
129.61	*0.0920*	0.1311	0.1375	0.1071	0.1103	0.0975	0.1191	0.1108	0.1696
129.63	*0.1165*	0.1657	0.1777	0.1250	0.1321	0.1212	0.1517	0.1325	0.1513
129.67	*1.0774*	1.4436	1.1627	1.1403	0.9879	1.1351	1.1530	1.1417	1.1714
129.68	*0.7222*	0.9493	0.7393	0.7180	0.6336	0.7742	0.8098	0.7540	0.7347
129.83	*0.1192*	0.1975	0.1859	0.1461	0.1496	0.1440	0.1830	0.1415	0.1550
129.84	*0.1070*	0.1634	0.1391	0.1168	0.1294	0.1251	0.1650	0.1256	N/a

E7

Peak (ppm)	Unadulterated	2% Sunfl	5% Sunfl	2% Soya	5% Soya	2% Corn	5% Corn	2% Cotton	5% Cotton
127.63	*0.1144*	0.1358	0.1636	0.2775	0.2837	0.1343	0.1435	0.1543	0.1661
127.64	*0.1071*	0.1520	0.1920	0.2855	0.2972	0.1425	0.1634	0.1555	0.1749
127.81	*0.1147*	0.1356	0.1627	0.2428	0.2641	0.1237	0.1431	0.1389	0.1544
127.82	*0.0896*	0.1178	0.1377	0.2189	0.2208	0.1084	0.1176	0.1212	0.1358
129.35	*0.7185*	0.7489	0.7741	1.5079	1.2559	0.7102	0.6974	0.8294	0.7729
129.37	*1.1139*	1.2035	1.2763	2.3429	1.9775	1.1383	1.0957	1.2597	1.2170
129.61	*0.1042*	0.1257	0.1526	0.2592	0.2614	0.1236	0.1382	0.1489	0.1626
129.63	*0.1181*	0.1334	0.1750	0.2835	0.2925	0.1398	0.1587	0.1633	0.1827
129.67	*1.2862*	1.2118	1.2715	2.4111	2.0425	1.1325	1.1334	1.3075	1.2216
129.68	*0.7808*	0.7917	0.8642	1.4467	1.2523	0.7234	0.7170	0.8028	0.7786
129.83	*0.1513*	0.1590	0.2128	0.2888	0.2955	0.1481	0.1818	0.1581	0.1841
129.84	*N/a*	0.1612	0.2124	0.2657	0.2643	0.1417	0.1613	0.1539	0.1769

E8

Peak (ppm)	Unadulterated	2% Sunfl	5% Sunfl	2% Soya	5% Soya	2% Corn	5% Corn	2% Cotton	5% Cotton
127.63	*0.1324*	0.1267	0.1531	0.1414	0.1488	0.1366	0.1477	0.1220	0.1477
127.64	*0.1415*	0.1575	0.1961	0.1695	0.1849	0.1699	0.1905	0.1494	0.1905
127.81	*0.1251*	0.1325	0.1606	0.1426	0.1522	0.1433	0.1573	0.1244	0.1573
127.82	*0.1022*	0.1129	0.1278	0.1189	0.1301	0.1223	0.1319	0.1070	0.1319
129.35	*0.7956*	0.7189	0.7146	0.7662	0.6622	0.7553	0.7277	0.7045	0.7277
129.37	*1.190*	1.149	1.115	1.1915	1.0894	1.2119	1.1223	1.1061	1.1223
129.61	*0.1234*	0.1249	0.1415	0.1288	0.1436	0.1269	0.1435	0.1200	0.1435
129.63	*0.1515*	0.1482	0.1750	0.1469	0.1668	0.1493	0.1772	0.1459	0.1772
129.67	*1.233*	1.130	1.133	1.1842	1.0598	1.1856	1.1602	1.0980	1.1602
129.68	*0.7813*	0.8219	0.7886	0.8341	0.7725	0.8409	0.8177	0.7713	0.8177
129.83	*0.1441*	0.1679	0.1942	0.1702	0.1836	0.1771	0.1950	0.1515	0.1950
129.84	*0.1382*	0.1588	0.1796	0.1673	0.1770	0.1595	0.1874	0.1458	0.1874

E9									
Peak (ppm)	Unadult -erated	2% Sunfl	5% Sunfl	2% Soya	5% Soya	2% Corn	5% Corn	2% Cotton	5% Cotton
127.63	*0.1319*	0.1695	0.1803	0.1422	0.1764	0.1880	0.1555	0.1875	0.1817
127.64	*0.1344*	0.1942	0.2193	0.1500	0.1896	0.2059	0.1852	0.1997	0.2136
127.81	*0.1129*	0.1535	0.1721	0.1295	0.1581	0.1832	0.1518	0.1814	0.1604
127.82	*0.1053*	0.1509	0.1511	0.1153	0.1448	0.1534	0.1316	0.1705	0.1595
129.35	*0.8315*	0.9876	0.8694	0.7951	0.8263	1.0751	0.7735	1.0989	0.7998
129.37	*1.2569*	1.5699	1.4201	1.2701	1.2713	1.7346	1.2194	1.7927	1.2875
129.61	*0.1305*	0.1645	0.1656	0.1379	0.1649	0.1838	0.1427	0.1951	0.1399
129.63	*0.1417*	0.1744	0.1982	0.1509	0.1847	0.1991	0.1604	0.1970	0.1562
129.67	*1.2872*	1.5425	1.3753	1.2358	1.3079	1.7124	1.2279	1.7809	1.2402
129.68	*0.8530*	1.0509	0.9706	0.8186	0.9163	1.1422	0.8234	1.2205	0.8894
129.83	*0.1457*	0.1934	0.2238	0.1492	0.1946	0.2061	0.1839	0.2237	0.2148
129.84	*0.1359*	0.1995	0.2185	0.1587	0.1924	0.2168	0.1832	0.2323	0.1757

Cooman's Plots

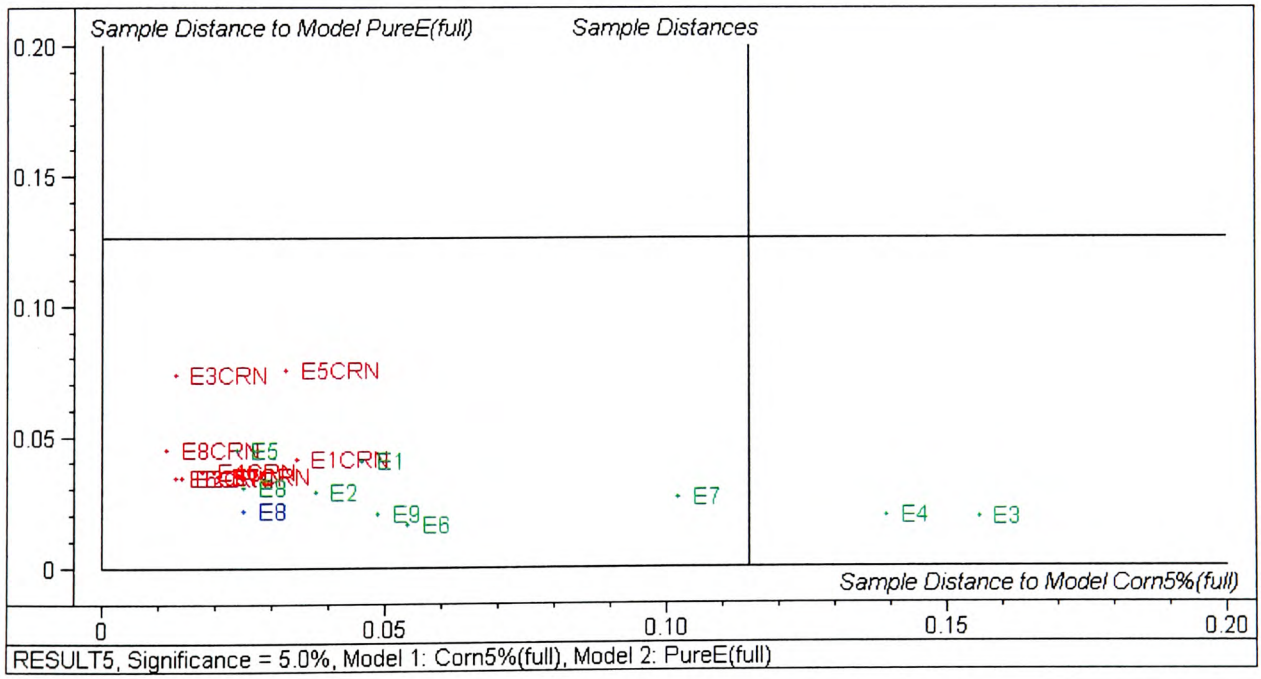

Figure B.1 – Cooman's plot to show separation between pure Crete oils (red E1-9) and 5% corn adulterated oils (green) using all variables

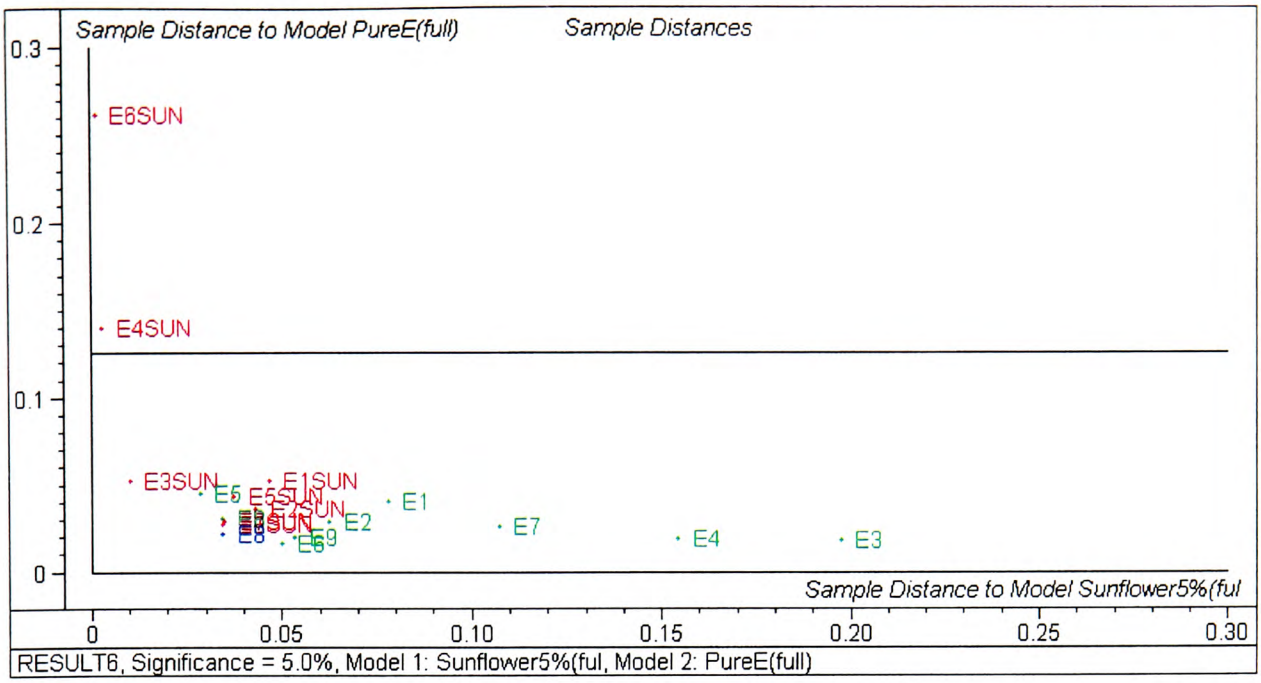

Figure B.2 - Cooman's plot to show separation between pure Crete oils (green E1-9) and 5% sunflower adulterated oils (red) using all variables

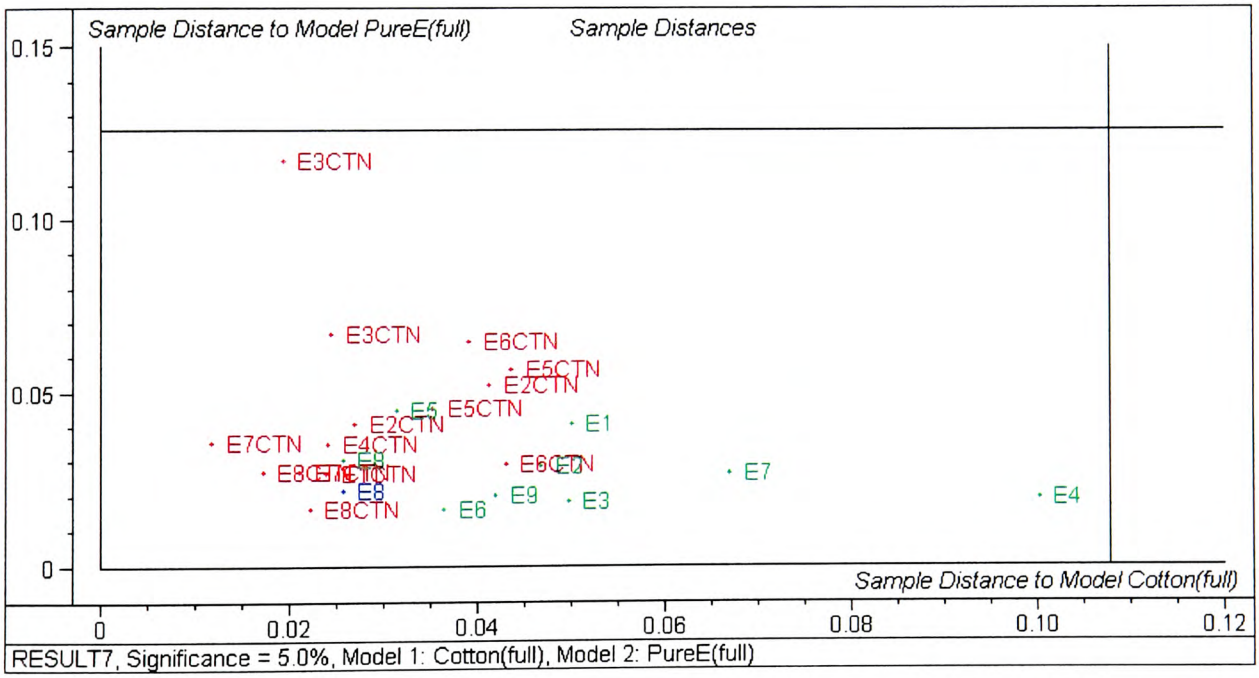

Figure B.3 - Cooman's plot to show separation between pure Crete oils (green E1-9) and 5% cotton adulterated oils (red) using all variables

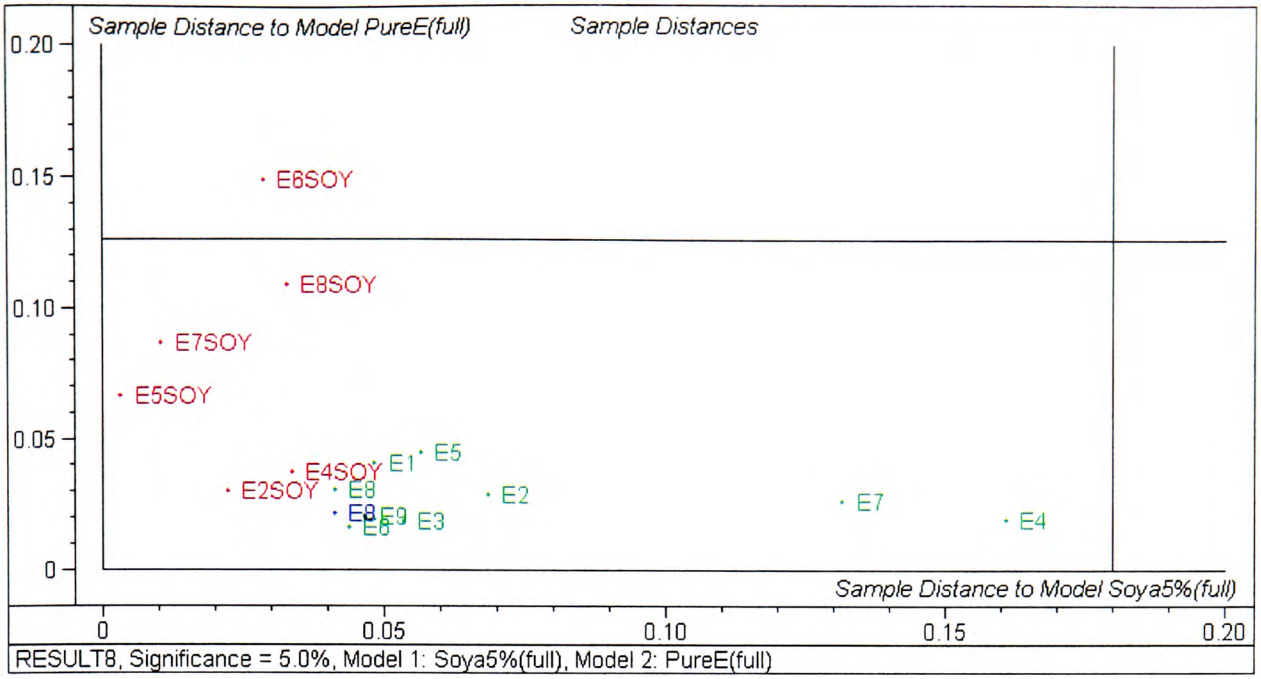

Figure B. 4 - Cooman's plot to show separation between pure Crete oils (green E1-9) and 5% soya adulterated oils (red) using all variables

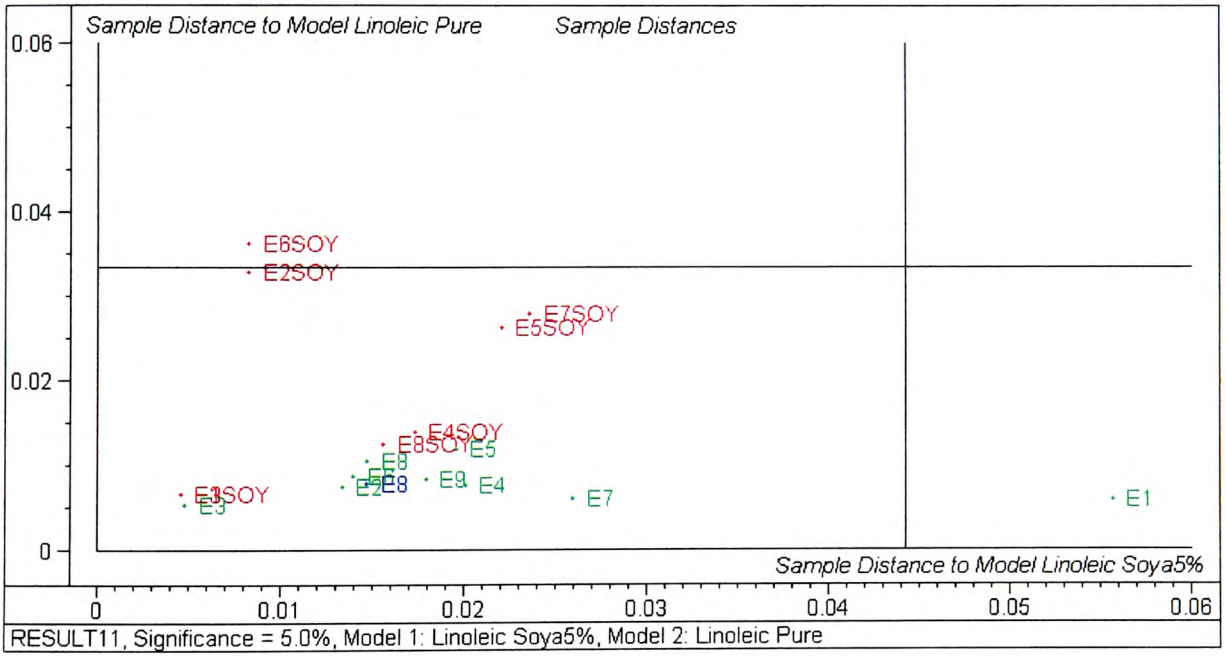

Figure B. 5 - Cooman's plot to show separation between pure Crete oils (green E1-9) and 5% soya adulterated oils (red) using linoleic peaks

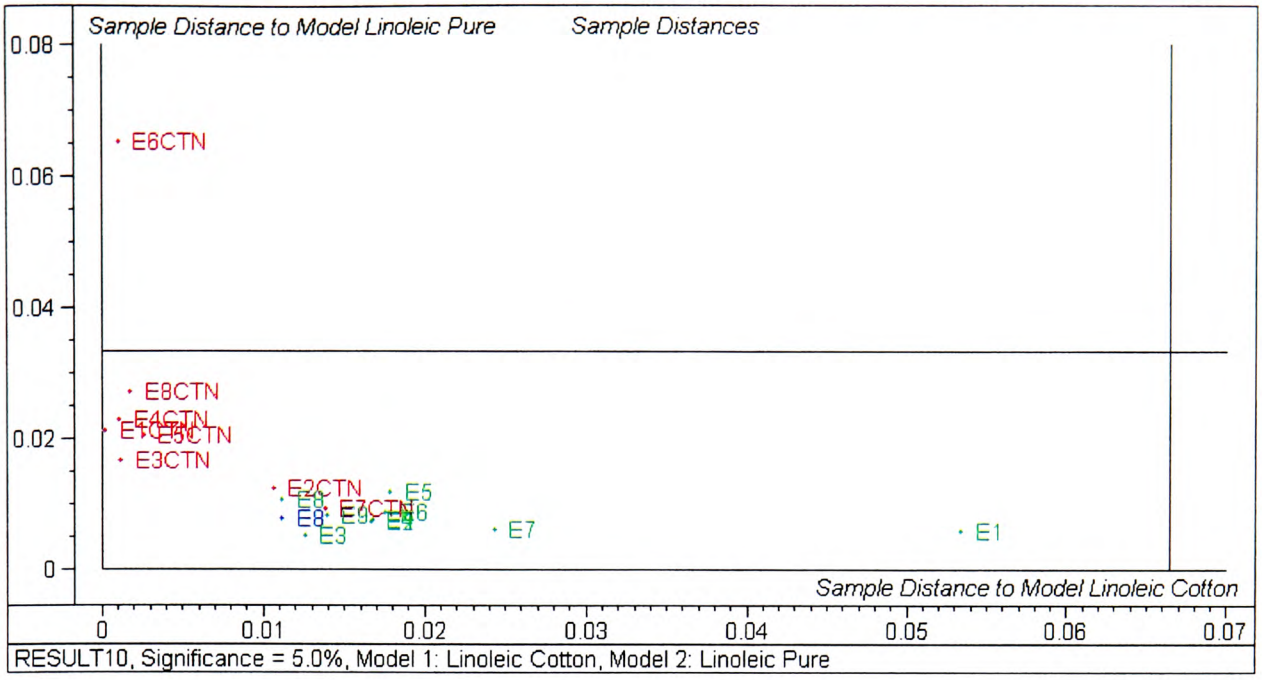

Figure B.6 - Cooman's plot to show separation between pure Crete oils (green E1-9) and 5% cotton adulterated oils (red) using linoleic peaks

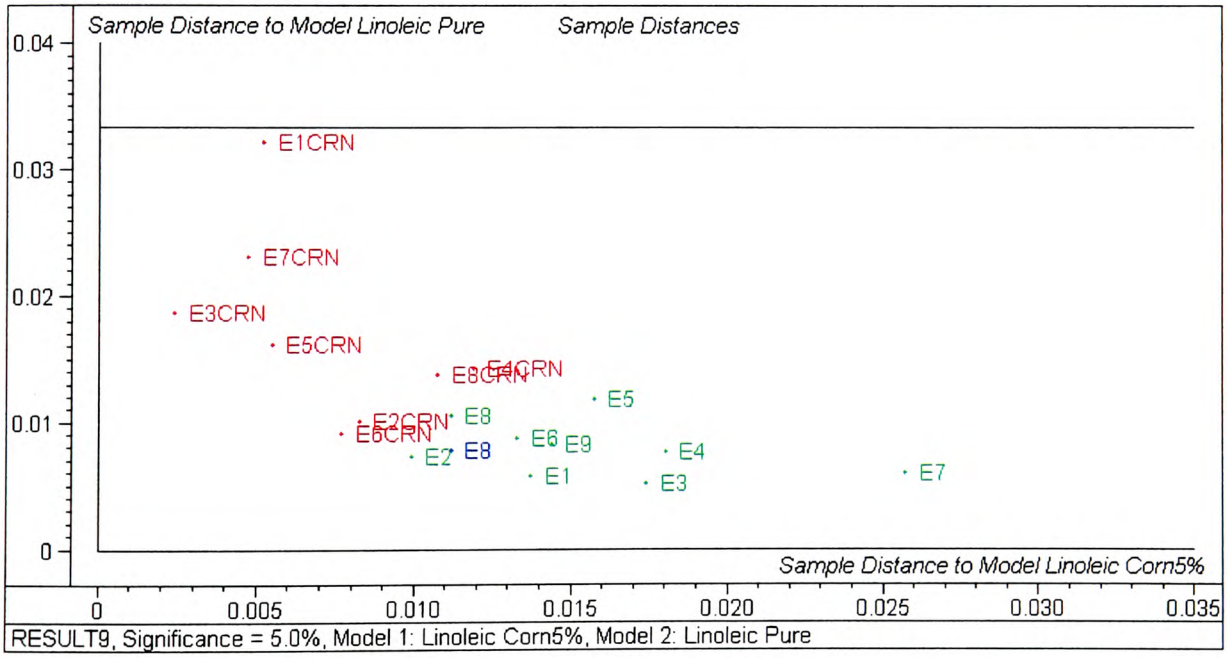

Figure B.7 - Cooman's plot to show separation between pure Crete oils (green E1-9) and 5% cotton adulterated oils (red) using linoleic peaks

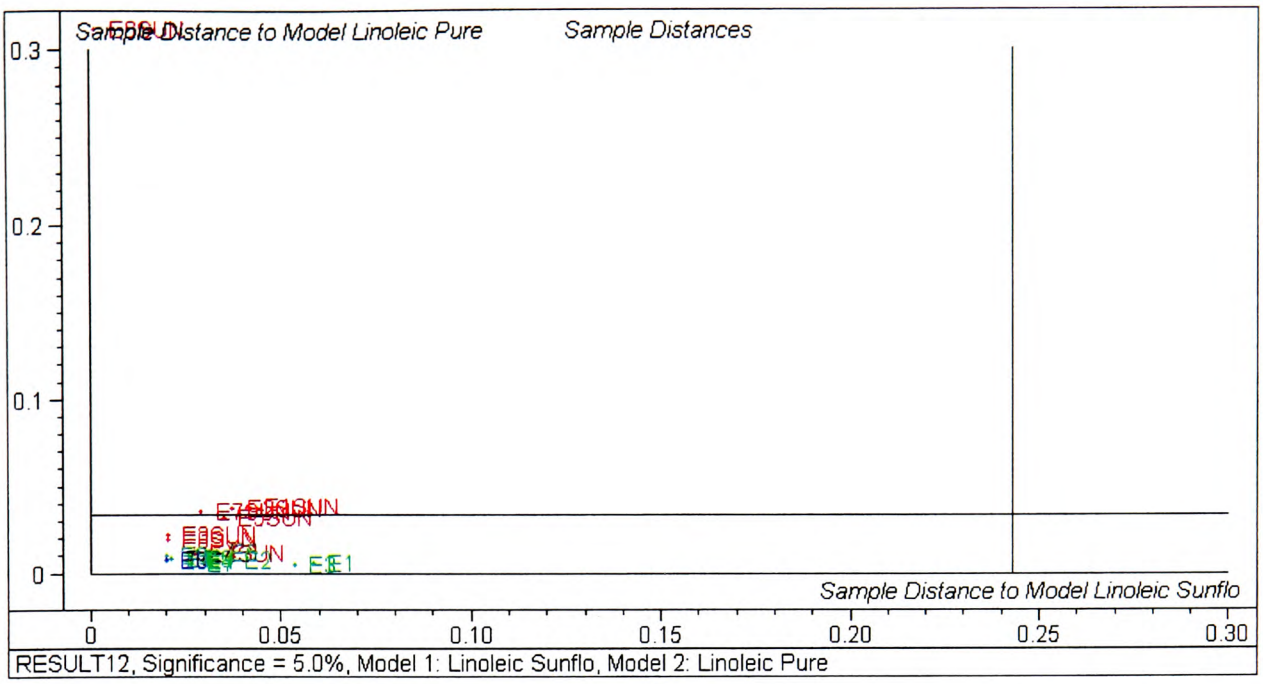

Figure B.8 - Cooman's plot to show separation between pure Crete oils (green E1-9) and 5% sunflower adulterated oils (red) using linoleic peaks

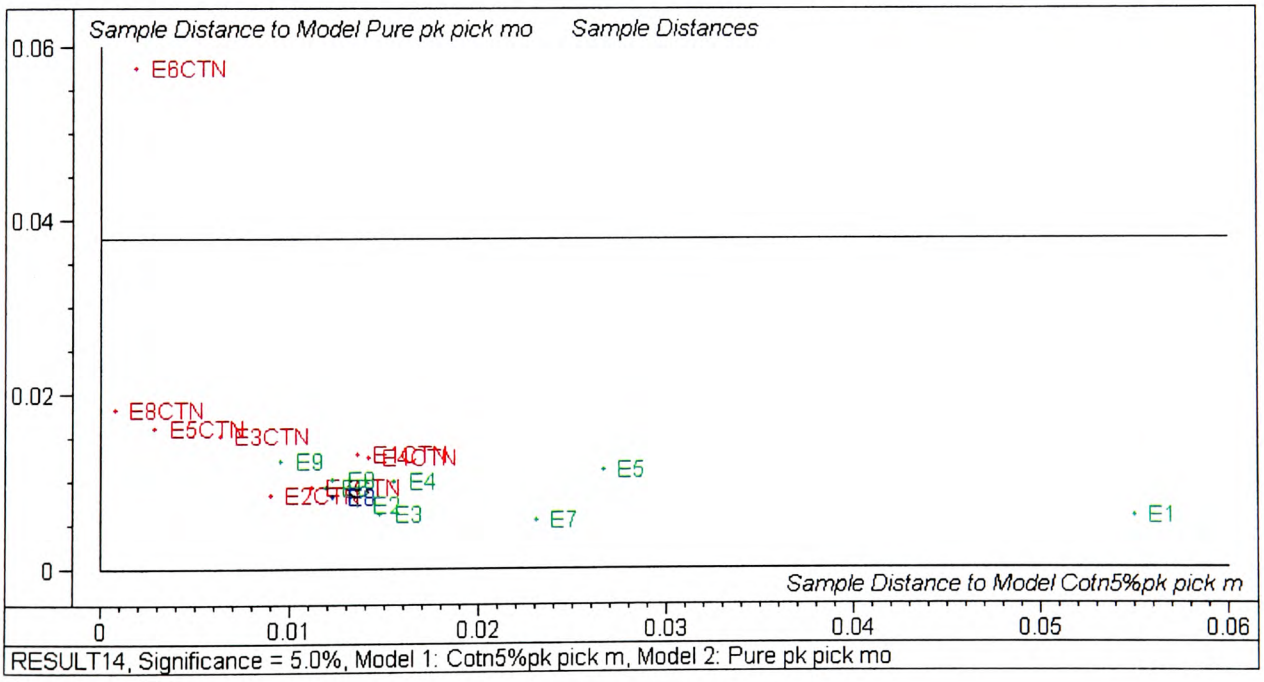

Figure B.9 - Cooman's plot to show separation between pure Crete oils (green E1-9) and 5% cotton adulterated oils (red) using model picked peaks

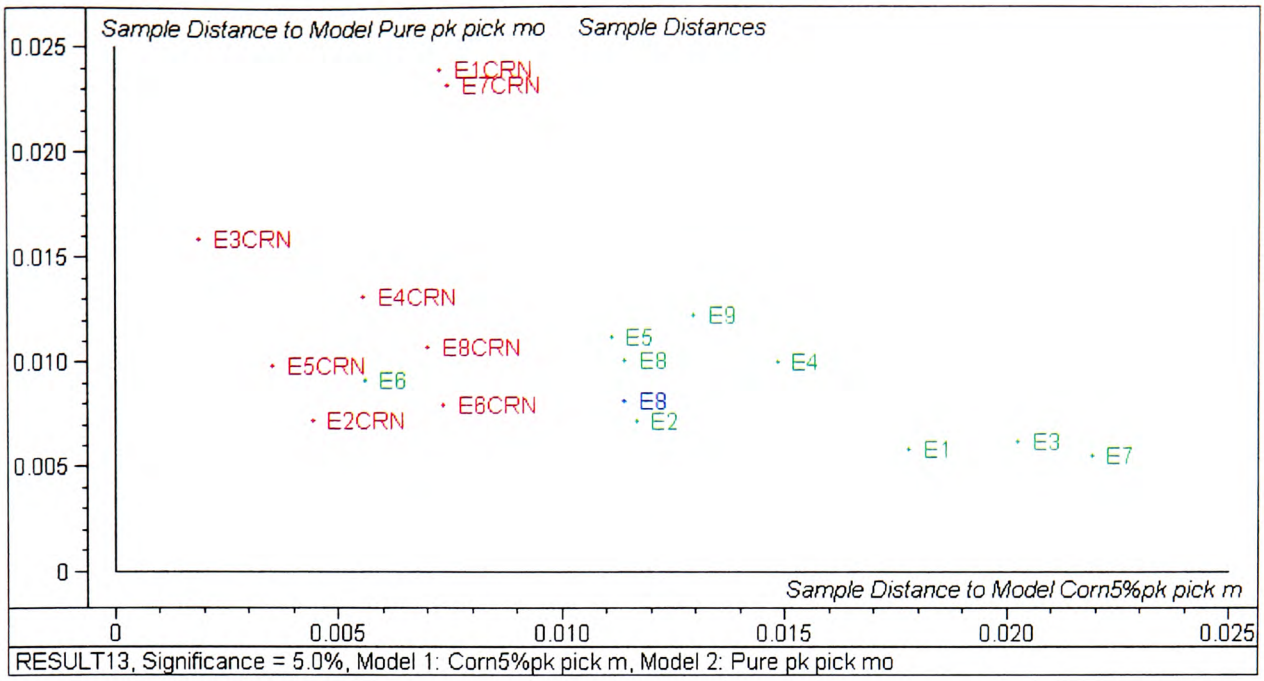

Figure B.10 - Cooman's plot to show separation between pure Crete oils (green E1-9) and 5% corn adulterated oils (red) using model picked peaks

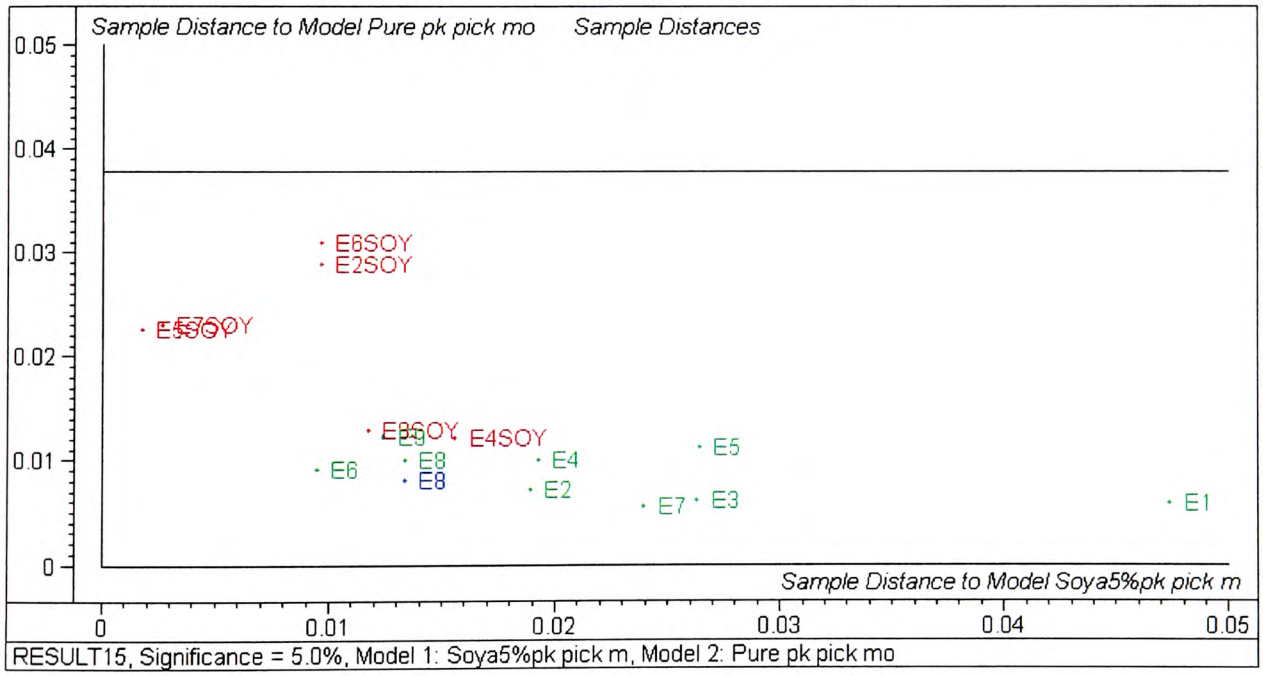

Figure B.11 - Cooman's plot to show separation between pure Crete oils (green E1-9) and 5% soya adulterated oils (red) using model picked peaks

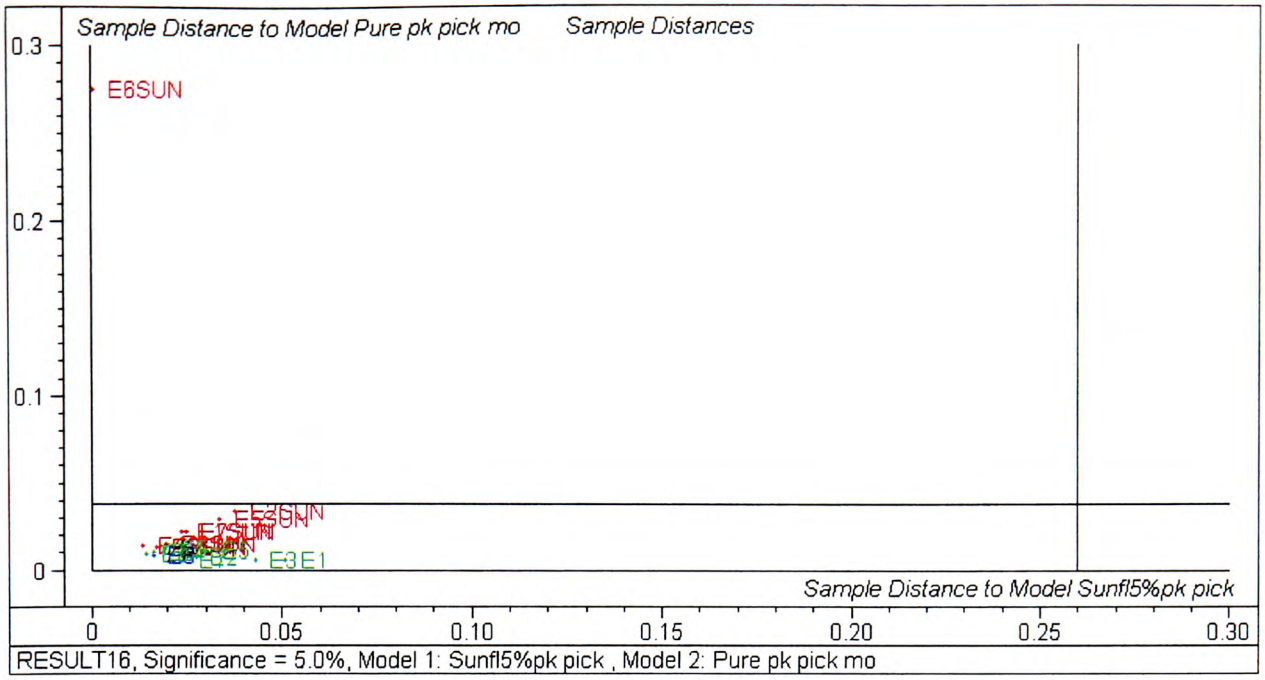

Figure B.12 - Cooman's plot to show separation between pure Crete oils (green E1-9) and 5% sunflower adulterated oils (red) using model picked peaks

Reference

Mavromoustakos, T., M. Zervou, E. Theodoropoulou, D. Panagiotopoulos, G. Bonas, M. Day and A. Helmis (1997). "^{13}C NMR analysis of the triacylglycerol composition of Greek virgin olilve oils." Magnetic Resonance in Chemistry **35**: S3-S7.

APPENDIX C

^{1}H NMR

Appendix C – Index of Tables

Appendix C – Index of Figures

E set Crete Oils

Table C.1 – NMR sample weights, pure oils E set

Pure Olive Oil			
Sample	**NMR Sample weighing (g)**	**NMR Filename**	**2.7ppm weighted integral**
E1	0.4303	apj-e1	755411193.8
E2	0.4099	apj-e2	4726242.5
E3	0.4422	apj-e3	5546963.4
E4	0.4609	apj-e4	6520906.1
E5	0.442	apj-e5	11330810
E6	0.4276	apj-e6	6862981.3
E7	0.4796	apj-e7	7288272.7
E8	0.404	apj-e8	7196576.2
E9	0.4436	apj-e9	7790233.544
E10	0.3707	apj-e10	6589966.01
E11	0.4735	apj-e11	6818467.582
E12	0.4192	apj-e12	9502917.939
E13	0.4379	apj-e13	7557287.052
E14	0.4763	apj-e14	7782204.493
E15	0.3814	apj-e15	5718987.939
E16	0.4051	apj-e16	5442652.185
E17	0.4239	apj-e17	6412299.127
E18	0.3804	apj-e18	7196433.228

Table C.2 - NMR sample weights, 1%, 5% and 10% sunflower adulterated oils, Crete E set

1% Sunflower Oil						
Sample	**Wt of Sunflower Oil (g)**	**Wt of Olive Oil (g)**	**Total Weight (g)**	**% adulteration**	**NMR Sample weighing**	**NMR Filename**
E1	0.118	9.899	10.017	1.18	0.4577	apj-e1-1%
E2	0.120	9.931	10.051	1.19	0.5645	apj-e2-1%
E3	0.107	9.906	10.013	1.07	0.4118	apj-e3-1%
E4	0.125	9.910	10.035	1.25	0.5207	apj-e4-1%
E5	0.110	9.894	10.004	1.10	0.4499	apj-e5-1%
E6	0.115	9.910	10.025	1.15	0.3754	apj-e6-1%
E7	0.105	9.896	10.001	1.05	0.4655	apj-e7-1%
E8	0.118	9.902	10.020	1.18	0.4281	apj-e8-1%
E9	0.113	9.916	10.029	1.13	0.4082	apj-e9-1%
E10	0.117	9.920	10.037	1.17	0.4006	apj-e10-1%
E11	0.121	9.900	10.021	1.21	0.4475	apj-e11-1%
E12	0.113	9.910	10.023	1.13	0.3967	apj-e12-1%
E13	0.138	9.903	10.041	1.37	0.4447	apj-e13-1%
E14	0.126	9.905	10.031	1.26	0.4301	apj-e14-1%
E15	0.116	9.903	10.019	1.16	0.3966	apj-e15-1%
E16	0.113	9.902	10.015	1.13	0.3661	apj-e16-1%
E17	0.117	9.907	10.024	1.17	0.4196	apj-e17-1%
E18	0.131	9.908	10.039	1.30	0.4309	apj-e18-1%
5% Sunflower Oil						
Sample	**Wt of Sunflower Oil (g)**	**Wt of Olive Oil (g)**	**Total Weight (g)**	**%**	**NMR Sample weighing**	**NMR Filename**
E1	0.530	9.488	10.018	5.29	0.4800	apj-e1-5%
E2	0.509	9.482	9.991	5.09	0.4438	apj-e2-5%
E3	0.522	9.515	10.037	5.20	0.4408	apj-e3-5%
E4	0.495	9.477	9.972	4.96	0.4258	apj-e4-5%
E5	0.495	9.511	10.006	4.95	0.4144	apj-e5-5%
E6	0.491	9.487	9.978	4.92	0.4121	apj-e6-5%
E7	0.484	9.507	9.991	4.84	0.4416	apj-e7-5%
E8	0.488	9.485	9.973	4.89	0.4234	apj-e8-5%

E9	0.495	9.486	9.981	4.96	0.4320	apj-e9-5%
E10	0.496	9.509	10.005	4.96	0.4120	apj-e10-5%
E11	0.505	9.507	10.012	5.04	0.3763	apj-e11-5%
E12	0.252	0.475	5.002	5.04	0.4114	apj-e12-5%
E13	0.498	9.525	10.023	4.97	0.3888	apj-e13-5%
E14	0.494	9.502	9.996	4.94	0.4045	apj-e14-5%
E15	0.498	9.511	10.009	4.98	0.4458	apj-e15-5%
E16	0.483	9.506	9.989	4.84	0.4061	apj-e16-5%
E17	0.518	9.520	10.038	5.16	0.4229	apj-e17-5%
E18	0.559	9.505	10.064	5.55	0.3683	apj-e18-5%
10% Sunflower Oil						
Sample	**Wt of Sunflower Oil (g)**	**Wt of Olive Oil (g)**	**Total Weight (g)**	**%**	**NMR Sample weighing**	**NMR Filename**
E1	1.004	8.974	9.978	10.06	0.4188	apj-e1-10%
E2	1.007	8.995	10.002	10.07	0.3898	apj-e2-10%
E3	1.001	9.009	10.010	10.00	0.3956	apj-e3-10%
E4	1.001	8.995	9.996	10.01	0.3980	apj-e4-10%
E5	1.022	8.999	10.021	10.20	0.4543	apj-e5-10%
E6	1.007	9.015	10.022	10.05	0.4114	apj-e6-10%
E7	1.010	8.992	10.002	10.10	0.4378	apj-e7-10%
E8	1.015	8.999	10.014	10.14	0.4304	apj-e8-10%
E9	1.020	9.016	10.036	10.16	0.4132	apj-e9-10%
E10	1.018	9.008	10.026	10.15	0.4411	apj-e10-10%
E11	1.052	9.011	10.063	10.45	0.3842	apj-e11-10%
E12	1.041	8.991	10.032	10.38	0.4504	apj-e12-10%
E13	1.025	9.005	10.030	10.22	0.4133	apj-e13-10%
E14	1.020	9.061	10.081	10.12	0.4445	apj-e14-10%
E15	1.025	9.043	10.068	10.18	0.4369	apj-e15-10%
E16	1.035	9.004	10.039	10.31	0.4186	apj-e16-10%
E17	1.009	9.019	10.028	10.06	0.4489	apj-e17-10%
E18	1.015	9.059	10.074	10.08	0.4291	apj-e18-10%

F set Crete Oils

Table C.3 - NMR sample weights, pure oils F set

Pure Olive Oil			
Sample code	**NMR Sample weighing (g)**	**NMR Filename**	**2.7 ppm weighted integral**
F1	0.4709	apj-f1	3488326.694
F2	0.4179	apj-f2	4615855.908
F3	0.4345	apj-f3	4470530.55
F4	0.4590	apj-f4	4031781.002
F5	0.3860	apj-f5	4572467.876
F6	0.4392	apj-f6	3315247.268
F7	0.4238	apj-f7	5123046.909
F8	0.4055	apj-f8	5900990.481
F9	0.4099	apj-f9	4256650.305
F10	0.3927	apj-f10	4751115.865
F11	0.4514	apj-f11	5325104.121
F12	0.3999	apj-f12	5729651.413
F13	0.4754	apj-f13	5191609.592
F14	0.4133	apj-f14	5525193.322
F15	0.4774	apj-f15	5115693.339
F16	0.4420	apj-f16	4637861.538
F17	0.4670	apj-f17	5167953.747
F18	0.4396	apj-f18	3895965.423
F19	0.4279	apj-f19	8742010.75
F20	0.4079	apj-f20	6854686.933
F21	0.4886	apj-f21	5900362.669
F22	0.3949	apj-f22	7474556.597

Table C.4 - NMR sample weights, 1% and 10% sunflower adulterated oils, F set

1% Sunflower Oil						
Sample	**Wt of Sunflower Oil (g)**	**Wt of Olive Oil (g)**	**Total Weight (g)**	**%**	**NMR Sample weighing**	**NMR Filename**
F1	0.077	4.951	5.028	1.53	0.4694	apj-f1-1%
F2	0.061	4.971	5.032	1.22	0.4142	apj-f2-1%
F3	0.093	4.970	5.063	1.83	0.4885	apj-f3-1%
F4	0.054	4.963	5.017	1.07	0.4333	apj-f4-1%

F5	0.061	4.971	5.032	1.22	0.4915	apj-f5-1%
F6	0.050	4.963	5.013	1.00	0.5567	apj-f6-1%
F7	0.064	4.948	5.012	1.28	0.4684	apj-f7-1%
F8	0.060	4.946	5.006	1.20	0.4232	apj-f8-1%
F9	0.055	4.972	5.027	1.09	0.4558	apj-f9-1%
F10	0.060	4.964	5.024	1.19	0.5060	apj-f10-1%
F11	0.063	4.978	5.041	1.25	0.4834	apj-f11-1%
F12	0.063	4.960	5.024	1.26	0.4738	apj-f12-1%
F13	0.059	4.990	5.050	1.18	0.3811	apj-f13-1%
F14	0.059	4.952	5.012	1.18	0.4786	apj-f14-1%
F15	0.062	4.950	5.011	1.23	0.5234	apj-f15-1%
F16	0.058	4.940	4.998	1.16	0.4064	apj-f16-1%
F17	0.061	4.951	5.012	1.21	0.4940	apj-f17-1%
F18	0.059	4.960	5.019	1.18	0.4901	apj-f18-1%
F19	0.061	4.956	5.017	1.21	0.4826	apj-f19-1%
F20	0.060	4.981	5.041	1.19	0.4810	apj-f20-1%
F21	0.060	4.958	5.018	1.20	0.4891	apj-f21-1%
F22	0.060	4.951	5.011	1.19	0.4516	apj-f22-1%
5% Sunflower Oil						
Sample	**Wt of Sunflower Oil (g)**	**Wt of Olive Oil (g)**	**Total Weight (g)**	**%**	**NMR Sample weighing**	**NMR Filename**
F1	0.269	4.754	5.023	5.35	0.4315	apj-f1-5%
F2	0.269	4.759	5.028	5.35	0.4162	apj-f2-5%
F3	0.251	4.743	4.994	5.02	0.4882	apj-f3-5%
F4	0.267	4.755	5.022	5.32	0.4753	apj-f4-5%
F5	0.270	4.746	5.016	5.38	0.4836	apj-f5-5%
F6	0.289	4.743	5.033	5.75	0.4822	apj-f6-5%
F7	0.284	4.781	5.065	5.61	0.4701	apj-f7-5%
F8	0.290	4.737	5.027	5.76	0.4476	apj-f8-5%
F9	0.279	4.742	5.021	5.56	0.4452	apj-f9-5%
F10	0.277	4.734	5.011	5.52	0.4317	apj-f10-5%
F11	0.287	4.770	5.057	5.67	0.4659	apj-f11-5%
F12	0.290	4.750	5.040	5.74	0.4607	apj-f12-5%
F13	0.261	4.734	4.995	5.22	0.3753	apj-f13-5%
F14	0.249	4.779	5.028	4.96	0.4112	apj-f14-5%
F15	0.268	4.733	5.001	5.36	0.4810	apj-f15-5%
F16	0.257	4.748	5.004	5.13	0.4279	apj-f16-5%
F17	0.257	4.755	5.012	5.12	0.4877	apj-f17-5%
F18	0.270	4.776	5.046	5.35	0.4046	apj-f18-5%

F19	0.270	4.745	5.015	5.38	0.4834	apj-f19-5%
F20	0.269	4.770	5.039	5.34	0.4517	apj-f20-5%
F21	0.287	4.802	5.089	5.63	0.4857	apj-f21-5%
F22	0.276	4.759	5.035	5.49	0.4837	apj-f22-5%

E samples (non-Crete) weighings

Table C.5 - NMR sample weights, 1% and 5% sunflower adulterated oils, non-Crete E set

Sample	Sunflwr Oil (g)	Olive oil (g)	Total (g)	%	Sample	Sunflwr Oil (g)	Olive oil (g)	Total (g)	%
E19	0.0409	3.959	3.9999	1.023	E19	0.2002	3.8009	4.0011	5.004
E20	0.042	3.961	4.003	1.049	E20	0.203	3.7992	4.0022	5.072
E21	0.0398	3.9587	3.9985	0.995	E21	0.1989	3.801	3.9999	4.973
E22	0.04	3.9651	4.0051	0.999	E22	0.1999	3.803	4.0029	4.994
E23	0.0419	3.9631	4.005	1.046	E23	0.202	3.8015	4.0035	5.046
E24	0.0396	3.9609	4.0005	0.990	E24	0.1999	3.7999	3.9998	4.998
E25	0.047	3.9684	4.0154	1.170	E25	0.1993	3.8	3.9993	4.983
E26	0.0396	3.9611	4.0007	0.990	E26	0.339	3.9	4.239	7.997
E27	0.0416	3.9614	4.003	1.039	E27	0.2001	3.8019	4.002	5.000
E28	0.0406	3.9596	4.0002	1.015	E28	0.199	3.8005	3.9995	4.976
E29	0.0424	3.963	4.0054	1.059	E29	0.2005	3.8021	4.0026	5.009
E30	0.043	3.9641	4.0071	1.073	E30	0.1998	3.8023	4.0021	4.992
E31	0.0467	3.9676	4.0143	1.163	E31	0.2086	3.8087	4.0173	5.193
E32	0.0445	3.9638	4.0083	1.110	E32	0.2021	3.802	4.0041	5.047
E34	0.0408	3.9621	4.0029	1.019	E34	0.2003	3.8011	4.0014	5.006
E35	0.0406	3.9609	4.0015	1.015	E35	0.2006	3.8009	4.0015	5.013
E36	0.041	3.9614	4.0024	1.024	E36	0.2023	3.803	4.0053	5.051
E37	0.0407	3.9614	4.0021	1.017	E37	0.2088	3.8027	4.0115	5.205
E38	0.0411	3.962	4.0031	1.027	E38	0.1999	3.8003	4.0002	4.997
E39	0.042	3.9613	4.0033	1.049	E39	0.2041	3.804	4.0081	5.092
E40	0.0415	3.9613	4.0028	1.037	E40	0.2019	3.8069	4.0088	5.036
E41	0.0409	3.9625	4.0034	1.022	E41	0.2016	3.7998	4.0014	5.038
E42	0.0443	3.9689	4.0132	1.104	E42	0.2029	3.8041	4.007	5.064
E43	0.04	3.9618	4.0018	1.000	E43	0.2017	3.801	4.0027	5.039
E44	0.041	3.9621	4.0031	1.024	E44	0.2034	3.8036	4.007	5.076
E45	0.042	3.9616	4.0036	1.049	E45	0.2022	3.8038	4.006	5.047
E46	0.0395	3.9602	3.9997	0.988	E46	0.1992	3.8015	4.0007	4.979
E47	0.0441	3.9618	4.0059	1.101	E47	0.2007	3.8014	4.0021	5.015
E48	0.0415	3.9605	4.002	1.037	E48	0.2002	3.8017	4.0019	5.003
E49	0.0431	3.9676	4.0107	1.075	E49	0.2029	3.8025	4.0054	5.066
E50	0.0404	3.9621	4.0025	1.009	E50	0.2	3.8001	4.0001	5.000
E51	0.0405	3.961	4.0015	1.012	E51	0.2	3.8013	4.0013	4.998
E52	0.0406	3.9605	4.0011	1.015	E52	0.204	3.8052	4.0092	5.088
E53	0.0405	3.9625	4.003	1.012	E53	0.2012	3.8005	4.0017	5.028
E54	0.0405	3.9621	4.0026	1.012	E54	0.2044	3.8012	4.0056	5.103
E55	0.0417	3.9601	4.0018	1.042	E55	0.2017	3.803	4.0047	5.037
E56	0.0411	3.9605	4.0016	1.027	E56	0.2116	3.813	4.0246	5.258
E57	0.042	3.9621	4.0041	1.049	E57	0.2017	3.809	4.0107	5.029

E58	0.0401	3.9604	4.0005	1.002	E58	0.2029	3.8005	4.0034	5.068
E59	0.0406	3.9618	4.0024	1.014	E59	0.203	3.8042	4.0072	5.066
E60	0.041	3.9652	4.0062	1.023	E60	0.2	3.8034	4.0034	4.996
E61	0.0401	3.9617	4.0018	1.002	E61	0.2017	3.8022	4.0039	5.038
E62	0.0403	3.962	4.0023	1.007	E62	0.2001	3.8015	4.0016	5.000
E63	0.04	3.9603	4.0003	1.000	E63	0.2008	3.8	4.0008	5.019
E64	0.0416	3.9605	4.0021	1.039	E64	0.2018	3.8011	4.0029	5.041
E65	0.042	3.9602	4.0022	1.049	E65	0.2002	3.8026	4.0028	5.001

F samples (non-Crete) weighings

Table C.6 - NMR sample weights, 1% and 5% sunflower adulterated oils, non-Crete F set

Oil code	Olive oil (g)	Sample	1% sun (g)	Olive oil (g)	Total (g)	%	Oil code	5% sun (g)	Olive oil (g)	Total (g)
F23	3.9985	F23	0.041	3.9612	4.0022	1.0244	F23	0.2025	3.8028	4.0053
F24	4.0024	F24	0.0398	3.9575	3.9973	0.9957	F24	0.2002	3.8011	4.0013
F25	4.0011	F25	0.0401	3.9613	4.0014	1.0021	F25	0.2005	3.7992	3.9997
F26	4.0008	F26	0.0405	3.9599	4.0004	1.0124	F26	0.202	3.802	4.004
F27	4.0013	F27	0.0404	3.962	4.0024	1.0094	F27	0.2021	3.8004	4.0025
F28	4.0014	F28	0.0408	3.9606	4.0014	1.0196	F28	0.2007	3.8001	4.0008
F29	4	F29	0.0398	3.96	3.9998	0.9950	F29	0.2015	3.802	4.0035
F30	4.0021	F30	0.042	3.962	4.004	1.0490	F30	0.2005	3.802	4.0025
F31	4.001	F31	0.0415	3.963	4.0045	1.0363	F31	0.203	3.805	4.008
F32	39991	F32	0.0404	3.9606	4.001	1.0097	F32	0.2017	3.8041	4.0058
F33	4.006	F33	0.0429	3.964	4.0069	1.0707	F33	0.2016	3.8018	4.0034
F34	3.9998	F34	0.0399	3.9604	4.0003	0.9974	F34	0.2029	3.801	4.0039
F35	3.9933	F35	0.0418	3.9614	4.0032	1.0442	F35	0.1991	3.820	4.0191
F36	4.0054	F36	0.0400	3.9608	4.0008	0.9998	F36	0.2002	3.804	4.0042
F37	4.0004	F37	0.0423	3.9613	4.0036	1.0565	F37	0.202	3.8028	4.0048
F38	3.9979	F38	0.0408	3.9624	4.0032	1.0192	F38	0.1991	3.797	3.9961
F39	4.0000	F39	0.0405	3.9607	4.0012	1.0122	F39	0.2021	3.8005	4.0026
F40	3.9991	F40	0.0406	3.9598	4.0004	1.0149	F40	0.2004	3.8042	4.0046
F41	3.9975	F41	0.0394	3.9584	3.9978	0.9855	F41	0.2003	3.8001	4.0004
F42	4.0001	F42	0.0401	3.9614	4.0015	1.0021	F42	0.202	3.7994	4.0014
F43	4.0005	F43	0.0416	3.962	4.0036	1.0391	F43	0.2002	3.8002	4.0004
F44	4.003	F44	0.0434	3.9634	4.0068	1.0832	F44	0.1998	3.7994	3.9992
F45	3.9961	F45	0.0441	3.9666	4.0107	1.0996	F45	0.2005	3.7998	4.0003
F46	4.0045	F46	0.0394	3.967	4.0064	0.9834	F46	0.2012	3.8025	4.0037
F47	3.9975	F47	0.042	3.9628	4.0048	1.0487	F47	0.2009	3.802	4.0029
F48	4.0024	F48	0.0413	3.9621	4.0034	1.0316	F48	0.2067	3.81	4.0167
F50	4.0063	F50	0.0397	3.9601	3.9998	0.9925	F50	0.2015	3.8009	4.0024
F51	3.9969	F51	0.0411	3.96	4.0011	1.0272	F51	0.2002	3.8005	4.0007
F52	4.0074	F52	0.0492	3.9688	4.018	1.2245	F52	0.200	3.7996	3.9996
F53	3.995	F53	0.0396	3.9599	3.9995	0.9901	F53	0.2015	3.8016	4.0031
F54	4.0005	F54	0.0425	3.968	4.0105	1.0597	F54	0.2014	3.8015	4.0029
F55	4.0007	F55	0.0399	3.9618	4.0017	0.9971	F55	0.2019	3.8011	4.003

F56	4.0004	F56	0.0399	3.9606	4.0005	0.9974	F56	0.2007	3.802	4.0027
F57	3.9991	F57	0.0414	3.9609	4.0023	1.0344	F57	0.2006	3.8029	4.0035
F58	4.0193	F58	0.0411	3.9641	4.0052	1.0262	F58	0.2016	3.8036	4.0052
F59	4.0014	F59	0.0406	3.961	4.0016	1.0146	F59	0.2004	3.7995	3.9999

^{1}H NMR E set regression plots

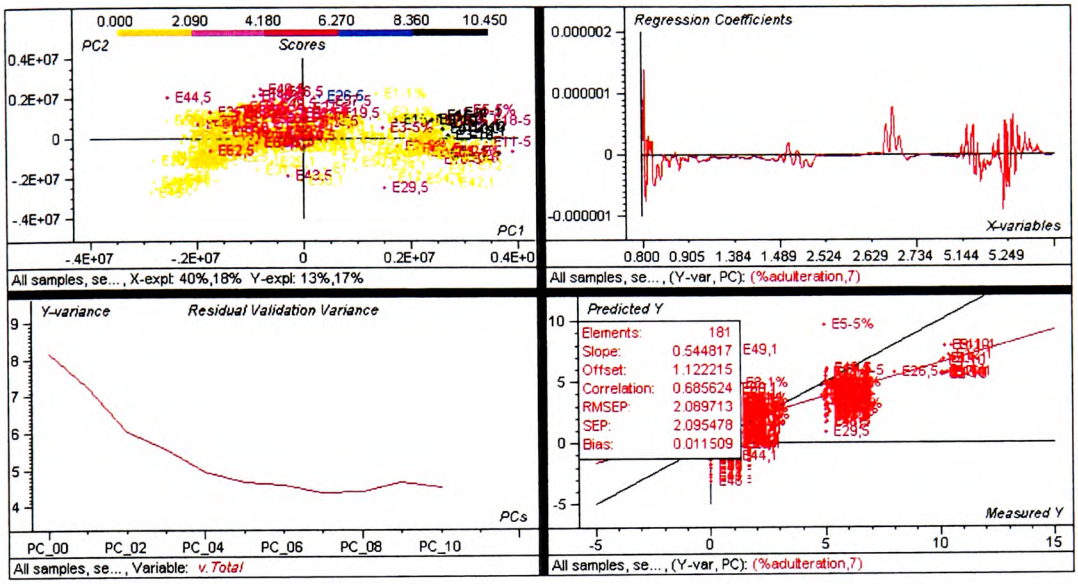

Figure C.1 – ^{1}H NMR E samples (full set) PLS1 regression plots, selected peaks-outlier (E13)

Crete oils

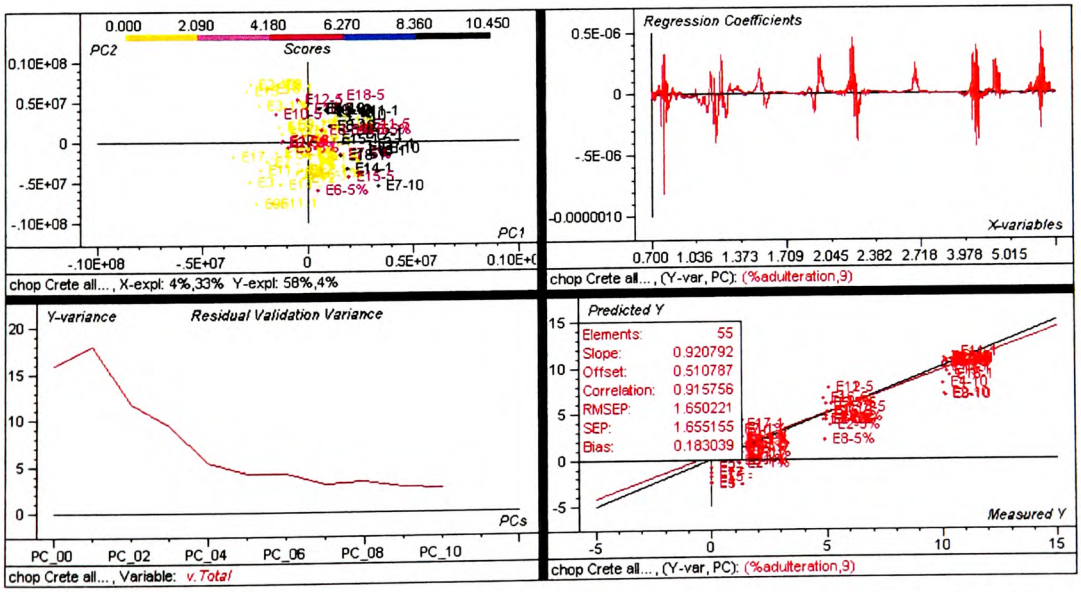

Figure C.2 - ^{1}H NMR E Crete samples, PLS1 regression plot using all variables-outlier (E13)

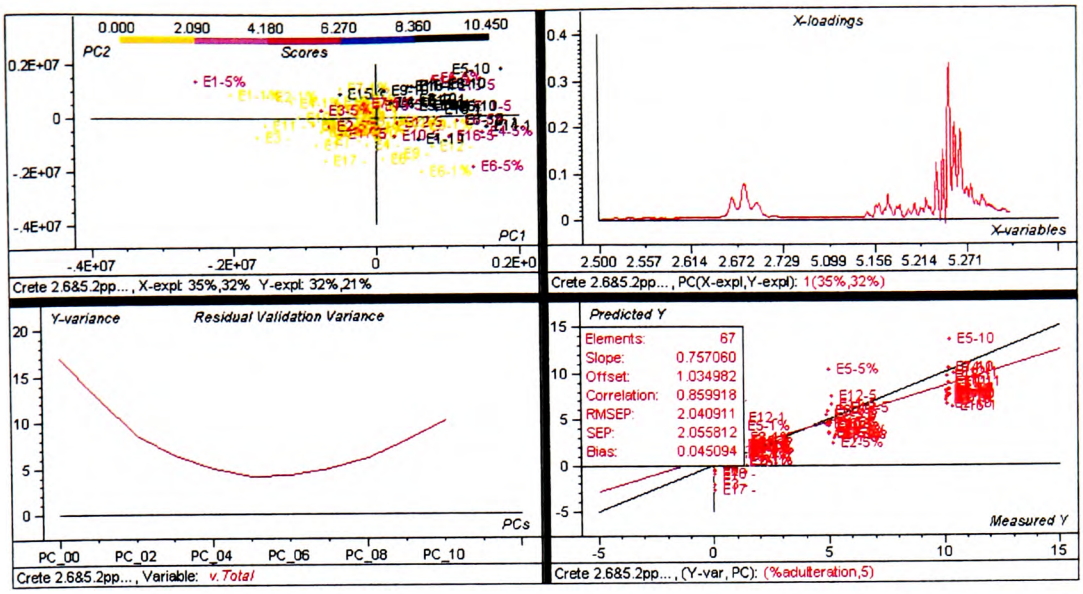

Figure C.3 - ^{1}H NMR E Crete samples, PLS1 regression plot using variables at 2.6 and 5.2 ppm-outlier (E13)

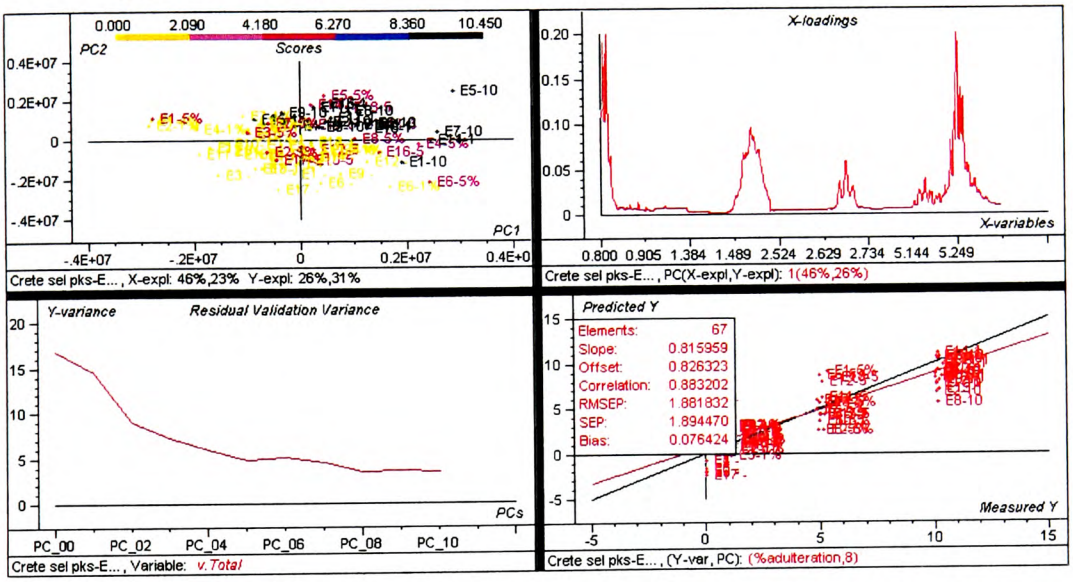

Figure C.4 - ^{1}H NMR E Crete samples, PLS1 regression plot using selected peaks-outlier (E13)

Non-Crete oils regression plots

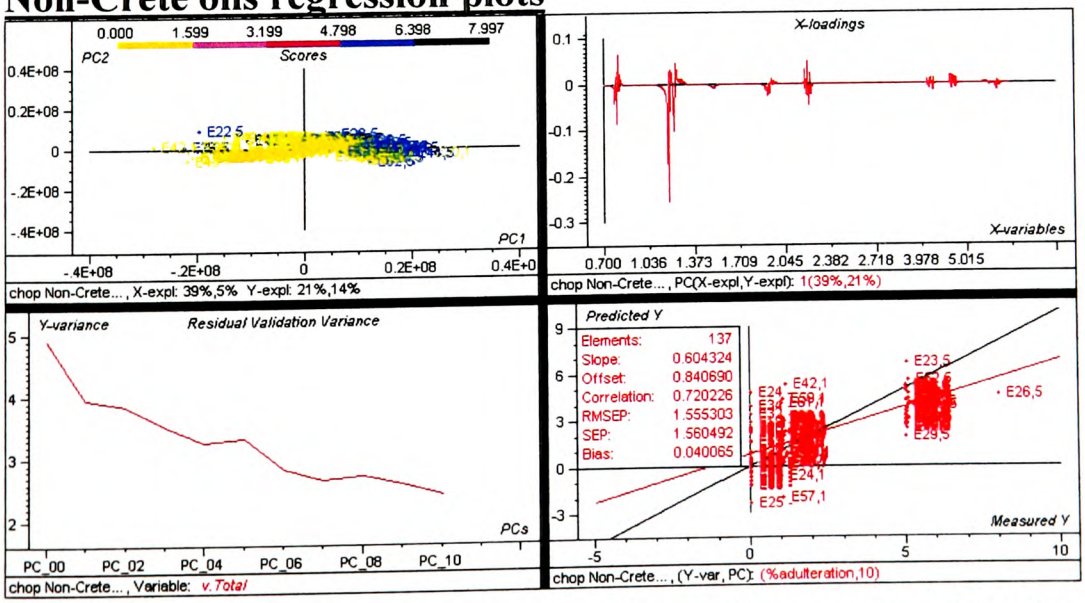

Figure C.5 - ^{1}H NMR E non-Crete samples, PLS1 regression plot using all variables

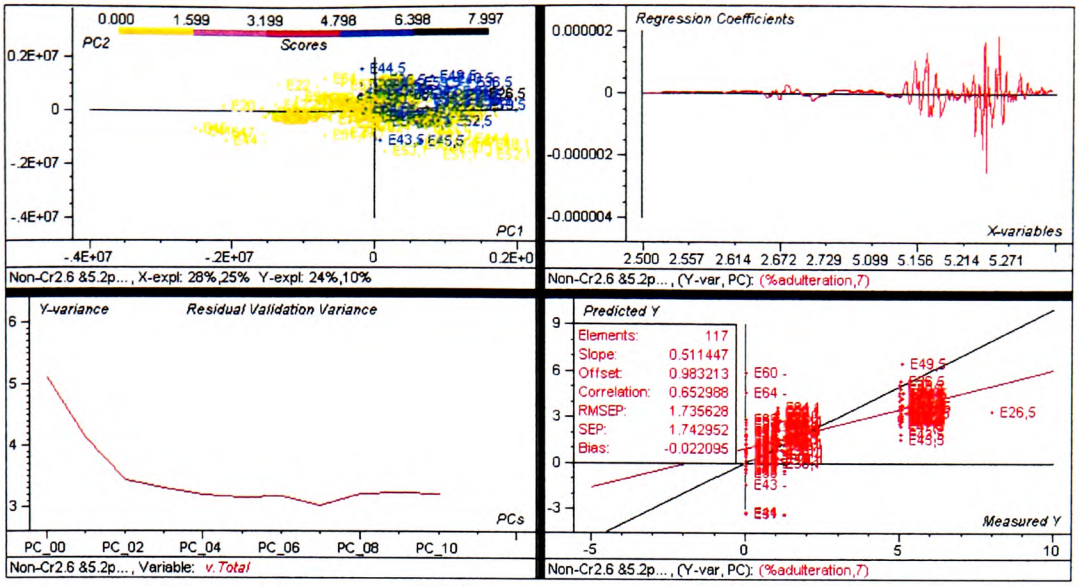

Figure C.6 - ^{1}H NMR E non-Crete samples, PLS1 regression plot using variables at 2.6 and 5.2 ppm-outlier

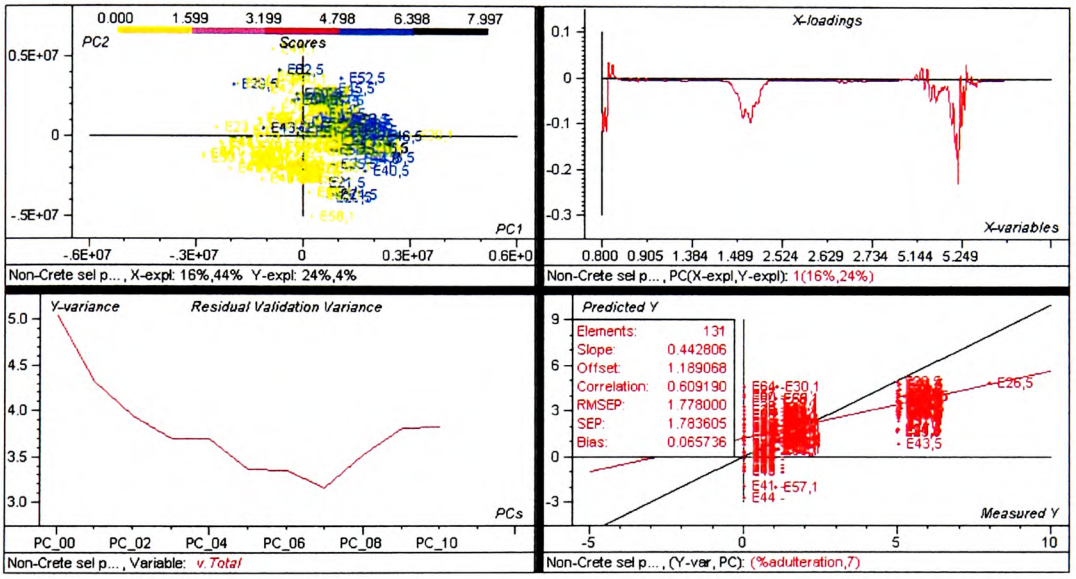

Figure C.7 - ^{1}H NMR E non-Crete samples, PLS1 regression plot using selected peaks-outliers

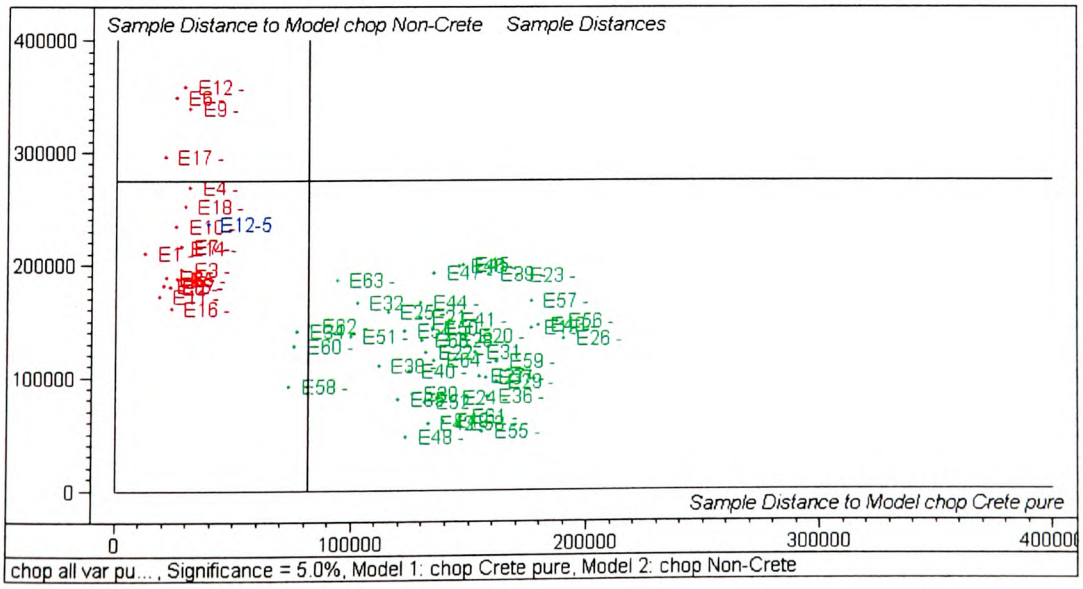

Figure C.8 – ^{1}H NMR Cooman's plot E set Crete (red) v non-Crete (green) over all variables with a 5% adulterated test sample (blue)

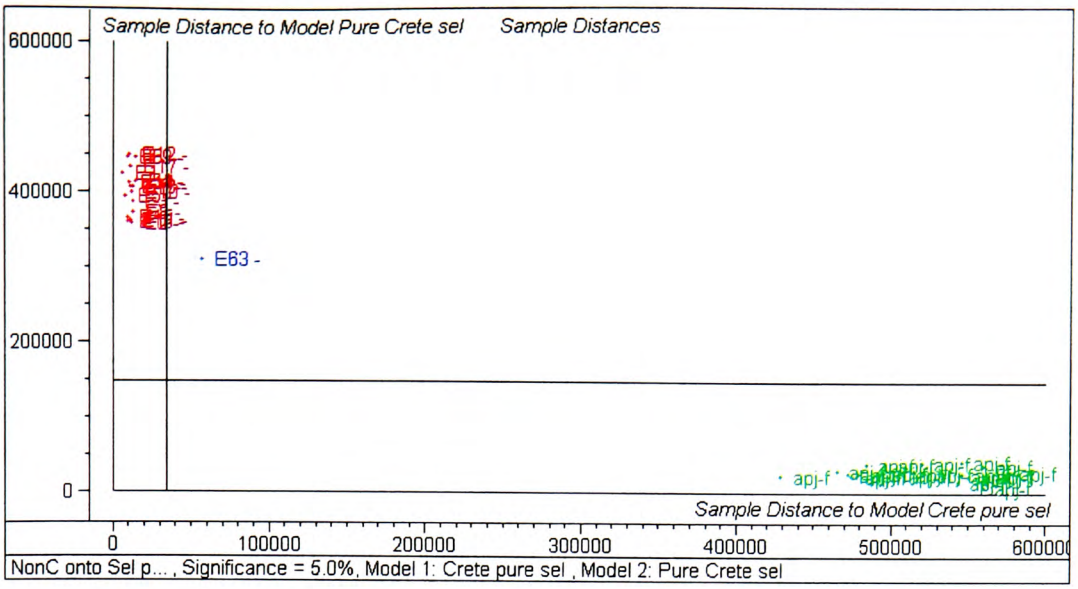

Figure C.9 – ^{1}H NMR Cooman's plot of E (red) v F (green)Crete oils selected peaks with non-Crete oil test sample (blue)

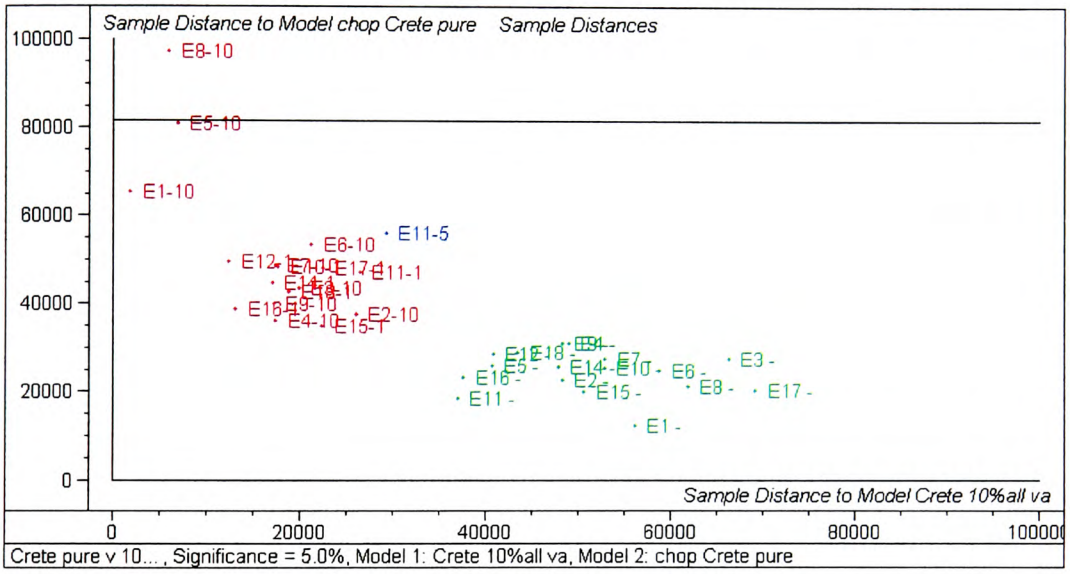

Figure C.10 – ^{1}H NMR Cooman's plot of E Crete pure (green) v 10% sunflower adulterated oils (red) over all variables with a 5% sunflower test sample (blue)

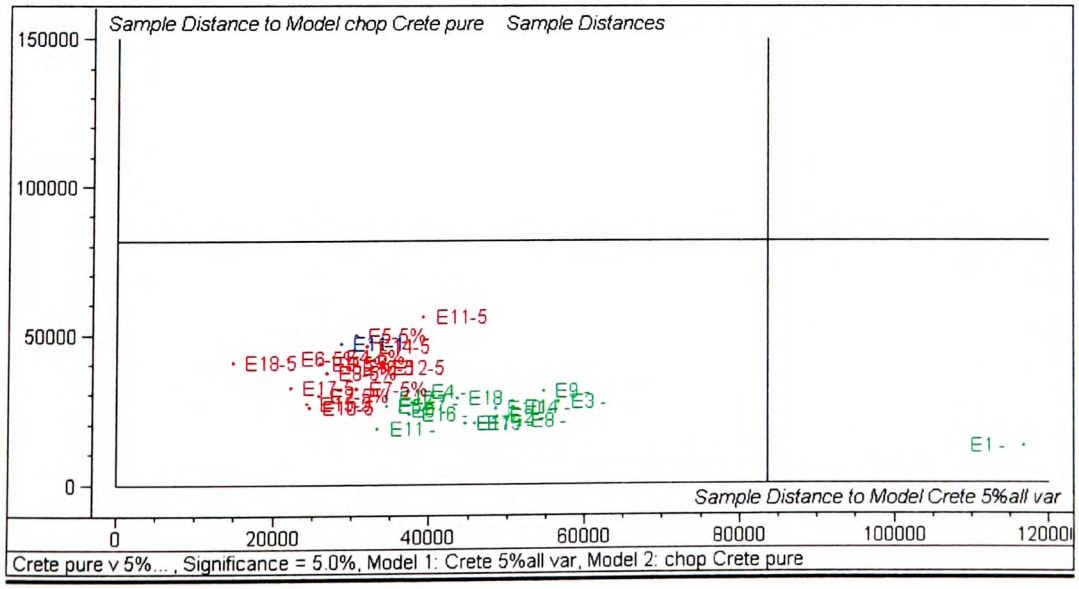

Figure C.11 – ^{1}H NMR Cooman's plot of E Crete pure oils (green) v 5% sunflower adulterated oils (red) over all variables with a 5% adulterated test sample (blue)

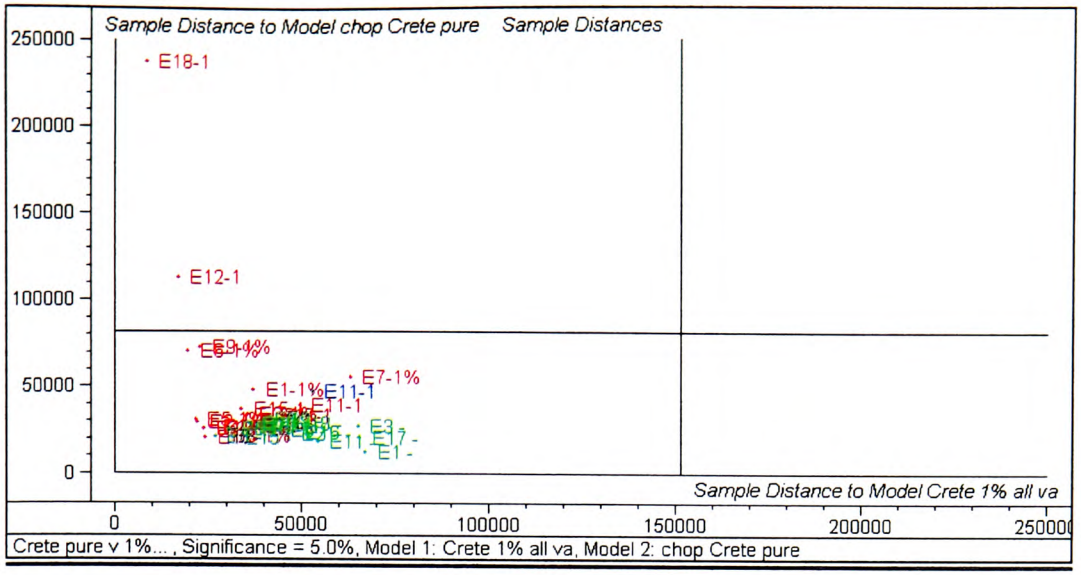

Figure C.12 - ^{1}H NMR Cooman's plot of E Crete pure oils (green) v 1% sunflower adulterated oils (red) over all variables

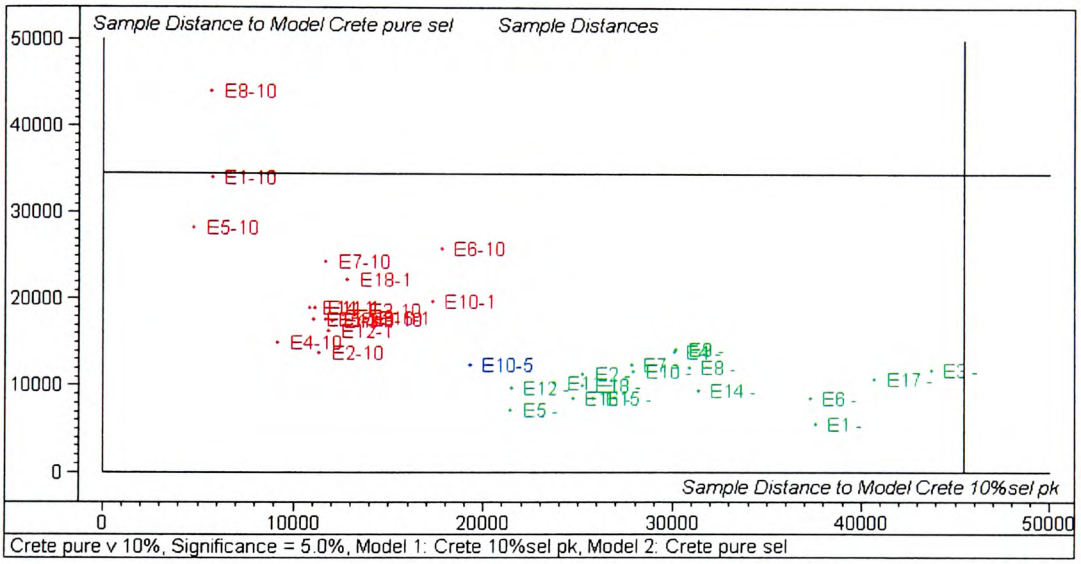

Figure C.13 - ^{1}H NMR Cooman's plot of E Crete pure oils (green) v 10% sunflower adulterated oils (red) over selected peaks with a 5% adulterated test sample (blue)

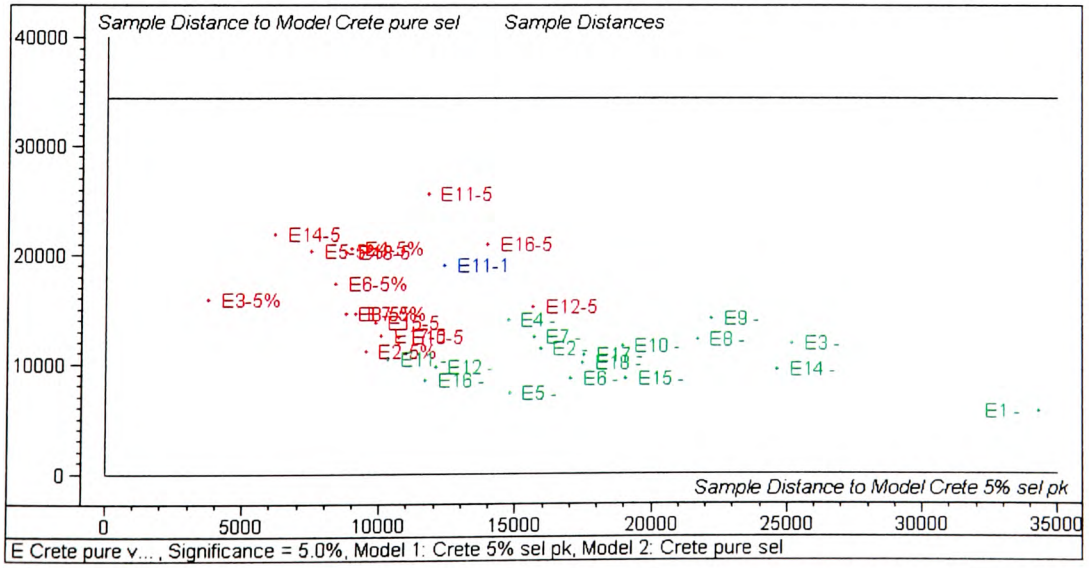

Figure C.14 - ^{1}H NMR Cooman's plot of E Crete pure oils (green) v 5% sunflower adulterated oils(red) over selected peaks with a 1% adulterated oil test sample(blue)

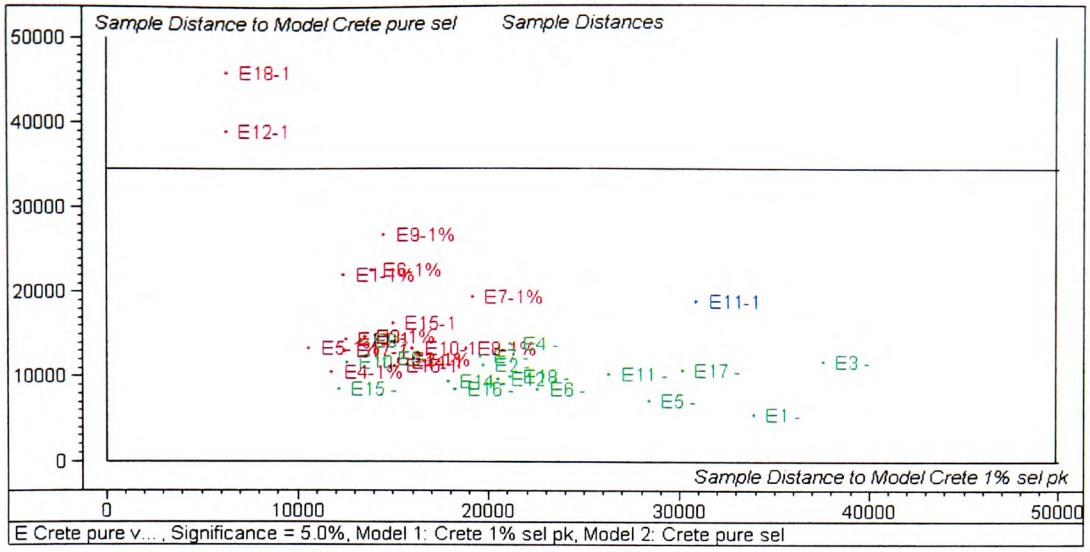

Figure C.15 - ^{1}H NMR Cooman's plot of E Crete pure oils (green) v 1% sunflower adulterated oils(red) over selected peaks with a 1% adulterated oil test sample(blue)

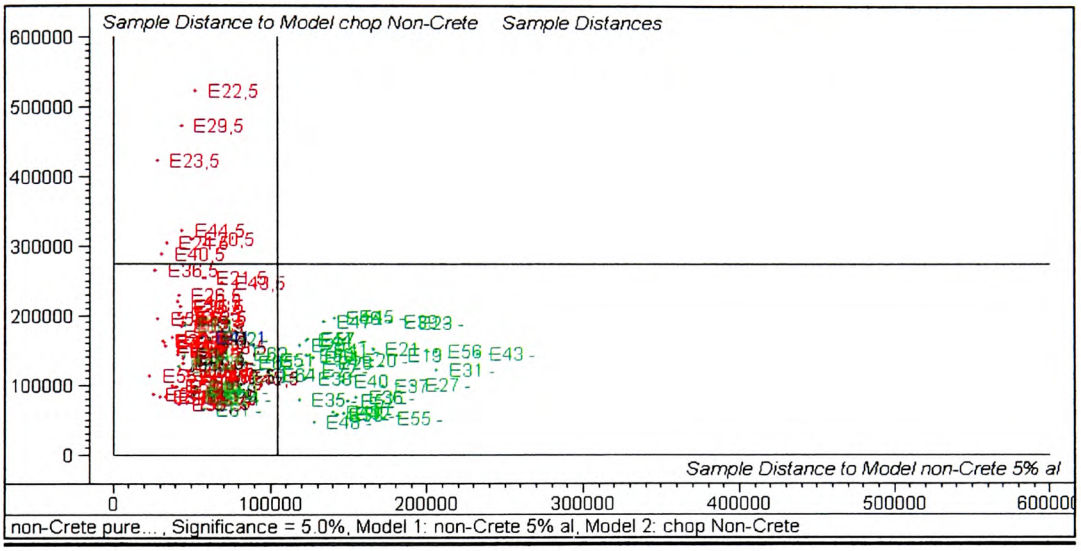

Figure C.16 - ^{1}H NMR Cooman's plot of E non-Crete pure oils (green) v 5% sunflower adulterated oils (red) over all variables with a 1% adulterated oil test sample (blue)

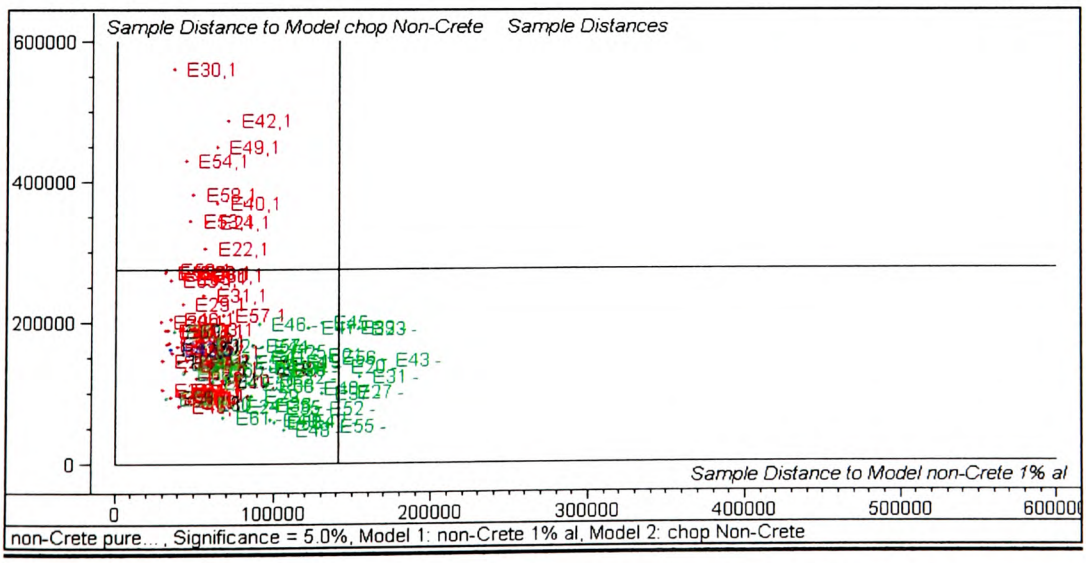

Figure C.17 - ^{1}H NMR Cooman's plot of E non-Crete pure oils (green) v 1% sunflower adulterated oils (red) over all variables with a 5% adulterated oil test sample (blue)

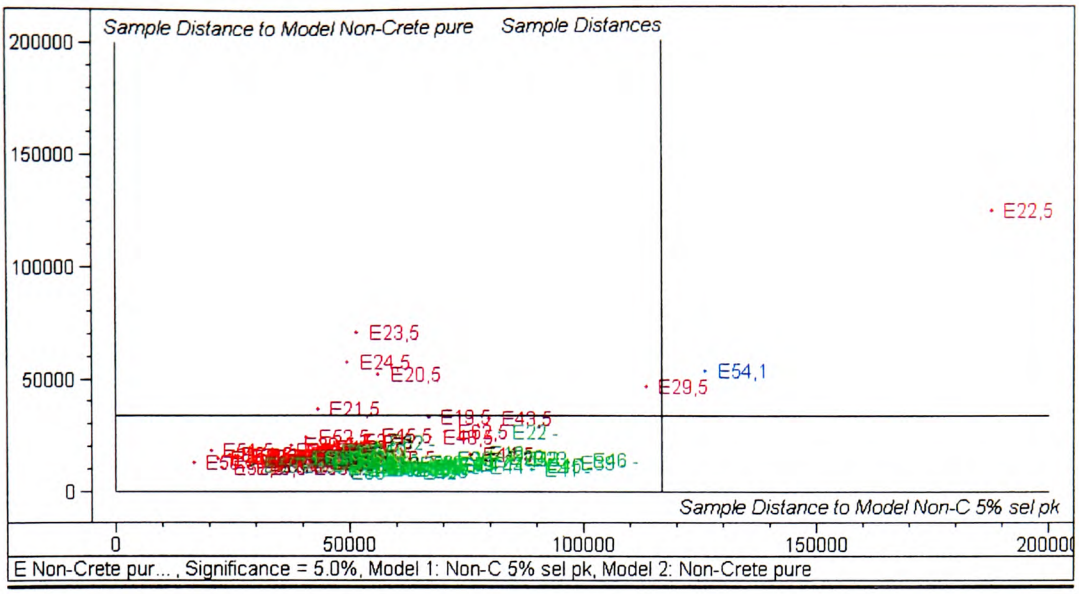

Figure C.18 - ^{1}H NMR Cooman's plot of E non-Crete pure oils (green) v 5% sunflower adulterated oils (red) over selected peaks with a 1% adulterated oil test sample (blue)

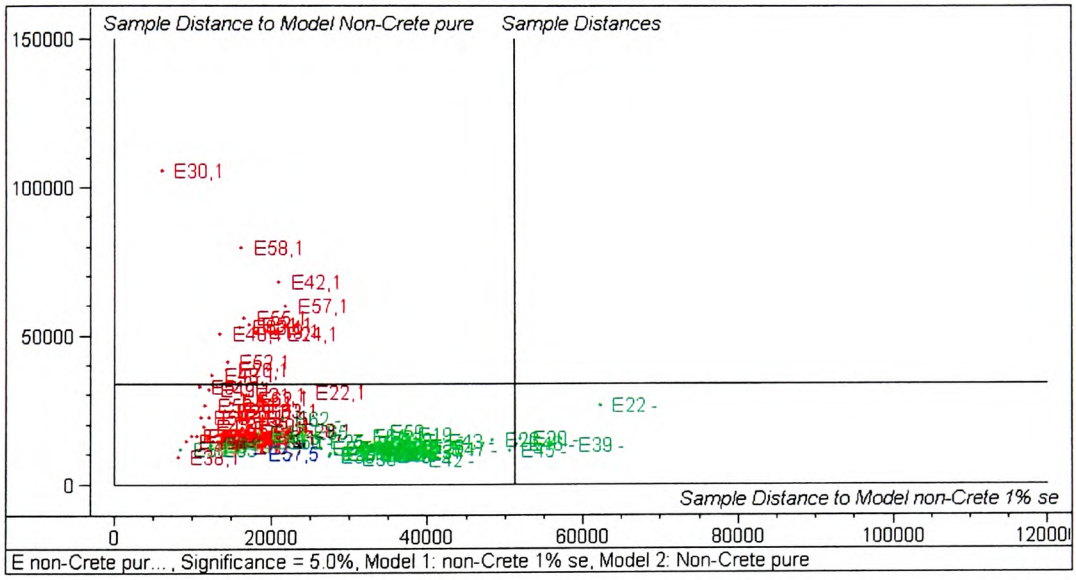

Figure C.19 - ^{1}H NMR Cooman's plot of E non-Crete pure oils (green) v 1% sunflower adulterated oils (red) over selected peaks with a 5% adulterated test sample (blue)

F set

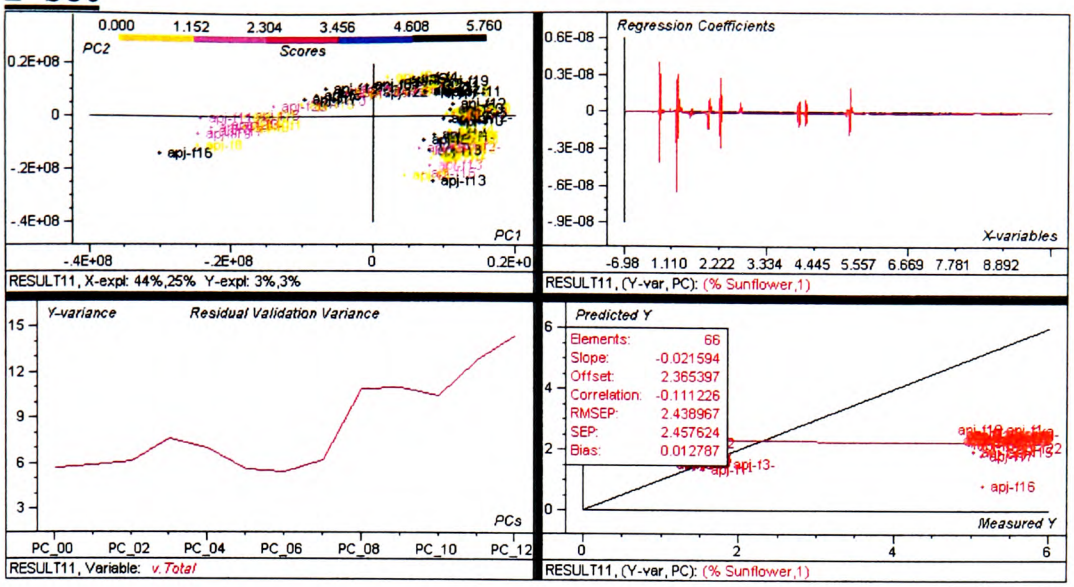

Figure C.20 – F set, Crete oils PLS1 regression plot over all variables

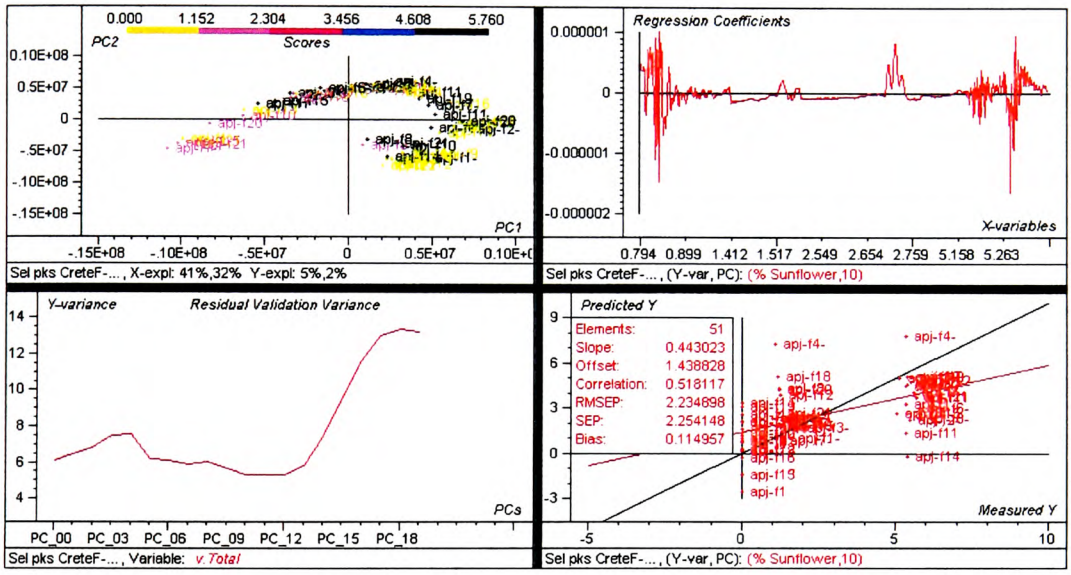

Figure C.21 – F set, Crete oils PLS1 regression plot over selected peaks-outlier

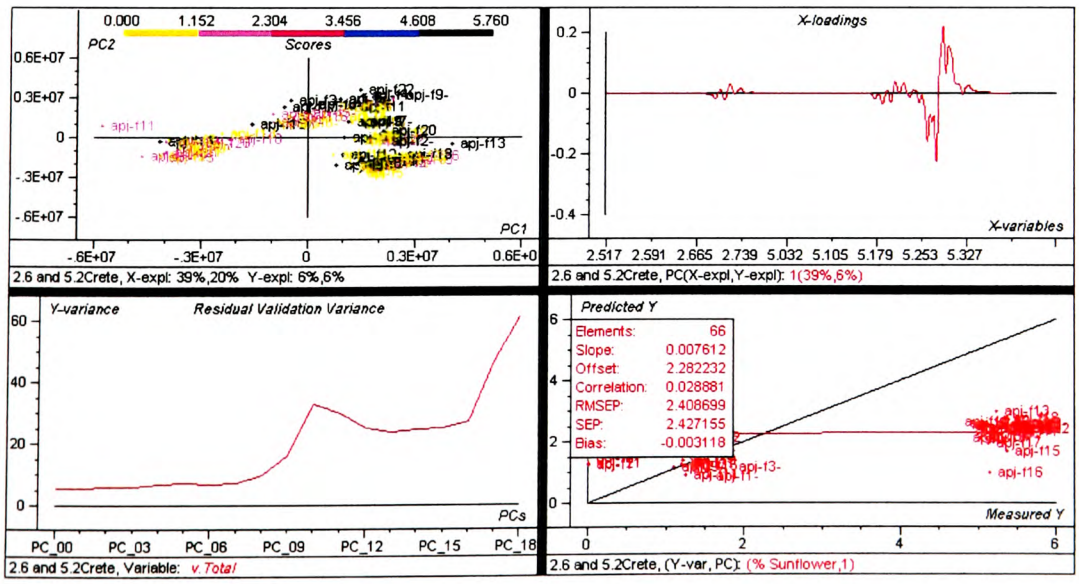

Figure C.22 – F set, Crete oils PLS1 regression plot over variables at 2.6 & 5.2ppm

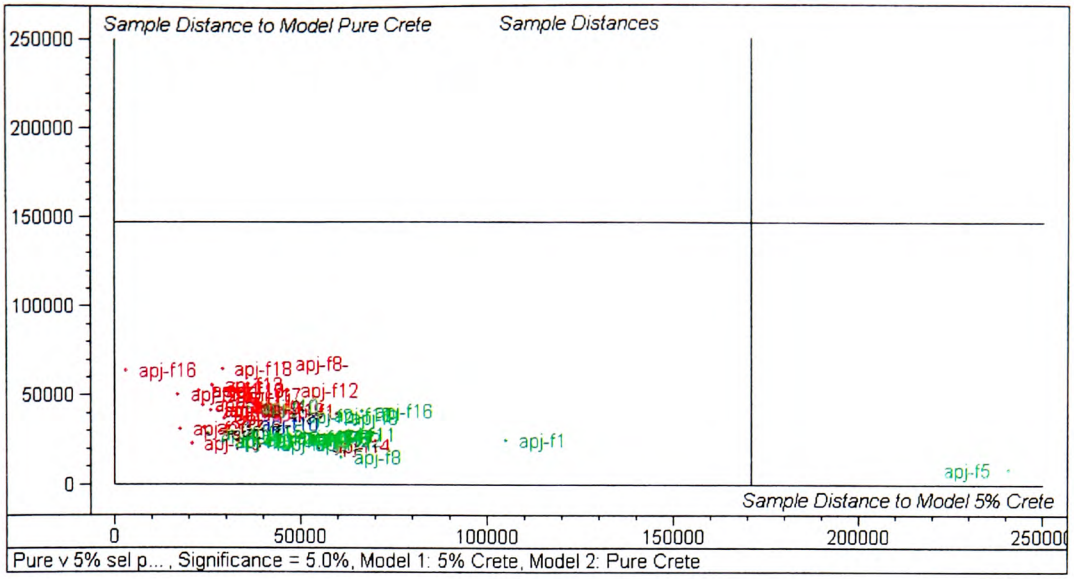

Figure C.23 – ^{1}H NMR Cooman's plot F set Crete pure oils (green) v 5% sunflower adulterated oils (red) with a 10% adulterated test sample (blue)

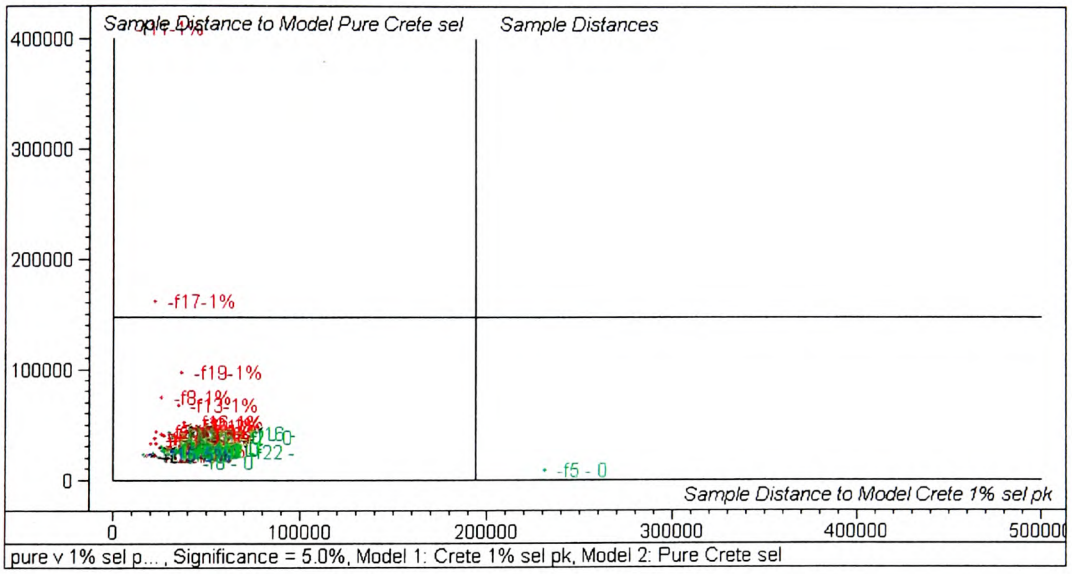

Figure C.24 - ^{1}H NMR Cooman's plot F set Crete pure oils (green) v 1% sunflower adulterated oils (red) over selected peaks with a 5% adulterated test sample (blue)

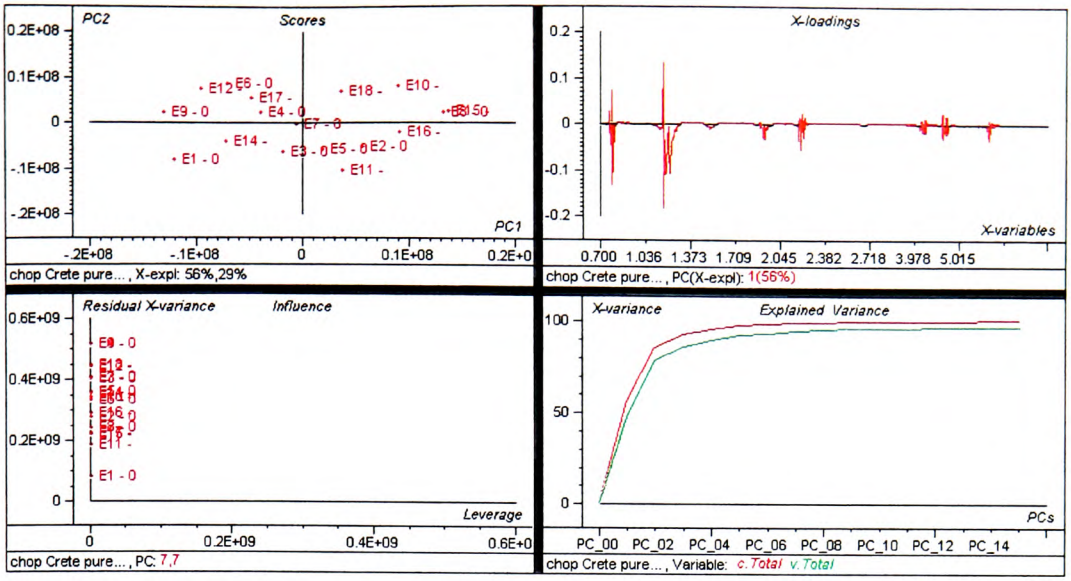

Figure C.25 - PCA overview of E Crete pure oils(-E13) over all variables

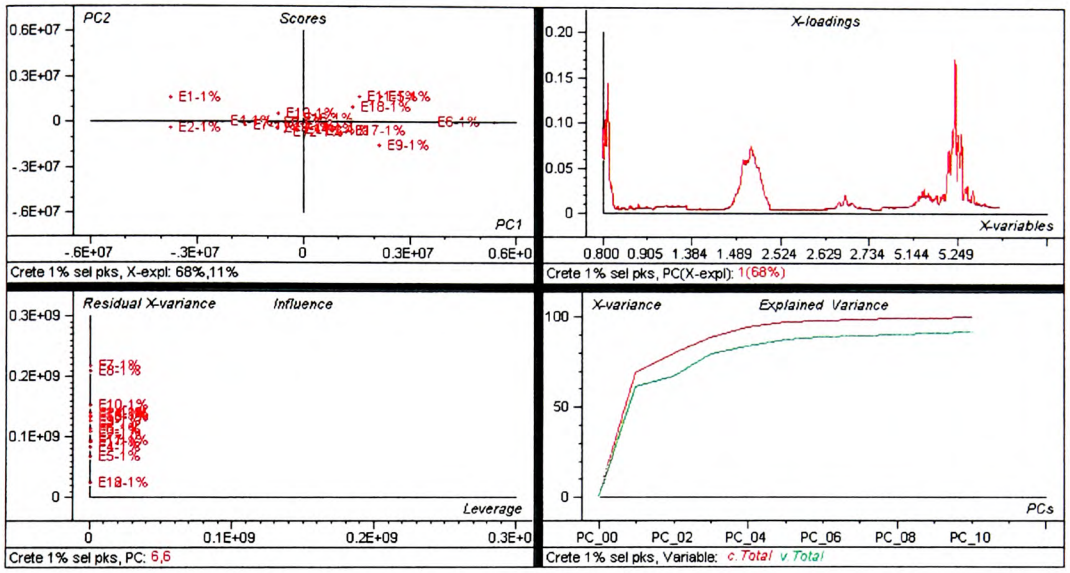

Figure C.26 - PCA overview plot E Crete 1% sunflower adulterated oils over selected peaks

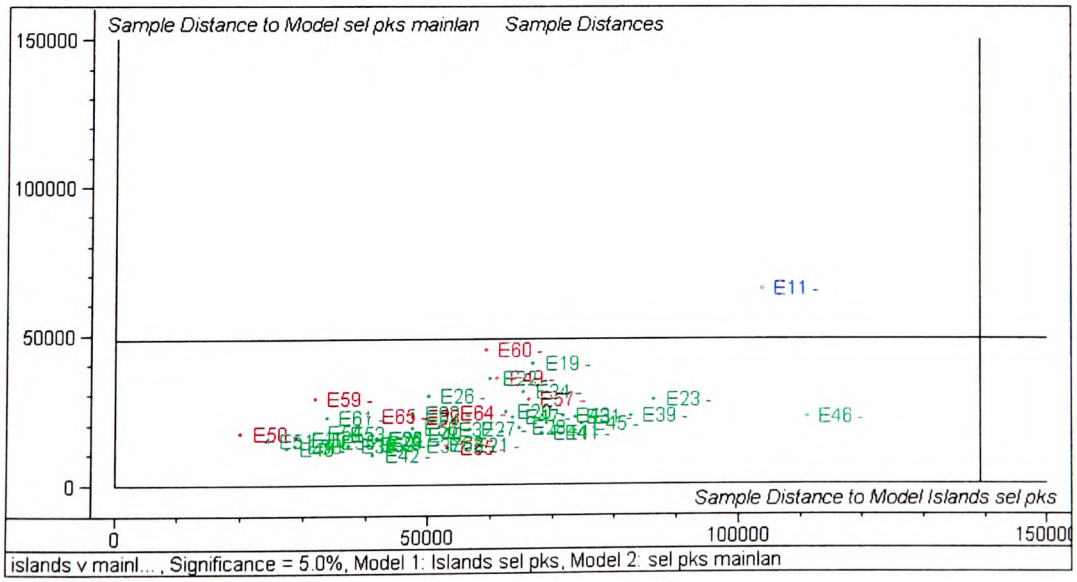

Figure C.27 – Cooman's plot to show separation between E set islands (red) oils (not Crete) v mainland Greece oils (green) with a Crete oil (blue) as a test sample

APPENDIX D

IR

Appendix D – Index of Figures

D SET

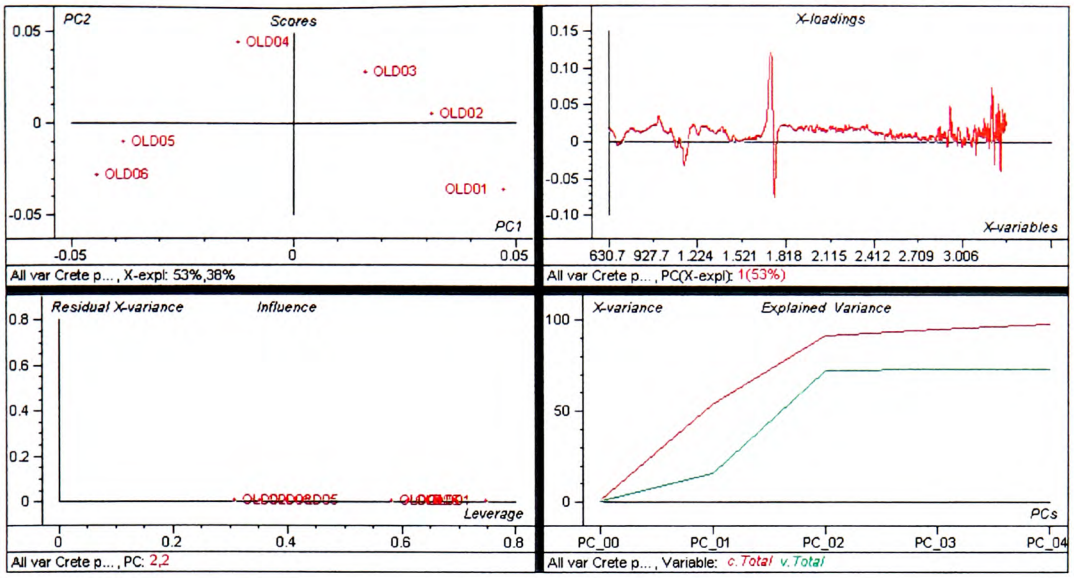

Figure D.1 – PCA overview of D Set Crete pure oils over all variables

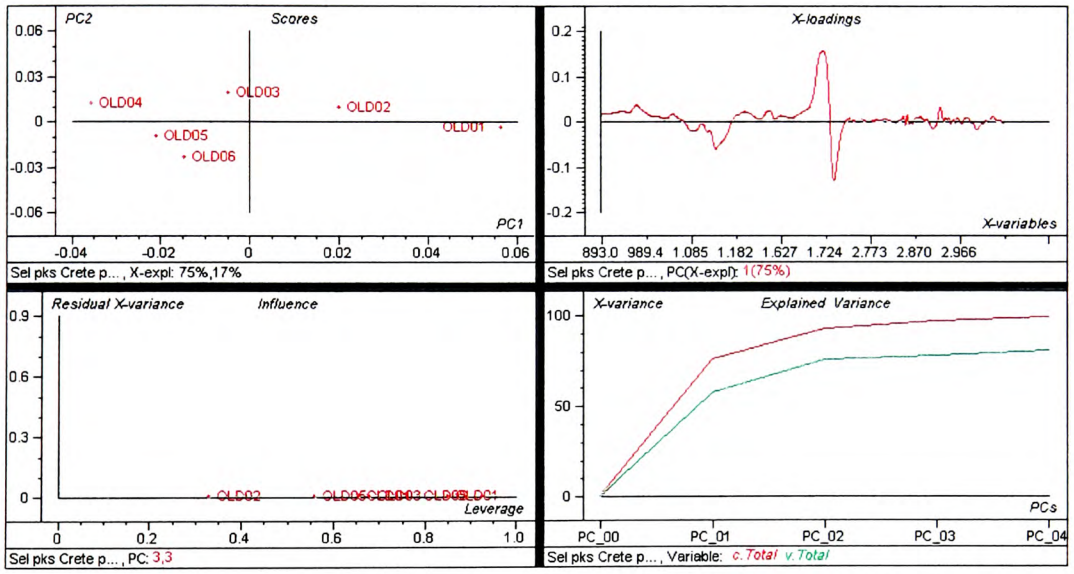

Figure D.2 – PCA overview of D Set Crete pure oils over selected peaks

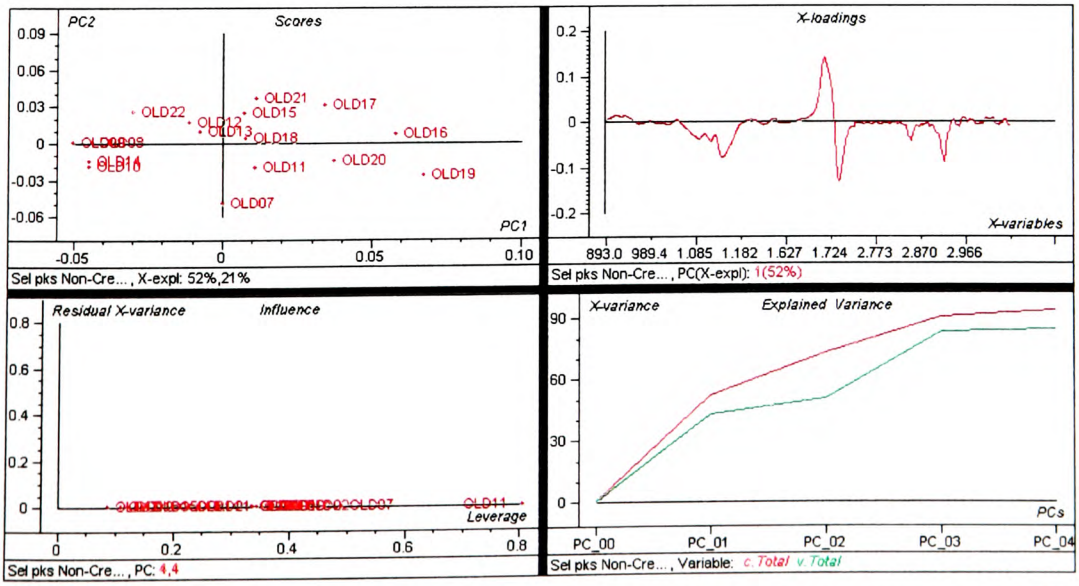

Figure D.3 – PCA overview of D Set non-Crete pure oils over selected peaks

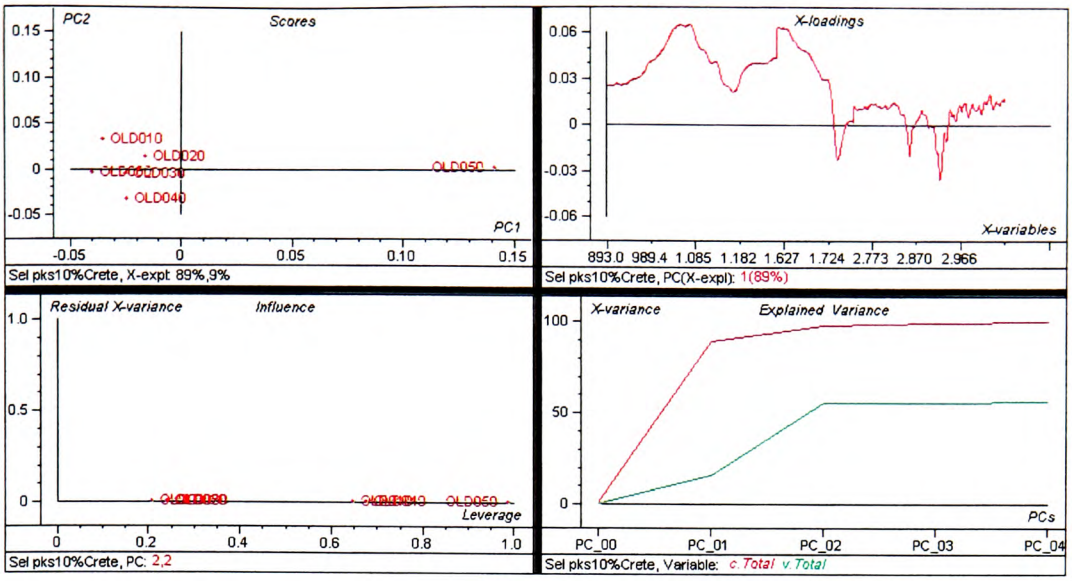

Figure D.4 –PCA overview of D Set Crete oils with 10% sunflower adulteration over selected peaks

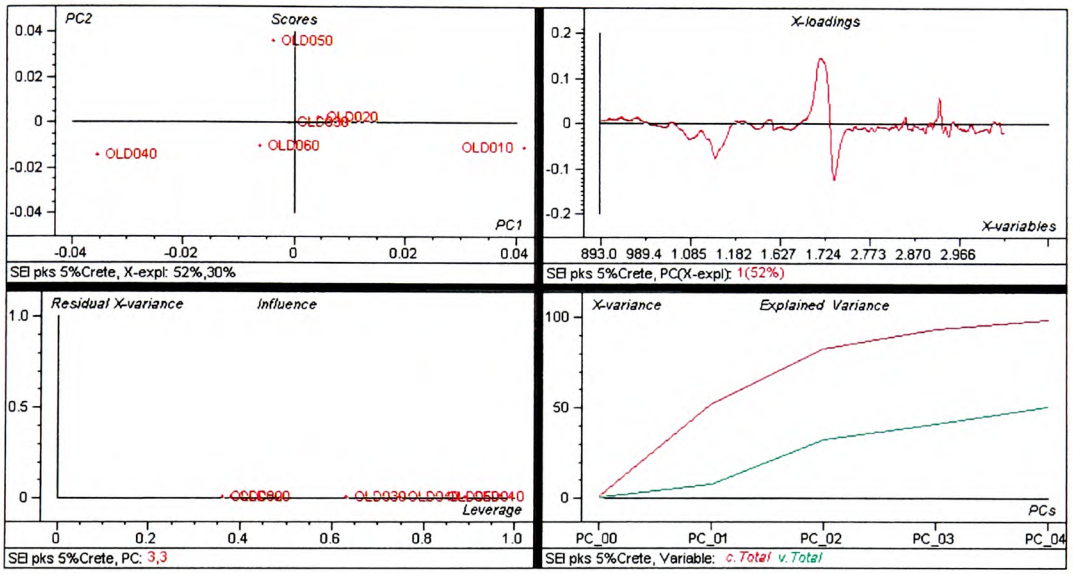

Figure D.5 – PCA overview of D Set Crete oils with 5% sunflower adulteration over selected peaks

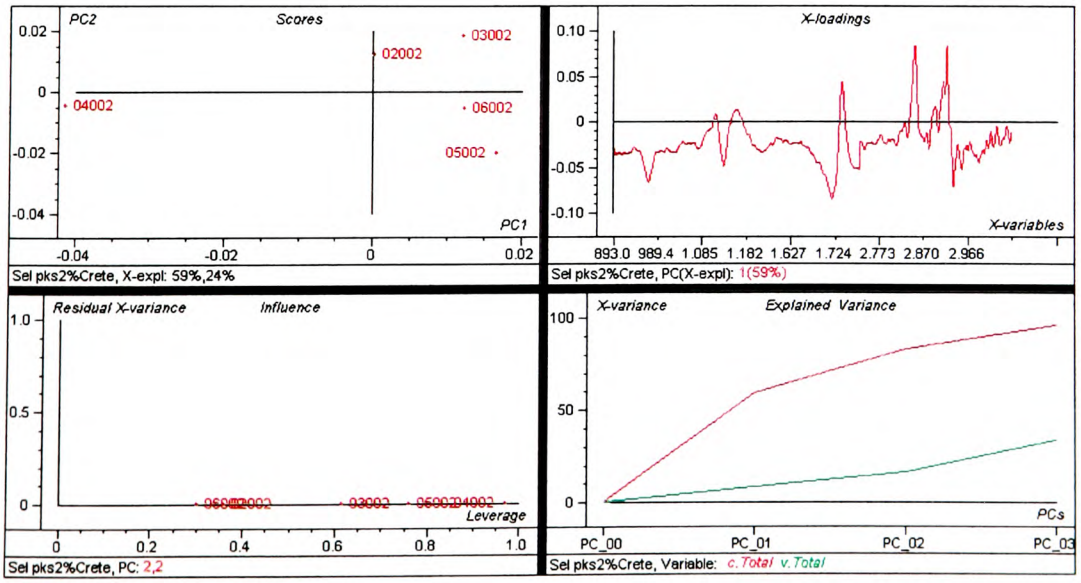

Figure D.6 – PCA overview of D Set Crete oils with 2% sunflower adulteration over selected peaks

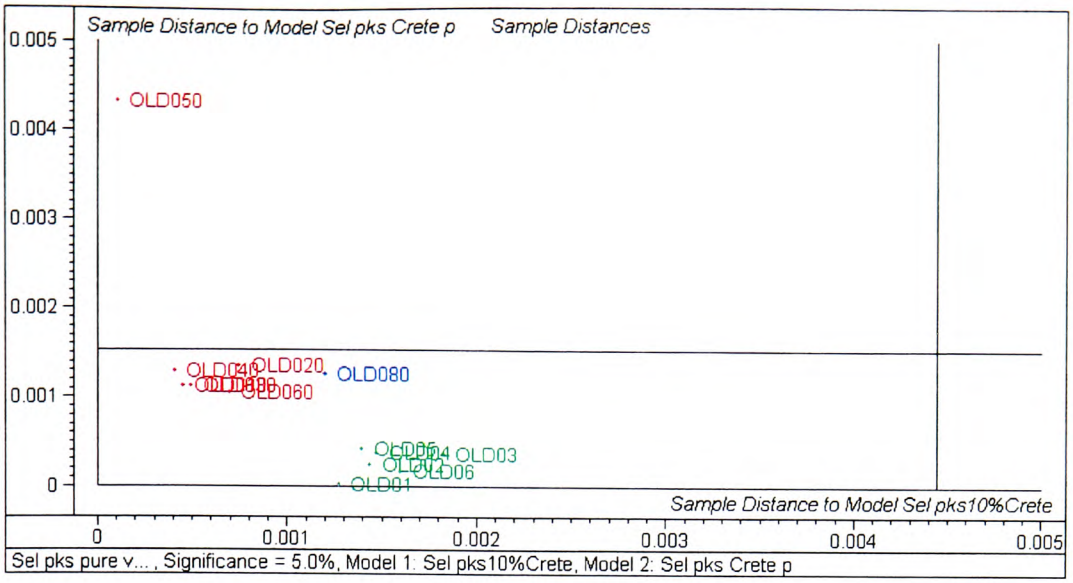

Figure D.7 – Cooman's plot of D Set Crete oils pure (green) v 10% sunflower adulterated (red) oils over selected peaks with a 5% sunflower adulterated test sample (blue)

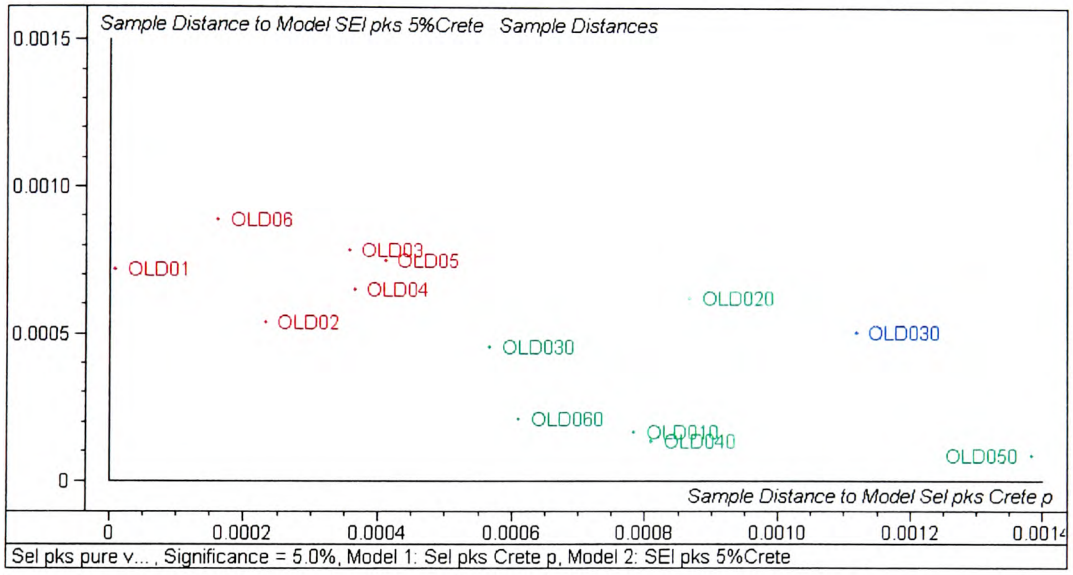

Figure D.8 – Cooman's plot of D Set Crete oils pure (red) v 5% sunflower adulterated oils (green) over selected peaks with a test sample (blue)

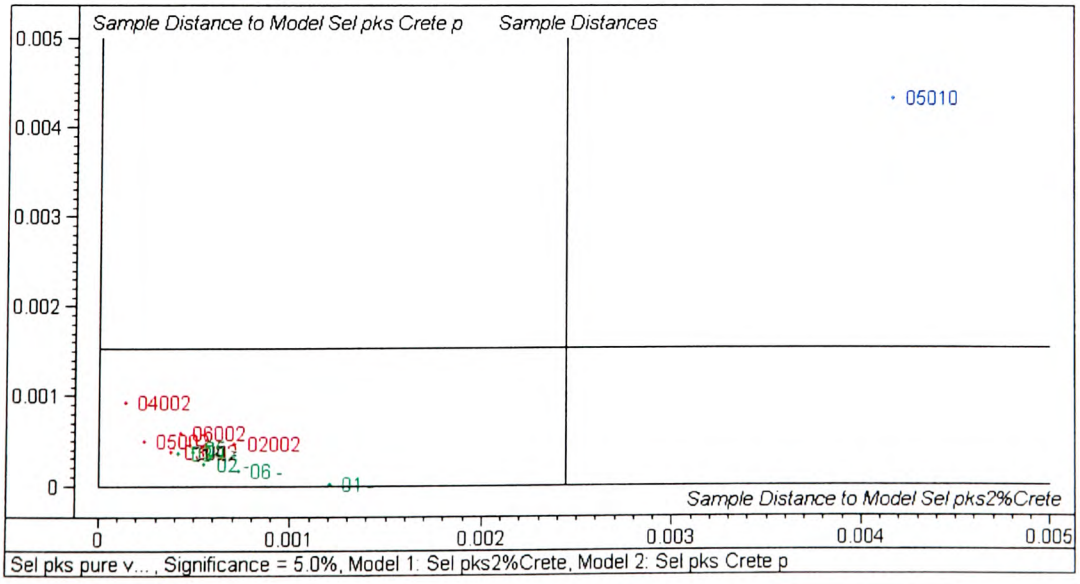

Figure D.9 – Cooman's plot of D Set Crete oils pure (green) v 2% sunflower adulterated oils (red) over selected peaks with a 10% adulterated test sample (blue)

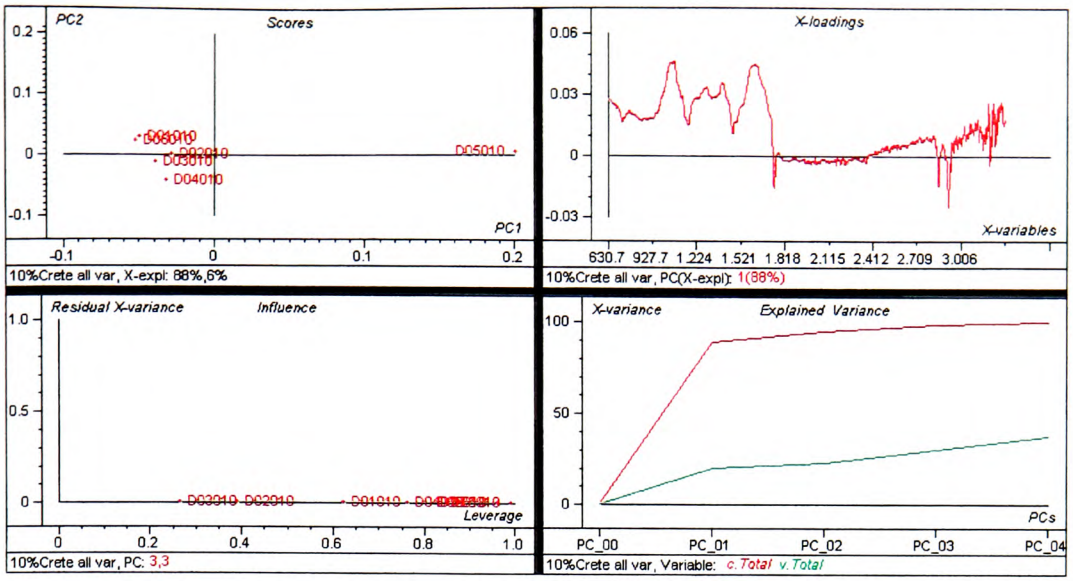

Figure D.10 – PCA overview of D Set Crete oils adulterated with 10% sunflower oil over all variables

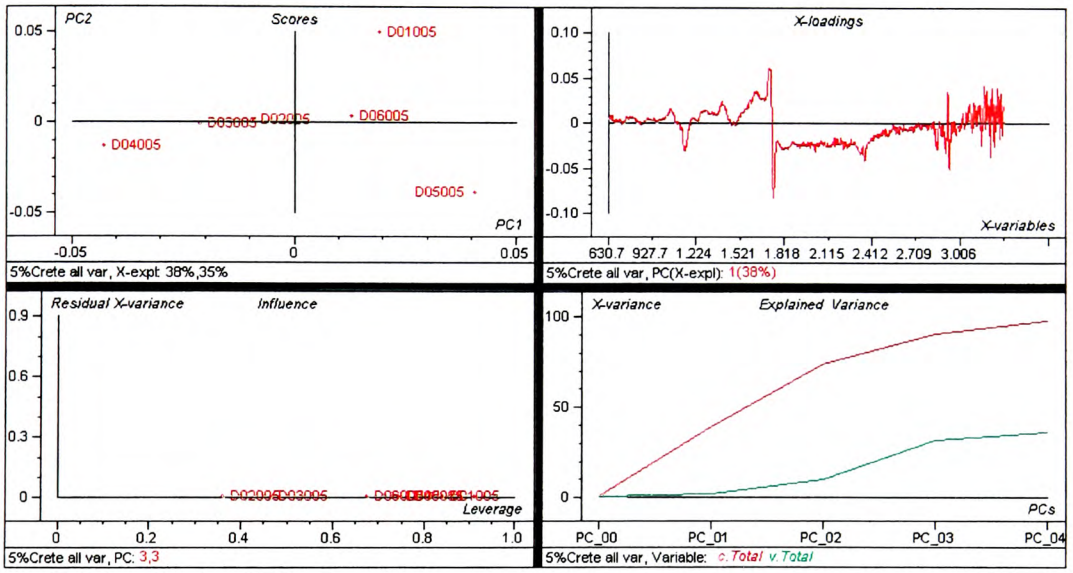

Figure D.11 – PCA overview of D Set Crete oils adulterated with 5% sunflower oil over all variables

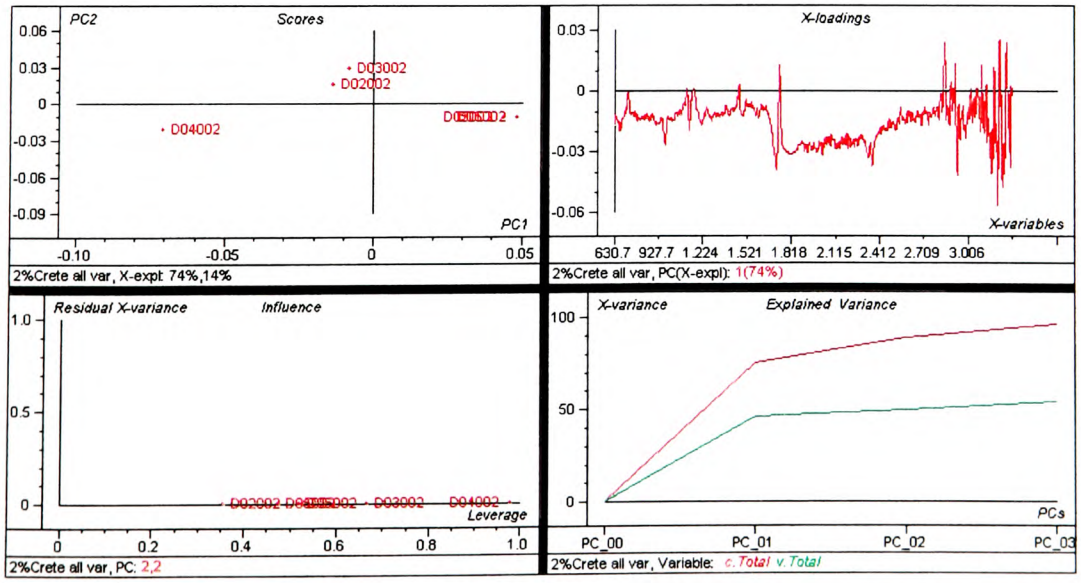

Figure D.12 - PCA overview of D Set Crete oils adulterated with 2% sunflower oil over all variables

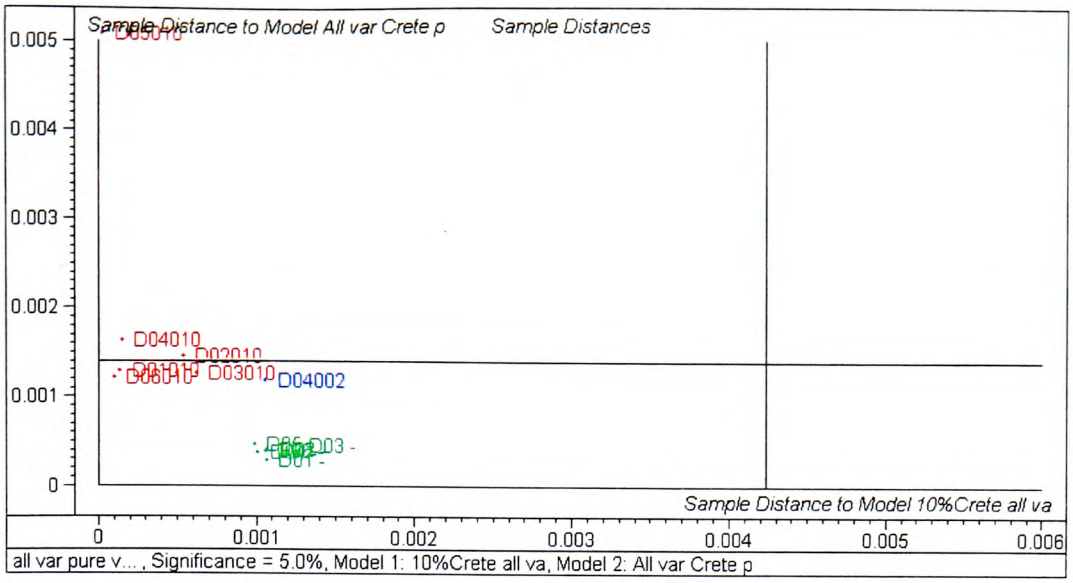

Figure D.13 – Cooman's plot of D Set Crete oils pure (green) v 10% sunflower adulterated oils (red) over all variables with a 2% adulterated test sample (blue)

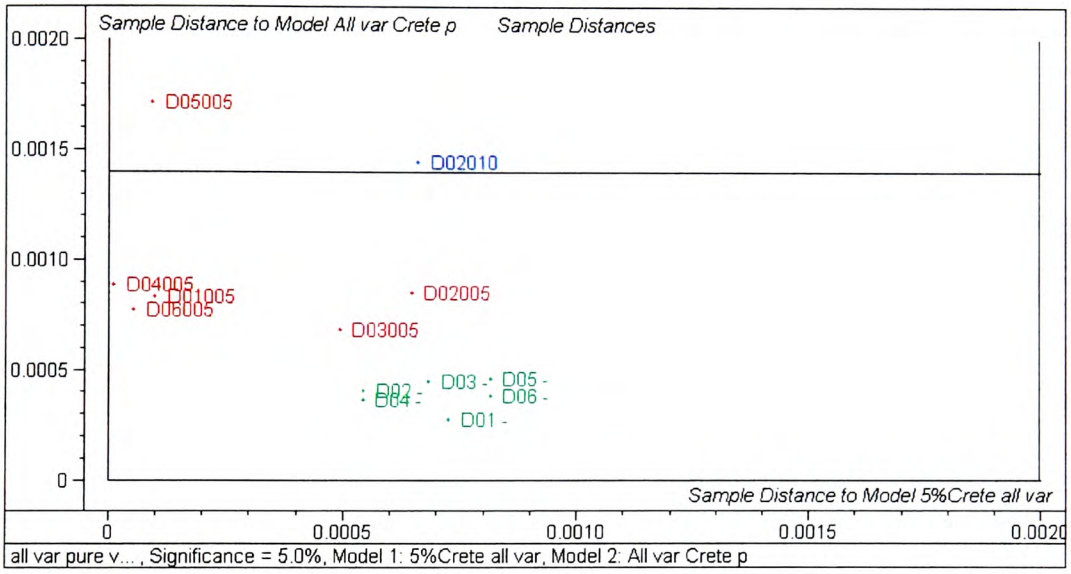

Figure D.14 - Cooman's plot of D Set Crete oils pure (green) v 5% sunflower adulterated oils (red) over all variables with a 10% adulterated test sample (blue)

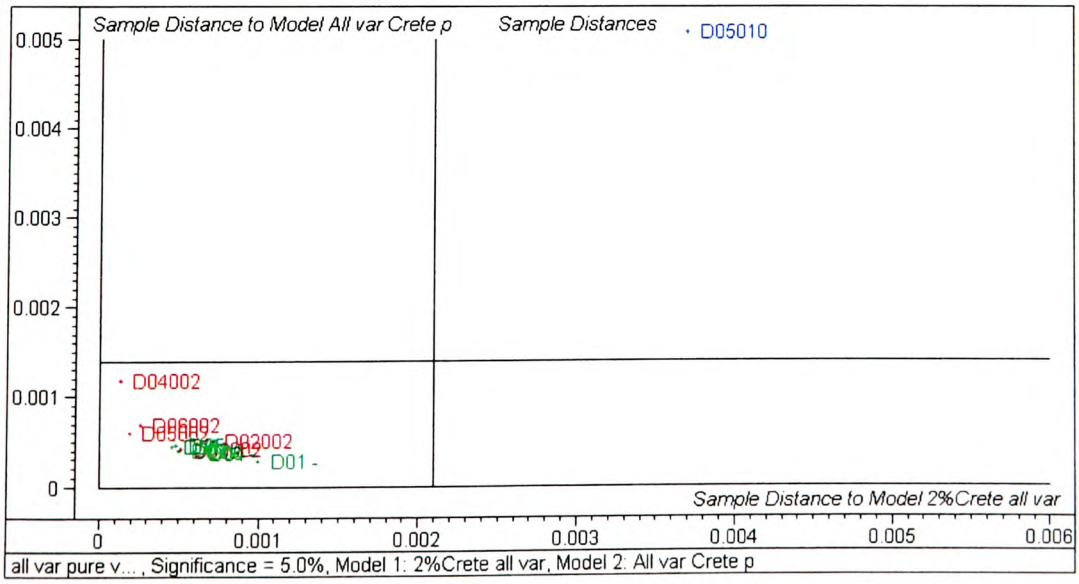

Figure D.15 - Cooman's plot of D Set Crete oils pure (green) v 2% sunflower adulterated oils (red) over all variables with a 10% adulterated test sample (blue)

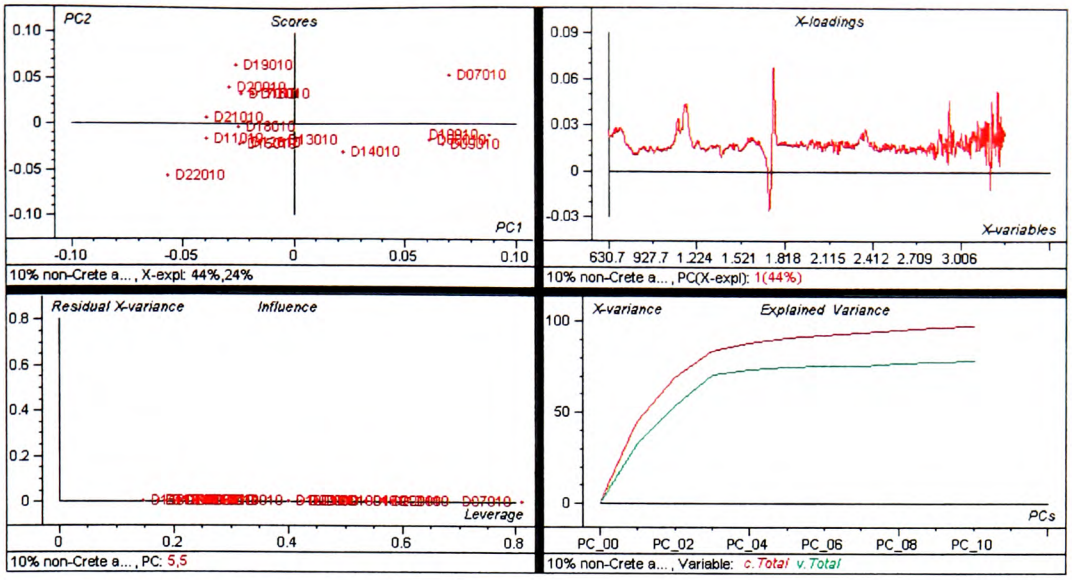

Figure D.16 – PCA overview of D Set non-Crete oils adulterated with 10% sunflower oil over all variables

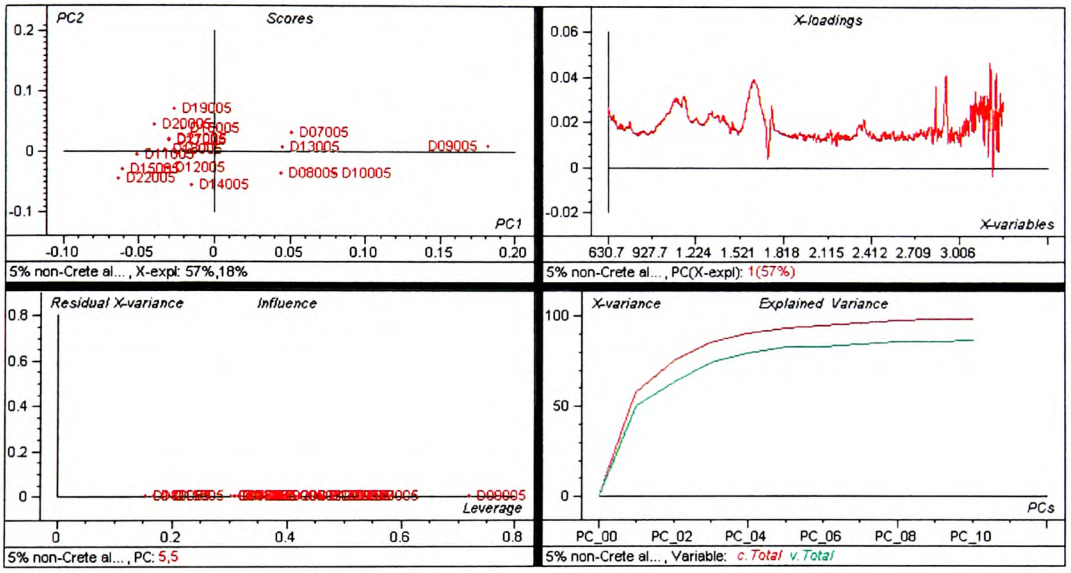

Figure D.17 – PCA overview of D Set non-Crete oils adulterated with 5% sunflower oil over all variables

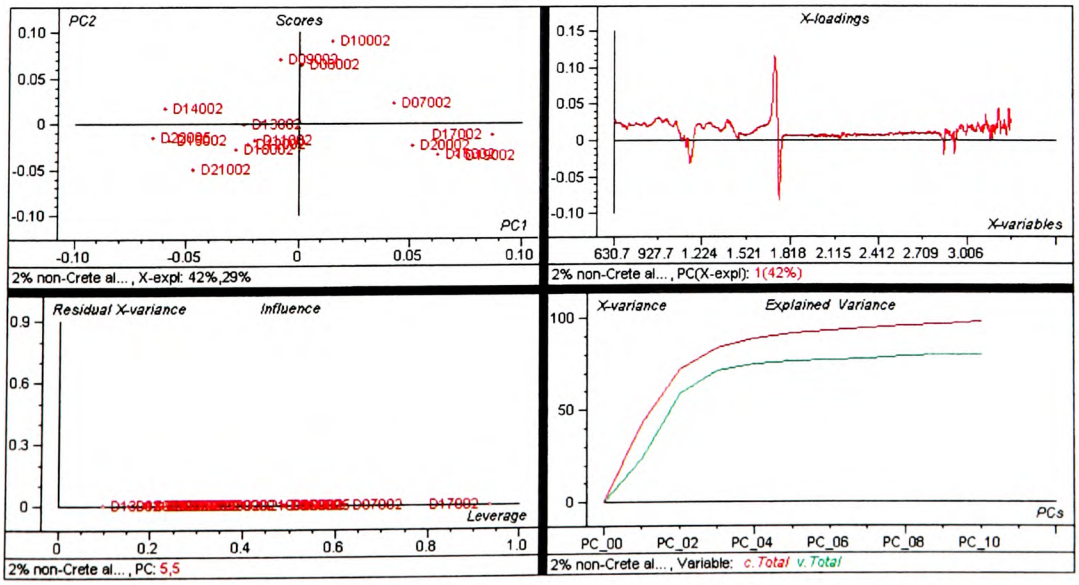

Figure D.18 – PCA overview of D Set non-Crete oils adulterated with 2% sunflower oil over all variables

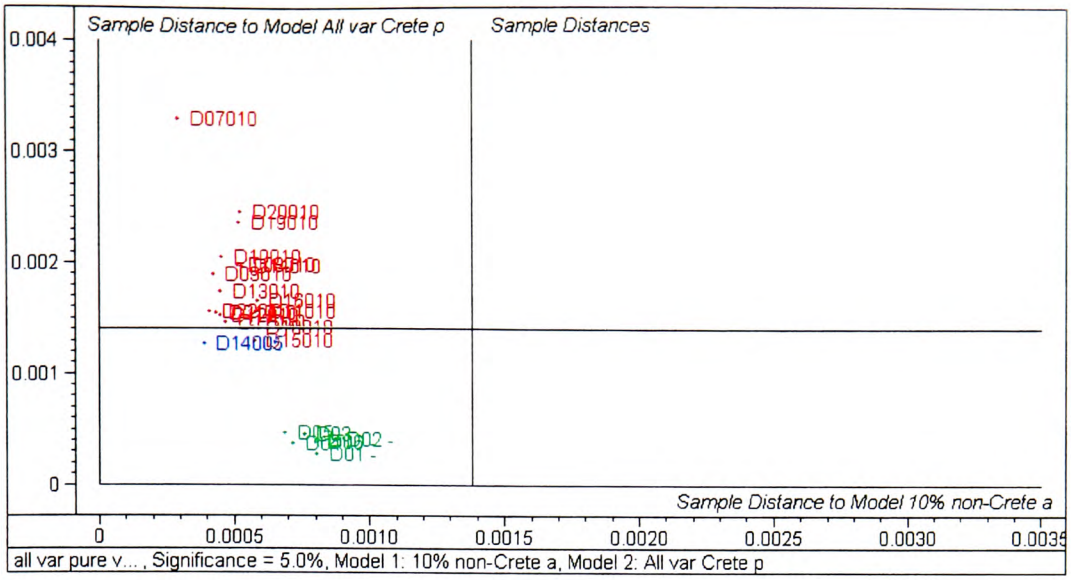

Figure D.19 – Cooman's plot of D Set non-Crete oils pure (green) v 10% sunflower adulterated oils over all variables with a 5% adulterated test sample (blue)

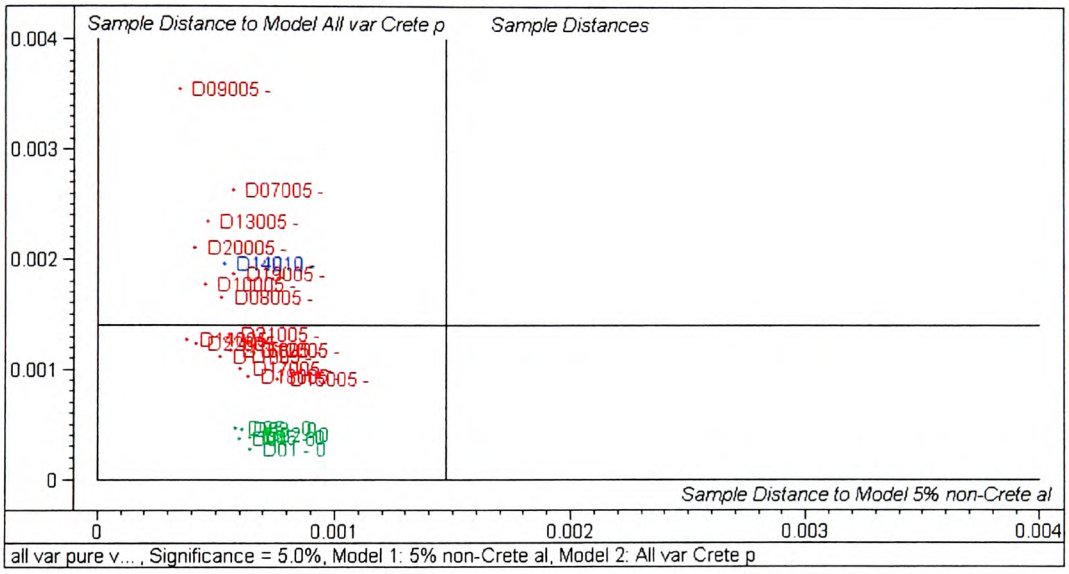

Figure D.20 – Cooman's plot of D Set non-Crete oils pure (green) v 5% sunflower adulterated oils over all variables with a 10% adulterated test sample (blue)

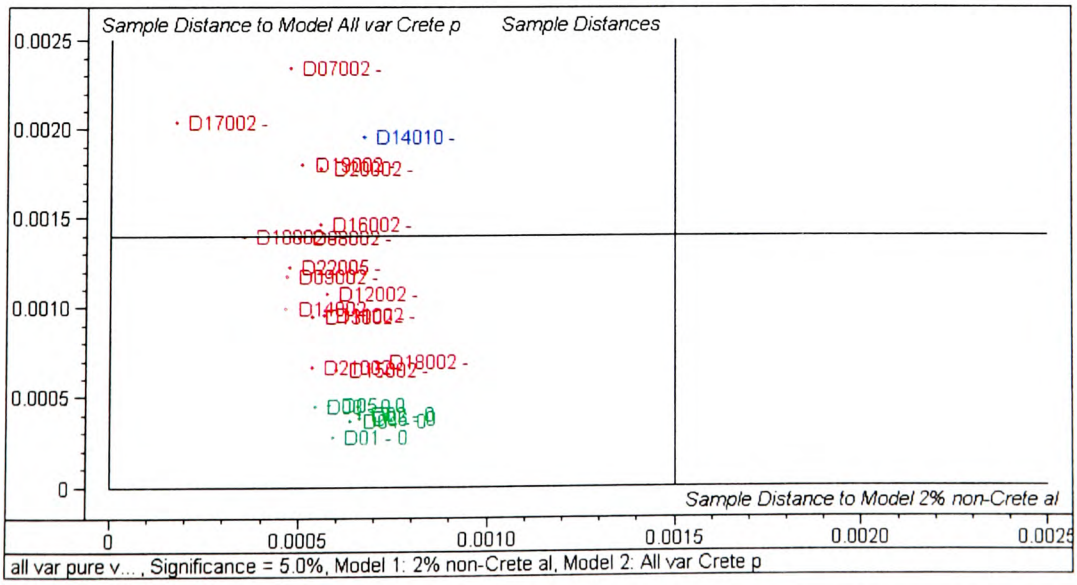

Figure D.21 – Cooman's plot of D Set non-Crete pure oils (green) v 2% sunflower adulterated oils (red) over all variables with a 10% adulterated test sample (blue)

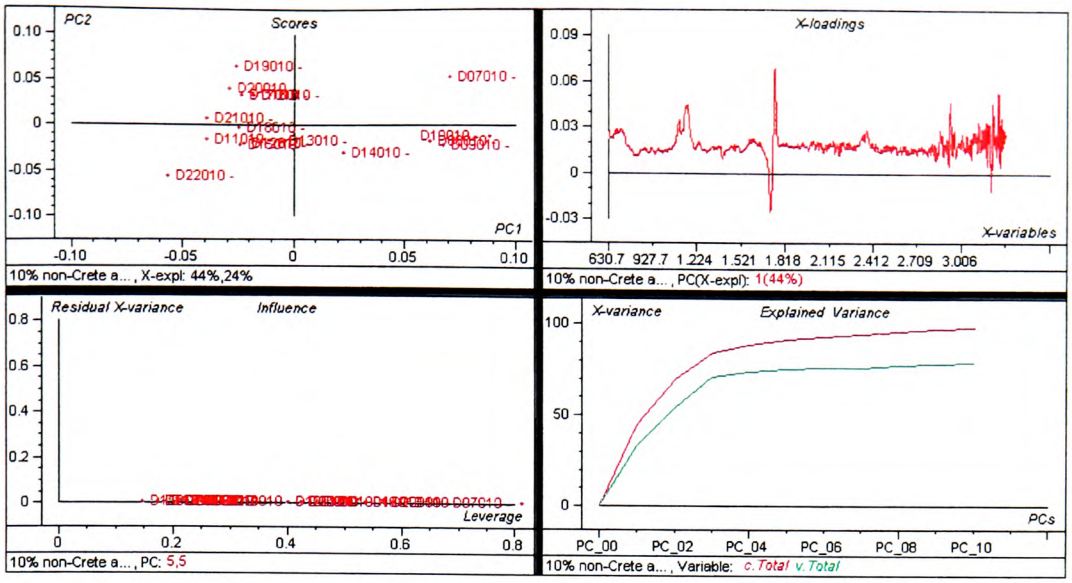

Figure D.22 – PCA overview of D Set non-Crete oils adulterated with 10% sunflower oil over selected peaks

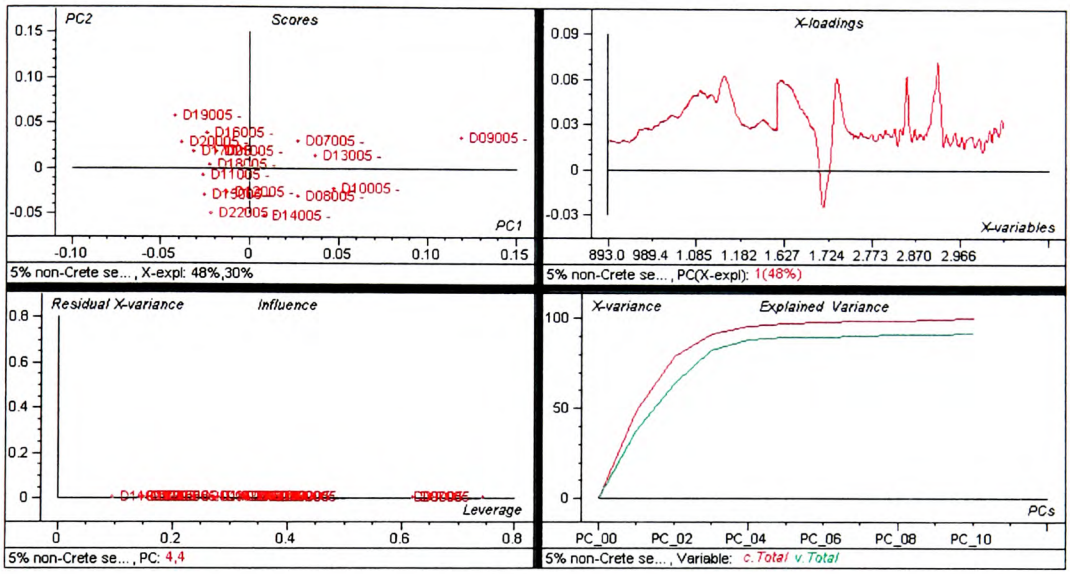

Figure D.23 - PCA overview of D Set non-Crete oils adulterated with 5% sunflower oil over selected peaks

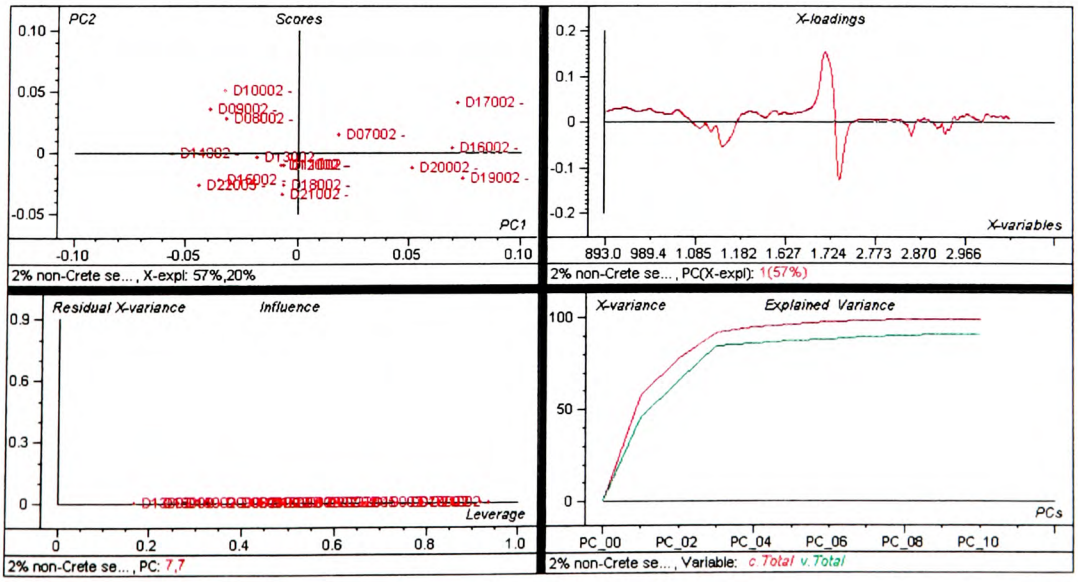

Figure D.24 - PCA overview of D Set non-Crete oils adulterated with 2% sunflower oil over selected peaks

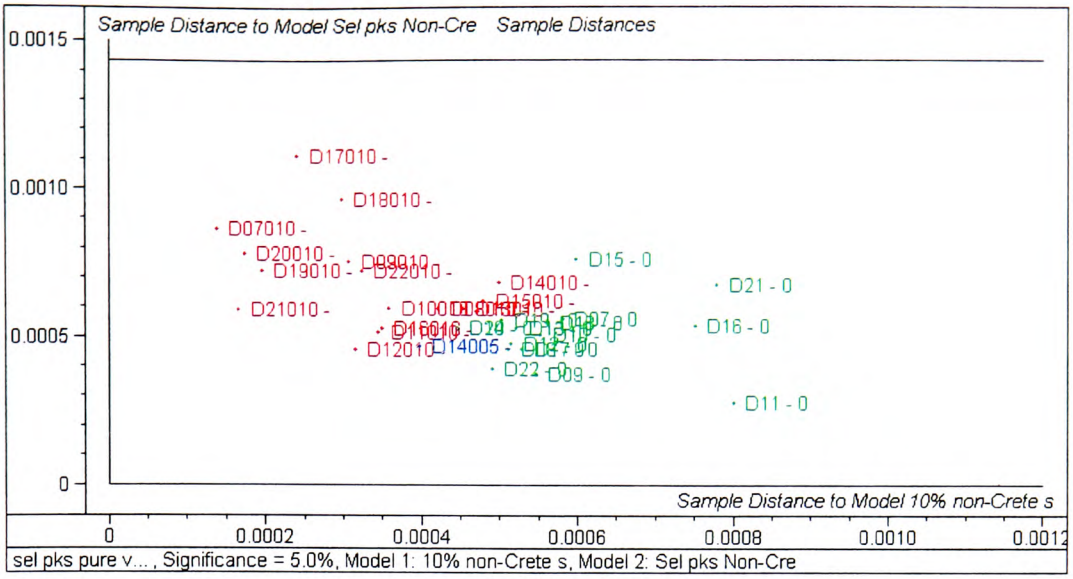

Figure D.25 – Cooman's plot of D Set non-Crete oils pure (green) v 10% (red) over selected peaks with a 5% adulterated test sample (blue)

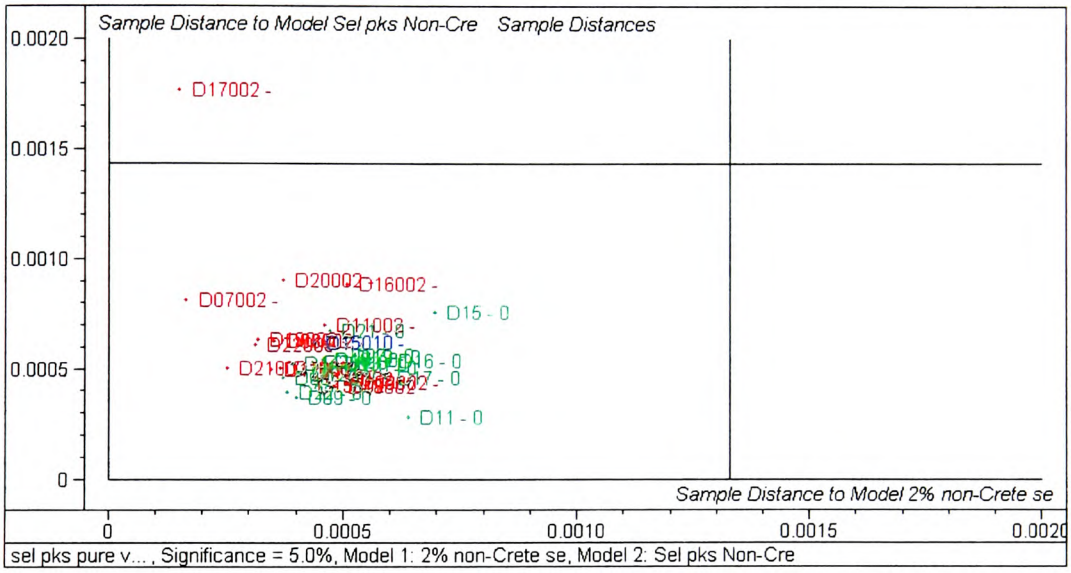

Figure D.26 - Cooman's plot of D Set non-Crete oils pure (green) v 2% (red) over selected peaks with a 10% adulterated test sample (blue)

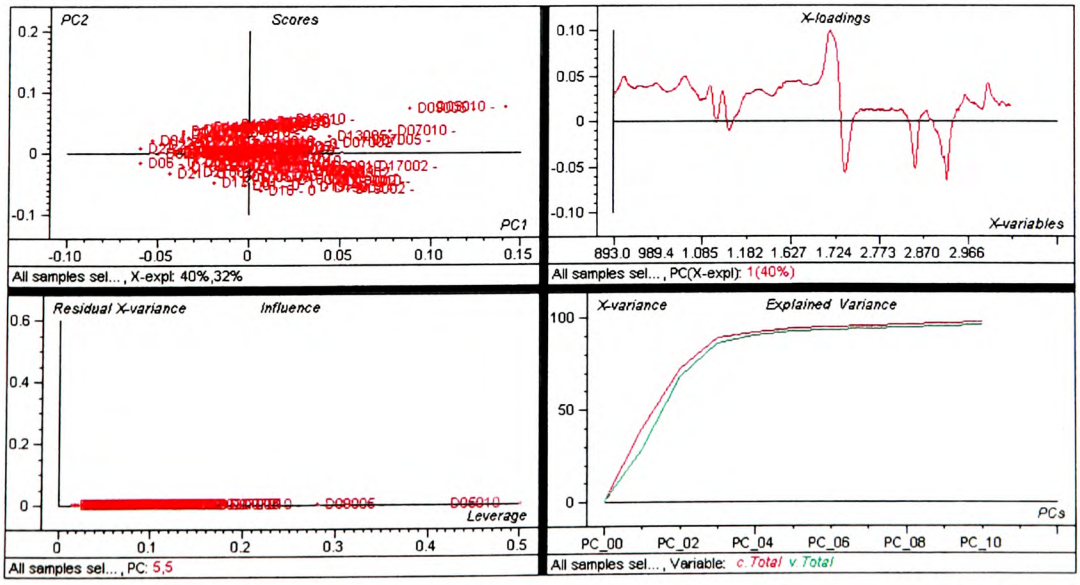

Figure D.27 – PCA overview of all samples in the D set over selected peaks

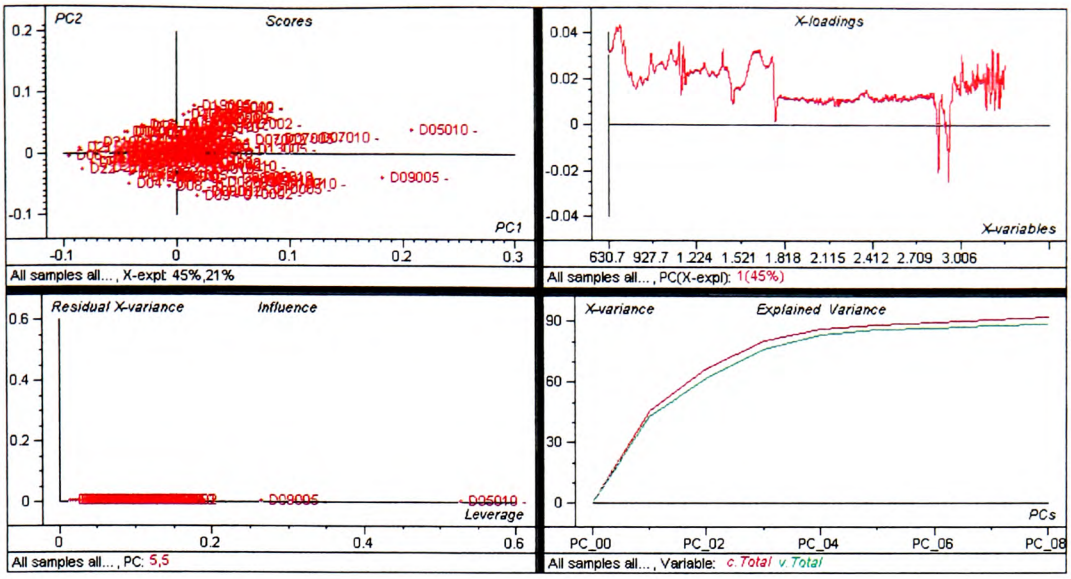

Figure D.28 – PCA overview of all samples in the D set over all variables

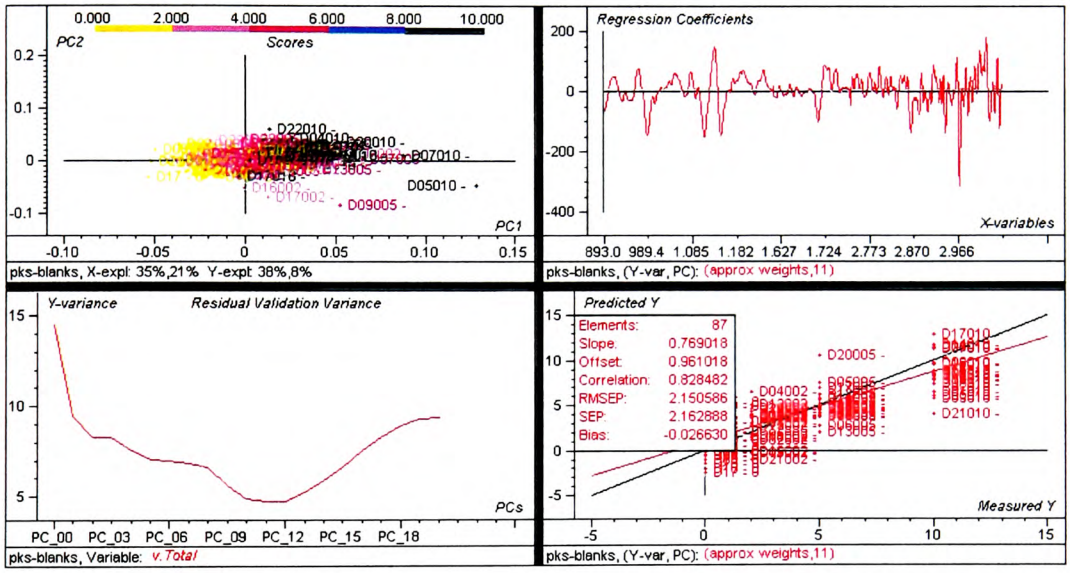

Figure D.29 – PLS1 regression overview of all D set samples over selected peaks using 11 PCs

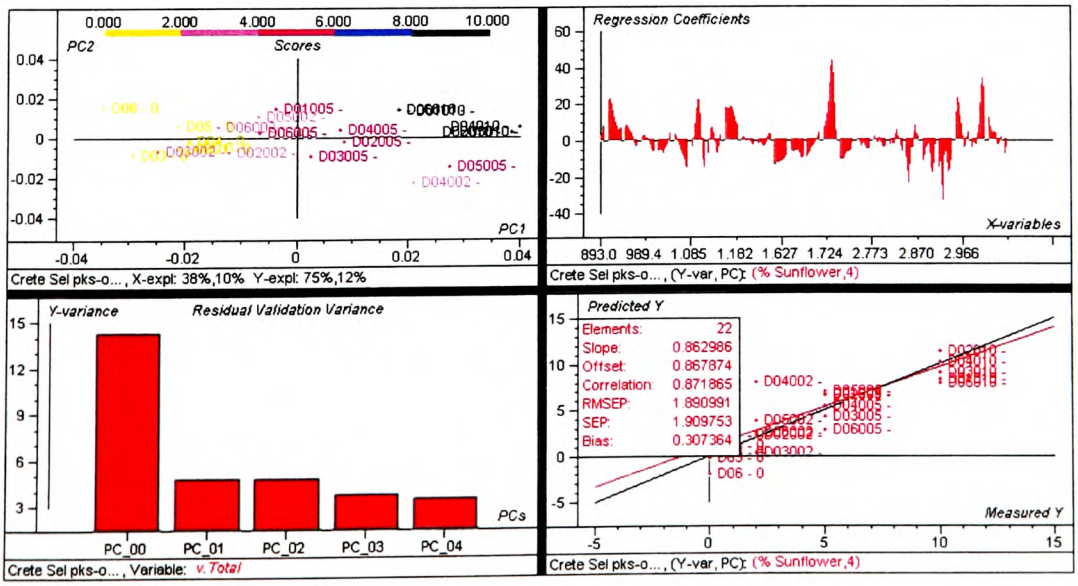

Figure D.30 – PLS1 regression overview of Crete D set oils over selected peaks-outliers using 4 PCs

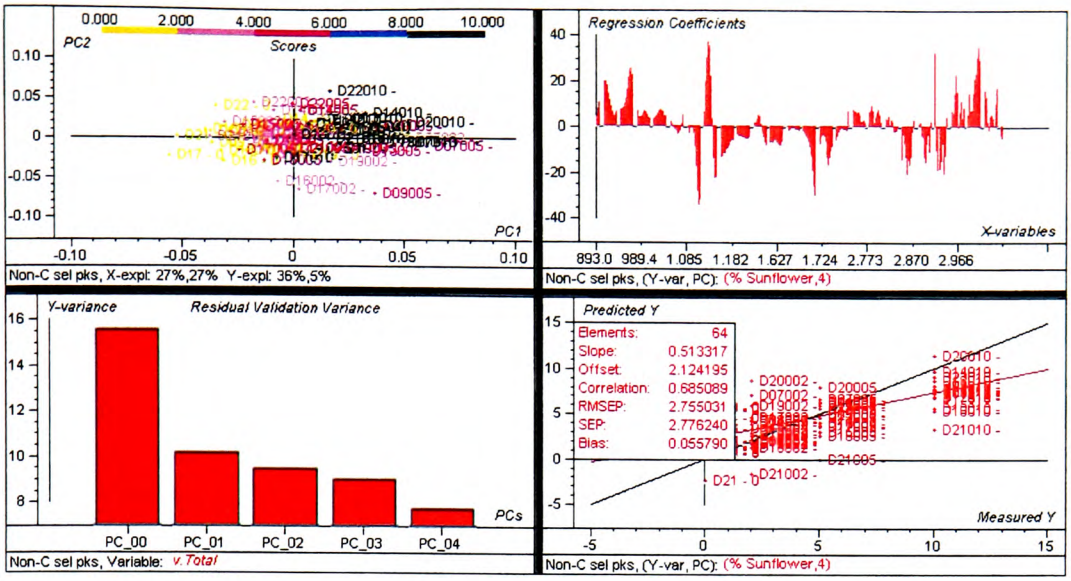

Figure D.31 - PLS1 regression overview of non-Crete D set oils over selected peaks-outliers using 4 PCs

E SET

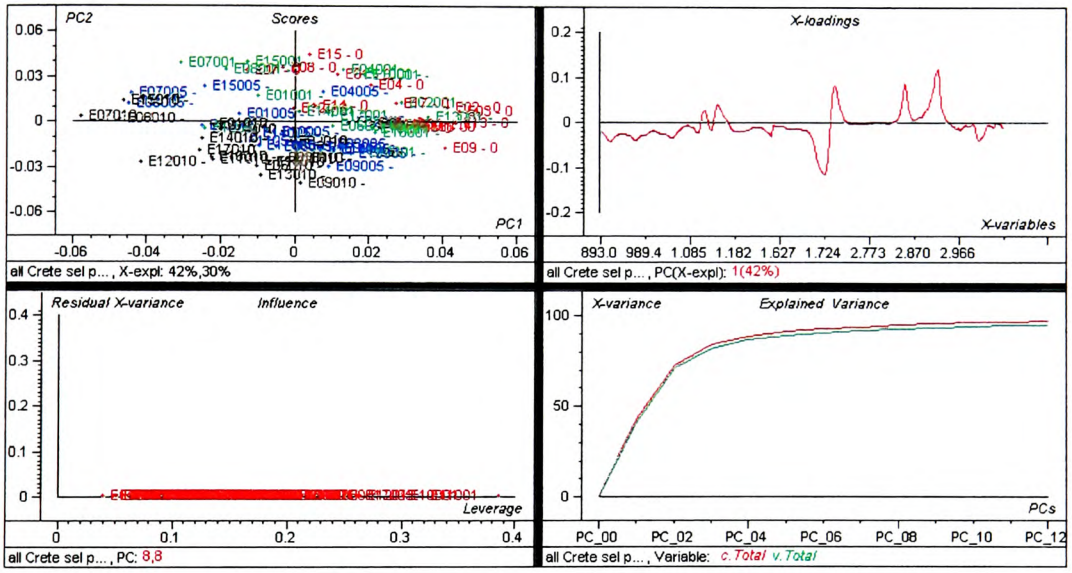

Figure D.32 - PCA overview of E set Crete samples over selected peaks

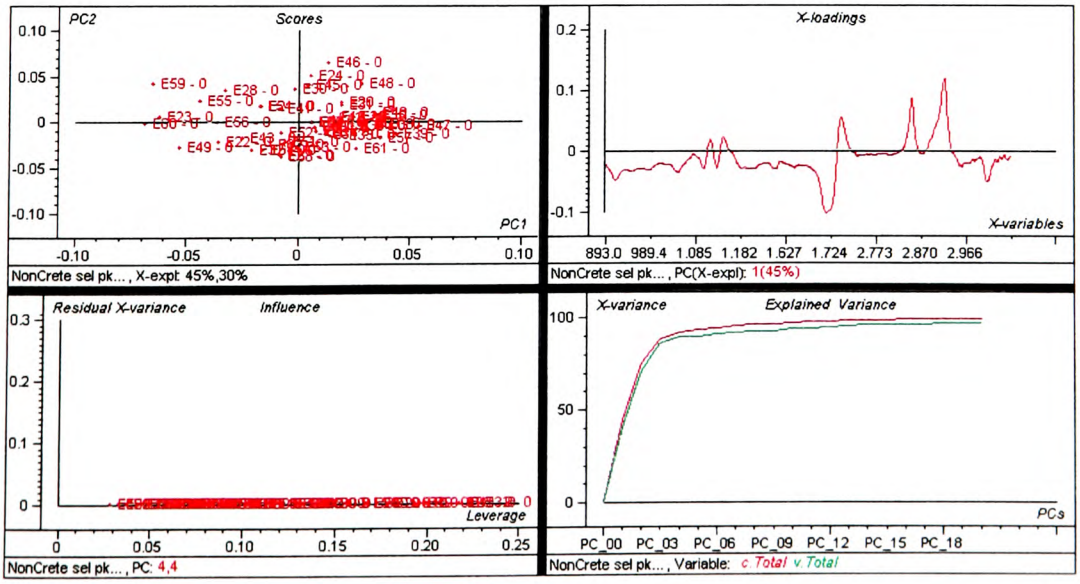

Figure D.33 - PCA overview of E set non-Crete samples over selected peaks

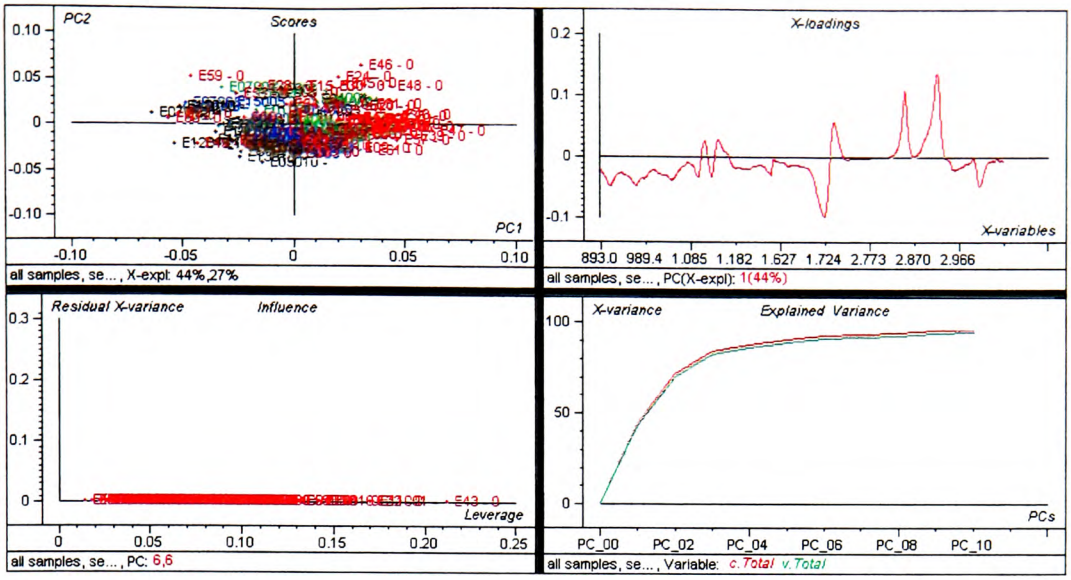

Figure D.34 - PCA overview of all E set samples-outliers over selected peaks

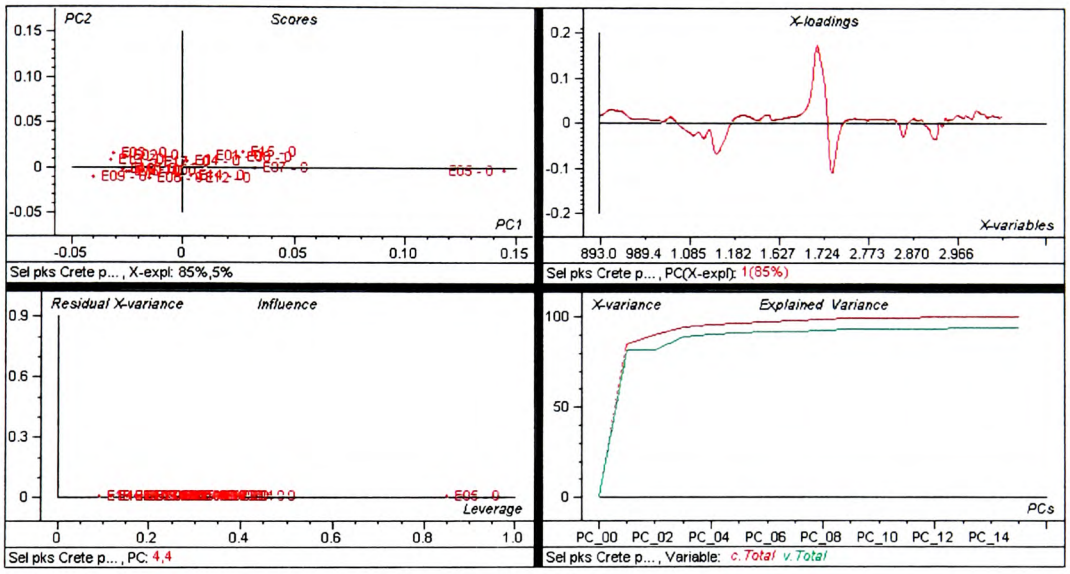

Figure D.35 - PCA overview of E set Crete pure oils over selected peaks

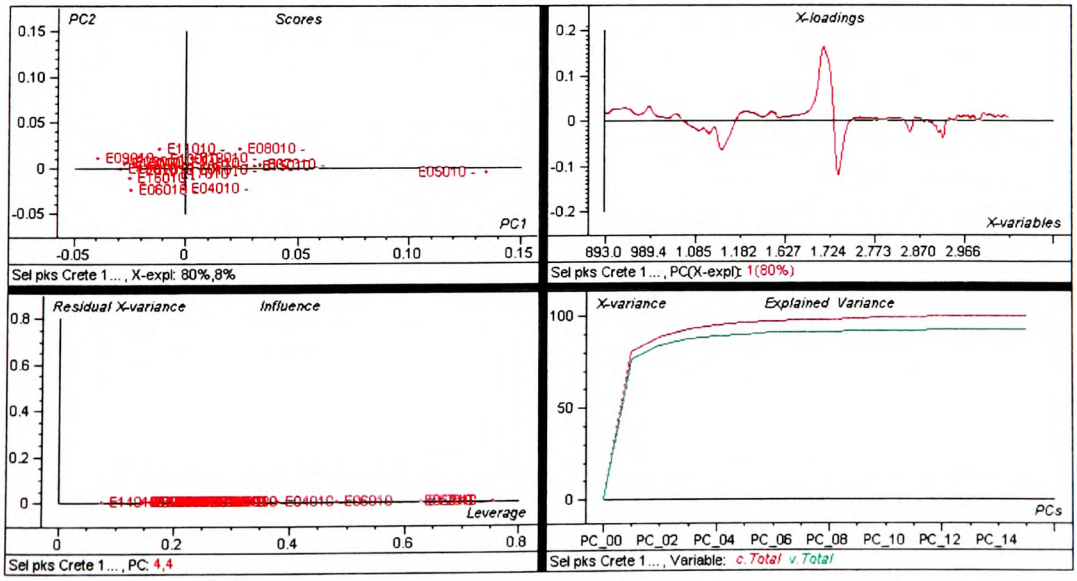

Figure D.36 – PCA overview of E set Crete oils adulterated with 10% sunflower oil over selected peaks

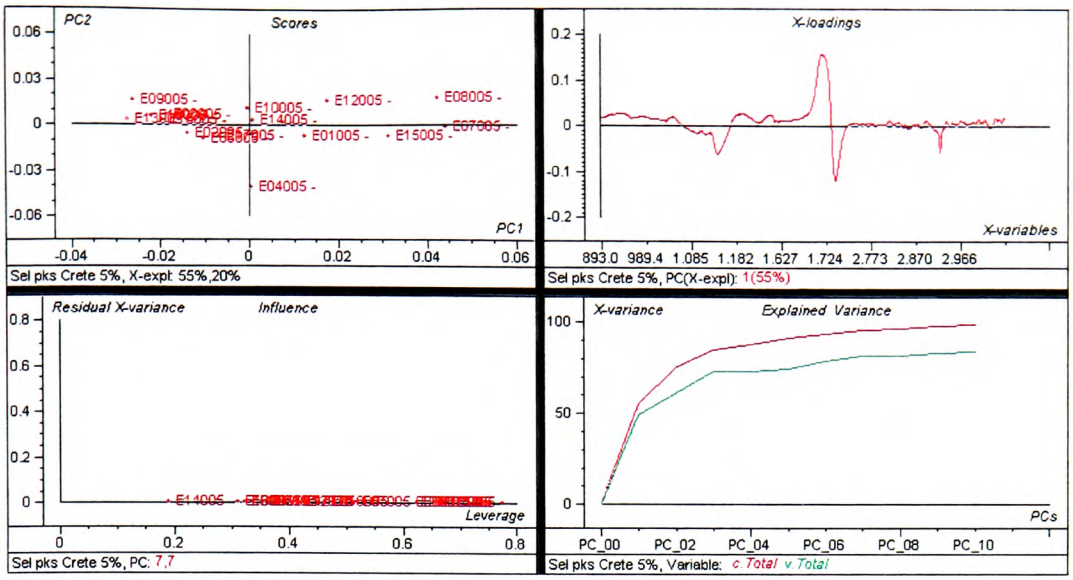

Figure D.37 - PCA overview of E set Crete oils adulterated with 5% sunflower oil over selected peaks

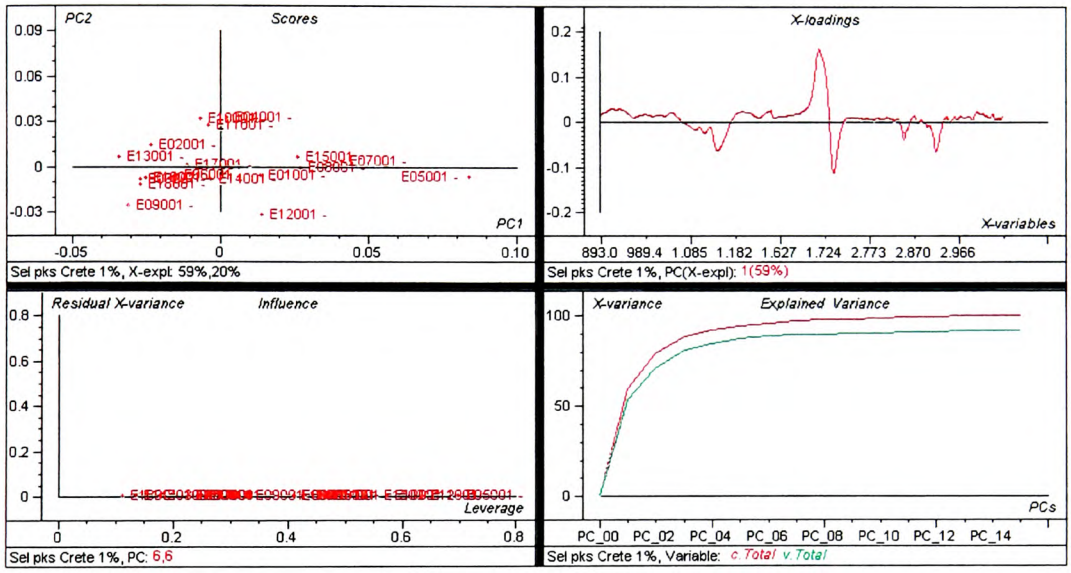

Figure D.38 - PCA overview of E set Crete oils adulterated with 1% sunflower oil over selected peaks

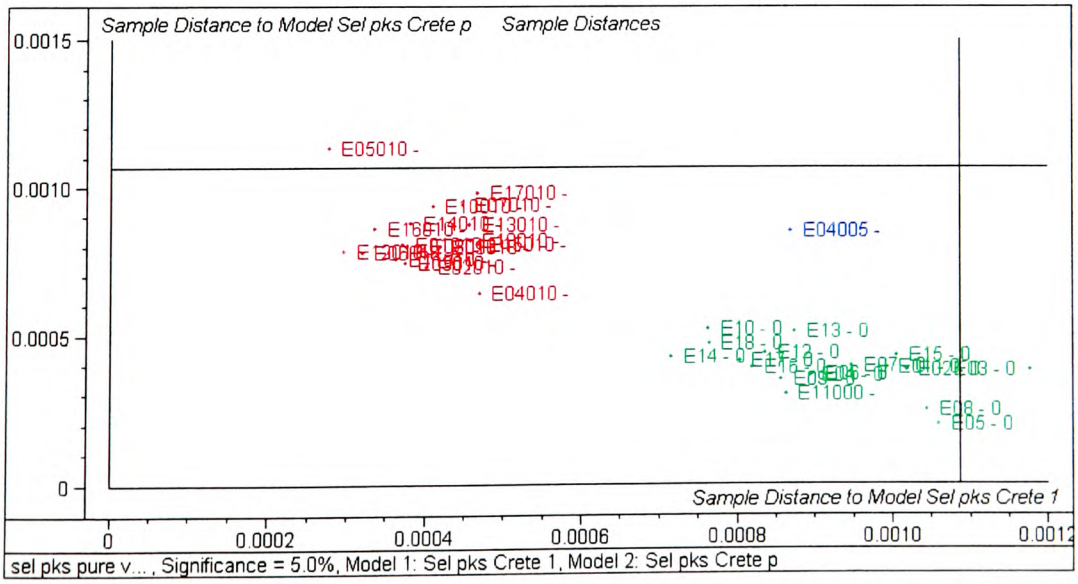

Figure D.39 – Cooman's plot of E set Crete pure oils (green) v 10% sunflower adulterated oils (red) over selected peaks with a 5% adulterated test sample

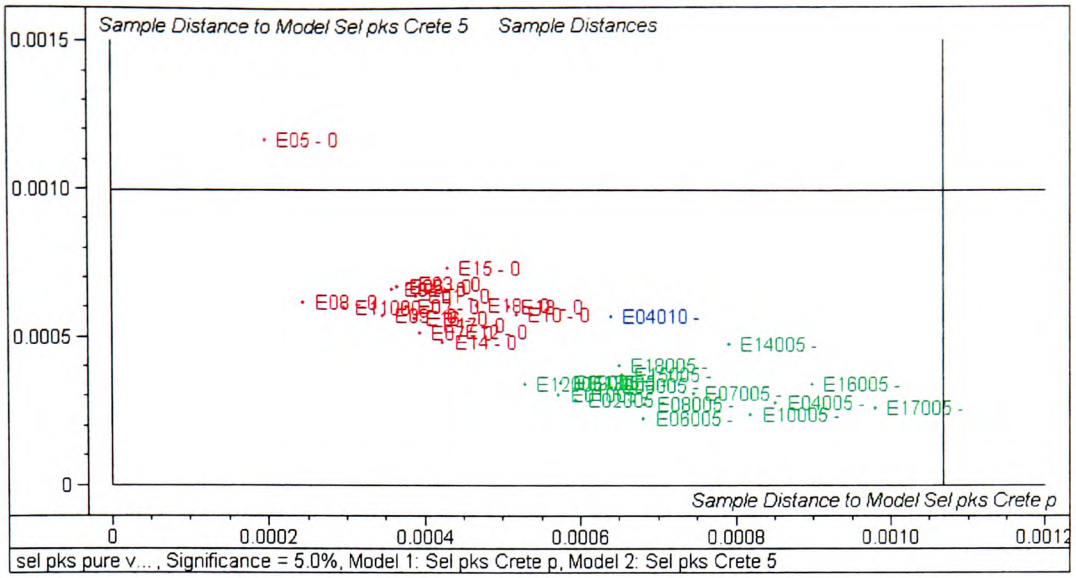

Figure D.40 – Cooman's plot of E set Crete pure oils (red) v 5% sunflower adulterated oils (green) over selected peaks with a 10% adulterated test sample

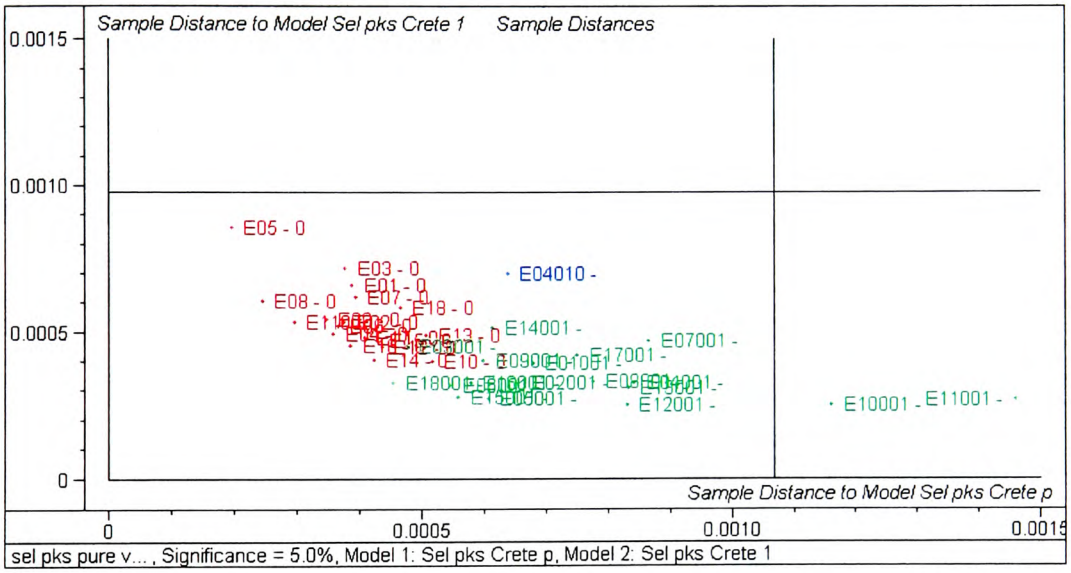

Figure D.41 – Cooman's plot of E set Crete pure oils (red) v 1% sunflower adulterated oils (green) over selected peaks with a 10% adulterated test sample

F SET

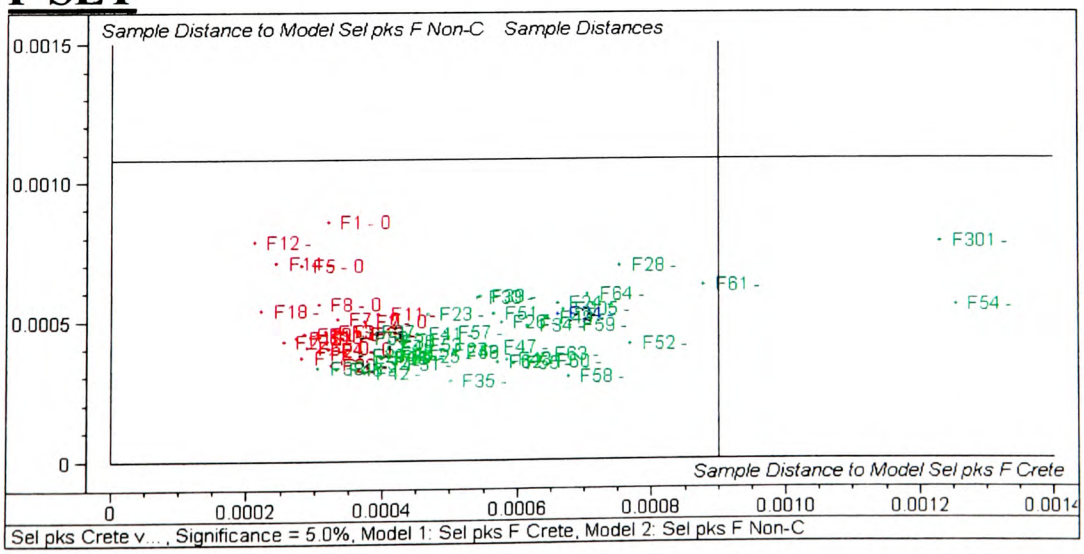

Figure D.42 – Cooman's plot of F set Crete (red) v non-Crete oils (green) over selected peaks with a non-Crete test sample (blue)

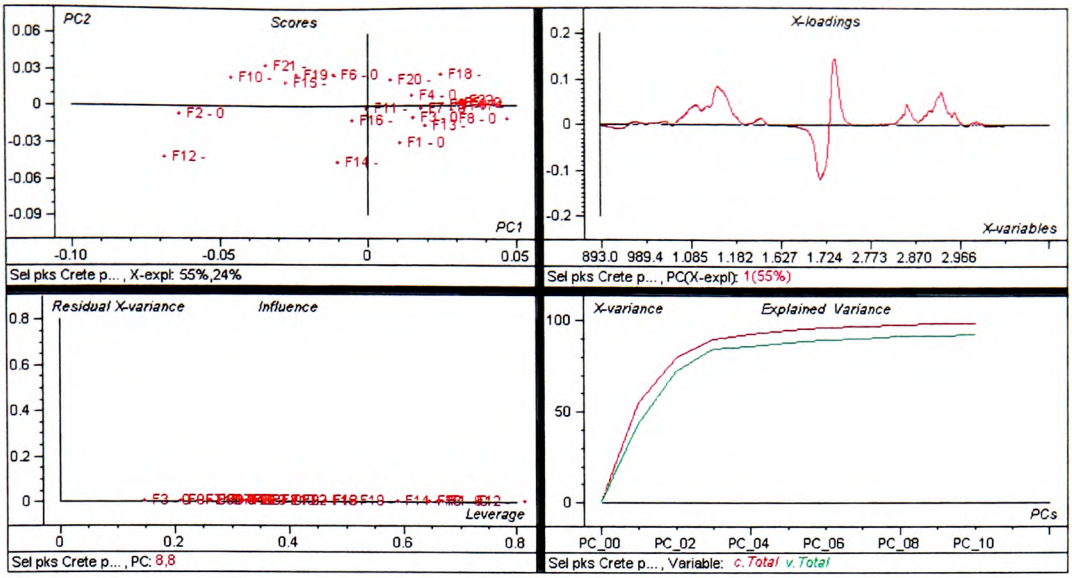

Figure D.43 - PCA overview of F set Crete pure oils over selected peaks

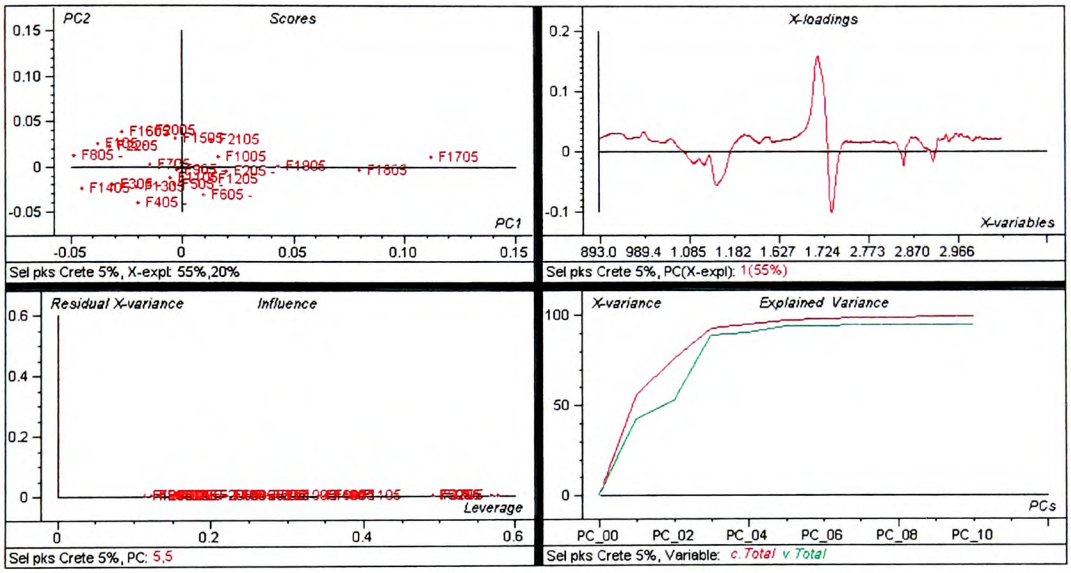

Figure D.44 - PCA overview of F set Crete oils adulterated with 5% sunflower oil over selected peaks

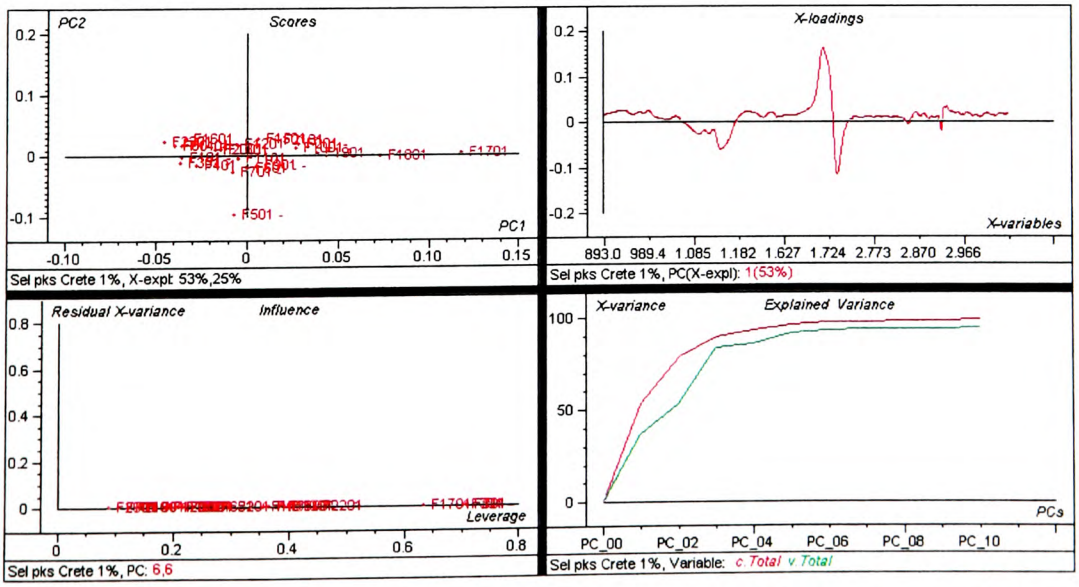

Figure D.45 - PCA overview of F set Crete oils adulterated with 1% sunflower oil over selected peaks

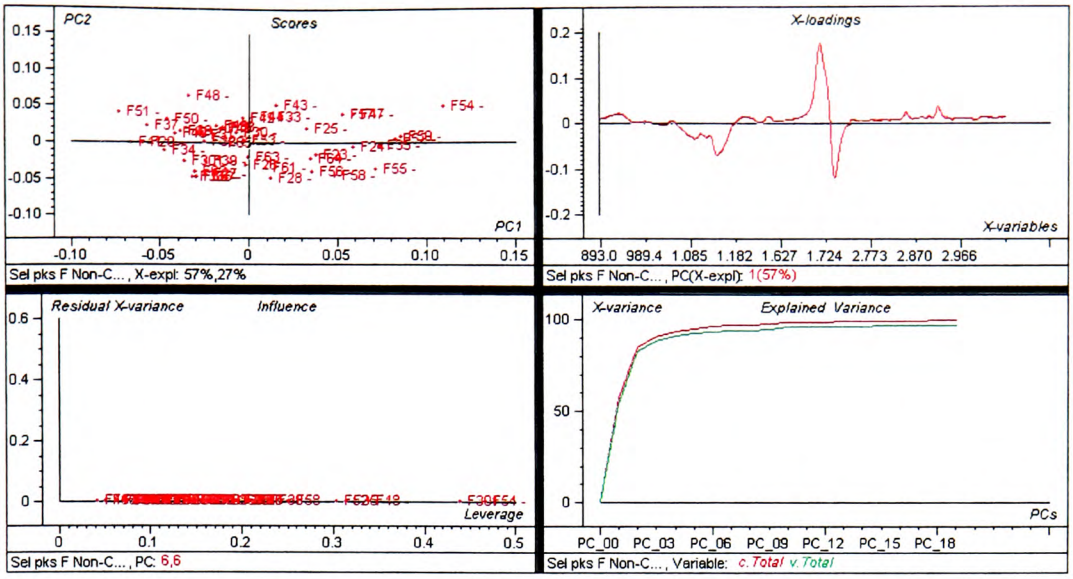

Figure D.46 - PCA overview of F set non-Crete pure oils over selected peaks

Harvest Comparisons

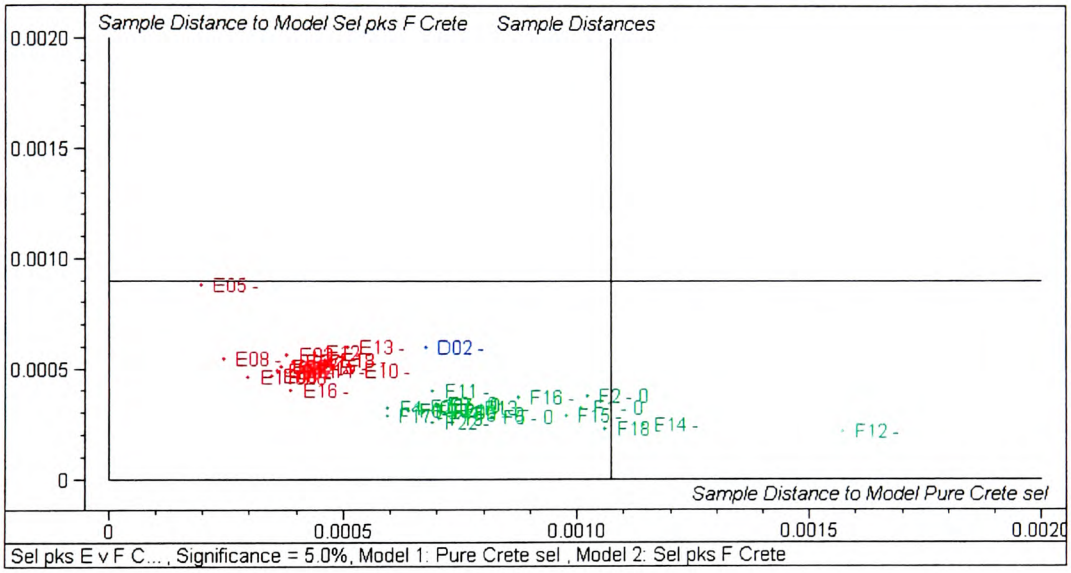

Figure D.47 – Cooman's plot of Crete oils E (red) v F (green) harvest over selected peaks with a D harvest test sample (blue)

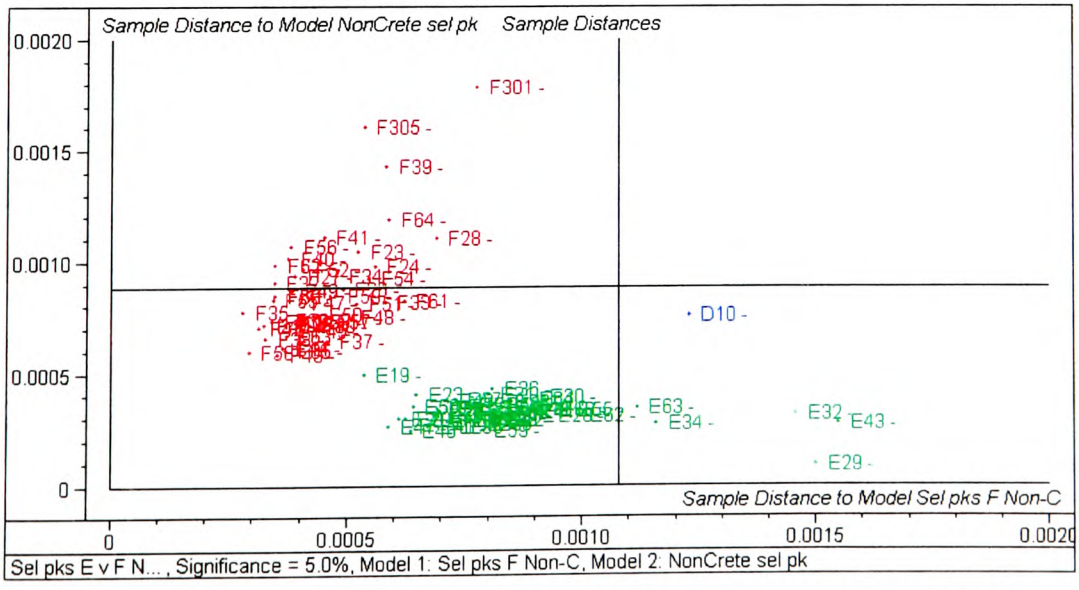

Figure D.48 – Cooman's plot of non-Crete oils E (green) v F (red) harvest over selected peaks with a D harvest test sample (blue)

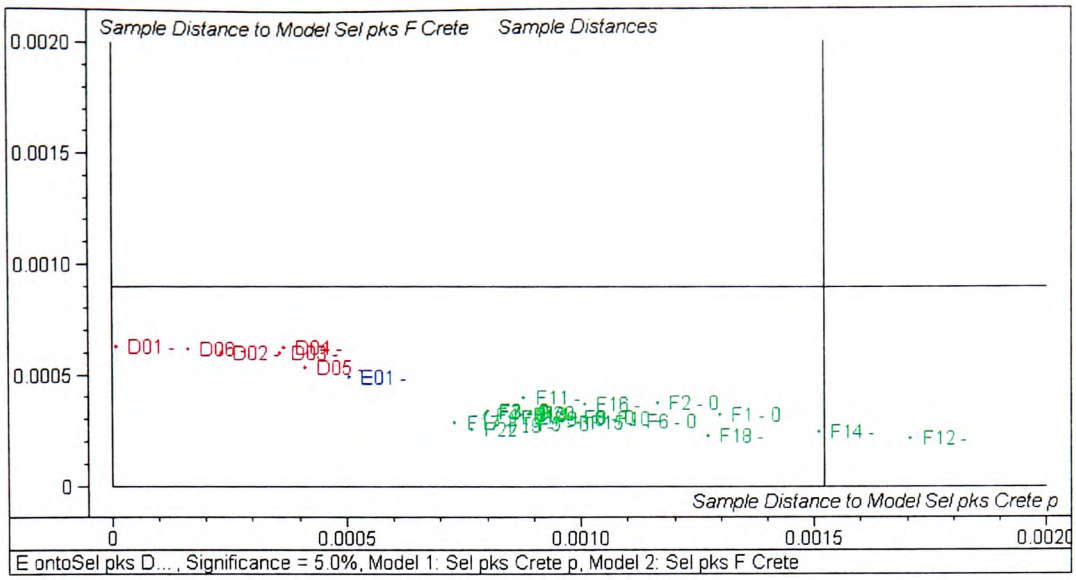

Figure D.49 – Cooman's plot of Crete oils D (red) v F (green) harvest over selected peaks with an E harvest test sample (blue)

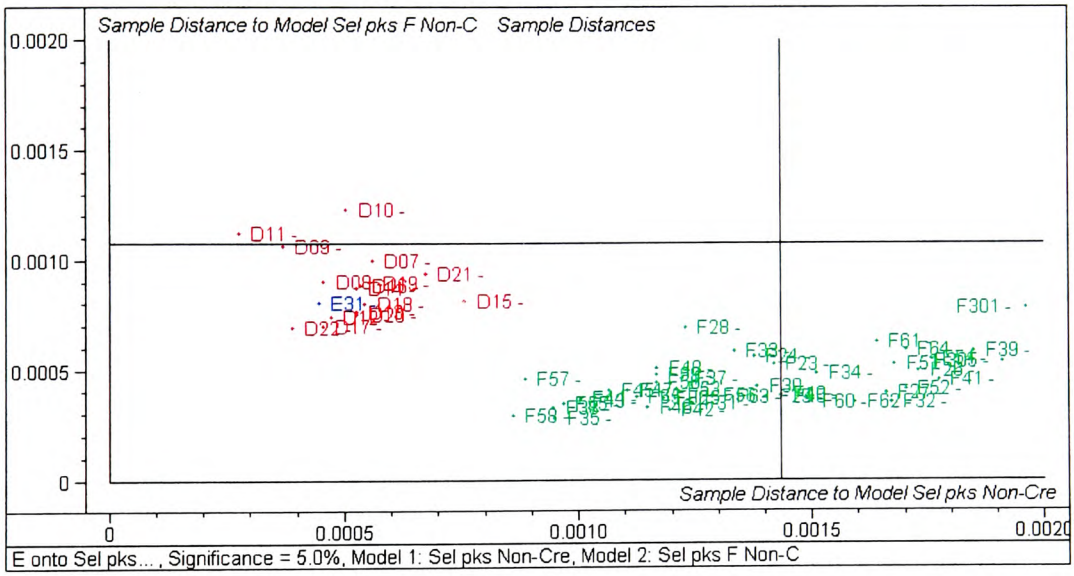

Figure D.50 – Cooman's plot of non-Crete oils D(red) v F (green) harvest over selected peaks with an E harvest test sample (blue)

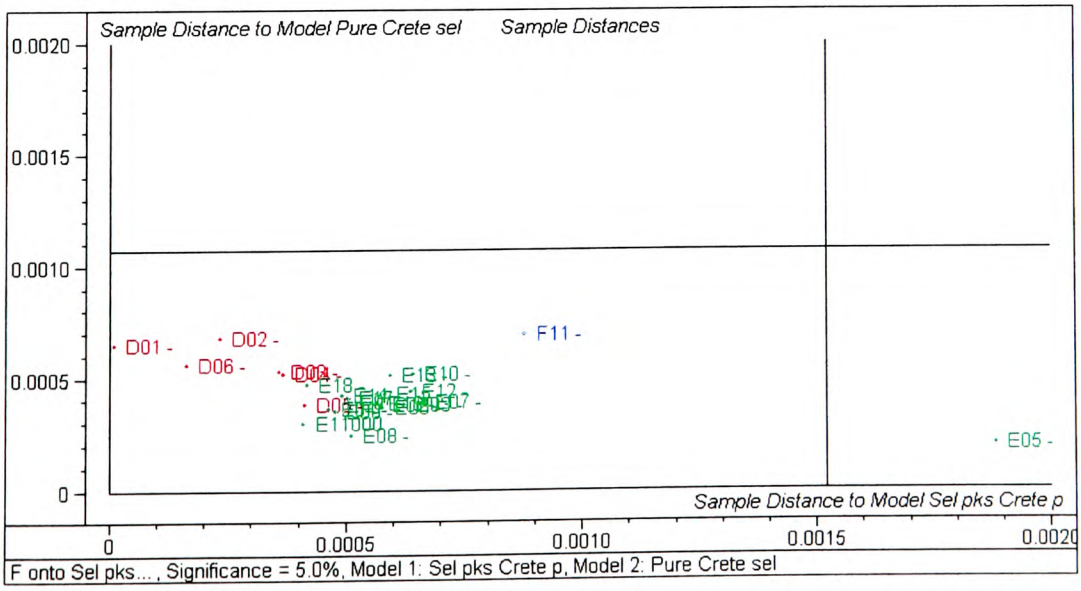

Figure D.51 – Cooman's plot of Crete oils D (red) v E (green) harvest over selected peaks with an F harvest test sample (blue)

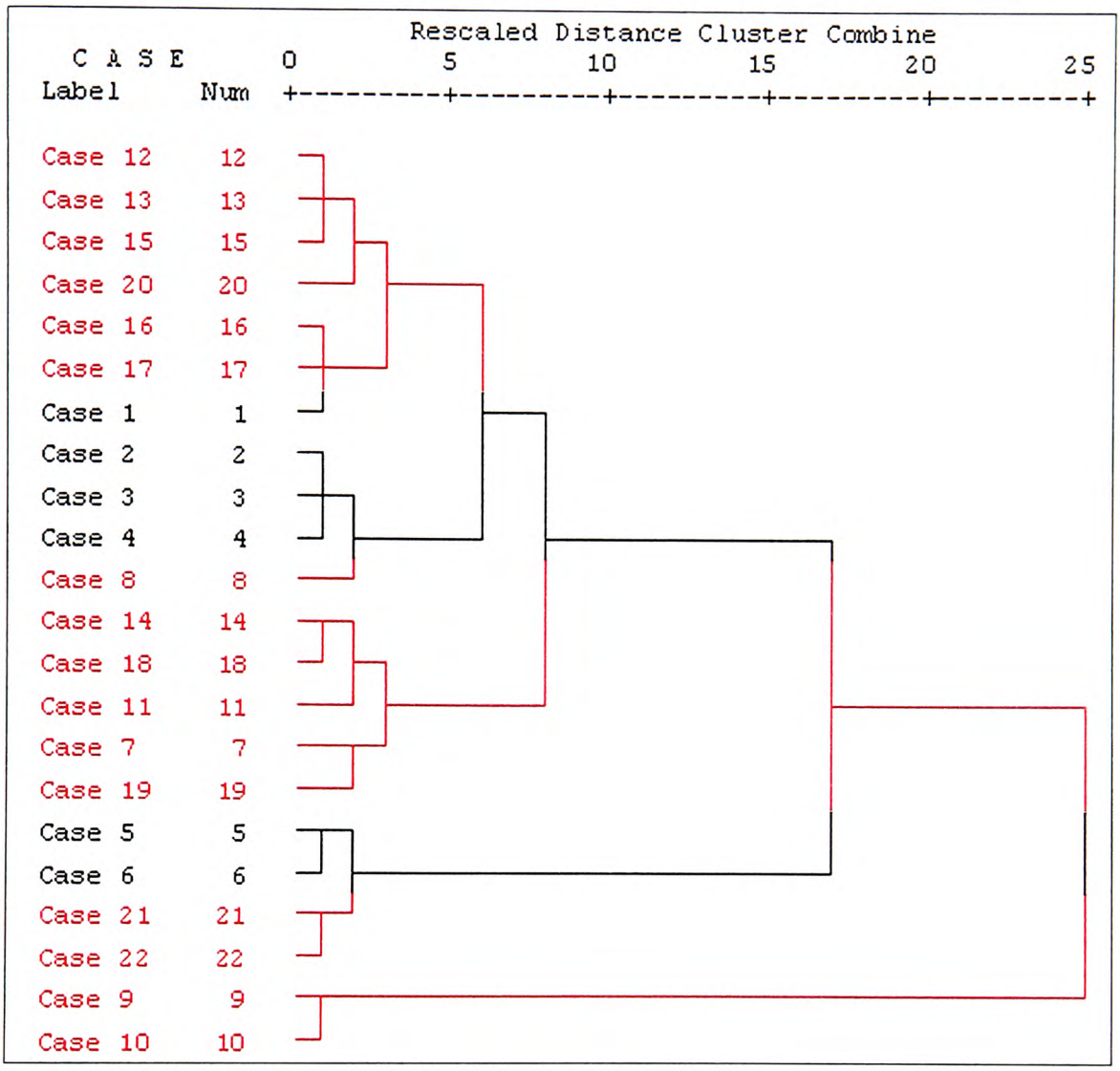

Figure D.52 – D set dendrogram of hierarchical clustering using Ward's method and squared Euclidean distance measurement (Crete oils – black, non-Crete oils – red)

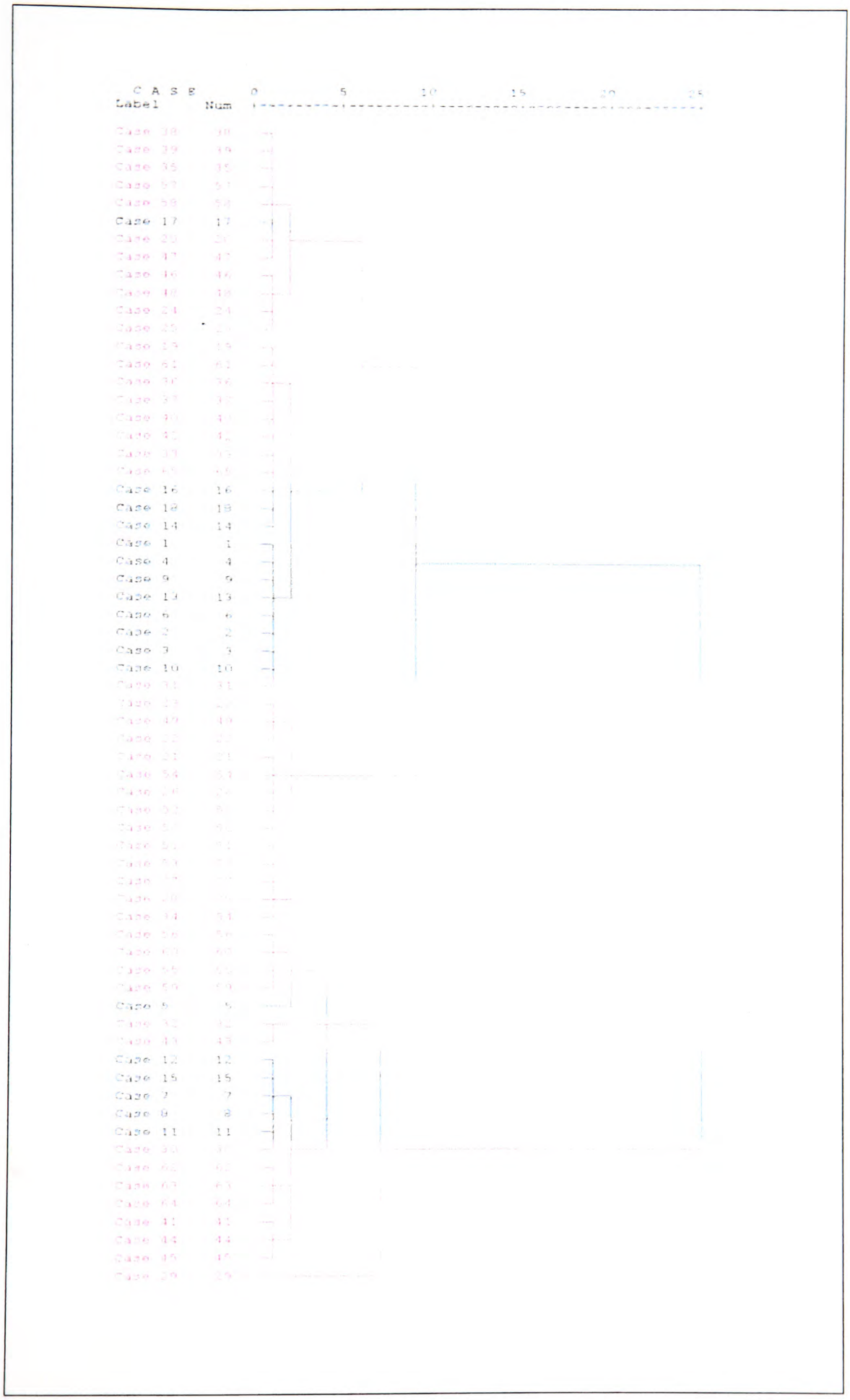

Figure D.53 - E set dendrogram of hierarchical clustering using Ward's method and squared Euclidean distance measurement (Crete oils – black, non-Crete oils – red)

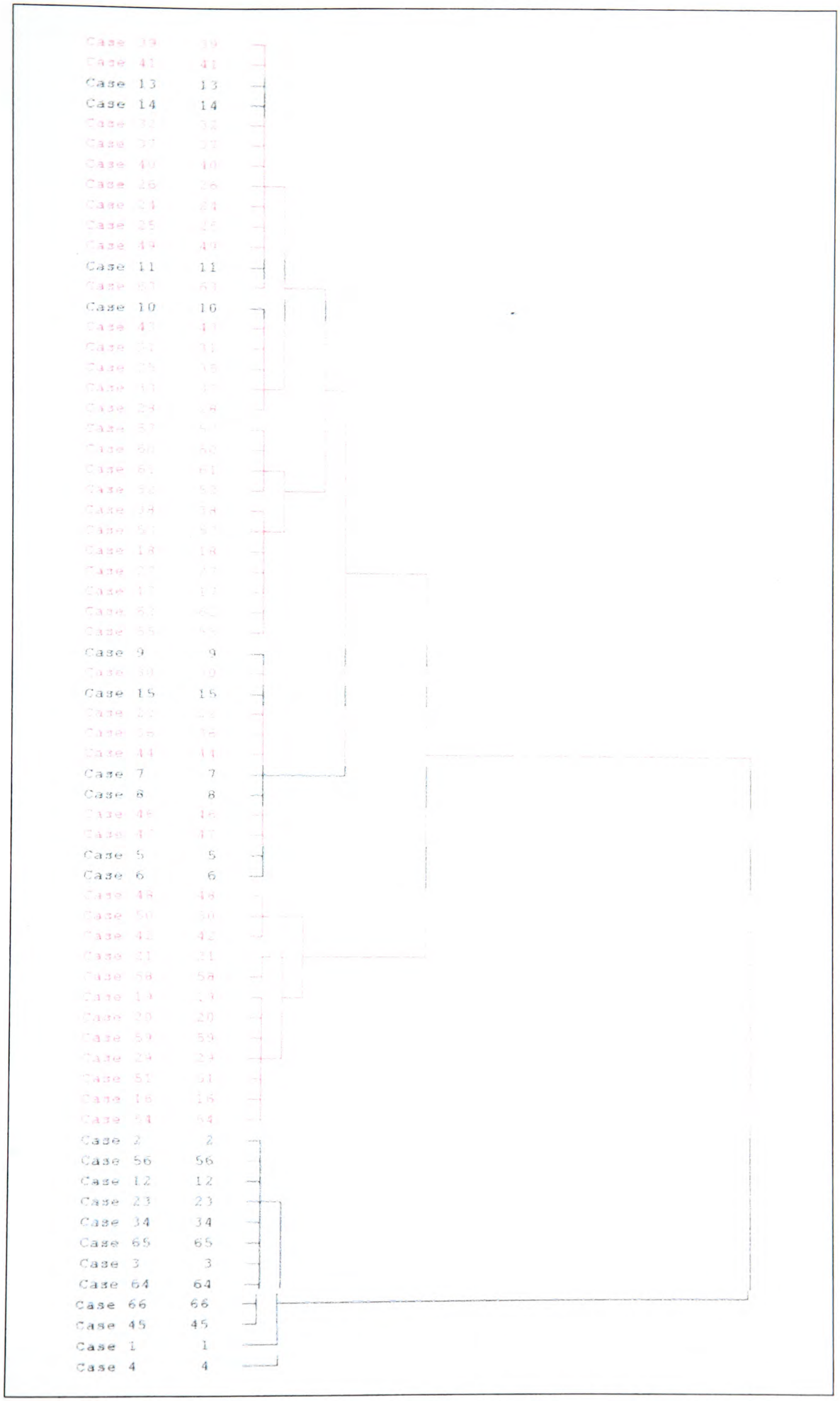

Figure D.54 - F set dendrogram of hierarchical clustering using Ward's method and squared Euclidean distance measurement (Crete oils – black, non-Crete oils – red)

APPENDIX E

SFE

Appendix E – Index of Figures

Appendix E – Index of Tables

Total Ion Chromatograms (TIC) for standard solutions to check retention times and fragmentation patterns

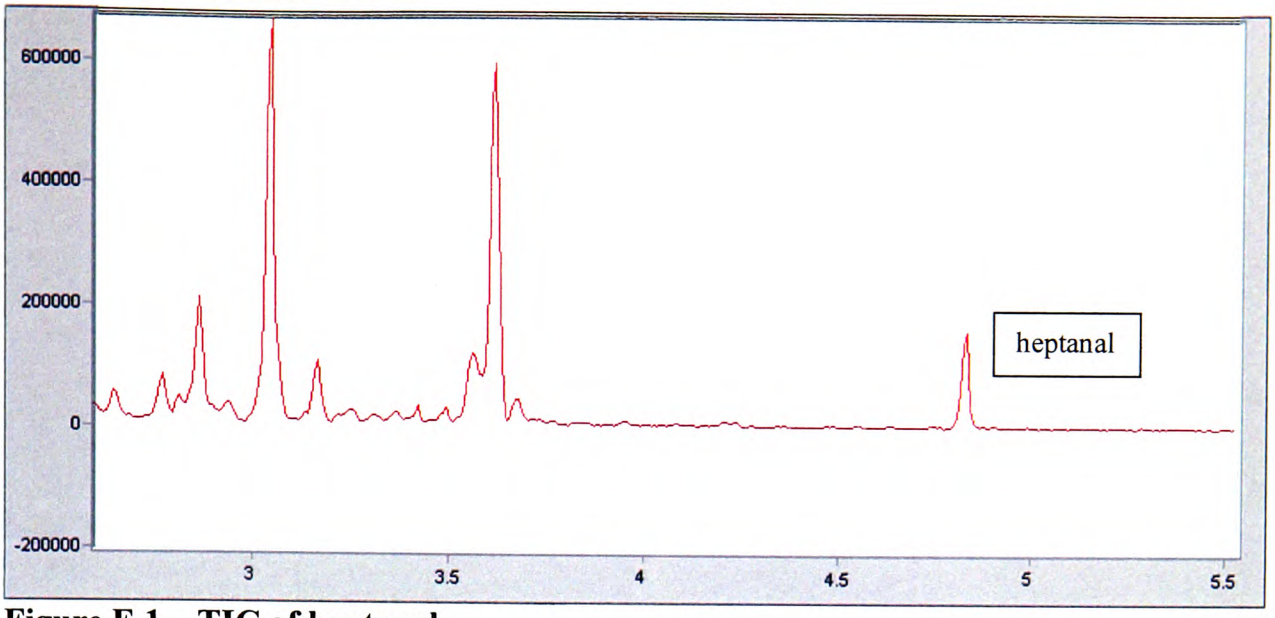

Figure E.1 – TIC of heptanal

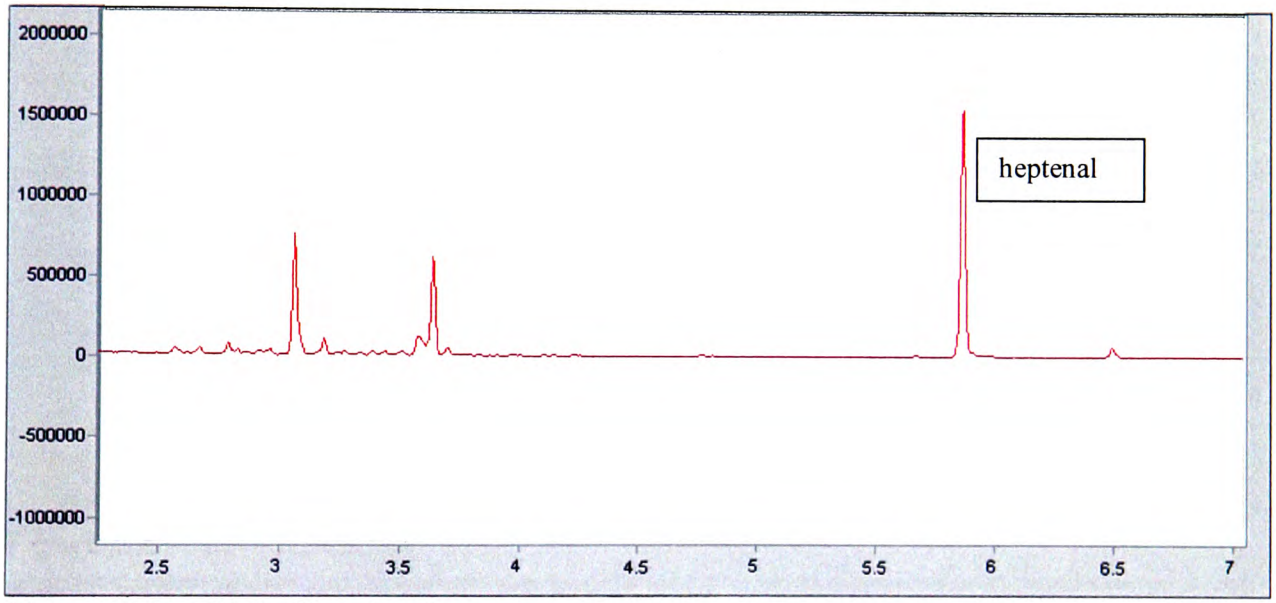

Figure E.2 – TIC of heptenal

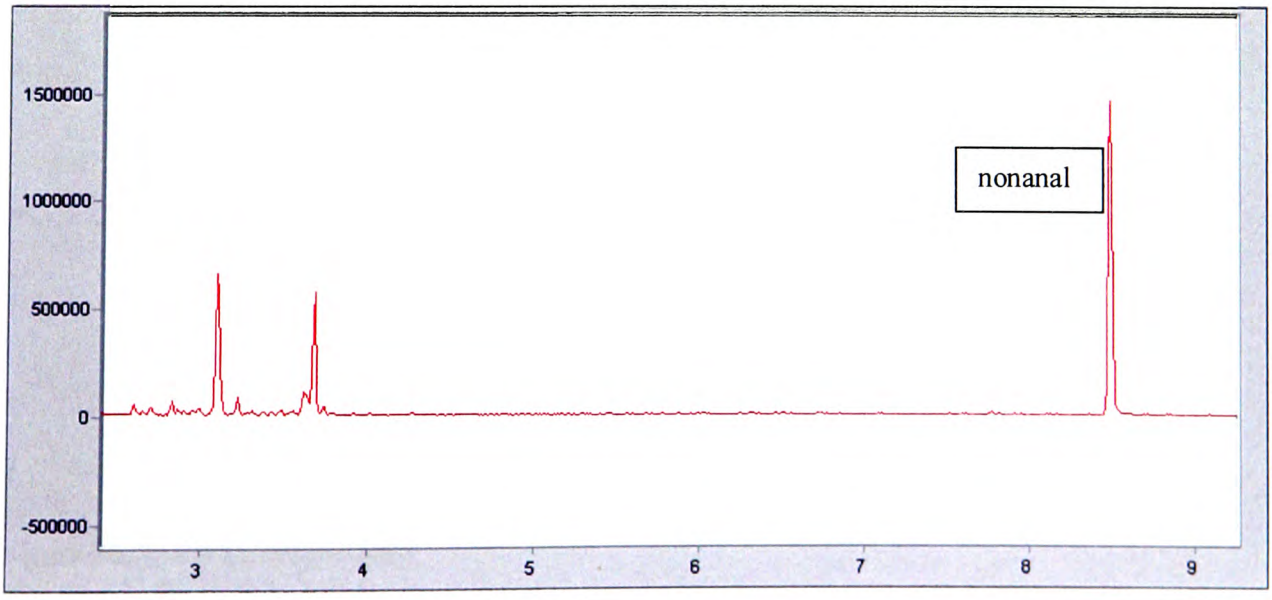

Figure E.3 – TIC of nonanal

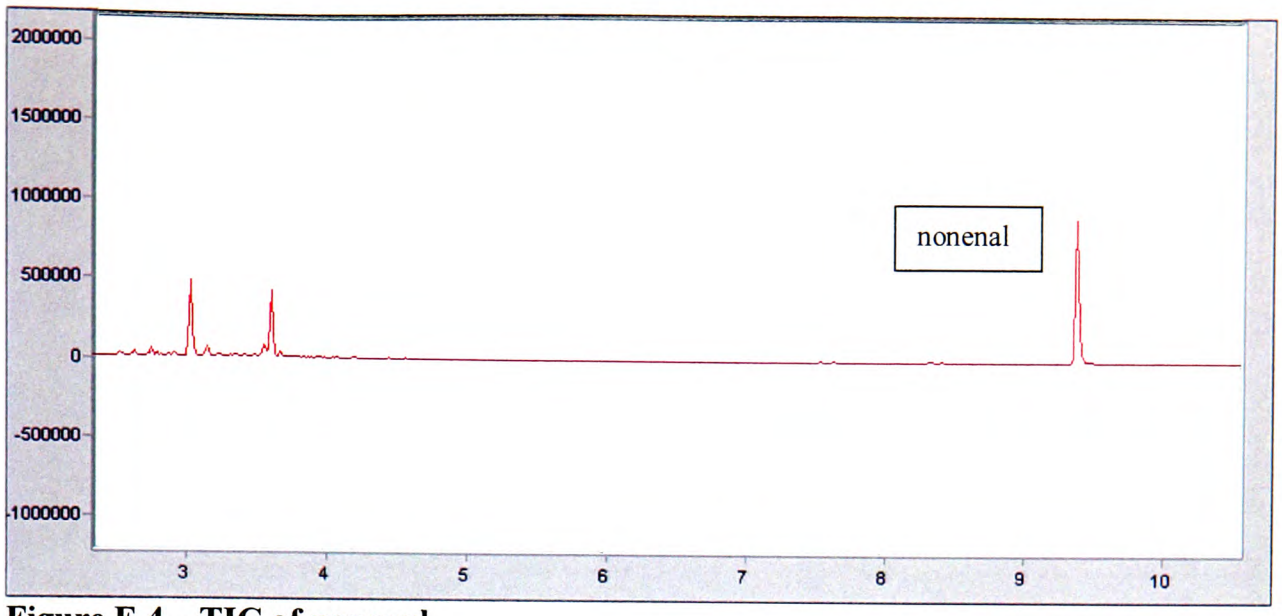

Figure E.4 – TIC of nonenal

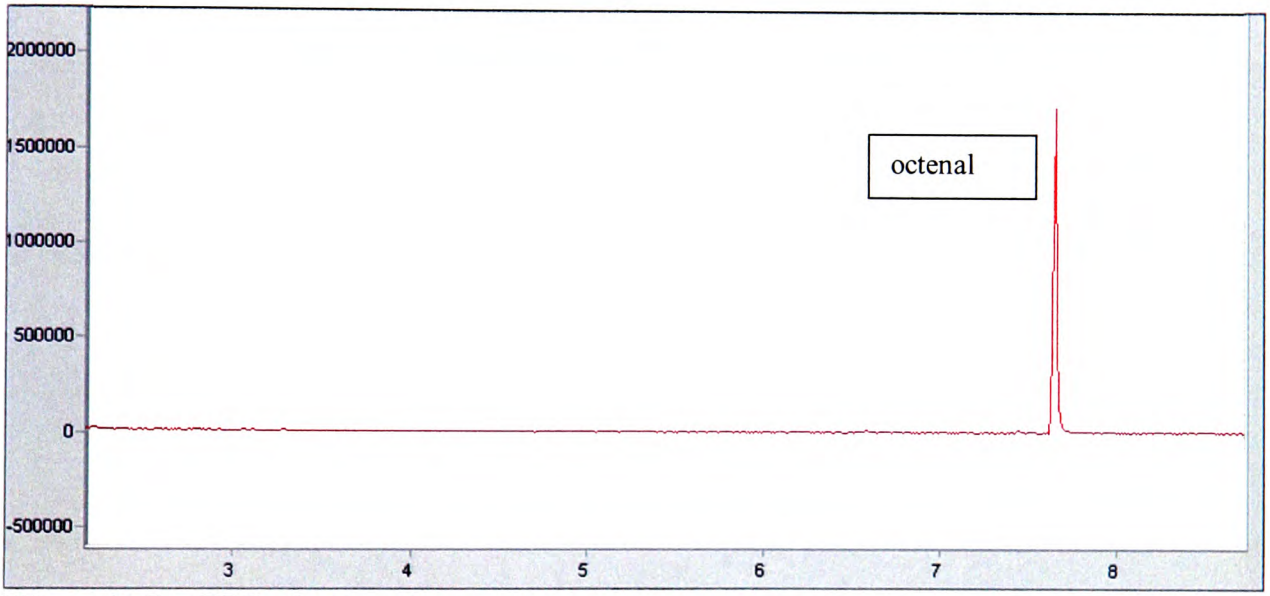

Figure E.5 – TIC of octenal

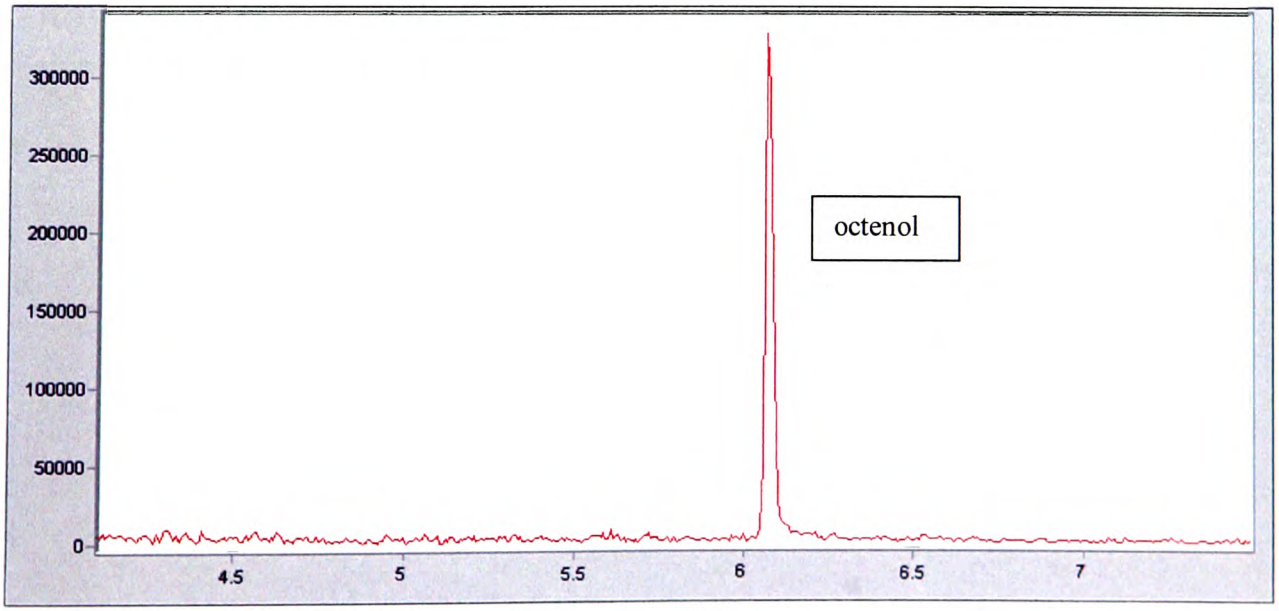

Figure E.6 – TIC of octenol

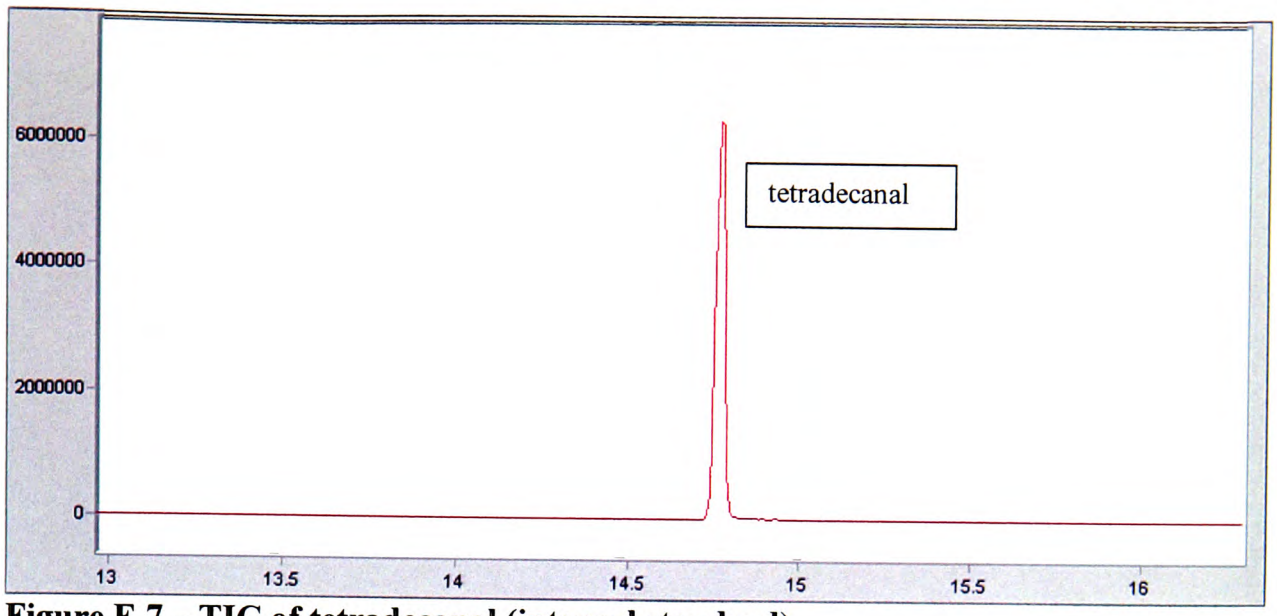

Figure E.7 – TIC of tetradecanal (internal standard)

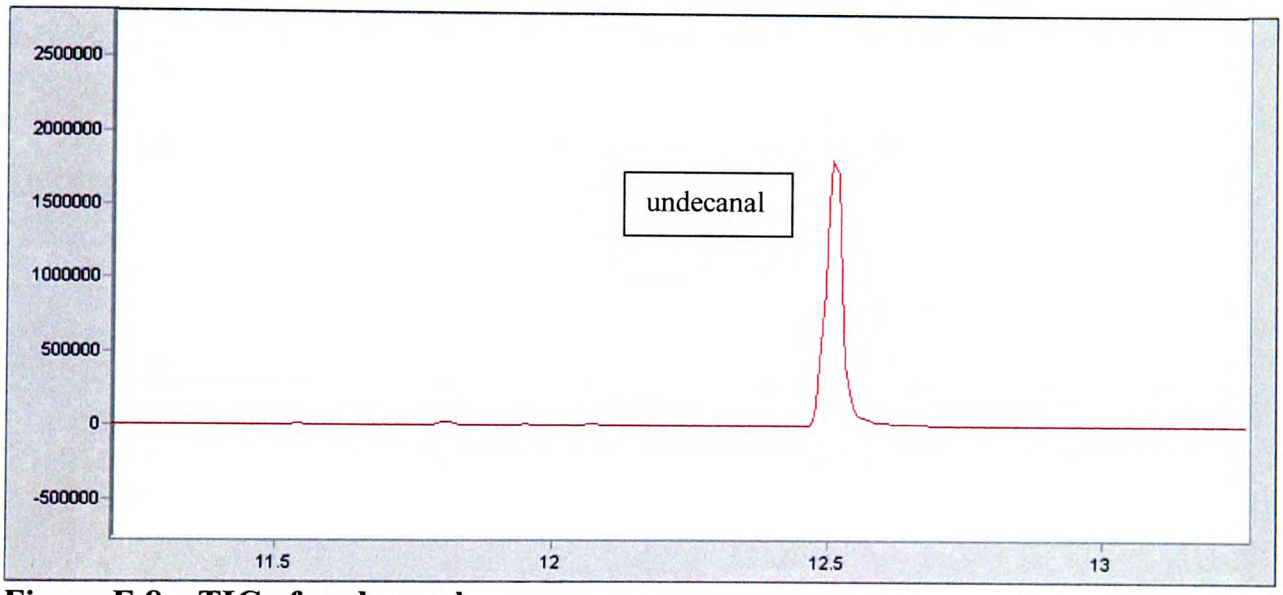

Figure E.8 – TIC of undecanal

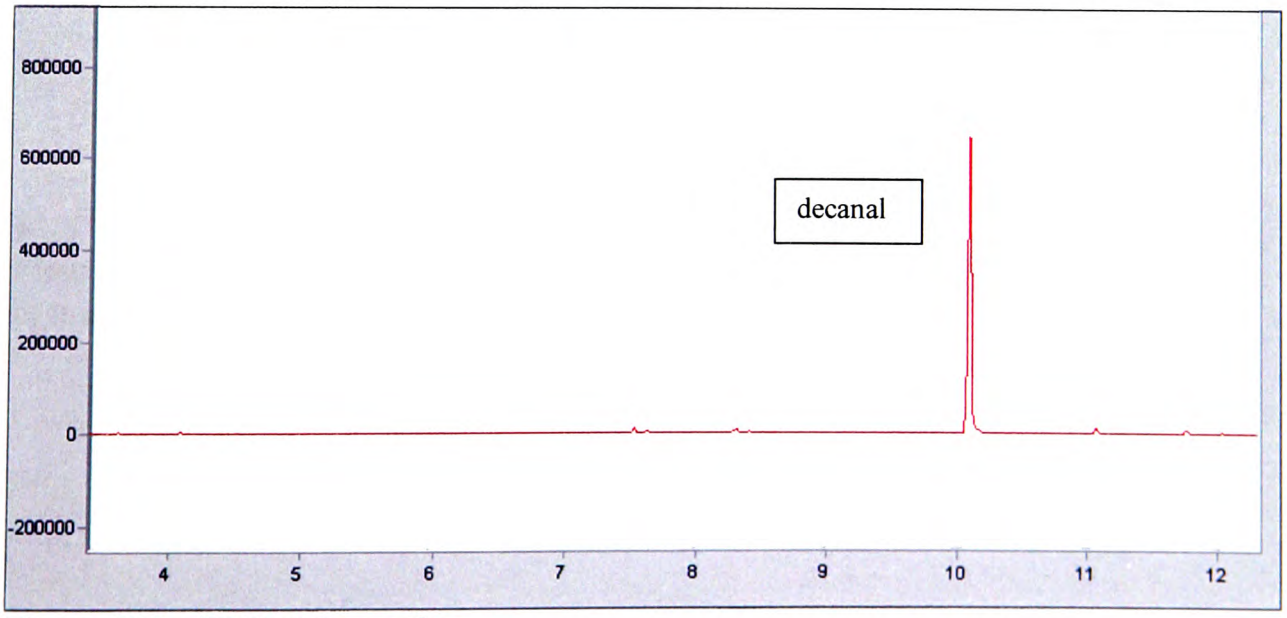

Figure E.9 – TIC of decanal

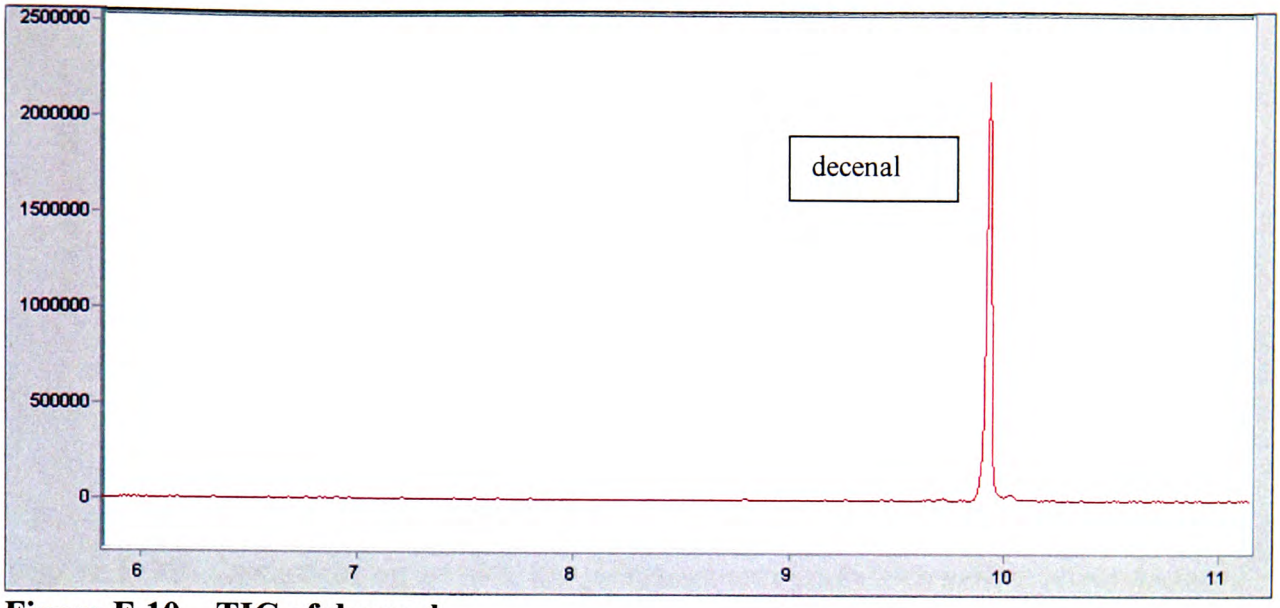

Figure E.10 – TIC of decenal

Optimisation of SFE Temperature and Static Extraction Parameters

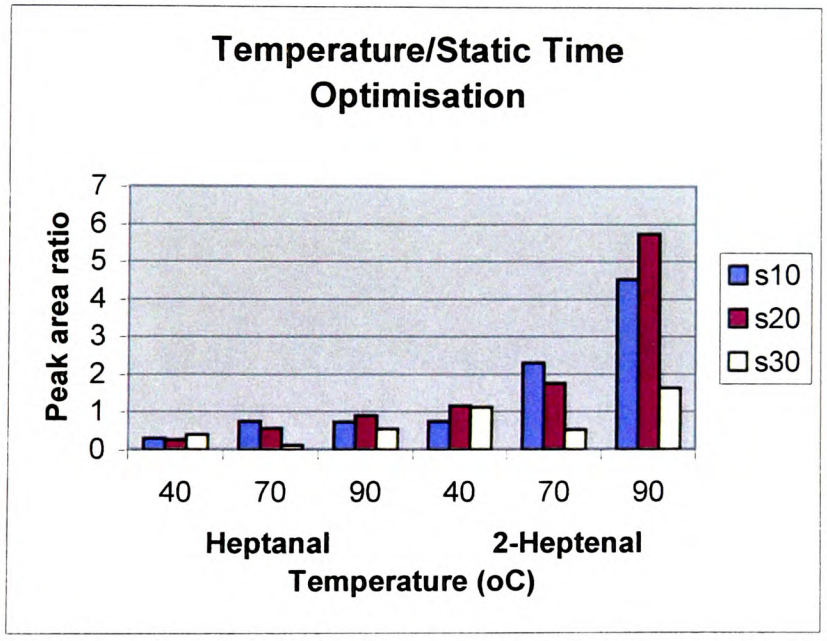

Figure E.11 - Optimisation of SFE temperature and static extraction parameters (s in minutes) for heptanal and 2-heptenal

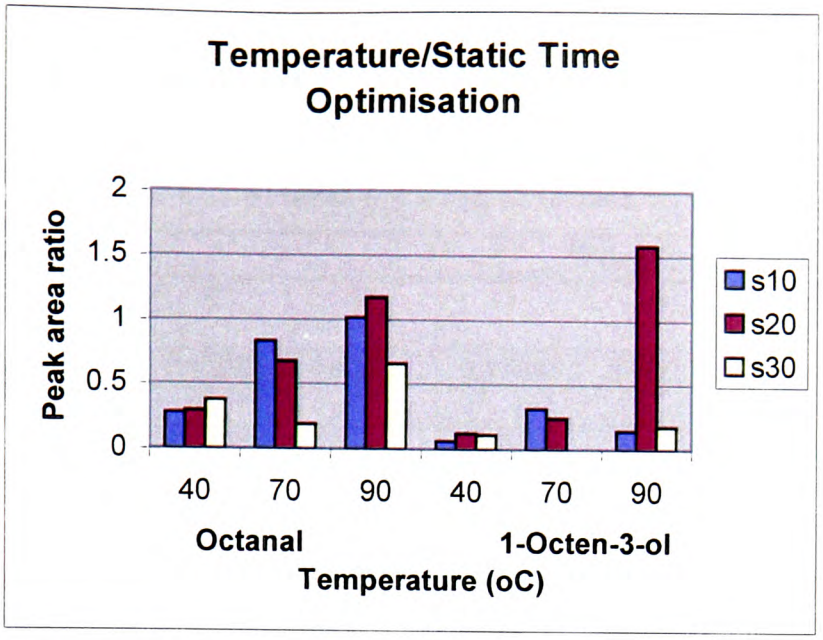

Figure E.12 - Optimisation of SFE temperature and static extraction parameters (s in minutes) for octanal and 1-octen-3-ol

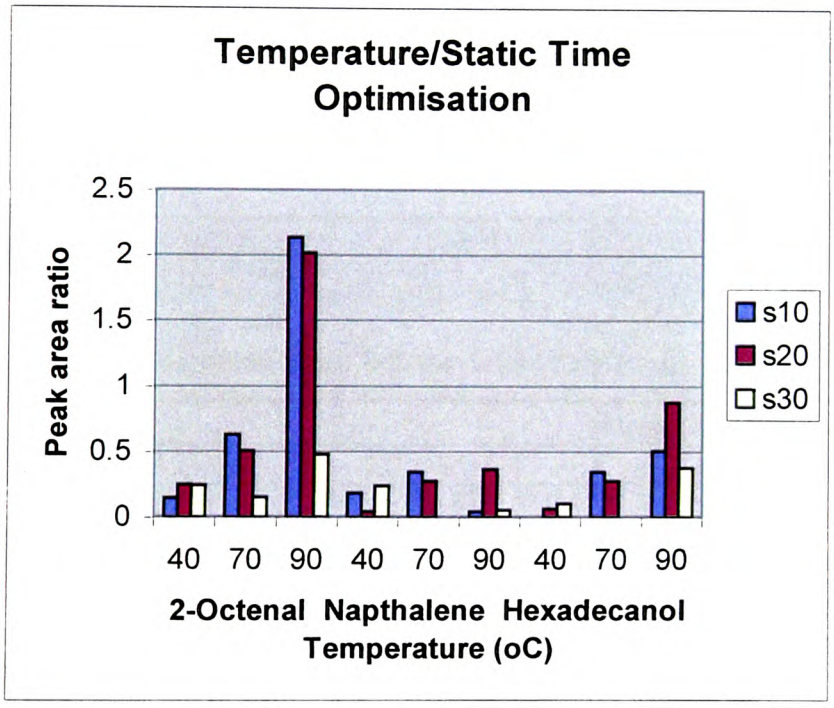

Figure E.13 - Optimisation of SFE temperature and static extraction parameters (s in minutes) for 2-octenal, napthalene and hexadecanol

Tables to show ratio of detected compound (by retention time) to internal standard for the SFE extractions of the Greek olive oils with the mean value, standard deviation and number of samples shown

Table E.1 – Extractions 1-4 for E14 (Crete oil), mean, s.d. and number of runs

E14	Runs ratio						
Retention time	1	2	3	4	Mean	SD	n
2.93	0.44089	0.43305	0.47938	0.40639	0.439928	0.030163	4
3.8					0	0	
4.63	0.02059	0.0322	0.03723	0.046145	0.034041	0.010661	4
5.62	0.036004	0.07588	0.079904	0.08713	0.06973	0.02296	4
5.88	0.030002				0.030002		1
6.08		0.01588	0.01915		0.017515	0.002312	2
6.28	0.10262	0.11373	0.128999	0.113801	0.114788	0.010834	4
6.48	0.06155	0.08247	0.091099	0.19813	0.108312	0.06115	4
6.9							
7.44	0.04062	0.0323	0.038199	0.03192	0.03576	0.004331	4
7.67	0.019404	0.03305	0.09178	0.03197	0.044051	0.032417	4
8.05	0.14394	0.13439	0.153621	0.13178	0.140933	0.009943	4
8.22		0.18103	0.18492	0.16554	0.177163	0.010252	3
9.14	0.03665	0.05568	0.02973	0.04034	0.0406	0.010973	4
9.86	0.049889	0.049995		0.050543	0.050142	0.000351	3
10.72			0.013003	0.034254	0.023629	0.015027	2
12.22	0.047586	0.045692	0.042043	0.043378	0.044675	0.002457	4
14.19							

Table E.2 - Extractions 1-8 for E15 (Crete oil)

E15	Runs ratio							
R/T	1	2	3	4	5	6	7	8
2.93	0.46425	0.48334	0.55578	0.45204	0.620696	0.497508	0.55711	0.6741
3.8								
4.63	0.02199	0.022867	0.027136	0.02049	0.02766	0.023507		0.03251
5.62	0.04785	0.05199	0.05406	0.04447	0.05924	0.05974	0.046662	0.06031
5.88		0.017655	0.020584	0.018338	0.02997	0.026037		0.019866
6.08				0.015233				
6.28	0.09294	0.09153	0.10244	0.098417	0.202071	0.18771	0.17952	0.26513
6.48	0.08939	0.096888	0.105322	0.085564	0.09638	0.0942	0.078866	0.10154
6.9								
7.44	0.04721	0.04373	0.04334	0.046606	0.04567	0.06176	0.03425	0.041814
7.67	0.02684	0.019817	0.024962	0.02022	0.03541	0.03082		
8.05	0.16923	0.153785	0.16842	0.182383	0.08352	0.10078	0.02743	0.024035
8.22	0.23826	0.206862	0.255871	0.22898	0.22608	0.2693	0.14442	0.175594
9.14	0.051826	0.039554	0.04108	0.03803	0.108096	0.17583	0.05115	0.06269
9.86	0.050875	0.082832	0.088598	0.085036	0.064028	0.090741		0.025389
10.72	0.047141	0.030887	0.057253	0.05073	0.055357	0.085056		
12.22	0.060997	0.065841	0.071292	0.06681	0.074679	0.109427	0.032768	0.03296
14.19								

Table E.3 - Mean, s.d. and number of runs for E15 extractions

E15	Mean	SD	n
2.93	0.538103	0.078829	8
3.8			0
4.63	0.025166	0.004164	8
5.62	0.05304	0.006318	8
5.88	0.022075	0.004871	6
6.08	0.015233		1
6.28	0.15247	0.065256	8
6.48	0.093519	0.008608	8
6.9			0
7.44	0.045548	0.007714	6
7.67	0.026345	0.006074	8
8.05	0.113698	0.064323	8
8.22	0.218171	0.041401	8
9.14	0.071032	0.048058	8
9.86	0.069643	0.02435	7
10.72	0.054404	0.017708	7
12.22	0.064347	0.024463	8

Table E.4 - Extractions 1-4 for E16 (Crete oil), mean, s.d. and number of runs

E16	Runs ratio						
R/T	1	2	3	4	Mean	SD	n
2.93	0.553	0.467	0.395	0.404	0.45475	0.072913	4
3.8		0.0043	0.0188		0.01155	0.010253	2
4.63	0.032	0.03	0.031		0.031	0.001	3
5.62	0.056	0.059	0.053	0.032	0.056	0.012247	4
5.88							
6.08							
6.28	0.259	0.247	0.224	0.189	0.22975	0.030804	4
6.48	0.086	0.077	0.072	0.0666	0.0754	0.008245	4
6.9							
7.44			0.02		0.02		
7.67							
8.05		0.049	0.065	0.057	0.057	0.008	3
8.22							
9.14		0.096	0.058		0.077	0.02687	2
9.86							
10.72							
12.22							
14.19							

Table E.5 - Extractions 1-4 for E17 (Crete oil), mean, s.d. and number of runs

E17	Runs ratio						
R/T	1	2	3	4	Mean	SD	n
2.93	0.5944	0.49324		0.56426	0.550633	0.051938	3
3.8							
4.63	0.01959			0.01851	0.01905	0.000764	2
5.62	0.03358	0.02713		0.03417	0.031627	0.003905	3
5.88				0.006165	0.006165		
6.08				0.00475	0.00475		1
6.28	0.10087	0.08729		0.09977	0.095977	0.007543	3
6.48	0.07439	0.0676		0.07766	0.07766	0.005132	3
6.9							
7.44	0.02969	0.02912		0.02664	0.02664	0.001622	3
7.67				0.004036	0.004036		1
8.05	0.11304	0.09282		0.10039	0.102083	0.010216	3
8.22	0.17241	0.15602		0.18998	0.172803	0.016983	3
9.14	0.03413	0.04692		0.03108	0.037377	0.008404	3
9.86	0.061875	0.070958		0.028219	0.053684	0.022516	3
10.72				0.004519	0.004519		1
12.22	0.031467	0.038496		0.014946	0.028303	0.01209	3
14.19							

Table E.6 - Extractions 1-4 for E18 (Crete oil), mean, s.d. and number of runs

E18	Runs ratio						
R/T	1	2	3	4	Mean	SD	n
2.93	0.10667	0.115004	0.109384		0.110353	0.004251	3
3.8		0.007715	0.006283		0.006999	0.001013	2
4.63	0.00986	0.010909	0.011767		0.010845	0.000955	3
5.62	0.01546	0.017447	0.015853	0.009137	0.014474	0.00366	4
5.88			0.002971		0.002971		1
6.08			0.003195		0.003195		1
6.28	0.07013	0.067487	0.074616	0.05759	0.067456	0.007205	4
6.48	0.02005	0.020885	0.019746		0.020227	0.00059	3
6.9							
7.44		0.007029	0.005577		0.006303	0.001027	2
7.67			0.00553		0.00553		1
8.05	0.01102		0.01064		0.01083	0.000269	2
8.22	0.11874	0.113833	0.119932	0.08007	0.108144	0.018901	4
9.14	0.02069	0.029477	0.022985		0.024384	0.004557	3
9.86	0.018354	0.019171	0.017456		0.018327	0.000858	3
10.72							
12.22							
14.19							

Table E.7 - Extractions 1-4 for E33 (non-Crete oil), mean, s.d. and number of runs

E33	Runs ratio						
R/T	1	2	3	4	Mean	SD	n
2.93	0.14462	0.161334	0.162802	0.159867	0.157156	0.008443	4
3.8		0.022542	0.024545	0.021781	0.022956	0.001428	3
4.63	0.00685	tr	0.013821		0.010336	0.004929	2
5.62	0.010635	tr	0.015461		0.013048	0.003412	2
5.88	0.006128				0.006128		1
6.08		tr	tr				
6.28	0.012903	0.16669	0.16102	0.158795	0.124852	0.074707	4
6.48	0.015393	0.035836	0.033877	0.036416	0.03038	0.010051	4
6.9			0.17977		0.17977		1
7.44	0.008426	tr	tr		0.008426		1
7.67	0.014817		0.019752		0.017285	0.00349	2
8.05	0.03655	0.037979	0.047228	0.040539	0.040574	0.004733	4
8.22	0.178233	0.190368	0.205749	0.21261	0.19674	0.01545	4
9.14	0.041347	0.044565	0.051658	0.054763	0.048083	0.006196	4
9.86							
10.72	0.036385	0.04247	0.046086	0.045956	0.042724	0.004546	4
12.22		0.014458	0.019514		0.016986	0.003575	2

Table E.8 - Extractions 1-4 for E34 (non-Crete oil), mean, s.d. and number of runs

E34	Runs ratio						
R/T	1	2	3	4	Mean	SD	n
2.93	0.071439	0.067028	0.055526	0.06268	0.064168	0.006781	4
3.8	0.0108	0.009479	0.009486	0.01012	0.009971	0.000629	4
4.63		0.006547		0.005731	0.006139	0.000577	2
5.62		0.005616		0.005603	0.00561	9.05E-06	2
5.88							
6.08							
6.28	0.080374	0.076748	0.073115	0.072899	0.075784	0.003533	4
6.48	0.019759	0.017466	0.015119	0.017052	0.017349	0.001905	4
6.9							
7.44							
7.67	0.010973		0.008902		0.009937	0.001464	2
8.05	0.03152			0.029503	0.030512	0.001426	2
8.22	0.149591	0.134152	0.129702	0.126798	0.135061	0.010148	4
9.14	0.01616	0.017194	0.014296	0.016545	0.016049	0.001244	4
9.86							
10.72	0.029982	0.035626	0.026554	0.019491	0.027913	0.006747	4
12.22	0.009231	0.016669	0.008255	0.00801	0.010541	0.004119	4
14.19		0.01227	0.007824	0.007349	0.009148	0.002714	3

Table E.9 - Extractions 1-4 for E35 (non-Crete oil), mean, s.d. and number of runs

E35	Runs ratio						
R/T	1	2	3	4	Mean	SD	n
2.93	0.062459	0.055737	0.047403	0.052515	0.054529	0.006303	4
3.8	0.014298	0.014805	0.014572	0.01418	0.014464	0.000281	4
4.63	0.006367		0.008341	0.009213	0.007974	0.001458	3
5.62	0.006007		0.004506	0.005714	0.005409	0.000796	3
5.88			0.002859	0.003375	0.003117	0.000365	2
6.08							
6.28	0.057515	0.051105	0.044994	0.040318	0.048483	0.007468	4
6.48	0.015071	0.013168	0.01548	0.01261	0.014082	0.001406	4
6.9							
7.44	0.017889	0.01652		0.003731	0.012713	0.007809	3
7.67			0.007173	0.008006	0.00759	0.000589	2
8.05			0.02361	0.02341	0.02351	0.000141	2
8.22	0.091504	0.0882	0.088573	0.089347	0.089406	0.001478	4
9.14	0.015489	0.013815	0.014542	0.01408	0.014482	0.000736	4
9.86							
10.72	0.010277	0.014063	0.013792	0.014951	0.013271	0.002056	4
12.22	0.007046		0.00618	0.006611	0.006612	0.000433	3
14.19			0.003919	0.00486	0.00439	0.000665	2

Table E.10 - Extractions 1-4 for E36 (non-Crete oil), mean, s.d. and number of runs

E36	Runs ratio						
R/T	1	2	3	4	Mean	SD	n
2.93	0.060097	0.061078	0.05429	0.053994	0.057365	0.003745	4
3.8	0.005702	0.006375	0.007756	0.006443	0.006569	0.000859	4
4.63	0.005689	0.004653	0.005642	0.005426	0.005352	0.00048	4
5.62	0.005574	0.003389	0.004163	0.003951	0.004269	0.000929	4
5.88							
6.08				0.002484	0.002484		1
6.28	0.049599	0.04896	0.0483	0.04604	0.048225	0.00155	4
6.48	0.009669	0.009304	0.009454	0.008667	0.009274	0.000431	4
6.9							
7.44							
7.67							
8.05							
8.22	0.035203	0.034383	0.03274	0.032126	0.033613	0.001425	4
9.14	0.005113	0.004355			0.004734	0.000536	2
9.86							
10.72							
12.22							
14.19							

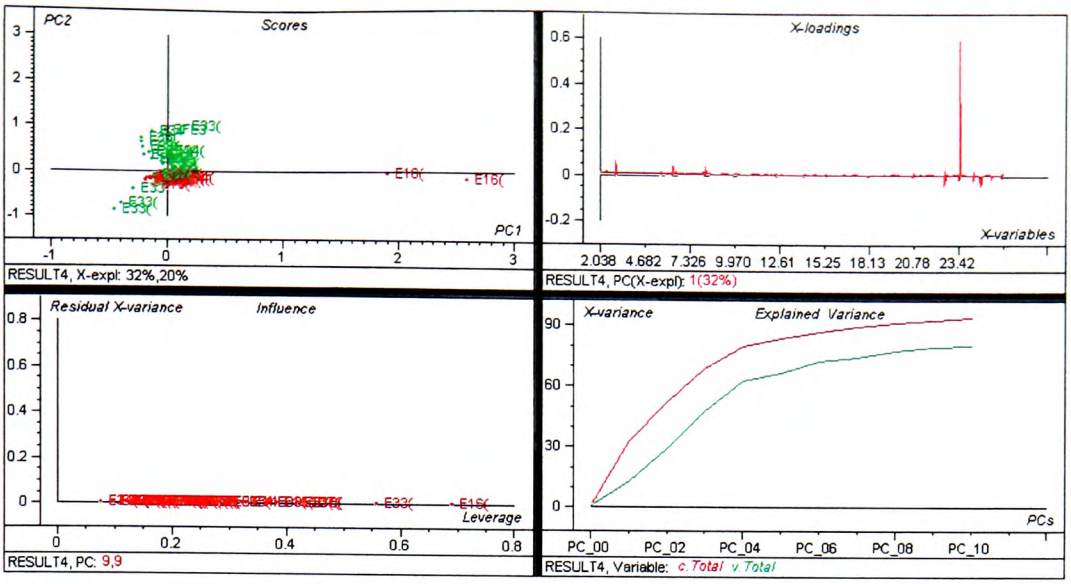

Figure E.14 - PCA overview of SFE extraction of Crete (red, top left) and non-Crete (green, top left) oils, all samples over all variables

APPENDIX F

SPME

Appendix F – Index of Tables

Appendix F – Index of Figures

Tables to compare retention times and peak areas for SFE and SPME extractions of the Greek olive oils

Table F.1– Table showing retention times and peak areas for extraction of volatile fraction of oil E14 by SFE and SPME

Compound	SFE		SPME	
	RT	Pk area	RT	Pk area
2-pentenal			2.24	296464
Hexanal	2.96	6561671	2.87	7314864
2-hexenal			3.73	571626
3-hexen-1-ol				
Heptanal				
2,4-hexadienal				
2,4-octadienal				
2-heptenal	5.62	1149699	5.60	4325391
Heptanol				
1-octen-3-ol	6.06	240673	6.05	2987974
2,4 nonadienal			6.27	1524132
Octanal	6.46	1249598	6.45	3565417
Limonene				
3-octen-2-one				
2-octenal	7.42	489413	7.42	6310033
Nonanal			7.66	2081856
4-nonenal	8.05	2036367		
2-nonen-1-ol	8.22	2742952	8.22	9965791
Nonanol			9.32	952829
Naphthalene			9.48	939371
Decanal				
2-decenal	10.73	571196	10.71	9208827
2,4-decadienal			11.51	3526937
2-undecenal	12.24	692327	12.20	6031355
α -Farnesene				

Table F.2 - Table showing retention times and peak areas for extraction of volatile fraction of oil E15 by SFE and SPME

Compound	SFE		SPME	
	RT	Pk area	RT	Pk area
2-pentenal			2.26	330794
Hexanal	2.96	6844805	2.90	6698597
2-hexenal			3.75	213963
3-hexen-1-ol			4.02	783370
Heptanal				
2,4-hexadienal				
2,4-octadienal	4.48?	228030		
2-heptenal	5.61	705514	5.61	4134368

Heptanol	5.89	228894	5.90	581380
1-octen-3-ol			6.07	3820637
2,4 nonadienal	6.27	1370279	6.28	1328777
Octanal	6.46	1317888		
Limonene				
2-octenal	7.40	696080	7.44	5986265
Nonanal			7.68	1459440
4-nonenal	8.04	2495158	8.05	3619954
2-nonen-1-ol	8.21	3512832	8.23	8778476
Naphthalene				
Decanal				
2-decenal	10.70	695036	10.73	7018099
2,4-decadienal			11.54	1958063
2-undecenal	12.22	899329	12.22	3399576
α -Farnesene				

Table F.3 - Table showing retention times and peak areas for extraction of volatile fraction of oil E16 by SFE and SPME

Compound	**SFE**		**SPME**	
	RT	**Pk area**	**RT**	**Pk area**
2-pentenal				
Hexanal	2.96	3248710	2.82	3048397
2-hexenal	3.80	129853	3.70	608054
3-hexen-1-ol			3.98?	444632
Heptanal	4.66	206648	4.67	Tr
2,4-hexadienal				
2,4-octadienal				
2-heptenal	5.63	413183	5.60	1752039
1-octen-3-ol	6.08	Tr	6.04	586049
2,4 nonadienal	6.29	1716550		
Octanal	6.48	532417	6.46	1323661
Limonene				
2-octenal	7.42	Tr	7.42	1988053
Nonanal	7.67	Tr	7.67	783533
4-nonenal	8.05	340878		
2-nonen-1-ol				
Naphthalene			9.50	691502
Decanal				
2-decenal				
2,4-decadienal				
2-undecenal				
α -Farnesene				

Table F.4 - Table showing retention times and peak areas for extraction of volatile fraction of oil E17 by SFE and SPME

Compound	SFE		SPME	
	RT	Pk area	RT	Pk area
2-pentenal			2.22	199321
Hexanal	2.99		2.86	4624716
2-hexenal				
3-hexen-1-ol			4.00	155233
Heptanal	4.66			
2,4-hexadienal				
2,4-octadienal				
2-heptenal	5.62		5.59	2767547
Heptanol			5.88	485346
1-octen-3-ol	6.06		6.05	1212957
2,4 nonadienal	6.28		6.26	808323
Octanal	6.46		6.45	2219394
Limonene				
3-octen-2-one			7.08	159846
2-octenal	7.42		7.42	4289304
Nonanal				
4-nonenal				
2-nonen-1-ol	8.21		8.22	5359748
2-nonenal			9.12	605755
Naphthalene			9.48	789159
Decanal			9.86	866751
2-decenal			10.72	4861136
2,4-decadienal			11.19	1057826
2-undecenal			12.20	3141533
α -Farnesene				

Table F.5 - Table showing retention times and peak areas for extraction of volatile fraction of oil E18 by SFE and SPME

Compound	SFE		SPME	
	RT	Pk area	RT	Pk area
2-pentenal				
Hexanal	2.95	1608060	2.85	999197
2-hexenal	3.78	107882	3.72	1058715
3-hexen-1-ol			3.79	298982
Heptanal	4.63	152529		
2,4-hexadienal				
2,4-octadienal				
2-heptenal	5.60	243952	5.58	1178656
Heptanol				
1-octen-3-ol			6.04	356194
2,4 nonadienal	6.26	943644		
Octanal	6.44	292032	6.45	476186
Limonene			6.91	100504

3-octen-2-one			7.08	141122
2-octenal	7.40	98281	7.41	547376
Nonanal				
4-nonenal				
2-nonen-1-ol	8.19	1591677	8.22	5965930
Naphthalene			9.48	648079
Decanal				
2-decenal			10.71	1223704
2,4-decadienal				
2-undecenal				
α -Farnesene				

Table F.6 - Table showing retention times and peak areas for extraction of volatile fraction of oil E33 by SFE and SPME

Compound	**SFE**		**SPME**	
	RT	**Pk area**	**RT**	**Pk area**
2-pentenal			2.59	35738
Hexanal	2.92	2453495	2.82	923904
2-hexenal	3.76	342806	3.68	1786999
3-hexen-1-ol			3.76	664521
Heptanal	4.16	Trace		
2,4 hexadienal				
2,4-octadienal			5.36	227509
2-heptenal	5.58	Trace	5.56	222954
1-octen-3-ol	6.02	Trace	6.02	60972
2,4 nonadienal	6.24	2534967	6.24	172658
Octanal	6.42	544978	6.43	627184
Limonene			6.89	756923
2-octenal	7.4	Trace	7.4	162186
nonanal				
4-nonenal	8.00	577563		
2-nonen-1-ol	8.18	2895043	8.2	2073912
2-decenal	10.68	645852	10.70	2009347
Naphthalene			9.47	172297
2-undecenal	12.18	219864	12.21	325678
α -Farnesene			14.16	210948

Table F.7 - Table showing retention times and peak areas for extraction of volatile fraction of oil E35 by SFE and SPME

Compound	SFE		SPME		SFE onto SPME	
	RT	Pk area	RT	Pk area	RT	Pk area
2-pentenal						
Hexanal	2.99		2.79	559977	2.86	393572
2-hexenal	3.83		3.66	3803269	3.75	200849
3-hexen-1-ol			3.74	452695		
Heptanal	4.69					
2,4-hexadienal						
2,4-octadienal						
2-heptenal	5.65					
Heptanol					5.91	201290
1-octen-3-ol			6.01	143355		
2,4 nonadienal	6.32				6.29	1461301
Octanal	6.50				6.48	586078
Limonene			6.87	40097		
3-octen-2-one						
2-octenal			7.40	92739	7.44	522470
Nonanal						
4-nonenal						
2-nonen-1-ol	8.25		8.19	1932242	8.25	5401284
Nonanol						
Naphthalene			9.46	756657	9.52	427346
Decanal					9.89	823393
2-decenal	10.76		10.72	424177	10.75	1382907
2,4-decadienal					11.58	254153
2-undecenal	12.26				12.24	962441
α -Farnesene			14.17	398051		

SPME extraction optimisation

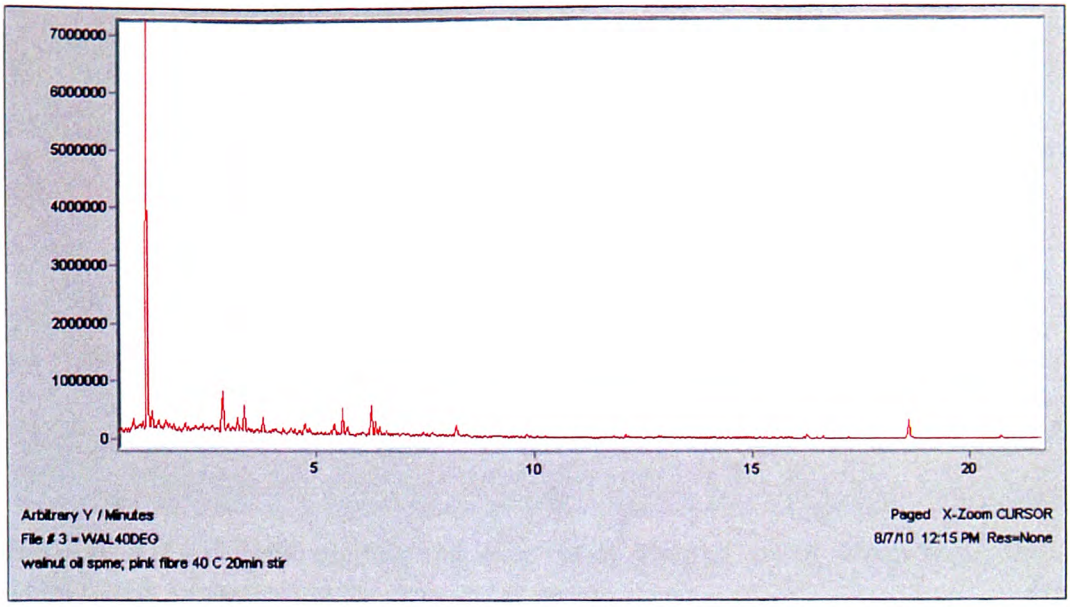

Figure F.1 – SPME extraction of 2 ml of walnut oil for 20 minutes at 40°C

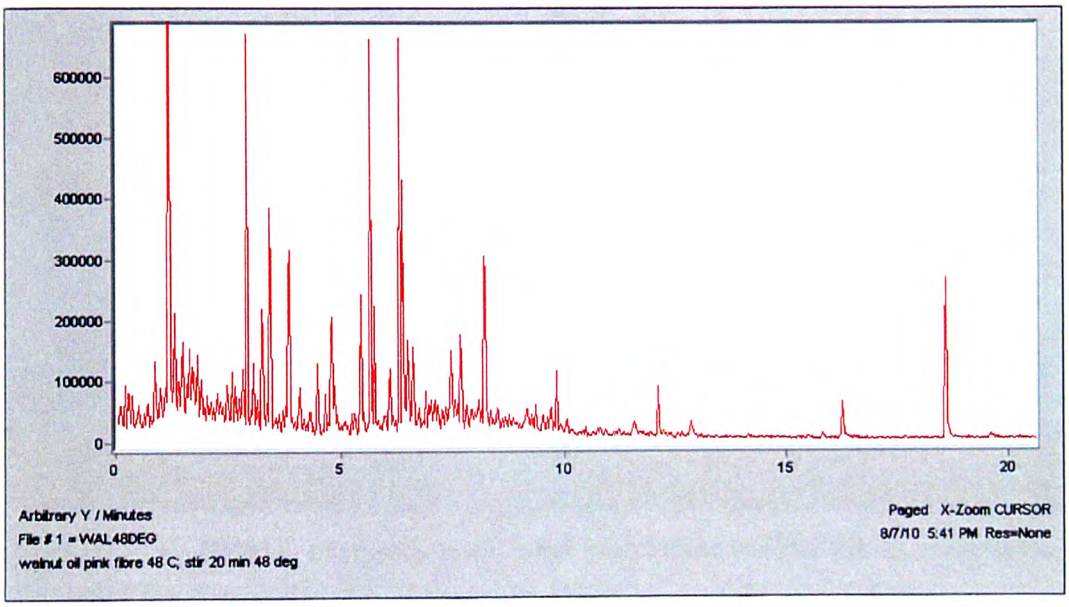

Figure F.2 - SPME extraction of 2 ml of walnut oil for 20 minutes at 48°C

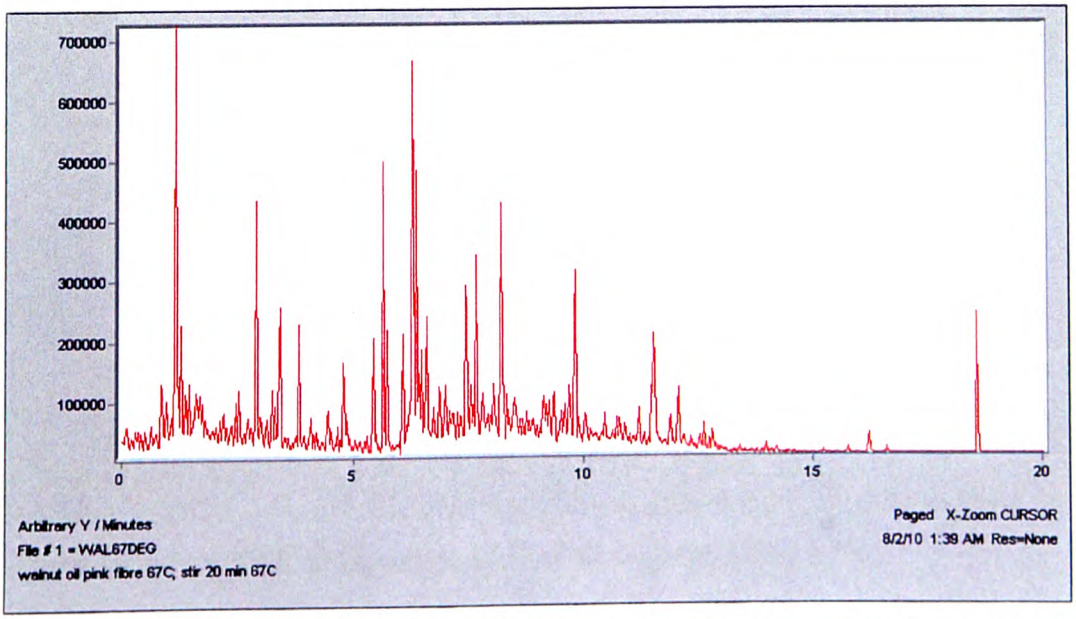

Figure F.3 - SPME extraction of 2 ml of walnut oil for 20 minutes at 67°C

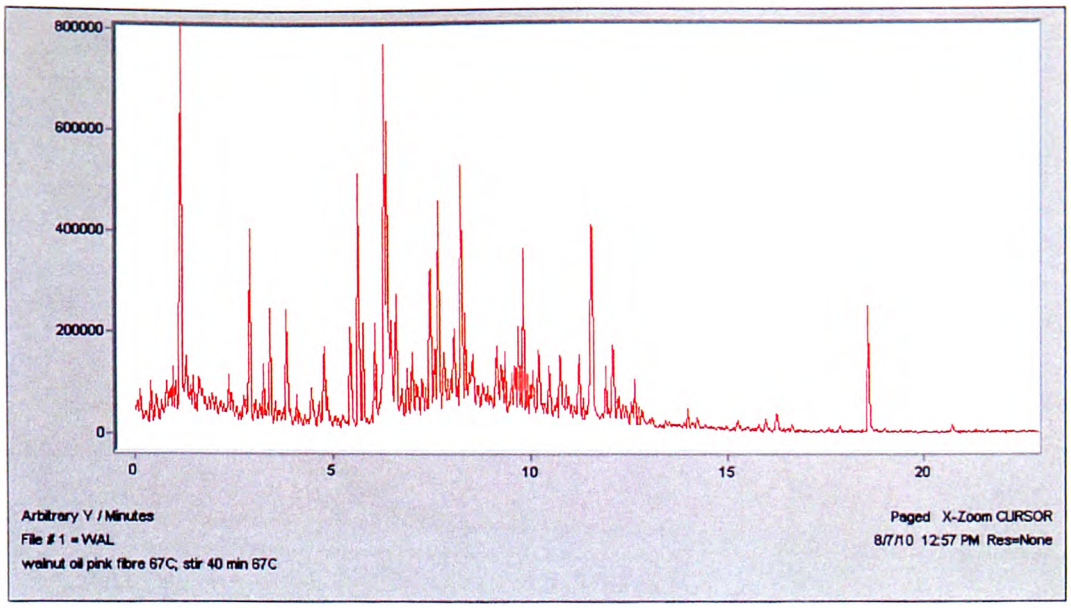

Figure F.4 – SPME extraction of 2 ml of walnut oil for 40 minutes at 67°C

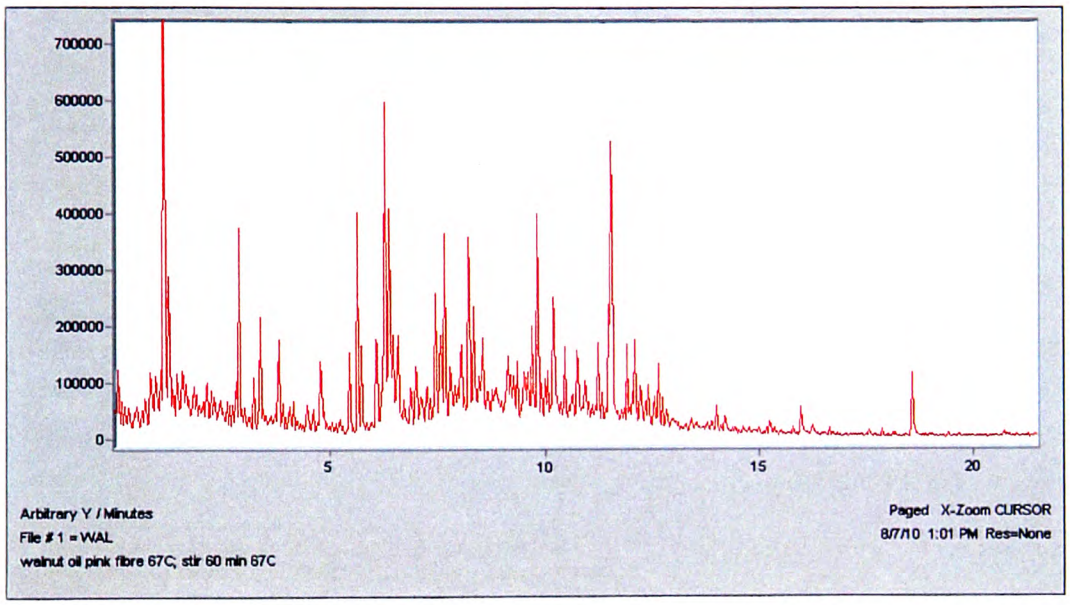

Figure F.5 - SPME extraction of 2 ml of walnut oil for 60 minutes at 67°C

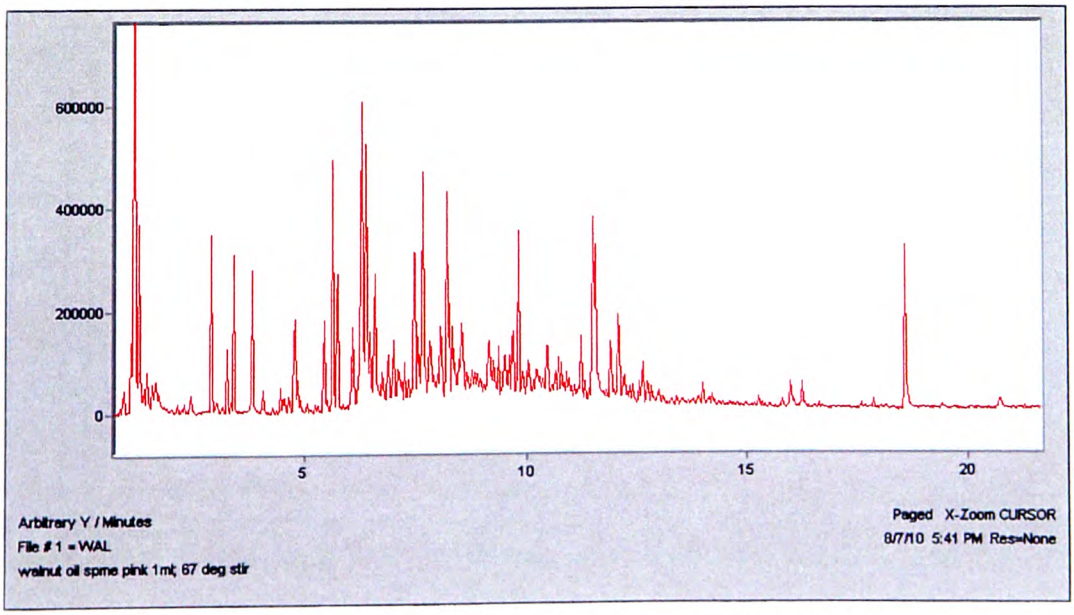

Figure F.6 - SPME extraction of 1ml of walnut oil at 67°C

Statistical analysis

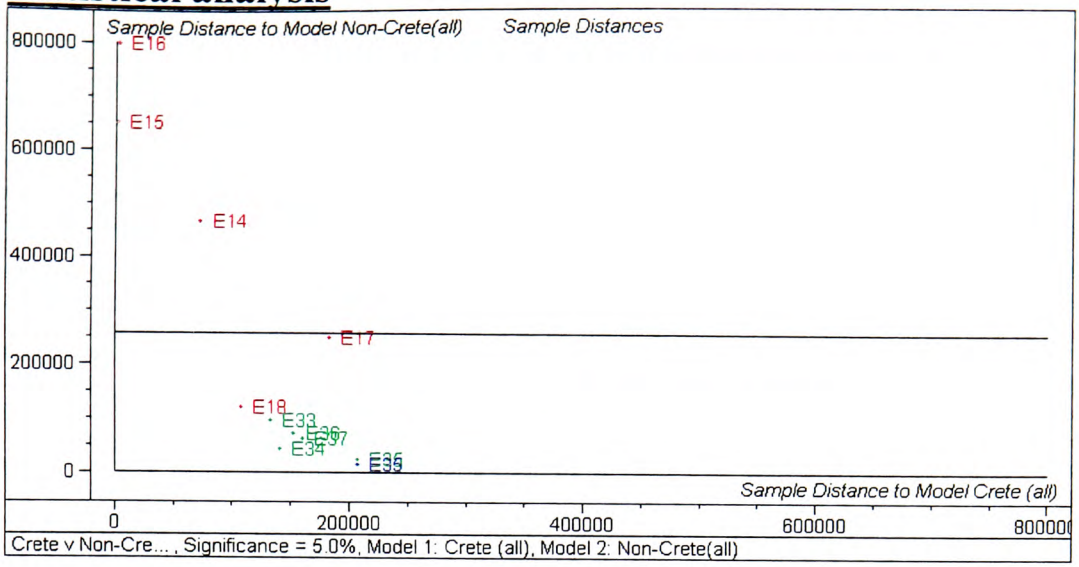

Figure F.7 – Cooman's Plot of the E set SPME extracted volatiles, Crete (red) v Non-Crete (green) over all variables

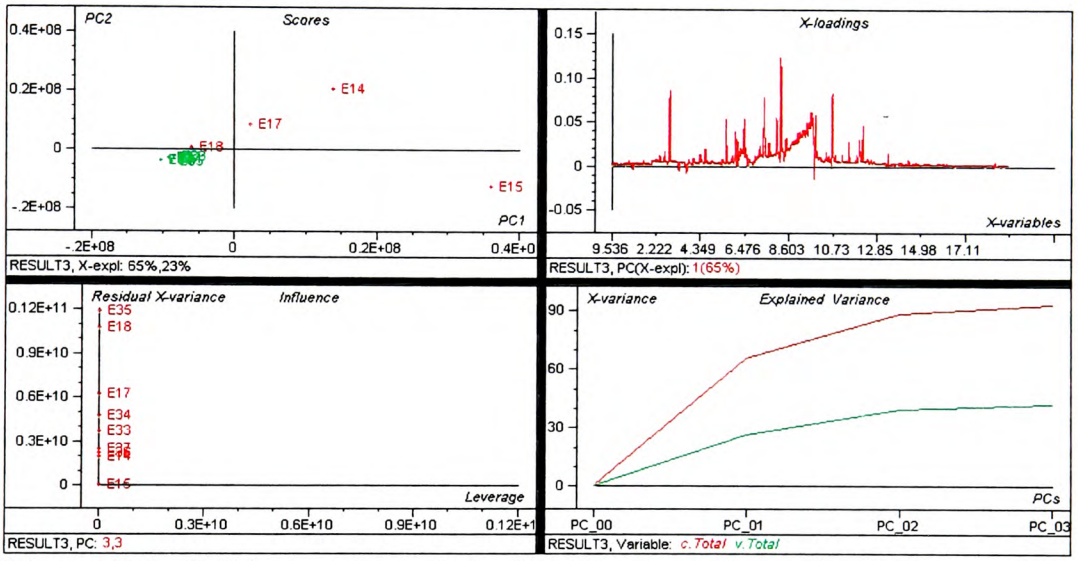

Figure F.8 - PCA overview of the SPME extractions of volatile fraction of olive oil – outlier. Scores plot (top left), Crete oils – red, non-Crete oils – green.

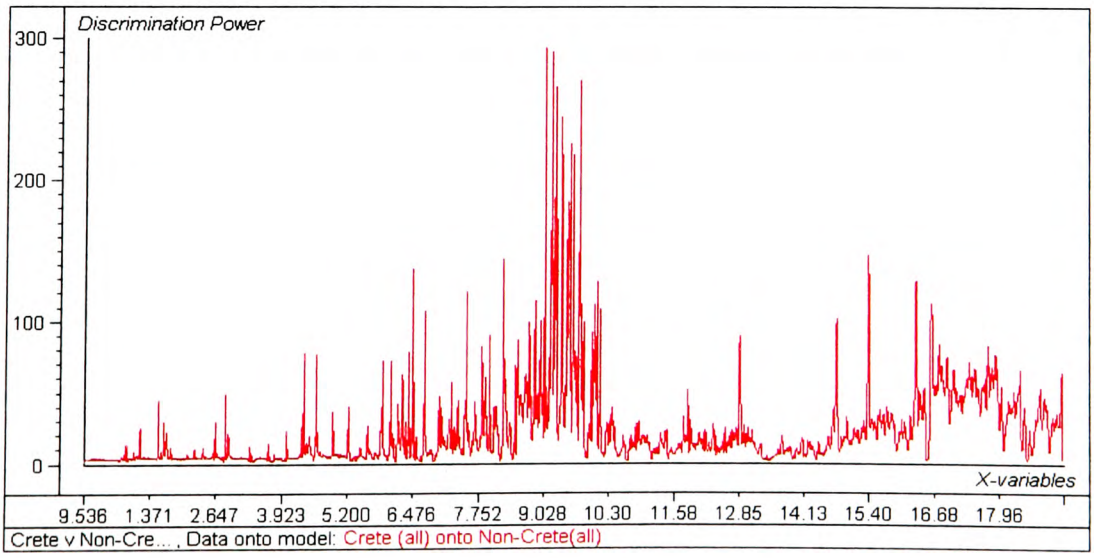

Figure F.9 – Discrimination plot showing that all the variables are considered to be important variables in distinguishing between the SPME data from the Crete oils and the non-Crete PCA model